When physical experiments meet machine learning experiments for the understanding and prediction of the ageing of refrigerated transport vehicles

Claudia Capo

N°d'ordre NNT : 2021LYSEI017

THESE de DOCTORAT DE L'UNIVERSITE DE LYON
opérée au sein de
INSA de Lyon

Ecole Doctorale N° 162
Mécanique – Energétique – Génie civil - Acoustique

Spécialité/ discipline de doctorat : Thermique - énergétique

Soutenue publiquement le 16/03/2021, par :
Claudia Capo

When physical experiments meet machine learning experiments for the understanding and prediction of the ageing of refrigerated transport vehicles

---

Devant le jury composé de :

Tréméac, Brice	Maître de conférences HDR, CNAM Paris	Rapporteur
Minetto, Silvia	Senior Researcher, ITC-CNR Padova	Rapporteure, Présidente
Roncancio, Claudia	Professeur des universités, Ensimag Grenoble	Examinatrice
Monti, Arthur	Docteur, Chereau Avranches	Examinateur
Bonjour, Jocelyn	Professeur des universités, CETHIL Lyon	Directeur de thèse
Revellin, Rémi	Professeur des universités, CETHIL Lyon	Co-directeur de thèse
Petit, Jean-Marc	Professeur des universités, LIRIS Lyon	Co-directeur de thèse
Cavalier, Gérald	Ingénieur-Directeur, CEMAFROID Fresnes	Examinateur

Département FEDORA – INSA Lyon - Ecoles Doctorales – Quinquennal 2016-2020

SIGLE	ECOLE DOCTORALE	NOM ET COORDONNEES DU RESPONSABLE
CHIMIE	**CHIMIE DE LYON** **http://www.edchimie-lyon.fr** Sec. : Renée EL MELHEM Bât. Blaise PASCAL, 3e étage **secretariat@edchimie-lyon.fr** INSA : R. GOURDON	**M. Stéphane DANIELE** Institut de recherches sur la catalyse et l'environnement de Lyon IRCELYON-UMR 5256 Équipe CDFA 2 Avenue Albert EINSTEIN 69 626 Villeurbanne CEDEX **directeur@edchimie-lyon.fr**
E.E.A.	**ÉLECTRONIQUE,** **ÉLECTROTECHNIQUE,** **AUTOMATIQUE** **http://edeea.ec-lyon.fr** Sec. : M.C. HAVGOUDOUKIAN **ecole-doctorale.eea@ec-lyon.fr**	**M. Gérard SCORLETTI** École Centrale de Lyon 36 Avenue Guy DE COLLONGUE 69 134 Écully Tél : 04.72.18.60.97 Fax 04.78.43.37.17 **gerard.scorletti@ec-lyon.fr**
E2M2	**ÉVOLUTION, ÉCOSYSTÈME,** **MICROBIOLOGIE, MODÉLISATION** **http://e2m2.universite-lyon.fr** Sec. : Sylvie ROBERJOT Bât. Atrium, UCB Lyon 1 Tél : 04.72.44.83.62 INSA : H. CHARLES **secretariat.e2m2@univ-lyon1.fr**	**M. Philippe NORMAND** UMR 5557 Lab. d'Ecologie Microbienne Université Claude Bernard Lyon 1 Bâtiment Mendel 43, boulevard du 11 Novembre 1918 69 622 Villeurbanne CEDEX **philippe.normand@univ-lyon1.fr**
EDISS	**INTERDISCIPLINAIRE** **SCIENCES-SANTÉ** **http://www.ediss-lyon.fr** Sec. : Sylvie ROBERJOT Bât. Atrium, UCB Lyon 1 Tél : 04.72.44.83.62 INSA : M. LAGARDE **secretariat.ediss@univ-lyon1.fr**	**Mme Sylvie RICARD-BLUM** Institut de Chimie et Biochimie Moléculaires et Supramoléculaires (ICBMS) - UMR 5246 CNRS - Université Lyon 1 Bâtiment Curien - 3ème étage Nord 43 Boulevard du 11 novembre 1918 69622 Villeurbanne Cedex Tel : +33(0)4 72 44 82 32 **sylvie.ricard-blum@univ-lyon1.fr**
INFOMATHS	**INFORMATIQUE ET** **MATHÉMATIQUES** **http://edinfomaths.universite-lyon.fr** Sec. : Renée EL MELHEM Bât. Blaise PASCAL, 3e étage Tél : 04.72.43.80.46 **infomaths@univ-lyon1.fr**	**M. Hamamache KHEDDOUCI** Bât. Nautibus 43, Boulevard du 11 novembre 1918 69 622 Villeurbanne Cedex France Tel : 04.72.44.83.69 **hamamache.kheddouci@univ-lyon1.fr**
Matériaux	**MATÉRIAUX DE LYON** **http://ed34.universite-lyon.fr** Sec. : Stéphanie CAUVIN Tél : 04.72.43.71.70 Bât. Direction **ed.materiaux@insa-lyon.fr**	**M. Jean-Yves BUFFIÈRE** INSA de Lyon MATEIS - Bât. Saint-Exupéry 7 Avenue Jean CAPELLE 69 621 Villeurbanne CEDEX Tél : 04.72.43.71.70 Fax : 04.72.43.85.28 **jean-yves.buffiere@insa-lyon.fr**
MEGA	**MÉCANIQUE, ÉNERGÉTIQUE,** **GÉNIE CIVIL, ACOUSTIQUE** **http://edmega.universite-lyon.fr** Sec. : Stéphanie CAUVIN Tél : 04.72.43.71.70 Bât. Direction **mega@insa-lyon.fr**	**M. Jocelyn BONJOUR** INSA de Lyon Laboratoire CETHIL Bâtiment Sadi-Carnot 9, rue de la Physique 69 621 Villeurbanne CEDEX **jocelyn.bonjour@insa-lyon.fr**
ScSo	**ScSo*** **http://ed483.univ-lyon2.fr** Sec. : Véronique GUICHARD INSA : J.Y. TOUSSAINT Tél : 04.78.69.72.76 **veronique.cervantes@univ-lyon2.fr**	**M. Christian MONTES** Université Lyon 2 86 Rue Pasteur 69 365 Lyon CEDEX 07 **christian.montes@univ-lyon2.fr**

*ScSo : Histoire, Géographie, Aménagement, Urbanisme, Archéologie, Science politique, Sociologie, Anthropologie.

Abstract

The thermal insulation of the vehicles'enclosures used in refrigerated transport is a critical element both for the quality of the cold chain and for the energy consumption of these vehicles. Its efficiency is characterized by the overall insulation coefficient ("K coefficient"), which tends to increase over time due to the ageing of the enclosure. This thesis presents the results of a work carried out according to three complementary approaches to understand the ageing phenomenon. The results from experimental test campaigns have been confronted with results produced by methods from the world of data science to support physical modeling efforts. The experiments consisted of measurements of the K coefficient of prototype vehicles after their manufacturing and in service-vehicles after 12 years of use. This made it possible to evaluate the impact of the refrigerating unit and to quantify the difference between the new vehicles and their prototypes. Besides, the thermal and energy performances of a new type of vehicle built with sandwich panels with vacuum inserts in the walls were determined. The availability of a large amount of data stored in Cemafroid's Datafrig® databases makes it possible to study the ageing phenomenon using a data-centric approach. The data were statistically analysed using simple probability density concepts and artificial intelligence techniques. A numerical model of ageing was developed using a random forest algorithm: it allows the prediction of the ageing with an error of less than 6%. Finally, a 1D physical model was developed in order to understand the ageing phenomenon from a thermal point of view. This model reproduces the initial insulation performances (K_p and K_0) of a refrigerated vehicle and allows to simulate the ageing of the vehicle after 12 years of life.

Resumé

L'isolation thermique de la caisse des véhicules utilisés dans le transport sous température dirigée est un élément critique tant pour la qualité de la chaîne du froid que pour la consommation énergétique de ces véhicules. Son efficacité est caractérisée par le coefficient d'isolation global ("coefficient K"), qui tend à augmenter au cours du temps en raison du vieillissement de la caisse. Cette thèse présente les résultats de travaux réalisés selon trois approches complémentaires pour comprendre le vieillissement. Des résultats de campagnes d'essais expérimentaux ont été confrontés à des résultats produits par des méthodes du monde de la science des données pour conforter des efforts de modélisation physique. Les expériences ont consisté à réaliser des mesures du coefficient K d'engins prototypes après leur fabrication et d'engins en service depuis 12 ans. Ceci a permis d'évaluer l'impact du groupe frigorifique et de quantifier la différence entre les nouveaux engins et leurs prototypes. Par ailleurs, les performances thermiques et énergétiques d'un nouveau type d'engin construit avec des panneaux sandwich ayant des inserts sous vide dans les parois ont été déterminées. La disponibilité d'un grand nombre de données stockées dans les bases de données Datafrig® du Cemafroid permet d'étudier le phénomène de vieillissement par une approche centrée sur les données. Les données ont été analysées statistiquement en utilisant des concepts simples de densité de probabilité et des techniques d'intelligence artificielle. Un modèle numérique de vieillissement a été développé à partir d'un algorithme de forêt aléatoire : il permet de prédire le vieillissement avec une erreur inférieure à 6%. Enfin, un modèle physique 1D a été développé afin de comprendre le phénomène de vieillissement d'un point de vue thermique. Ce modèle reproduit les performances d'isolation initiales (K_p et K_0) d'un véhicule frigorifique et permet de simuler le vieillissement du véhicule après 12 ans de vie.

Acknowledgement

It was the 11th September 2001. Sunlight was fading and the day was drawing to a close. In anticipation of the new school year, my father was sharpening my 13 year old mind with maths equations.

The most synonymous date in the 21st century marked an enormous shift in the world.

Personally, my memory of that fateful day is twofold: watching the scenes of terror on the streets of Manhattan but also of an unforgettable request my father made of me:

"*My Dear, promise me that you will continue your studies with seriousness and passion, that you will always nurture your education and that you will attend University".*

At the time my father was fighting his own personal battle against a terrible cancer and the sands were sadly quickly falling south in his hourglass. In the difficult times that have subsequently unfolded in my life, as well those that have marked our times, including the dramatic ones we are currently experiencing due to the Covid19 pandemic, I now understand the simple message my father hoped to impress upon me: education is the key and can save us from any terrible event.

It was on this day that my path toward his promise began and, if I could speak to him now, I would say: "*Dear Dad, sometimes it was difficult without you, but I tried to keep my promise*".

Any undertaking to complete a PhD is dotted with moments of triumph, despair and every emotion in between. Like all paths of life, a PhD, is also made up of people who remain with us in the good and bad moments. It is, for this reason, I wish to express my sincere gratitude to everyone who, in any way, helped me along this path.

First of all, I would like to thank the reviewers of this thesis: *Prof. Brice Trémeac* and *Dr. Silvia Minetto.* I already had the honour and the pleasure of discussing the topic of my thesis with you on several occasions during international congresses and conferences: your prestigious point of view, your advices on my research as well as your insights on this manuscript have been extremely valuable for me. A great thank you also to *Prof. Claudia Roncancio* and *Dr. Arthur Monti* for being the examiners of this thesis and for you your interesting insights.

My greatest acknowledgement is for the partners of this thesis: the *French Directorate-General for Food (DGAl), CHEREAU* company, *Petit Forestier* company. Without your implication, a large part of this work would not have been possible.

I wish to express my deepest gratitude to my academic supervisors, *Prof. Jocelyn Bonjour*, *Prof. Rémi Revellin* and *Prof. Jean-Marc Petit*. At the end of my internship at INSA you proposed me the beautiful challenge of a PhD with Cemafroid, thank you. You offered me a life experience whose richness will always be part of my personal cultural background. More generally, thank you for supporting me with dedication and rigour and teaching me to approach my PhD activities with a critical and constructive attitude and in an independent way.

To *Gérald Cavalier*, your guidance, whilst working by your side, helped me to grow in many ways and gain confidence personally, in work and in life. You introduced me to the world of refrigerated transport and your passionate enthusiasm taught me an invaluable lesson: *there is never a problem so long as there is a solution*. Despite the many varying tasks you already had in Cemafroid, you dedicated an enormous amount of time toward my development. This,

undoubtedly helped me progress my PhD thesis. Thank you. Your trust in me was truly supportive, given the nagging doubts that would, from time to time, creep into my head about living in France. While it has been an enriching experience, living in Paris was not always "oysters and champagne"! Thank you for understanding.

I would also like to express my sincere gratitude to my Professors at "Federico II", University of Napoli: *Prof. Alfonso William Mauro, Prof. Vincenzo Naso, Prof. Rita Mastrullo and Prof. Nicola Bianco*. You were the first to passionately introduce me to the study of heat transfer and refrigeration, many years ago. You exposed me to numerous opportunities that ensured my personal and professional growth and, for this, I will always be grateful. You gave me the opportunity to share my findings with your students : it was an honour for me. *Prof. Mauro*, my mission in France started thanks to you who, five years ago, trusted me and gave me the opportunity to spend five months at the INSA in Lyon to work on my Master's thesis project. I would never have imagined that those five months would turn into this very rich life experience. Thank you for keepeing an eye on my research from afar especially in the first period of my PhD and thank you for all your valuable advices.

Thank you to *Dr. Girolamo Panozzo*. Many years ago I had the chance to attend your lecture on refrigerated transport organised by my Professors at "Federico II", University of Napoli. I never thought I would continue a Research started many years earlier by you. Thank you for sharing your knowledge on the ageing of refrigerated transport vehicles, even after that lecture.

To all the Cemafroid Directors, you have always shown your interest in my PhD thesis and I have always felt you by my side in this beautiful challenge. Merci beaucoup!!!

To the Cemafroid teams of Fresnes, Cestas, Arras and Casal Monferrrato. Your daily work, ranging from certification, experiments in the laboratories to Datafrig®'s data management, but also communication and informatics…directly or indirectly, assisted my PhD project. Merci.

Frantz Latchan, thank you for the praiseworthy technical support you devoted throughout my PhD thesis. Thank you also for your valuable advices, not only in the technical matters.

Nicolas Boudet, thank you for enriching, with your expertise and knowledge of refrigerated transport, my study on the ageing of refrigerated transport vehicles, especially with regard to the physical model.

Mohammed, thank you for your advices during these last months of this work.

To *Prof. Jean-Marc Petit* and his team of experts at LIRIS laboratory, who accompanied me in discovering the fascinating world of Data Science. When we first met, we spoke totally different languages but with you it was not a problem, rather a source of richness and inspiration. Thank you very much for your support and help. A special thank you to *Marie Le Guilly* for the fruitful interaction and collaboration.

To my special colleagues with whom I spent most of my working days, *Tanina Bisaccia, Jacqueline Dacosta, Angela* and *Michele D'Ambrosio and Thomas Suquet*. It was a pleasure working by your side at Cemafroid. Thank you, because your sincere friendship helped me to overcome difficult moments in France. *Tanina*, your friendship has been a precious gift during these four years in France. I am sure it will always continue, no matter where life will take us.
Michele and *Angela*, thank you for welcoming me like a family member and making me feel at home, whilst I was away from my own. Your presence made many things easier. *Jacqueline*,

thank you for your sweetness and thoughtfulness. Thanks to all of you, you are angels that I was lucky enough to meet along the way.

Federica, my sweet friend, you have been in my life for twenty-two years and despite having spent these last four in France, we are even closer. This is proof that solid and true relationships exist despite the distance. Thank you for always being there in good and bad moments. You brought light and raised me up when everything seemed dark. With you I found the strength to never give up.

Luca, thank you because even though we haven't shared these years, meeting you again 25 years later in perhaps the most stressful months of this path, the ones before my PhD defence, was an unexpected and incredible gift. Thank you for your joyfull closeness. The smiles and laughs we shared helped me to reduce my stress.

My sincere thanks also to *Those* whom I did not mention directly but who have made me feel their closeness expressing, over the years, a caring and sensitive interest in my well-being and in my PhD project.

Last, and definitely not least I would like to sincerely thank my sweet *Mother* and *Brother*, who have continuously been by my side and always supported and encouraged me. Together with Dad, you paved a pathway full of love and meaning and for this I will be eternally grateful. Thank you because your closeness makes me feel strong.

During this life experience, in a foreign country, I grew on a professional and human level. Of all the lessons and principles I have learnt, the following is the one I most sincerely believe:

Those who truly love you, will never turn their back on you. Never.

In the end, the beginning. Always.

Claudia Capo

Fresnes, 16/03/2021

A mio Padre e mia Madre

Contents

List of Figures

List of Table

Layout of the thesis

The present thesis is divided in six chapters, organized as follows:

Chapter 1 provides a background to the study, by motivating the work and stating the research objectives.

Chapter 2 first introduces the fundamentals of refrigerated transport vehicles: the description of a refrigerated vehicle and its main components, the definitions given by the ATP regulation for refrigerated transport vehicles and the rule for testing their insulation performance. The process of ATP certificates issuing (which in France is carried out by the Cemafroid) and the production of data resulting from this process is also described.

Then, this chapter provides an overview of the state of the art related to the existing studies in open literature on:

- the evolution of materials and construction technologies insulated materials used for refrigerated transport vehicles,
- the ageing of refrigerated transport vehicles, including those studies that tried to model this phenomenon.

The existence of a large amount of data, made it possible to develop a data-centric approach which led to a statistical analysis and numerical modelling of the ageing phenomenon using artificial intelligence techniques. For this reason, this chapter also introduces those fundamental notions of big data and Machine Learning useful to implement such data learning approach. Hence, those steps to solve a given problem of supervised learning are highlighted. Among supervised algorithms a focus is done on classification and regression ones since they are those applied to the available data in Chapter 4.

Chapter 3 describes the experimental facility as well as the measurement instrumentation. All the experimental activities carried out during this thesis are presented in this chapter. The different results obtained are analyzed and commented.

Chapter 4 presents the implementation of a Data learning problem to study the ageing phenomenon of refrigerated vehicles. All the stages of such a data-centric study are presented:

- the available databases in Cemafroid;
- the selection of data from the available databases;
- the preprocessing phase of the selected data with the aim of improving their quality;
- a statistical analysis of the extracted data to gain insights from them;
- the study of the existence of a model and,
- the numerical modelling through classification and regression algorithms.

In *Chapter 5* a 1D model is proposed to reproduce the initial insulation performances (K_p and K_0) of a refrigerated vehicle of which the specific characteristics are known. This model also allows to simulate the ageing of the vehicle after 12 years of life.

Finally, *Chapter 6* summarizes the main outcomes of this thesis and the future perspectives.

Chapter 1

Introduction

Nomenclature of Chapter 1

Abbreviations

ANRT	Association Nationale Recherche Technologie	
ATP	Agreement on the International Carriage of Perishable Foodstuffs and on the Special Equipment to be Used for such Carriage	
COP	Coefficient of perfromance	
CETHIL	Centre d'Energétique et de THermIque de Lyon	
CAR	Chinese Association of Refrigeration	
CIFRE	Conventions Industrielles de Formation par la REcherche	
GHG	Greenhouse gas	
GWP	Global warming potential	[kg $CO_{2\ eq}$].
HC	Hydrocarbon	
HFC	Hydrofluorocarbures	
HFO	Hydrofluoroolefin	
IEA	International Energy Agency	
IIR	International Institute of Refrigeration	
IT	Information technology	
LIRIS	Laboratoire d'Informatique en Image et Systèmes d'Information	
PTV	Prototype vehicle	
SV	Series vehicle	
TEWI	Total equivalent warming impact	
UNECE	United Nations Economic Commission for Europe	
UNIDO	United Nation Industial Development Organization	
WHO	World Health Organization	
XPS	Extrude polystyrene	

Greek

β	Carbon dioxide emission factor	[g CO_2. kWh^{-1}]
Δ	Variation	

Roman

E	Energy consumption	[kWh]
K	Overall heat transfer coefficient	[W.m^{-2} K^{-1}]
L	Annual percentage leakage rate	[kg]
$\dot{L}$	Mechanical power	[W]
n	System running time	[hours]
N	Life of the system	[years]
$\dot{Q}$	Cooling power	[W]
S	Mean surface area	[m^2]
T	Temperature	[K]

Subscripts

a	Annual
$cooling$	Cooling
$compressor$	Compressor

1. Introduction

1.1 Context, motivations and background

The world is currently under serious threat due to climate change. The ever-increasing greenhouse gas (GHG) emissions can turned out a series of negative consequences, such as deteriorating the patterns and amounts of precipitation, weakening the ice and snow cover, raising the sea level, swelling the acidity of the oceans, shifting the ecosystem characteristics and increasing threats to human health. The transport sector is one of the most GHG-emitting economic sectors, accounting for a quarter of global emissions and a third in Europe according to the International Energy Agency (IEA, 2017). As another illustration of the importance of the transport sector, Estrada Flores and Platt (2007) suggested that the total energy spent in the Australian food industry to keep an unbroken cold-chain from farms to consumers is about 19 292 GWh.year^{-1}.

Today the refrigerated transport covers a wide range of services provided by a diversified and constantly evolving terrestrial fleet of equipment. In 2019, the IIR (International Institute of Refrigeration) estimated about 5 million refrigerated vehicles worldwide. Such a percentage has considerably and not negligible effect on the environment. As a matter of fact, refrigerated vehicles use refrigerants, which directly impact the environment and are energy consuming emitting large quantities of carbon dioxide, the major global warming gas.

As stated by Tassou et al. (2009), the 40 % of the greenhouse gas emissions results from vehicle's engine and refrigerant leakages. Moreover, a refrigerated semi-trailer travels about 100 000 km per year, consuming 42 000 liters of fuel; 20 % of which is used for the operation of the refrigeration unit. This consumption may be doubled due to poor thermal insulation performance.

Emissions of refrigerant fluids from leaks during vehicles' servicing directly impact the environment. On the other hand, the indirect effect is due to the energy required to keep the cold-chain intact. The generation of this energy contributes, in fact, to the production of large quantities of CO_2, which is the major global warming gas. The direct and indirect contributions to the environmental impact can be combined in a unique indicator, the Total Equivalent Warming Impact (TEWI), whose formula is introduced by Unido (2010) and applied by Makhnatcha and Khodabandeh (2014)

$$TEWI = \text{direct emissions} + \text{indirect emissions} = (GWP\ L\ N) + (E_a \beta n) \qquad \text{Eq. (1.1)}$$

Where:

- L is the annual percentage leakage rate of refrigerant in the system, kg (3% of refrigerant charge annually);
- N is the life of the system, years;
- n is the system running time, hours;
- $E_a$is the energy consumption, kWh per year (modelled for each refrigerant);

- β is the carbon dioxide emission factor, $CO_{2\text{-eq.}}$ emissions per kWh (g CO_{2eq}. kWh^{-1}) of each energy use to run the compressor.
- GWP, Global Warming Potential, is the refrigerant fluid index which compares the global warming impact of an emission of a greenhouse gas in relation to the impact from the emission of similar amount of CO_2. This estimation is made on a time horizon of 100 years. The contribution of a refrigerant to the global warming is lower if smaller is the GWP value.

The TEWI formula may be rewritten as:

$$\frac{TEWI}{N} = GWP\ L + \dot{L}_{compressor}\ \frac{n}{N}\beta \qquad \text{Eq. (1.2)}$$

$\dot{L}_{compressor}$ is the mechanical power expended by the compressor of the refrigerating unit to cool the inside of the vehicle and can be rewritten as:

$$\dot{L}_{compressor} = \frac{\dot{Q}_{cooling}}{COP} = \frac{K\Delta T\ S}{COP} \qquad \text{Eq. (1.3)}$$

Where:

- K is the overall heat transfer coefficient ($W.m^{-2}\ K^{-1}$) of the insulated body on which the refrigeration system is mounted;
- ΔT is the temperature difference between the mean inside temperature $T_{int}$and the mean outside temperature T_{ext}, during continuous refrigeration system operations;
- S is the mean surface (the square root of the product between the internal and external surfaces).
- COP is the coefficient of performance of the refrigeration unit.

Eq. (1.2) becomes:

$$\frac{TEWI}{N} = GWP\ L + \frac{K\Delta T\ S}{COP}\frac{n}{N}\beta \qquad \text{Eq. (1.4)}$$

The global environmental challenge of the refrigerated transport sector consists in reducing the contributions of both the direct and indirect emissions appearing in the TEWI indicator.

Eq. (1.4) allows considering that annual emissions of carbon dioxide indicator as a function of the following parameters:

- GWP value of the refrigerant fluid ;
- The annual percentage of refrigerant leaks, L depending on the manufacture and the wear of the refrigeration system;
- The *COP* value of the refrigeration unit, quantifying the efficiency of the refrigeration system.

- The K coefficient value of the insulated enclosure, representing the insulation performance of the enclosure of the vehicle on which the refrigeration system is mounted.

The dependence of the TEWI on these factors underlines the need to consider the refrigerated vehicle as composed of three fundamental parts:

- an insulated enclosure in which several accessories are installed and
- a refrigeration unit in which,
- a refrigerant fluid is circulating.

Reducing direct and indirect emissions is a global challenge to which refrigerated transport is called to respond. This challenge may be achieved by intervening on these three elementsas schematically illustrated in Figure 1.1.

Searching for new refrigerant fluids having a lower GWP value, new technologies with a better COP value and improving the insulation performance of the vehicle structure are processes that are closely interlinked and constantly evolving.

The achievement of these challenges allows refrigerated transport remaining one of the key links in the cold chain, having as objective to supply consumers with safe products of high quality. In this thesis, especially in Chapters 3, 4 and 5, the attention is focused on the challenges concerning the insulated enclosure: on how to improve the initial insulation performances and on the study of the ageing of these performances over the time from experimental, statistical and numerical points of view.

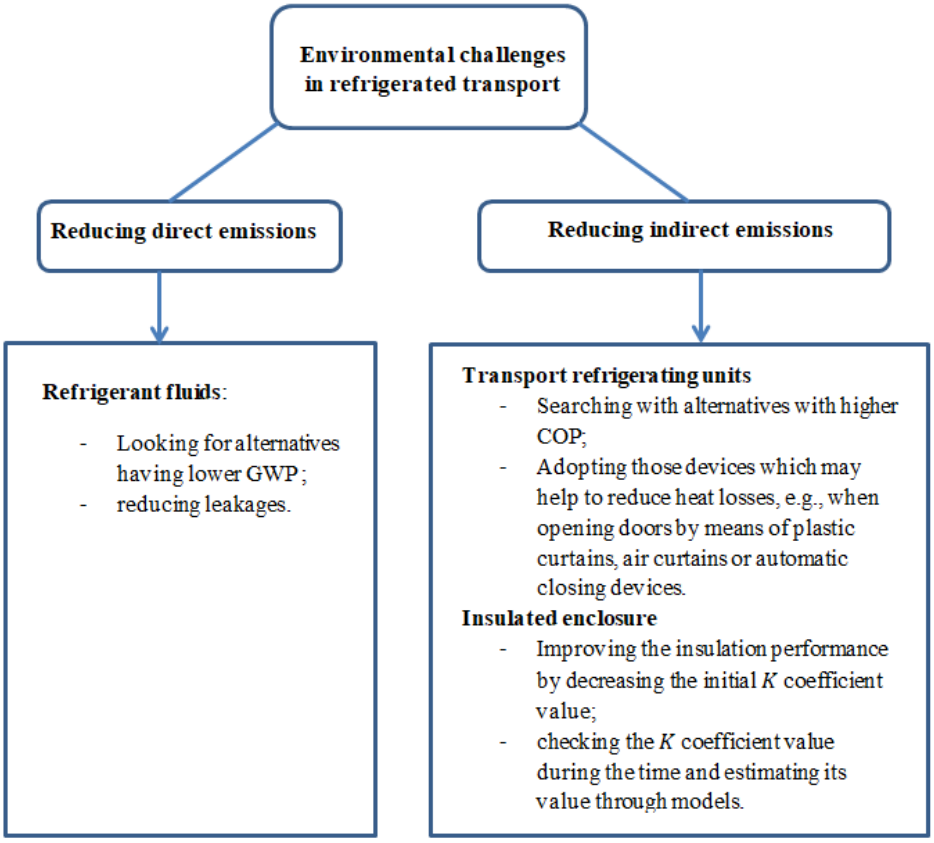

Figure 1.1 Environmental challenge of refrigerated transport sector

1.1.1 Cold chain and refrigerated transport

Food is lost or wasted worldwide throughout the supply chain, from initial agricultural production down to final household consumption (FAO, 2011). This problem is to be solved to feed those 795 million people in the world that were undernourished in the period 2014–16 (FAO, 2015). In this regard, refrigeration has a direct impact on human health through preservation of foods and pharmaceuticals, as well as through new low-temperature therapeutic techniques (IIR, 2019).Refrigeration inhibits the development of bacteria and toxic pathogens therefore preventing foodborne diseases. Refrigeration dramatically reduces the need for chemical preservatives in food. Since 1930, thanks to cold-chain enabled food preservation, a 90% decrease in the number of stomach cancer cases was noticed, according to a study (Boyle and Levin, 2008) by the World Health Organization (WHO). Whether in industrialized countries the food wastage problem is due to an excess in food production, in developing countries the causes of food losses and food insecurity are to be found in poor and unhygienic handling and storage conditions and in the lack of infrastructure for transportation, storage, cooling and adequate temperature control. The cold chain is a key element in solving the problems of food wastage and food insecurity, representing the continuity of means used in sequence to ensure the conservation at low temperature of perishable foodstuffs from the production phase to the final consumption.

Cold chain may be seen from three different points of view: it is a science, a technology, and a process. It is a science since it requires an understanding of the chemical and biological processes linked with perishability. It is a technology since it relies on physical means to ensure appropriate temperature conditions along the supply chain. It is a process since a series of tasks must be performed to prepare, store, transport and monitor temperature-sensitive products (Rodrigue and Notteboom, 2020).

Cold chain consists mainly of 5 steps, i.e.: production, packaging, storage in cold stores, transport and sale. However, among these steps there may be others intermediate warehouse and subsequent transport. An efficient cold chain is essential for the human health since it substantially reduces bacterial growth in food and the rate of many undesirable chemical and physiological reactions that jeopardize food's quality. Refrigeration is even more vital in those hot countries where bacterial activities are at a higher rate to ambient temperature. Refrigerated transport plays a central role in the cold chain reducing food losses and preserving its quality at all stages, from production to consumption but, at the same time, it is the most delicate link of this chain. For this purpose, vehicles are fitted with particular features and / or accessories such as insulating walls, refrigeration unit or eutectic plates, depending on the product and the transport regime. Refrigerated road transport saw its birth in the late 30s in USA and after the Second World War in Europe (Cavalier, 2016). Since then it continued to evolve, replacing the rail freight and recording an exponential growth all over the world in 1970. On this date the international agreement for transport of perishable foodstuffs ATP was signed in the frame of United Nations Economic Commission for Europe (UNECE). This Regulation was introduced with the aim of facilitating the international transport of perishable foodstuffs by harmonizing the relevant regulations and the administrative procedures and documentation requirements to which refrigerated transport is subject and setting common guidelines for testing and qualifying the refrigerated equipment. Nowadays, the role of refrigerated transport in the development of our modern societies is essential involving several sectors such as health, food processing, petrochemicals, aerospace or information technology (IT).

As highlighted in a recent socio-economic study carried out by Cemafroid (Fertell and Cavalier, 2020), at the end of 2019, The Economist predicted an average growth rate of 4.8 % per year by 2030 for the global refrigerated transport market. In view of the current health crisis, this rate is likely to be revised upwards. Indeed, the crisis has highlighted the very high level of interdependence of world economies and the fundamental role of supply chains in the structure of international trade. At the same time, the need for transport of pharmaceutical and food products will increase and evolve, and with them the performance requirements of equipment and its adequacy to the needs. The next paragraphs of this chapter present the evolution of the fleet in the world giving particular importance to the European fleet of which Cemafroid has a comprehensive knowledge. A focus is also made on the French fleet, whose data are used in this thesis for the study of the ageing of refrigerated vehicles.

1.1.2 Refrigerated transport fleet evolution

1.1.2.1 In the World

The 5 million refrigerated vehicles in the world are heterogeneously distributed in the various countries (see Table 1.1). Despite this disproportion, a general consideration that concerns all parts of the world is that temperature-controlled road transport is growing and, as indicated in a 2009 IIR study, is expected to increase by 2.5 per cent per year until 2030. This increase is essential to reduce the 360 million tons of perishable food that are wasted worldwide each year. Some governments have been made aware of the importance of temperature-controlled transport and, by 2030, will implement plans to expand the world fleet to meet food demand in emerging markets, particularly in Asia with China and India. In the European Union, before Brexit, the fleet of temperature-controlled transport equipment in service was estimated at between 1 and 1.1 million units, of which approximately 465 000 ATP units, or some 45 %, were ATP in service vehicles, as shown in Figure 1.2.

Table 1.1 Refrigerated vehicles in the world

	Number of refrigerated vehicles	**Number per inhabitants**
World	About 5 million of vehicles	1 for 1750 inhabitants
Europe	1.1 million of vehicles (Cemafroid)	1 for 450 inhabitants
China	140 000 (CAR 2019)	1 for 13 000 inhabitants
India	10 000 vehicles (NNCD 2018)	For 150 000 inhabitants

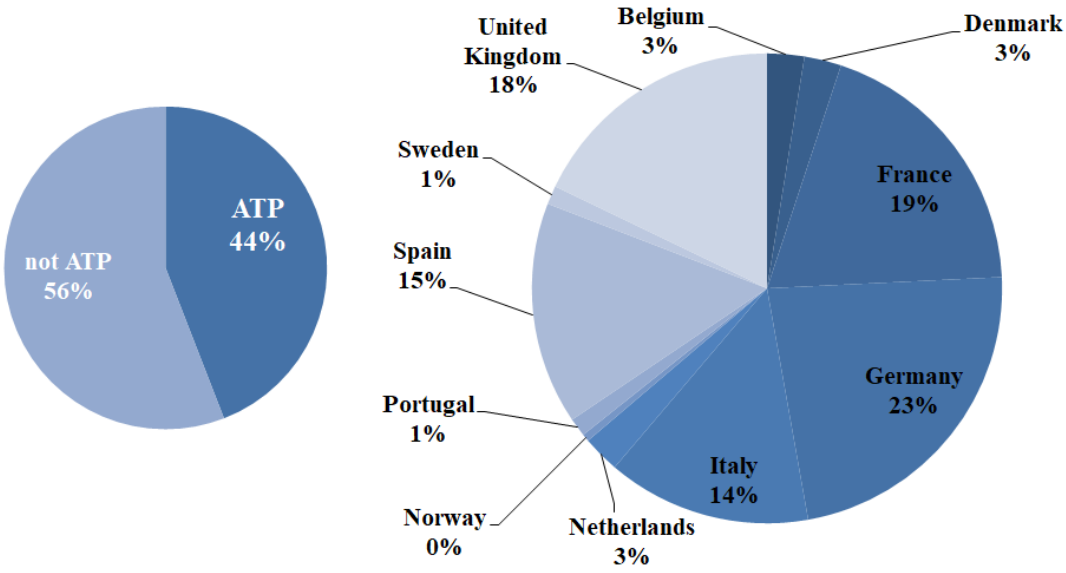

Figure 1.2 European fleet of refrigerated transport equipment.

In 2020 Cemafroid carried out a study (Fertell and Cavalier, 2020) to assess the European fleet at the end of 2018 through several methods: using UNECE data, population data, national and international transport data and their history. The results of this study are represented in Figure 1.3 where data are reported with their confidence levels (high, medium and low) and Table 1.2 which distinguishes the global fleet of each country from the corresponding ATP fleet. European market of refrigerated transport is now mature and rather oriented towards renewal. The relevant choices on how to renew the fleet should be made after a thorough knowledge of the ageing phenomenon. The French fleet is used for the ageing study: for this purpose its evolution is presented in the next subparagraph.

Table 1.2 European temperature-controlled transport fleet, global and ATP, at the end of 2018 (Cemafroid, 2020).

Country	Global fleet in 2018	ATP Fleet in 2018
Austria	14 843	2 000
Belgium	19 206	2 586
Bulgaria	12 778	2 000
Cyprus	1 848	350
Croatia	6 214	674
Czech Republic	18 945	2 845
Denmark	19 311	5 144
Finland	17 374	4 497
Estonia	3 482	804
France	149 081	119 368
Germany	167 244	30 000
Great Britain	113 837	8 300
Greece	14 417	1 002
Hungary	11 956	439
Ireland	12 450	2 800
Italy	96 964	47 837
Latvia	5 046	1 165
Lithuania	7 343	1 695
Luxembourg	1 432	300
Malta	1 173	250
Holland	30 845	4 657
Poland	83 990	25 079
Portugal	21 180	5 857
Romania	26 301	95
Slovakia	13 326	2 908
Slovenia	3 498	474
Spain	126 123	118 358
Sweden	18 125	2 703
Tot Europe and GB	1018 332	465 610

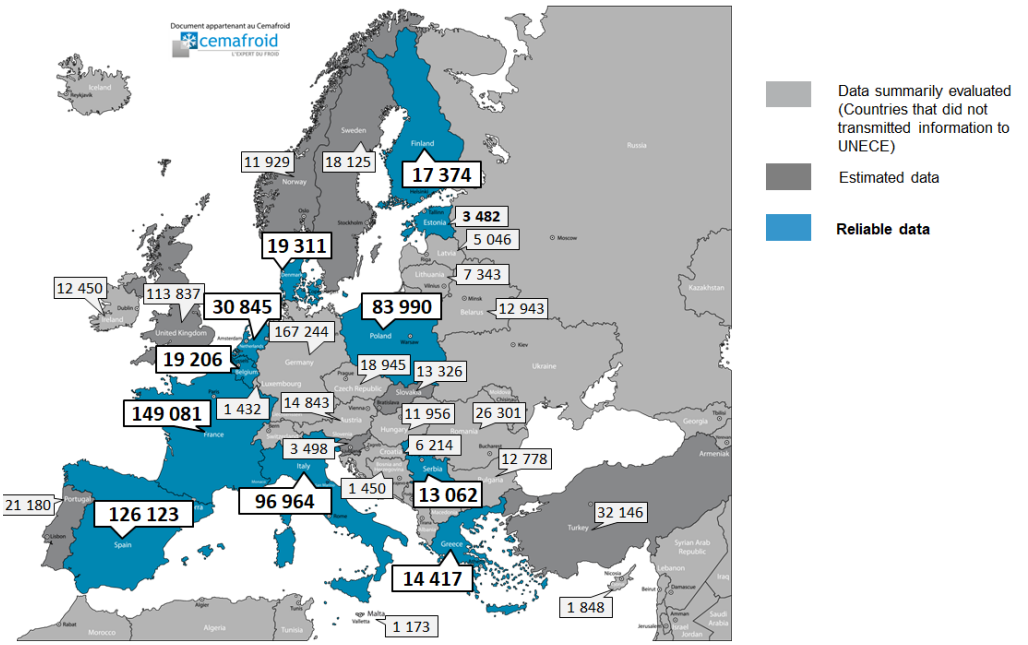

Figure 1.3 Map of the European temperature-controlled transport fleet at the end of 2018 (source Cemafroid 2020).

1.1.2.2 In France

The French fleet of ATP vehicles has steadily grown over the last ten years (Figure 1.4) and, at 31 December 2019, based on the Datafrig® data, counted 119 368 refrigerated transport equipment having a valid ATP certificate.

The Datafrig® database, managed by Cemafroid, allows the analysis of the trend of the ATP French fleet. As presented in Figure 1.5, these equipment are divided into different categories, the main ones: the vans (vehicles with a total weight allowed in charge smaller than 3.5 tons) representing the half of the fleet, the trucks (vehicles whose total weight allowed in charge varies from 3.5 to 29 tons) covering 20 % of the fleet and the semi-trailers (vehicles with total weight allowed in charge higher than 29 tons) for the remaining 26 %. Since 2018 France no longer has any refrigerated or isothermal wagons with a valid technical conformity certificate.

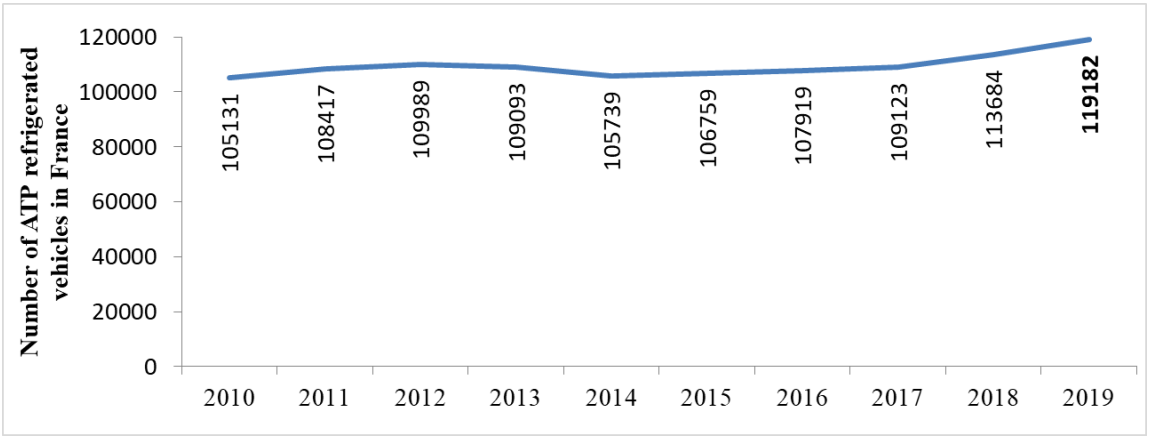

Figure 1.4 Evolution of the French fleet of refrigerated transport equipment (Datafrig® data).

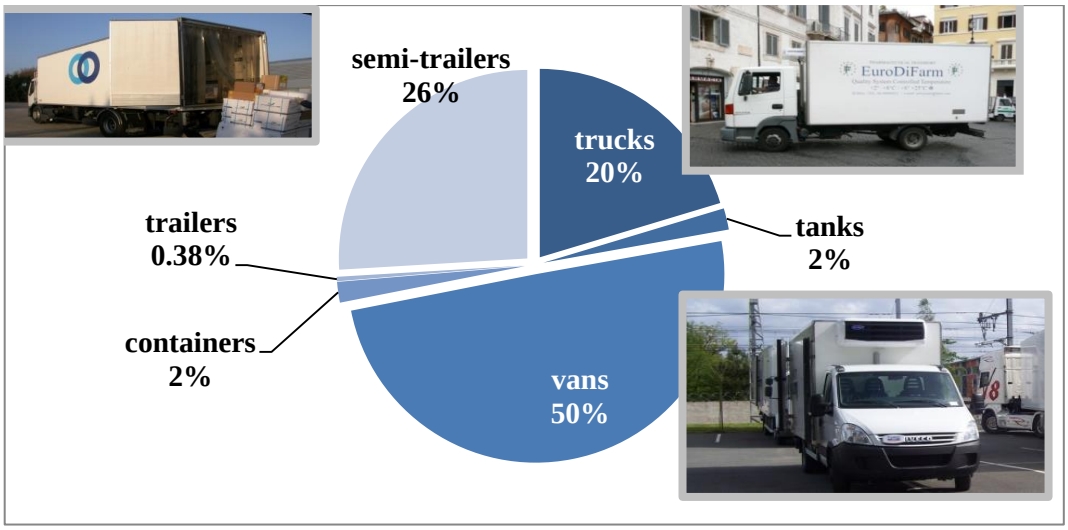

Figure 1.5 French fleet at 31 December 2019 based on Datafrig® data.

The vehicles involved in the cold chain have the peculiarity of generally being built with "sandwich" panels in which the insulation is made of polyurethane foams. The exceptional insulation properties are obtained by using blowing agents. Today the fleet is mainly made up of insulated enclosures realized with polyurethane foams expanded with cyclopentane or CO_2 (Capo et al., 2018)

Independently of the type of insulating foam, the nature of the insulated enclosures can be of two different types:

- integrated into the structure of the vehicle or,
- reported on the frame.

86 % of the French fleet, in 2019, is made up of vehicles with reported ion the frame insulated enclosures. Examples of integrated insulation and reported on the frame are shown in Figures 1.6a and 1.6b.

Figure 1.6 a) Integrated insuated vehicle; b) Reported insulated vehicle.

1.1.2.3 Life of a refrigerated vehicle and main challenges

Figure 1.6 presents the evolution of average age of the fleet in the last ten years. After a period of growth that took place from 2012 to 2015 and which led to a peak of 5.15 years, the average age of the fleet started to decrease to reach the value of 4.78 year in 2019.

This decrease was more pronounced for the semi-trailer category, 8% in the period between 2010 and 2019 (Figure 1.7). The analysis of the average age by type of vehicles shows, in Figure 1.8, that the average age of vans is significantly lower than that of semi-trailers and trucks. Nevertheless, semi-trailers have an average age that is 12.5% older than the rest of the fleet. Their operating life is longer and can be estimated to around 10 years on average.

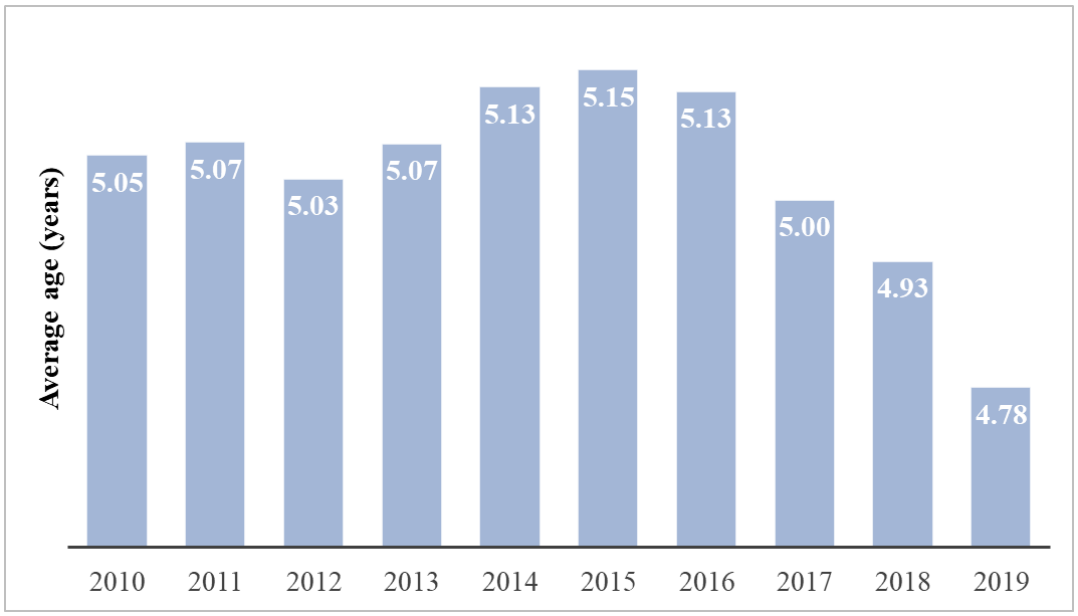

Figure 1.7 Evolution of the average age of the French fleet in the period 2010-2019 (Datafrig® data, Cemafroid 2020).

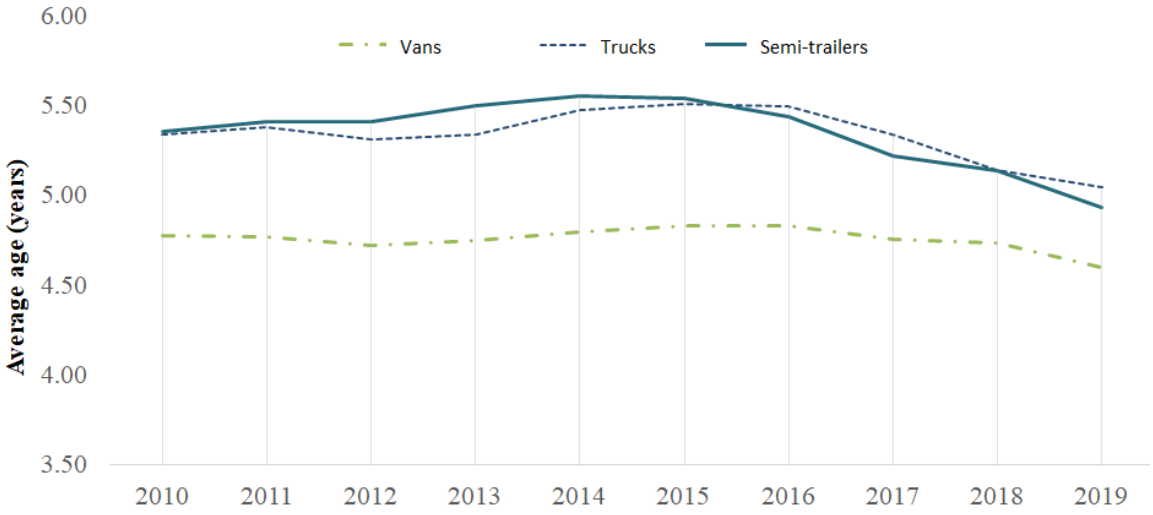

Figure 1.8 Evolution of the average age of the French fleet, by type of vehicles in the period 2010-2019 (Datafrig® data, Cemafroid 2020).

Today, the French refrigerated transport market is mature in terms of volume with the predominance of vehicles having insulated enclosures reported on their frames, but it is also changing very significantly in terms of both the nature of the body and the cold production system. The next few years will be characterized by many innovations that interest both body manufacturers and refrigerated unit manufacturers. As pointed out by Capo et al. (2018) in the short term, there will be changes that will affect the construction of the bodies of refrigerated vehicles.

Firstly, there will be the appearance of fourth generation refrigerant gases such as R-1234yf belonging to Hydrofluoro-Olefins (HFO) and which is being tested as a blowing agent in

polyurethane foams (PU). Despite a GWP equal to 4 tons equivalent of CO_2, slightly higher than hydrocarbons (HCs) and hydrofluorocarbures (HFCs), the expectations for the use of this refrigerant are to improve performance and consequently reduce vehicle consumption.

Concerning the extrude polystyrene bodies (XPS) expanded with R-134a, in order to reduce the increase in prices of HFCs and therefore to comply the imminent 2022 obligations of the F-Gas regulation, foam manufacturers are proposing two different approaches:

- reducing the quantity of R134a used for foam expansion,
- reducing the quantity of R134a and adding carbon to the foam matrix.

While the first approach will result in cost savings and lower performance, the second, by adding carbon, will result in the same or lower thermal conductivity and therefore similar or better insulating performance. More generally, the challenges towards which, body manufacturers and refrigerated unit manufacturers will direct their future solutions are: digitalization, connectivity and environment. The French fleet will make way for more productive and ergonomic innovations with the primary objective of reducing energy consumption and emissions.

1.2 Methodology of the study

This thesis, whose main objectives are to investigate and to model the phenomena related to the ageing of refrigerated transport vehicles, provides the results of a study developed in the context of a PhD activity carried out in the framework of a partnership, created within the CIFRE (Conventions Industrielles de Formation par la REcherche) of the ANRT (Association Nationale Recherche Technologie). This partnership (represented in the light blue frame at the center of the scheme of Figure 1.10) is composed of three different entities: the Cemafroid, recognized by the United Nations as ATP authority competent in France, and two academic laboratories of INSA Engineering School, based in Lyon, i.e. the CETHIL (Centre d'Energétique et de THermIque de Lyon) and the LIRIS (Laboratoire d'Informatique en Image et Systèmes d'Information). By means of a concatenated and complementary work, this partnership made it possible to develop different research activities which have led to the results presented in this manuscript. The strength of this partnership has been the diversity and wealth of competences. This has made it possible to study the phenomenon of ageing from different angles:

- experimental, thanks to the expertise of Cemafroid and its laboratories.
- physical modelling based on heat transfer analysis, thanks to the experience in this field of the CETHIL laboratory;
- data science, thanks to the presence of LIRIS which, through the use of artificial intelligence techniques, made it possible to use the large amount of data stored in the Cemafroid Datafrig® databases.

All the steps that led to the development of the study and to the achievement of its results are represented through a schematic outline in Figure 1.10.

The yellow parts of the scheme represent the process (and the actors involved in this process) which have fed the study, supplying the material to be tested. Cemafroid laboratories, set up by the Ministry of Agriculture in the 1950s to support the development of the cold chain in France, tests all the equipment used for the storage, transport and distribution of perishable products. Among this equipment there are the refrigerated vehicles built by manufacturers, i.e., new

prototype vehicles (PTV) and series vehicles (SV), and then used by refrigerated transport during their lifetime. After testing them, Cemafroid releases the ATP certificates for these vehicles through the Datafrig® information system. Hence, the vehicles tested and studied during this research project belong to the flow of vehicles arriving at Cemafroid ATP test station.

The main activities carried out throughout the thesis are shown in the frames of the graph of Figure 1.10, indicated with letters a) and b) and include both experimental activities carried out in the climatic chambers of the Cemafroid (several K coefficient tests) and analysis according to different approaches (i.e. thermodynamics, statistical and data learning ones) on the data extracted from Datafrig® databases. The whole of this process led to the development of models and performance indicators that cyclically return to all the entities presented in the outline of Figure 1.10, thus enriching them with new information useful for the development and the progress:

- of the manufacturing process carried out by the manufacturers,
- of use and maintenance of vehicles by transport companies,
- for the improvement of the ageing study itself but also for the development of new studies at Cemafroid, in partnership with the two academic laboratories.

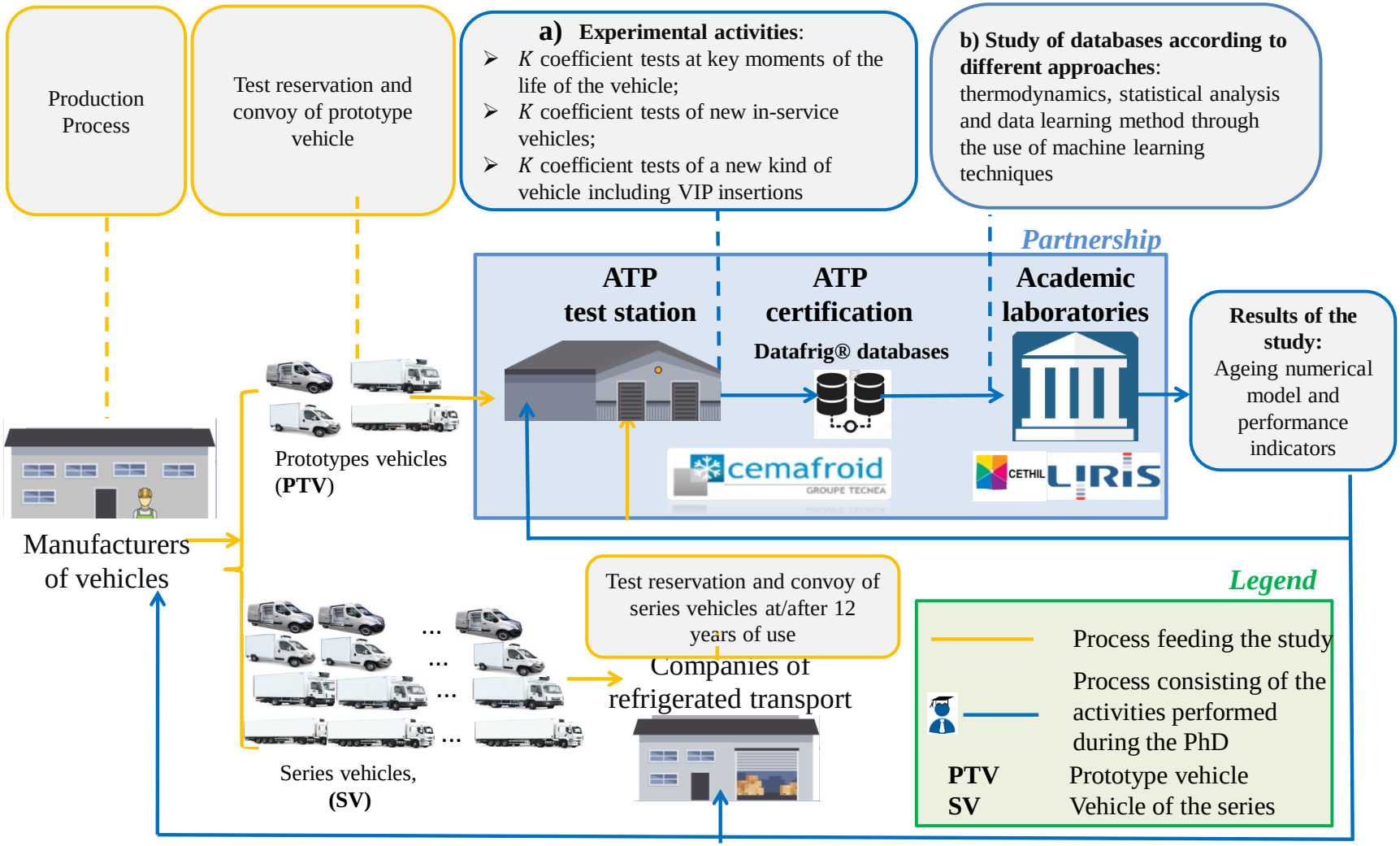

Figure 1.9 Outine of the Thesis

1.3 References

Boyle, P., Levin, B., 2008. World Cancer Report 2008. International Agency for Research on Cancer, 510 pages.

Capo, C., Bourez, D., Cavalier, G., 2018. Le parc de transport des engins sous température dirigée en 2017. Revue générale et du conditionnement d'air, Volume. Mai/Juin 2018, (25–32).

Cavalier, G., 2016. Sustainability in Transport Refrigeration Systems. Reference Module in Food Science, First Edition, (1–7).

Estrada Flores, S., Platt, G., 2007. Electricity usage in the Australian cold chain. Food Australia, 59 (8).

FAO, 2011. Global food losses and food waste – Extent, causes and prevention. Roma, Italy.

FAO, IFAD and WFP, 2015. The State of Food Insecurity in the World 2015. Meeting the 2015 international hunger targets: taking stock of uneven progress. Roma, Italy.

Fertell, C., Cavalier, G., 2020. L'innovation sur le marché des engins de transport sous température dirigée .Étude technico économique (Cemafroid Confidential study).

IEA, 2017. World Energy Outlook. Paris, France. Online source: https://www.iea.org/reports/world-energy-outlook-2017.

IIR, 2019. The role of refrigeration in Global Economy. 38th Informatory Note on Refrigeration Technologies.

Makhnatch, P., Khodabandeh, R., 2014. The role of environmental metrics (GWP, TEWI, LCCP) in the selection of low GWP refrigerant Energy Procedia 61, (2460–2463).

Rodrigue, J.P., Notteboom, T., 2020. The Cold Chain and its Logistics. The Geography of Transport Systems, fifth edition- New York: Routledge, 456 pages.

Tassou, S., De-Lille, G., Ge, Y.T., 2009. Food transport refrigeration. Approaches to reduce energy consumption and environmental impacts of road transport. Applied Thermal Engineering 29, (1467–1477).

Unido, 2010. Annual Report 2009 Industrial Development Board, thirty-seventh session Programme and Budget Committee,twenty-sixsession. Vienna

Chapter 2

State-of-the art

Nomenclature of Chapter 2

Abbreviations

AI	Artificial intelligence
ATP	Agreement on the International Carriage of Perishable Foodstuffs and on the Special Equipment to be Used for such Carriage
AUC	Area under the Roc curve
C.I.A.	Annual ageing coefficient
CE	Counterexamples
CFC	Chlorofluorocarbon
CPS	Cyber phiscal system
DBMS	Data base management system
EPAL	European Pallet Association
EPS	Expaned polystyrene
F_1	Weighted average of Precision and Recall
ERP	Enterprise resource planning
FD	Functional dependency
FN	Flase negative
FP	False positive
FPR	False positive rate
GRP	Glass reinforced plastic
HC	Hydrocarbon
HFC	Hydrofluorocarbure
HFO	Hydrofluoroolefin
IN	Normally insulated equipment
IoT	Internet of things
IR	Heavely insulated equipment
LIRIS	Laboratoire d'Informatique en Image et Systèmes d'Information
MAPE	Mean absolute percentage error
ML	Machine Learning
ODP	Ozone depletion potential
PCM	Phase change material
PU	Polyurethane foam

PVC	Polyvinyl chloride
QC	Quality coefficient
RFID	Radio-frequency identification
RMSE	Root-mean squared error
SQL	Structured query language
SVMs	Support vector machines
TMS	Tranport management system
TP	True positive
TPR	True positive rate
UNECE	United Nations Economic Commission for Europe
VIP	Vacuum insulation panel
XPS	Extruded polystyrene foam

Greek

Δ	Variation	
Δ	Thickness	[m]
λ.	Thermal conductivity,	[$W.m^{-1}.K^{-1}$]

Roman

A_{12}	Ageing coefficent	
A_t	Actual value	[same of A_t]
G_1	Proportion of counterexamples	
G_2	Proportion of tuples involved in counterexamples	
G_3	Size of the set of tuples in r to obtain a maximal new relation s satisfying $X \rightarrow Y$	
f	Mapping function	
K	Overall heat transfer coefficient	[$W.m^{-2}\ K^{-1}$]
k	Security coefficient	
k_1	Enlargment factor	
N	Number of year of the vehicle's life.	[years]
P	Power	[W]
P_t	Predicted value	[same of P_t]
$\dot{Q}$	Cooling power	[W]
r	Relation	

S	Mean surface area	[m^2]
T	Temperature	[K]
X	Domain of a function f	
Y	Codomain of the function f	

Subrscripts

12	12th year of the vehicle's life
ext	External
I	i-th
int	Internal
P	Prototype
N	n-th year of the vehicle's life
nom	Nominal
wall	Wall

2. State-of-the art

In refrigerated transport, the insulation of the enclosure is one of the basic elements of the refrigerated vehicle. First of all, insulation protects perishable food from temperature excursions and then plays a role for food safety, especially when there is a break in production of cold in the refrigerated vehicle. Moreover, reducing the need of refrigeration, it has also an environmental impact contributing to save energy. As a matter of fact, the cooling power to be produced to obtain the desired temperature inside the cargo primarily depends on the insulation efficiency, characterized by the so-called K coefficient value. This coefficient is a parameter increasing during the time due to the ageing of the enclosure's insulation and controlled as required by the ATP (the International Agreement for the Transport of Perishable Foodstuff). The ageing is a phenomenon depending on many factors. To understand it, it is necessary to start from the analysis of the materials and the technologies currently in use for the design and the construction of refrigerated transport vehicles to then analyze all the other factors due to the use of the vehicle. The techniques developed by engineers and manufacturers changed over the last 140 years to respond the evolution of refrigerated transport starting from the first cold rooms for boats, to rail insulated coaches that appeared at the beginning of the 20th century,finally to insulated trucks and trailers that appeared in the 1940s.

However, insulation techniques have faced and still face today economic, environmental and legal constraints such as the Kigali amendment or the European F-Gas regulation on F-Gas mitigation, that have an important impact both on insulated materials and construction techniques. Therefore, the construction designs, the used materials and technologies continue to adapt to face and prevent the ageing phenomena improving the insulation performance but also to meet the regulatory requirements and reduce the environmental impact.

This chapter has as main objectives:

- to introduce the fundamentals definitions for refrigerated transport and refrigerated vehicles and fundamental notions given by the ATP regulation;
- to review the evolution of insulated materials and technologies used for the design and construction of refrigerated transport vehicles, including those possible alternatives in the near and mid-term future ;
- to present a state-of-the-art review of the ageing of refrigerated transport vehicles, including those studies that tried to model this phenomenon;
- to introduce classical and fundamental tools for data science, especially those used in this thesis to study the ageing phenomenon through a data centric approach.

2.1 Fundamentals of refrigerated vehicles

This section aims at introducing all those fundamentals of refrigerated transport and logistics, used and mentioned in all parts of this manuscript. The various parts that make up a refrigerated vehicle are described and the most important notions defined by the regulations in force to distinguish these parts and test them are also provided.

2.1.1 Refrigerated transport and logistics

The “cold chain” refers to the various stages that a refrigerated product passes through, either until it is removed by a customer in a retail environment or unloaded from a delivery vehicle a few meters from its destination. From the moment a fruit or vegetable is harvested or an animal is slaughtered, the product starts to deteriorate. The deterioration of a product can be slowed by reducing the temperature at which it is transported and stored. As pointed out by Heap (2010), depending on the particular means of transport, the cold chain has to meet the following important requirements:

- speed: particularly important at the interfaces as well as in some intermediate stages of the chain, makes delivery possible with the least loss of shelf life;
- safety in product protection, including the maintaining of temperatures in the optimum range of each product;
- adaptability to quality-protection requirements, including for organoleptic qualities, freshness and appearance, which vary from one product to another.

Refrigerated transport is a fundamental link of the cold chain process and requires logistics. The linguistic roots of the word "logistics" come from the French term "Logis" which means the accommodation of the troops. Early in the 19th century, logistics was introduced and defined by the military as the planning and movement of troops (Bartodziej, 2017).

Amr et al. (2019) presented a historical background on logistics and supply chains highlighting how the different stages in the evolution of logistics coincided with the different industrial revolutions. From the 17th century to the present day, these authors identified four stages of logistics. Table 2.1 summarizes the time instants and the developments associated with each of these stages.

Table 2.1 The different stages in the evolution of logistic (Elkader et al., 2019) .

	Logistics 1.0	**Logistics 2.0**	**Logistics 3.0**	**Logistics 4.0**
Period of time	17th Century	1960	1968	2011
Associated development	Mechanizing the transportation	Cargo automation	Industrial robotic arm	Decentralization among different parties through digitalization

Logistics in the cold chain domain is considered as the art of coordinating and managing movement of products and information from the point of origin to the point of final destination (Panozzo et al., 1999) through the realization of a pre-established sequence of operations: packaging, preparation for transport, transport and intermediate handling and storage. These operations must be carried out continuously and refrigerated transport plays a a fundamental role in this process. However, to properly carry out the refrigerated transport several choices must be made also in the vehicle selection:

- the distance to be covered;

- the logistic scheme in which the vehicle is involved and the number of delivery points;
- the nature of the products to be transported and the temperature at which they must be maintained.

These topics are discussed in the next subparagraphs. The attention is focused on the fundamental concepts of logistics today in the field of the cold chain and to the digitalization process it has undergone through.

2.1.1.1 Refrigerated transport segments

The type of transport segment changes depending on the type of vehicle. As indicated in Table 2.2 it is possible to identify different types of segments depending on the total weight allowed in charge:

- long distance transport;
- urban , peri-urban and medium distances;
- short distance transport which may include: urban and peri-urban; and last kilometre delivery.

Table 2.2 Refrigerated transport segments.

Category	Total weight allowed in charge	Segment
Semi-trailers	≥ 29 tons	Suitable for all kind of distances deliveries but mainly used for long distance transport
Truck	between 3.5 and 29 tons	urban, peri-urban and medium distances
Light vehicles	≤ 3.5 tons	urban and peri-urban delivery
Small vehicles	≤2.7 tons	urban delivery – last kilometre

As pointed out by Heap (2010), long-distance transport includes that kind of transport from 300-500 km onwards without stopping for deliveries. In such type of transport because journeys are long and recharge facilities may be far apart, the vehicles must be reliable and supplied with some features such as: 2000 hours operating capability of refrigerating unit without need of maintenance, fuel reserve for at least a week, electric stand-by systems to ensure the continuity of the cold chain. Conversely "short-distance" transport identifies those journeys less than 300-500 km and for distribution journeys with several stops.

Once the transport segments have been clarified next subparagraph presents the logistic cold chain schemes in which the vehicles are inserted.

2.1.1.2 Logistic schemes in the cold chain

In the cold chain, various logistic schemes can be distinguished. These schemes have been described by Panozzo et al. (1999) and Casillo (2011) and are presented below.

The first scheme is the classical one (Figure 2.1). In this type of scheme there is a production point, a series of transports from the various production points to cold storage points, from which a new transport network branches off and ends in the distribution centres (supermarkets) for the sale, where the individual user picks up the product autonomously, thus creating the last link in the cold chain.

The general function of the cold store is to maintain the products delivered to a temperature value equal or lower than the regulatory temperature or the temperature prescribed by the manufacturer of the same product. Cold storages may have different forms:

- storage in production centers;
- storage in cold stores (public or private);
- storage at wholesalers' premises and in distribution platforms; and
- final stage storage at distributors (large and small); artisans or communities.

However, the first logistics scheme is completely irrational since, after the delivery, the vehicles follow the same route without load and this leads to a loss both in terms of optimization time and fuel consumption.

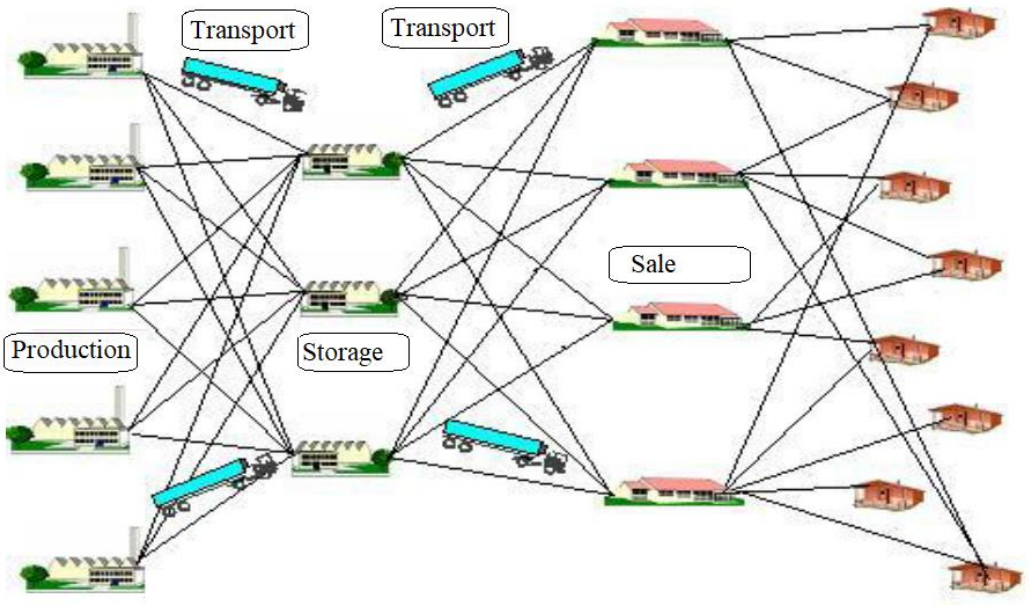

Figure 2.1 Classical logistic scheme (Casillo, 2011).

A first step to improve the classical scheme and make it more rational is to create a logistic scheme with concentrated warehouse (Figure 2.2), which provides for the presence of a few concentrated warehouses. This scheme allows reducing the route of each vehicle which was

forced, in the classical logistic scheme, to reach each warehouse individually. The introduction on the market of the multi-temperature vehicle (Figure 2.3) for the transport of product needing different temperatures, allowed the development of a third logistic scheme: the circular logistic (Figure 2.3). This kind of vehicle was introduced in the market between the 80s and 90s to take into account the needs of distribution and optimising deliveries, particularly in supermarkets and hypermarkets. These vehicles are able to maintain several compartments of the same vehicle at different temperatures: - 20°C for frozen products, + 2°C for fresh dairy or meat products and + 8°C for vegetables, for example. More recently, their use has been extended to the simultaneous transport of health products: blood products at - 25°C, fresh products at + 5°C and the so-called ambient temperature, e.g. + 22°C (Cavalier, 2010). Most multi-temperature vehicles are composed of 2 to 3 compartments and are equipped with a removable bulkhead that allows different configurations. Today, almost one out of four vehicles of the French fleet, is multi-temperature. The logistics scheme with multi-temperature vehicles involves a network in which the multi-temperature vehicle makes circular routes by picking and unloading cyclically and being always loaded, thus eliminating the dead times of return without load, typical of the classic scheme. This supposes that the vehicles are supported by a system that regulates their routes, which may vary according to the need.

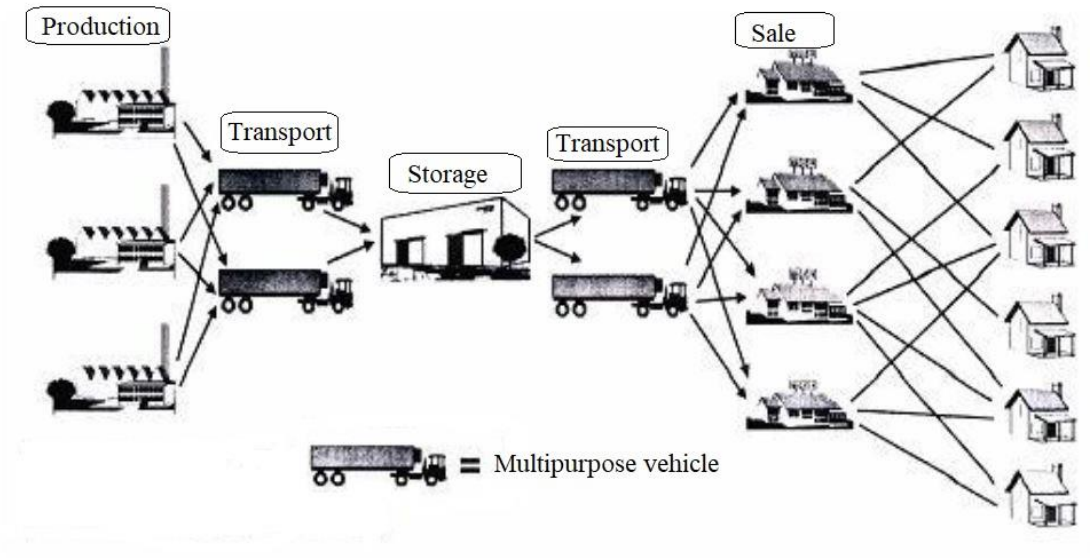

Figure 2.2 Centralized warehouse logistic scheme (Panozzo et al., 1999).

Figure 2.3 Multi-temperature vehicles (Cavalier 2010).

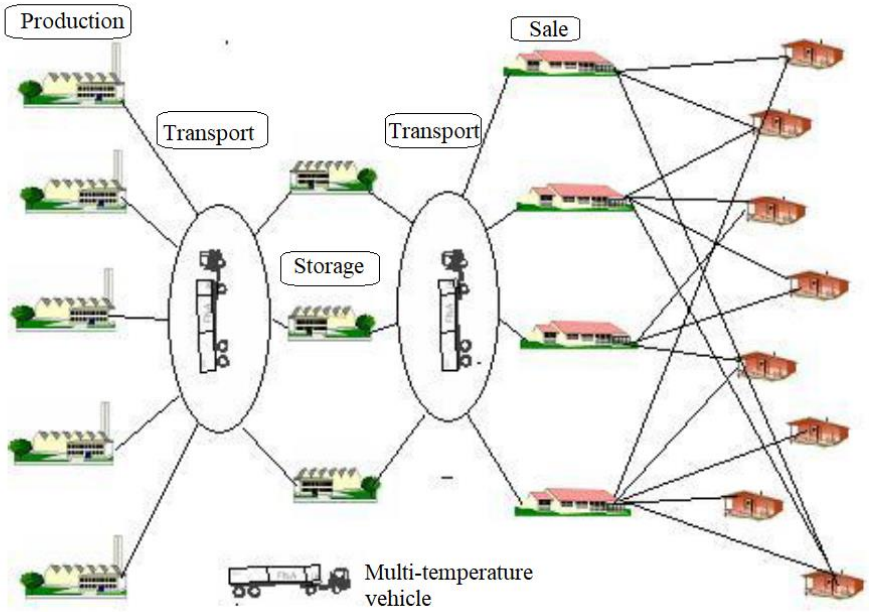

Figure 2.4 Circular logistic scheme (Casillo, 2011).

Another logistic scheme is the one that foresees the use of the mini-container . A mini container (Figure 2.5) is an insulated enclosure whose external dimensions, presented in Figure 2.6, are generally the same as those of a pallet. The concept of logistic with mini-containers is to have self-sufficient insulated containers, thus breaking the need for direct communication between vehicle and warehouse. The mini containers in fact, being self-sufficient, can be left out of the warehouse even for several hours. From a security point of view this logic is particularly safe, because it guarantees that there is no interruption in the cold chain between producer and

consumer. The use of small insulated mini-containers for refrigerated transport has strongly increased during the last ten years. Commonly used for the transport of food samples for a while, they are now used for transportation and distribution at an industrial level.

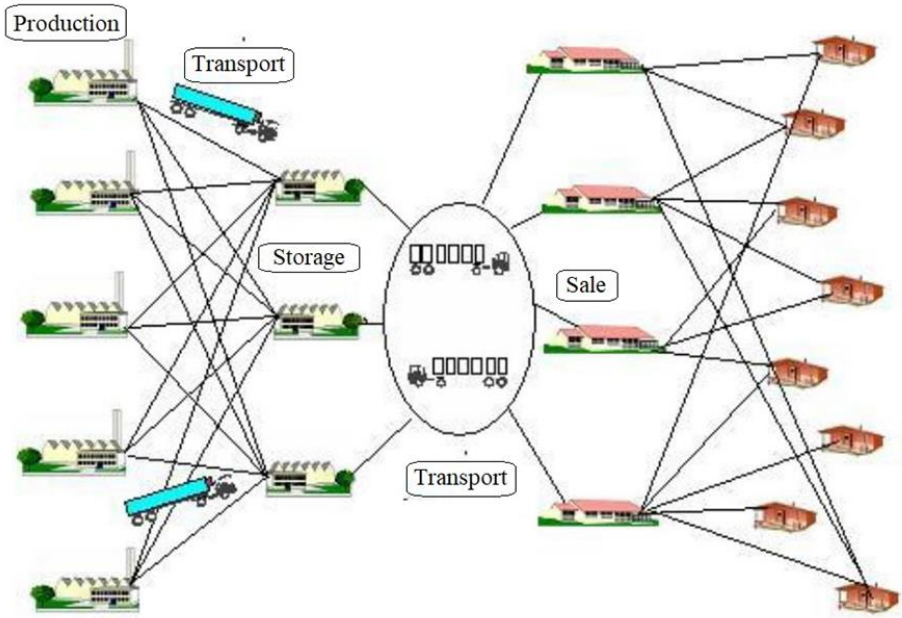

Figure 2.5 Logistic scheme with mini-container (Casillo, 2011).

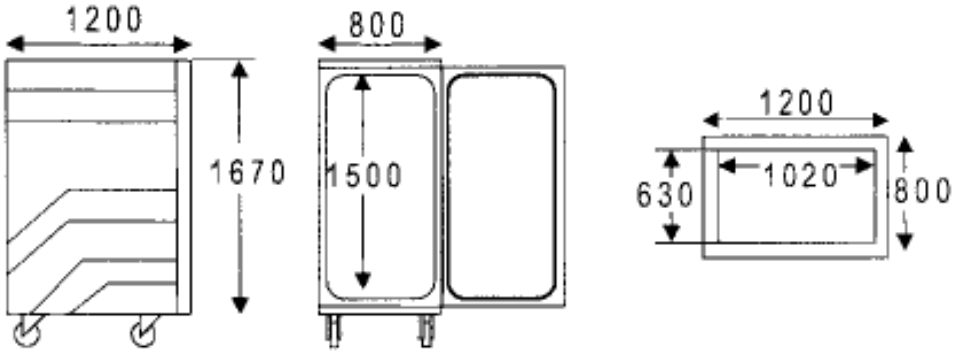

Figure 2.6 Dimension of mini-containers (Panozzo et al., 1999).

However, the most significant trend in recent years is the development of e-commerce. This development has led to an increase in demand for door-to door distribution of small packages.

This is a huge market, which has been growing rapidly for the last 10 years and which is expected to remain very dynamic, with sales expected to increase by 70 % between 2018 and 2021 (see Figure 2.7).

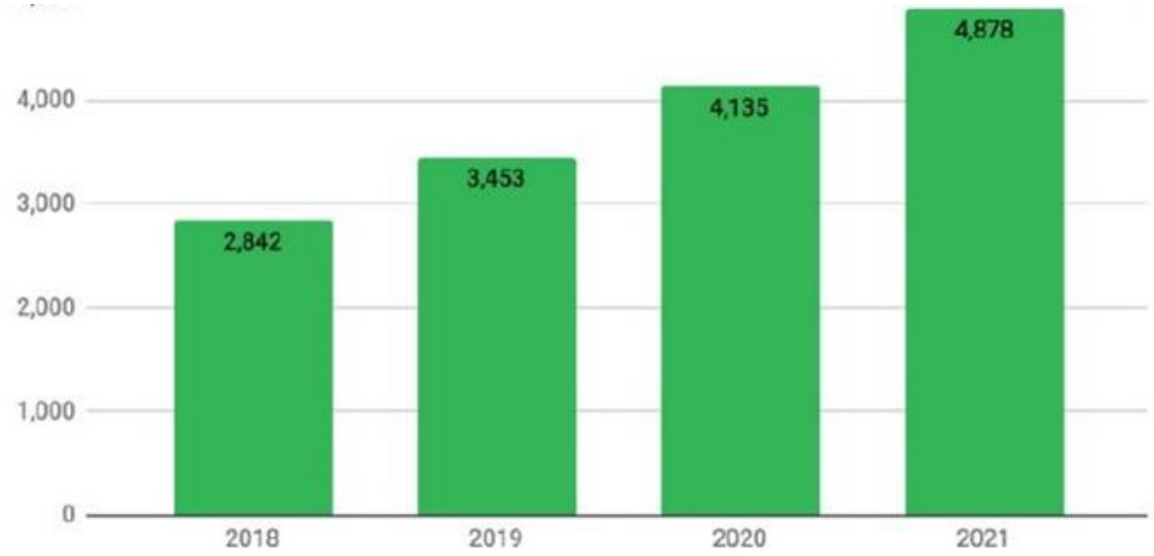

Figure 2.7 Forecast retail e-commerce sales (billions USD) between 2018 and 2021(Statista , online resource).

As documented in a recent Cemafroid study (Fertell and Cavalier, 2020) according to Les Echos (2019), food e-commerce is no longer a niche. Already in mid-2018, the Nielsen Institute made France the European champion in this consumption mode with 6.6 % of daily purchases made online. This is more than in the United Kingdom (6.3 %) and far more than in Germany (0.7 %) and the United States (4.7 %). China points to the trend where, according to Kantar, 10 percent of household baskets are being filled online. In the country of Alibaba and JD.com, growth is 30 % per year. South Korea already has a 20 % market share for this practice. As Figure 2.8 shows, France is just behind the United States in terms of the percentage of consumers delivered by a major distributor at least once a week.

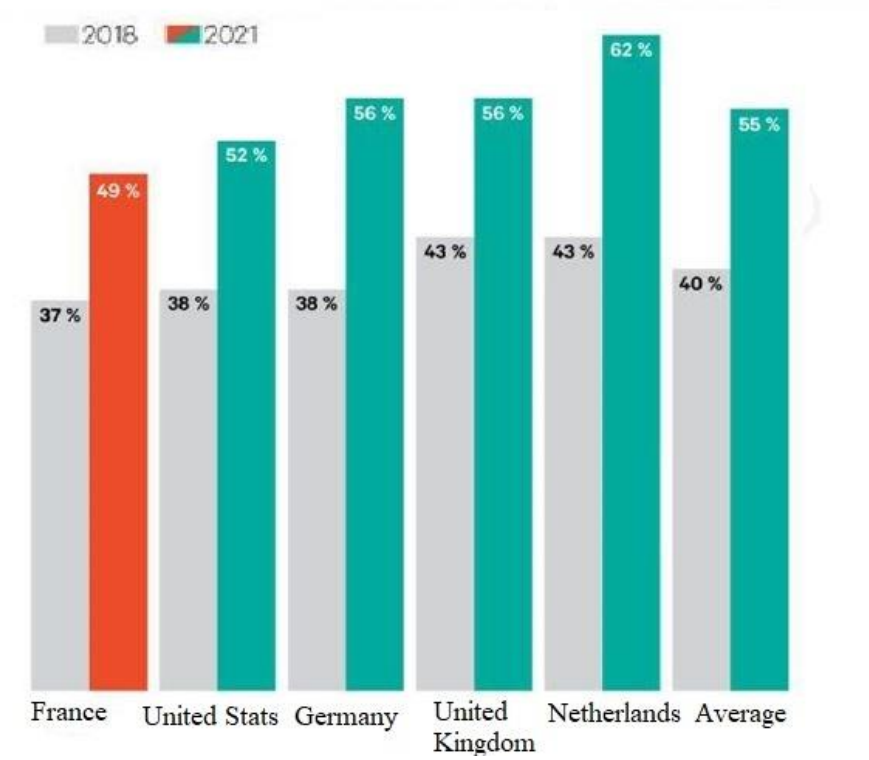

Figure 2.8 Number of consumers delivered by an e-merchant at least once a week (Statista, online resource).

The door-to-door distribution scheme, as shown in Figure 2.9, follows the classic pattern between the production and storage warehouses. From the storage phase, a series of small trucks are involved in the door-to-door distribution, completely skipping the market phase which is the most critical part of logistics. Eliminating the market phase, the weak link in the cold chain, may provide a greater guarantee of safety and quality of perishable products.

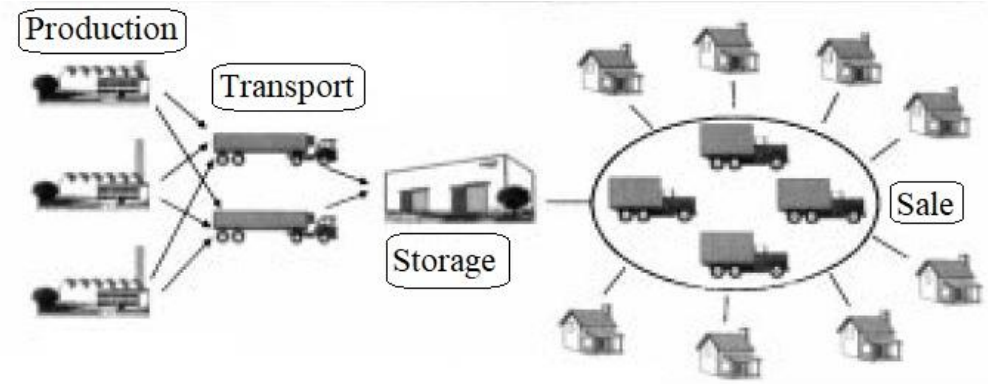

Figure 2.9 Door-to-door distribution (Panozzo et al., 1999).

The use of the different types of vehicles varies according to the needs and to the type of transported products, fitting more or less well into the different logistic schemes. Types of transported products are introduced below but first another aspect of logistics is tackled: its digitization thanks to the advent of technology and artificial intelligence. This digitalization process has given birth to what is called logistics 4.0.

2.1.1.3 Logistics 4.0

The progress and advancement of new technologies has pushed traditional logistics to experience a sort of upgrade: hence the concept of logistics 4.0. This upgrade was made possible through a deep process of digitization - the famous digital transformation - which affected and concerns the entire supply chain. Companies have begun to embrace a new organizational model that revolves around innovation and intelligent use of new technologies.

Logistics 4.0 consists of smart products and services that are initiated by the need for highly individualized services and products. As pointed out by Barreto et al. (2017), logistics 4.0 refers to incorporating the current concept of logistics with the innovations and applications added by Cyber Physical Systems (CPS). These latter are defined as those systems, that directly link real (physical) objects and processes with information processing (virtual) objects and processes via open, partially global and always interconnected information networks (Bartodziej, 2017).

The logistic schemes remain unchanged, but those technological systems and telematics solutions are integrated into them, opening a window into the real-time operations of the fleet and providing critical visibility of temperature sensitive cargo and their refrigeration equipment over the road. Some examples of technological systems and telematics solutions integrated in the logistics are presented as follows.

- Corporate computer systems from which structured and semi-structured data is derived (such as Enterprise Resource Planning (ERP)).
- Sensors and geolocation technologies including radio-frequency identification (RFID) (see Figure 2.10) and Internet of Things (IoT) freight tracking and tracing systems, systems able to connect devices, objects, and machines to the internet. Both these kind of systems can track merchandise during transport phases and provides complete temperature traceability with geolocation. For more information on RIFD in the cold chain see Flores and Tunner (2008).
- Transportation Management Systems (TMS) for transport fleet management which are specialized software for planning, executing and optimizing the shipment.
- Integration of temperature and reefer alarms, door status and fuel level notifications help fleet managers monitor unauthorized or extended usage of their refrigerated trailers as well as manage fuel usage and costs.
- Analyzing data over the time with the use of learning machine systems: this solution combines data from sensor, supply chain logistics, weather, traffic, and more and applies machine learning to detect repeatable patterns that managers can use to predict transit times and delays under a variety of circumstances. In this way it is possible to optimize routes and schedules to reduce travel time, plan cross-dock plans with fewer disconnects and manage which drivers provide the best results by route, season, and time of day.

- Blockchain, a technology that is mostly associated with cryptocurrencies, especially Bitcoin. It has many potential applications, which are just beginning to be explored. Blockchain is merely a digital ledger that cannot be altered. It can improve the speed of transaction execution and validation across multiple parties. These include digitally validating a transaction that has occurred between two entities and rendering it irrefutable. One application in the cold chain includes the possibility of recording that each temperature at each step in the chain. Another application that is mentioned in the literature is in international logistics by replacing a mostly paper process.

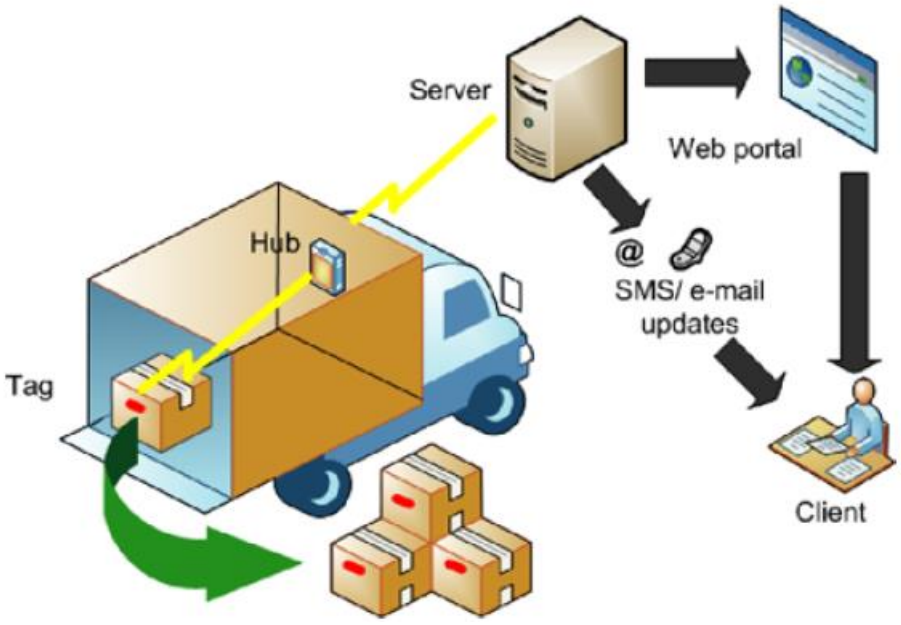

Figure 2.10 Conceptualization of a system based on the RFID for tracking cargo temperature and that of the air in a refrigerated transport system (Flores and Tunner, 2008).

Modern logistics is dynamic and constantly in evolution. The transformation affects everyone: people, warehouse, structures and software. Modern companies must be able to combine the needs of consumers, who expect immediate availability of products, with the complexities of physical management of goods. This is a delicate challenge, as it is necessary to be able to bring these two aspects together without generating confusion and extra costs for companies.

After this review on the development of logistics, the next subparagraph deals with the concerned transported products.

2.1.1.4 Types of transported products

The difference in the use of vehicles in the cold chain starts with the type of transported products (Cavalier, 2010). Perishable food products remain the most transported at a controlled temperature. ATP prescribes the types of perishable food to be transported under controlled temperature conditions and the temperatures at which refrigerated and refrigerated transport must be carried out. The perishable foodstuffs intended for human consumption to be transported under ATP controlled temperature regime are indicated in Table 2.3 with the associated temperatures. As shown in this Table, ATP does not take into account certain products which would otherwise require to be transported at a temperature-controlled condition due to their sensitivity. For instance, the ready-to-eat prepared raw vegetables and vegetable products category, indicated in the ATP list, only include raw vegetables which have been sliced or otherwise reduced in their size but exclude those vegetables which have only been washed, peeled or simply cut in half. Some delegations at the Geneva Working Party on the Transport of Perishable Foodstuffs propose from many years to introduce fruit and vegetables in the ATP list of perishable foodstuffs. The proposal has not been yet accepted, because quality of fruits and vegetables becomes critical much earlier than safety, and therefore unsafe food is usually discarded by people. However, the impact of a bad transport in terms of cost is not negligible, because of the high added value of such goods (Panozzo and Cortella, 2006). However, refrigerated transport does not only concern food and develops towards other uses. Vaccines, medicinal products for human and animal use, samples for laboratory diagnosis and labile blood products are some examples of these sensitive products which need to be maintained at a controlled temperature during transport (Cavalier, 2016). Figure 2.11 shows some trucks involved in medical and health products refrigerated transport. Refrigerated transport is growing for so-called ambient products (+ 15 °C / + 25 °C) which represent very large volumes of drugs, but also and above all for biotechnological products (+ 2 °C / + 8 °C) that represent extremely important values (Cavalier, 2010).

Figure 2.11 Transport and delivery of temperature-controlled medical and health products in refrigerated trucks (Cavalier, 2010).

Table 2.3 ATP list of perishable foodstuffs.

Chilled Foodstuff	
Product	**T (°C)**
Raw milk	+ 6 °C
Red meat and large game (other than red offal)	+ 7°C
- Meat products (except for products fully treated by salting, smoking, drying or sterilization), - pasteurized milk, butter, fresh dairy products , i.e., yoghurt, kefir, cream and fresh cheese (non-ripened and non-matured cheese which is ready for consumption shortly after manufacturing and which has a limited conservation period.), - ready cooked foodstuffs (meat, fish, vegetables), - ready to eat prepared raw vegetables and vegetable products, - concentrated fruit juice and fish products not listed below	Either at + 6 °C or at temperature indicated on the label and/or on the transport documents
Game (other than large game), poultry and rabbits	+ 4°C
Red offal	+ 3°C
Minced meat	Either at + 2°C or at temperature indicated on the label and/or on the transport documents
Untreated fish, mollusks and crustaceans (except for live fish, live mollusks and live crustaceans)	On melting ice or at temperature of melting ice
Frozen and quick frozen perishable foodstuffs	
Ice cream	- 20 °C
Frozen or quick (deep)-frozen fish, fish products, molluscs and crustaceans and all other quick (deep)-frozen foodstuffs	- 18°C
All other frozen foodstuffs (except butter)	- 12 °C
Butter	- 10°C

Derens et al. (2004) presented the residence times and the corresponding temperatures values of chilled products involved in real logistic circuits. These values are the results of study carried out by Ceamagref between 2001 and 2002, during which 400 temperature probes were placed on products such as yogurts, pre-packed meat, catering products and delicatessen. In this way the products were followed from the storage warehouses to the domestic refrigerators. As a result, it was possible to estimate the residence time of these products in each link of the chain as well as

the associated temperature values. The average and maximum residence times of these products in each link of the cold chain are presented in Table 2.4. The corresponding measured temperature values of these products in the same link of the chain are summarised in the Table 2.5.

Table 2.4 Average and maximum residence times of different products in each link of the chain (Derens et al., 2004).

	Fresh dairy products		Catering products and delicatessen		Pre-packed meat	
	Average time	**Maximum time**	**Average time**	**Maximum time**	**Average time**	**Maximum time**
Warehouses	3 days	8 days	6 and half days	12 and half days	/	/
Wholesale platforms	2 days	10 days	1 day	7 days	9 hours	4 days
Refrigerated transport	6 hours	2 days	6 hours	21 hours	5 hours	22 hours
Refrigerated display cabinet	4 days	21 days	5 days	18 days	4 days	13 days
Transport after sale	1 hour	7 hours	1 hour	13 hours	1 hour	6 hours
Domestic refrigerators	3 days	26 days	4 days	23 days	3 days	15 days

Table 2.5 Average and maximum temperature values of products in each link of the chain (Derens et al., 2004).

	Fresh dairy products		Catering products and delicatessen		Pre-packed meat	
	Average T (°C)	**Maximum T (°C)**	**Average T (°C)**	**Maximum T(°C)**	**Average T (°C)**	**Maximum T(°C)**
Warehouses	3.7	6.5	2.4	3.7		
Wholesale platforms	3.9	6.7	3.5	5.5	1.5	5
Refrigerated transport	4	8	3.3	7	1.8	6.4
Refrigerated display cabinet	4.2	9.8	3.1	10.2	3.4	7.7
Transport after sale	7.2	18	8.6	10.4	7.1	15.2
Domestic refrigerators	6.1	12.5	5.7	13.8	6	10.8

Perishables products typically undergo several handling transfers by the time they reach the final destination. Many of these products, in particular fresh fruits and vegetables, dairy products and meats, are susceptible to damage during handling. Additionally, labor availability and wages

continue to increase. For these reasons, perishables are increasingly being unitized prior to and/or during shipping. Unitizing is the process of combining individually packaged products into a larger, stable unit load convenient for handling, shipping, and storage (Laundrie, 1986). The materials used in this respect are, for example standardized pallets. The used base dimensions in Europe are 800 mm wide by 1200 mm long for a maximum weight of 30 kg, as specified as specified by the European Pallet Association (EPAL). Pallets must be fabricated out of a material of sufficient strength to minimize shifting or compression of the palletized product. Hardwood pallets are most common, although plastic and compressed pulp pallets are also utilized. An example of Euro-pallet is shown in Figure 2.12.

Figure 2.12 Euro-pallet (European Pallet Association (EPAL)).

2.1.2 Description of a refrigerated vehicle

A refrigerated vehicle used in the cold chain is characterized by the presence some fundamental components (Figure 2.13) of which the most important are:

- the insulated enclosure;
- the refrigeration system.

In addition, a refrigerated vehicle is completed by the following elements:

- an air circulation equipment;
- some accessories inside the enclosure;
- doors, which may be of different kinds.

These components are described in the next subparagraphs.

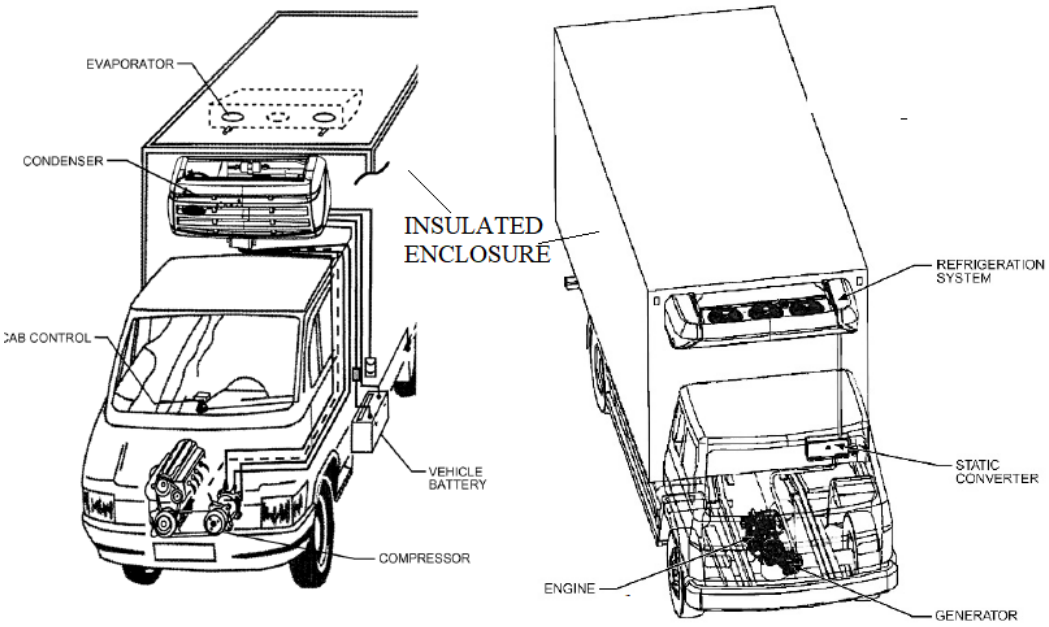

Figure 2.13 Components of a refrigerated vehicle.

2.1.2.1 Thermal insulated enclosure

Thermal insulation is the basis of refrigerated transport vehicles. First of all, because its main role is to limit the thermal load so that the refrigeration unit can always keep the required temperature: this is the key to reduce emissions related to the refrigeration unit. Additionaly, in case of a failure of the thermal device, it provides the time needed to get to a point of unloading without losing the merchandise and secondly because it limits temperature fluctuations and facilitates the regulation and homogeneity within the enclosure (Cavalier, 2010).

Insulating quality is measurable, and the industry standard is the K coefficient, as defined by the ATP Regulation. The lower the K factor, the better the insulation.

At the end of 2019, more than 95 % of the French fleet of temperature-controlled transport vehicles is classified as reinforced isothermal under the ATP or "R", i.e. with an overall heat transmission coefficient $K < 0.40$ W.m^{-2}.K^{-1}. Figure 2.14 gives the distribution of isothermal levels (K coefficient) of the equipment of the French fleet. It shows that currently only 3% of the fleet has an ATP isothermal rating of less than 0.30 W.m^{-2}.K^{-1}, whereas 57 % of the vehicles have an isothermal rating of between 0.36 and 0.40 W.m^{-2}.K^{-1}.

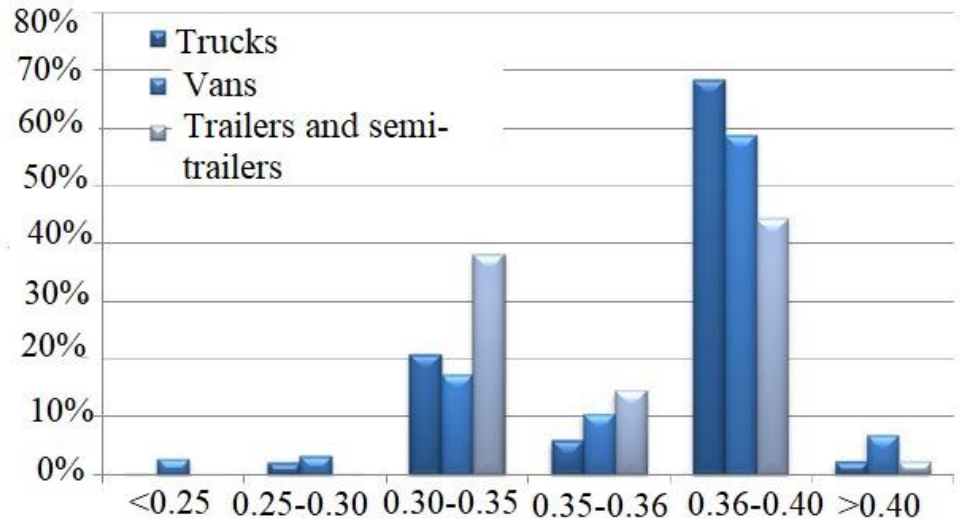

Figure 2.14 Thermal insulation performance of the French fleet at the end of 2019 for the entire fleet by type of vehicle (Source: DATAFRIG© - Cemafroid, 2020).

The insulation normally consists of expanded foam insulation sandwiched between two external skins. Each skin consists of a few millimetres of plywood covered with a glass reinforced polyester, steel or aluminium skin. The most popular insulation is expanded polyurethane (PU) foam with cyclopentane as the blowing agent. This construction achieves a thermal conductivity in the region of 0.025 W. m^{-1} K^{-1}. In side walls the thickness is constrained by the maximum permissible insulated vehicle width of 2.60 m and euro pallet dimensions this construction can accommodate 2 euro pallets side by side but insulation thickness is limited to 45-50 mm. Roofs and floors often have 100 mm or more insulation. This aspect, relating to insulation of the vehicle and the technologies used, is discussed in more detail in paragraph 2.2.

2.1.2.2 The refrigerating unit

Transport refrigeration units are designed to maintain the desired temperatures inside the vehicle. In a refrigerated transport unit, a temperature differential exists between the air entering the refrigeration unit, (i.e., the return air), and the air exiting the unit, (i.e., the supply air). This temperature differential continues into the cargo space, creating microenvironments within the cargo and the air surrounding the cargo. Microenvironments represent distinct and unique environments within the cargo space of the refrigerated container, trailer, truck, railcar, or air container. Controlling, modifying, and monitoring the characteristics of microenvironments inside insulated boxes are critical to maximizing the shelf life of the perishable cargo and optimizing the wholesomeness, safety and quality of food. A transport refrigeration system must have sufficient cooling capacity to remove the heat generated from all sources. Heat transfer into an insulated transport box is augmented by differences between outside and inside air temperatures, surface area of the insulated box, colour of exterior finishes, amount and effectiveness of insulation (*K* values) in walls, ceilings, floors, and doors, excessive air leakage into the insulated box caused by poor door seals and wall damage, and warm air infiltration when doors are opened and/or when the fresh air exchange vent setting is excessive.

Nowadays, the most common refrigeration system in use in refrigerated food transport applications today with more than 95 % of the market is the vapour-compression system with blown evaporators powered by either a diesel engine for so-called 'autonomous' systems or by the engine of the vehicle for so-called 'non-autonomous' systems.

According to Datafrig® data at the end of 2019 90% of refrigerated vehicles of the French fleet are equipped of such refrigeration system and only 3 % have eutectic devices composed of plates and tubes and very few are refrigerated by liquid cryogenic systems The 7 % remain of the fleet is made up of insulated equipment without refrigerating unit (Figure 2.15).

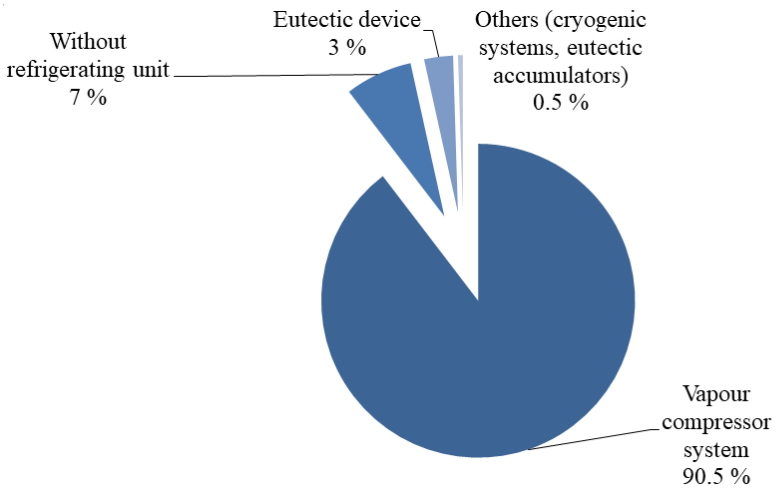

Figure 2.15 Distribution of the refrigeration units in the French fleet, 2019 (Cemafroid, 2020).

Refrigeration units shall have a power that allows compensating the thermal losses from the insulated enclosure body, those that are due to door openings as well as those due to the arrangement of the products and all other types f thermal losses that do not strictly depend on door openings. Concerning the thermal losses from the insulated enclosure, ATP Standard stipulates that the refrigeration unit must have a heat extraction of at least 1.75 the heat transfer through the walls in a 30°C ambient temperature. However, the mean refrigeration power depends on the size of the equipment and as shown in Figure 2.16, for refrigerated vehicles may vary between 500 W and 25 kW.

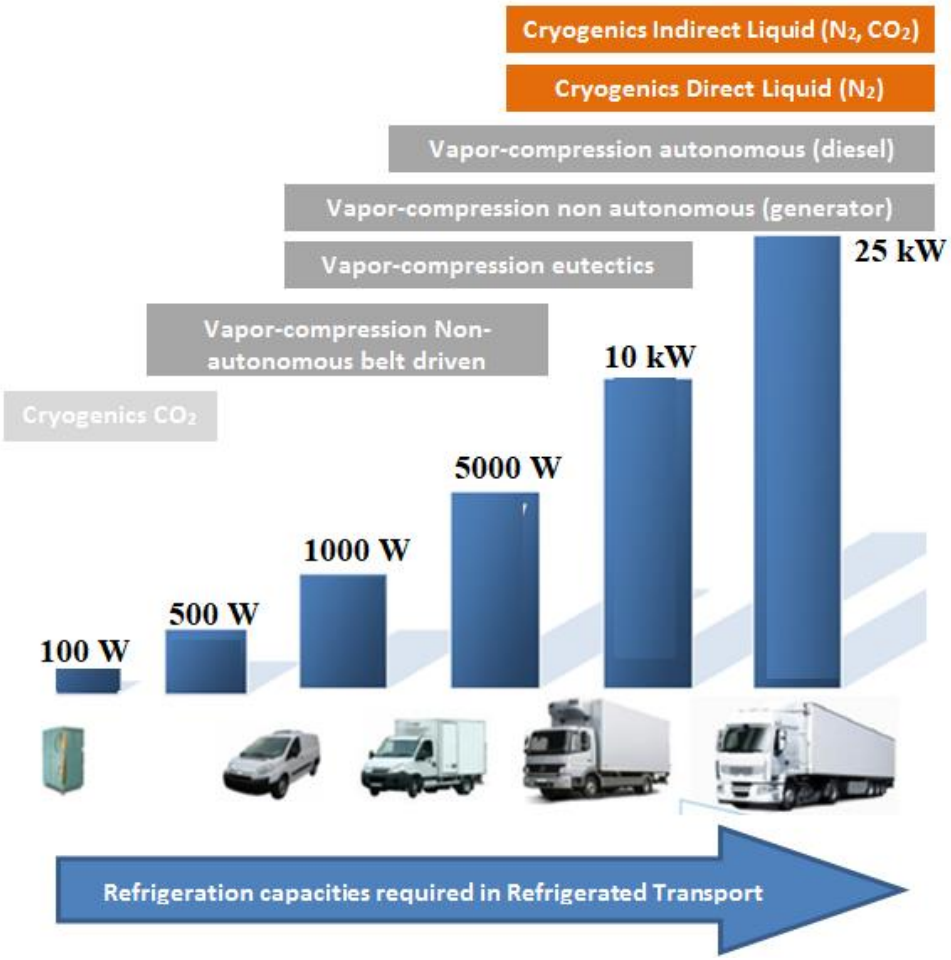

Figure 2.16 Average value of refrigeration power as a function of the equipment size (Cemafroid, 2020).

Refrigeration unit can be independent or non-independent and a wide range of options for compressor drive methods exists, depending on several criteria: duty required, weight, installation cost, environmental consideration and fuel taxation (Tassou et al., 2009).

In 2019, the French fleet is almost equally divided in independent and non-independent units. Different kind of independent and non-independent systems with their working principle are introduced below (Tassou et al., 2009).

- Independent diesel engine: this system has an engine built into the refrigeration unit, which drives the compressor with an integral or remote evaporator. This type of system is used in semi-trailers and it is able to operate while vehicle is parked through an electric stand-by. Its main disadvantage is to be heavy and noisy with additional maintenance requirements.

- Alternator unit: this system is a non-independent one. It has a compact size and a reduced weight and is characterized by the use of an alternator driven by a belt from the main traction engine which makes available the power to drive the electric motor placed in the refrigeration unit. Suitable vehicles for this system are semi-trailers

- Direct belt drive: this type of non-independent system is used mainly in van sized vehicles. The compressor of the refrigeration system is driven directly from the vehicle engine through a belt.

The major components of a vapour compressor refrigeration unit are its power source, a condenser, an evaporator, a compressor and an expansion valve, whose schematization is shown in Figure 2.17. The working fluid of the system, called refrigerant, cyclically crossing the various components of the system realizes the thermodynamic transformations that make up the refrigeration cycle and allow the fluid to transfer heat from a low temperature system (the inside of the case) to the external environment, through two heat exchangers called condenser and evaporator so named for the transformations that take place inside them, respectively the condensation and evaporation of the refrigerant. This transfer is possible, according to the second Law of Thermodynamics, by supplying energy to the fluid in the form of compression work through the compressor. In the expansion valve, instead, the fluid undergoes an expansion transformation, reducing its pressure and temperature and is ready to enter the evaporator. All components must withstand shock and vibration as well as extreme temperatures. Figure 2.17 shows the schematic diagram of a vapour compressor system run with an independent diesel engine.

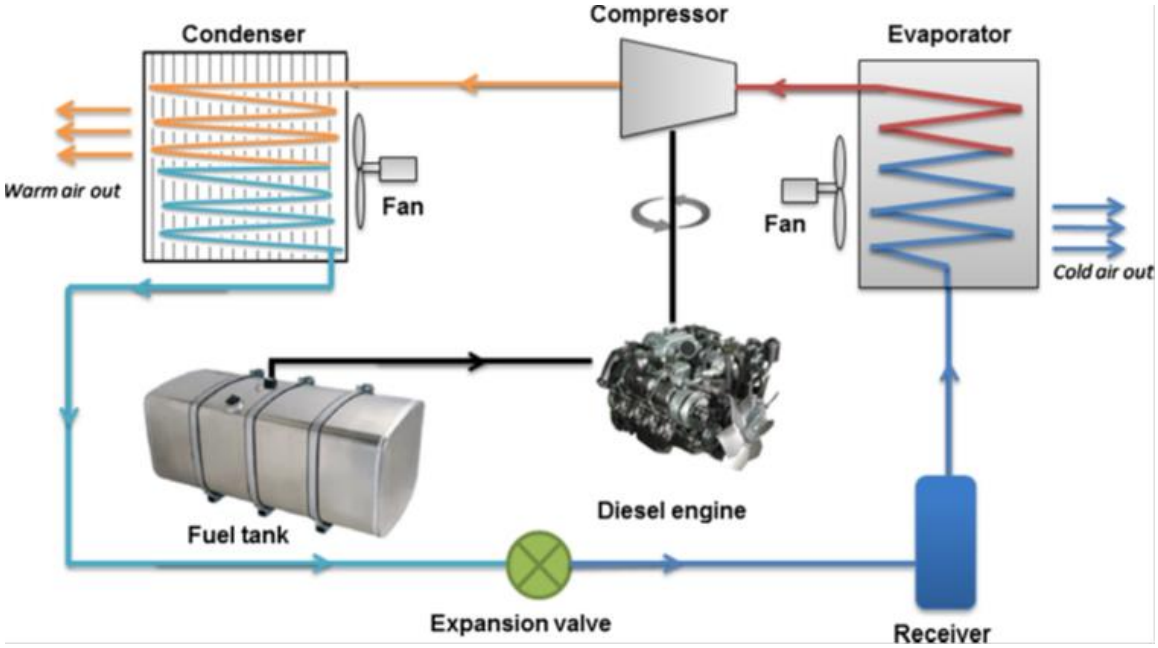

Figure 2.17 Vapour compressor system run with an independent diesel engine (Rai and Tassou, 2017).

In refrigerated transport it is possible to identify two different kind of refrigerating units' architectures:.

- the monobloc architecture and,
- the split one.

Depending on the architecture, performances may vary. The first one, the monobloc architecture (shown in Figure 2.18a and 2.18b), provides a cabinet which encloses the refrigeration circuit, the compressor and the fan. This cabinet is installed through a protrusion realized on the entire front side wall of the vehicle. The wall may have a reduced insulating performance, because of this perforation. The second one, the split system (Figure 2.18c), is characterized by an internal unit

and an external one connected through the passage of two pipes in the wall. It requires only the realization of holes for the passage of the pipes.

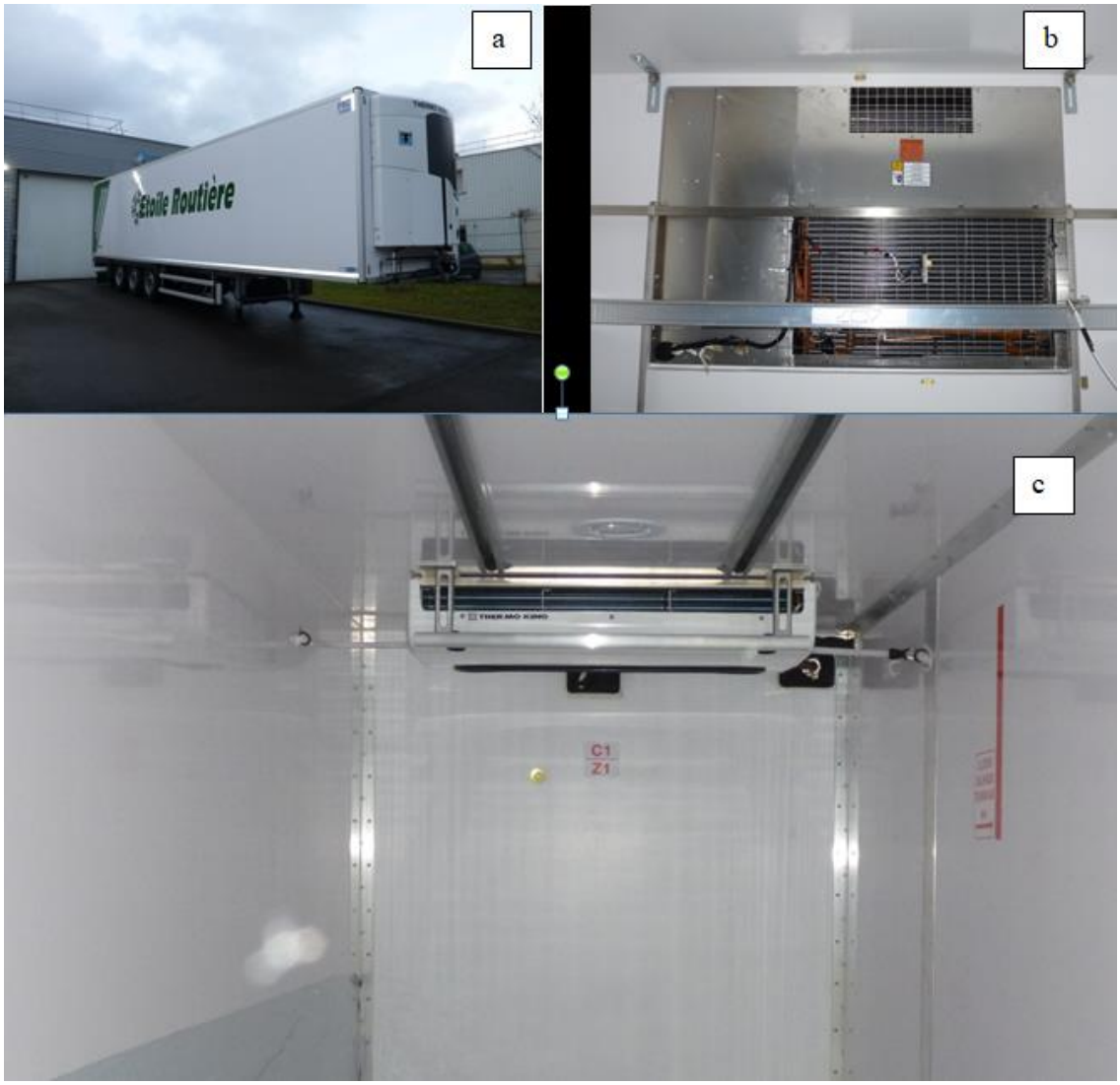

Figure 2.18 a) Monobloc architecture of a refrigerating unit, view from the outside; b) monobloc architecture of a refrigerating unit, view from the inside; c) split architecture of a refrigerating unit, view from inside.

2.1.2.3 Air circulation system

Air circulation is one of the most important factors in protecting refrigerated loads of perishable foods. Inadequate air distribution is probably the principal cause of improper cargo refrigeration during transport. Maintaining the cargo at the appropriate temperature is indispensable to assure quality, safety and preserve the shelf life of the perishable products. When designing an air circulation system, particular care should be taken with regard to the choice of the floor and to the accuracy of the products loading. Both may have an influence on the air circulation inside the vehicle. The most common types of floors found in refrigerated semi-trailers are flat floors (without any channels), duct board floors, duct-T floors, and T bar floors .

The latter, shown in Figure 2.19, provides more return air passage than any other design but it is more susceptible to forklift during loading and unloading operations. The temperature uniformity can be maintained around the load only if the floor of the trailer or container is completely covered with produce on pallets or in boxes the floor. By totally covering the floor, refrigerated air is forced up through and round the packages (Vigneault et al., 2009).

Two major methods for circulating air in refrigerated vehicles exist:

- top-air delivery system;
- bottom air-delivery system.

The top-air delivery system is the conventional one for refrigerated vehicles since the second system has been employed mainly in seagoing van containers for several decades. Top air delivery system is presented in Figure 2.20. In this kind of system, the air circulation starts with the air travelling above the load from the front to the rear part of the trailer. Some of the air flows downwards, lapping the sidewalls and passing through the load. When the air flow coming from above reaches the rear of the trailer it moves down passing through the space created between the door and load. Finally it passes through the space between the load and the floor of the trailer which acts as a plenum for return the air to the evaporator.

Figure 2.19 Interior view of a refrigerated container showing 'T' bar floor.

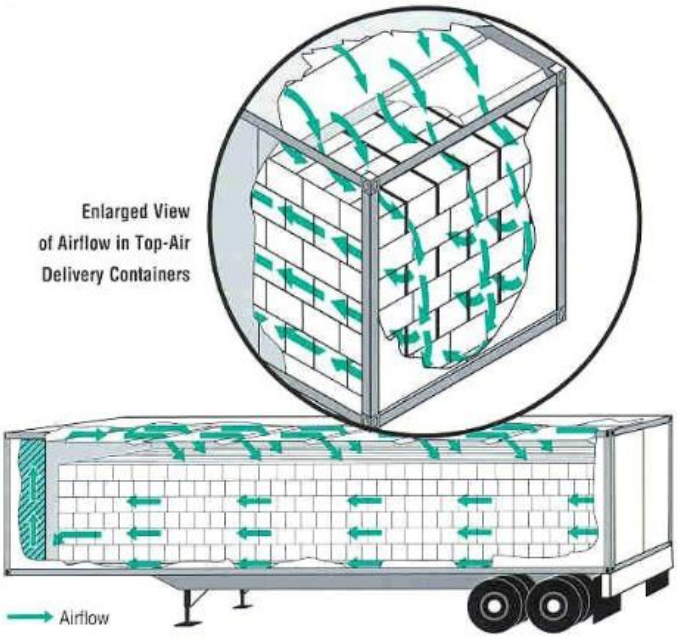

Figure 2.20 Top air delivery system (Brecht et al., 2019).

Studies carried out in the 1960s and 1970s led to the implementation of the place of device facilitating air circulation in the boxes. The air delivery ducts (Figure 2.21) conventionally fixed to the ceiling to distribute the flow from the evaporator to one-third and two-thirds of the body have been widespread. Open lashing rails (Figure 2.22a and Figure 2.22b) are also used not only for stowing the transported goods but also to create air recirculation inside the enclosure of the vehicle.

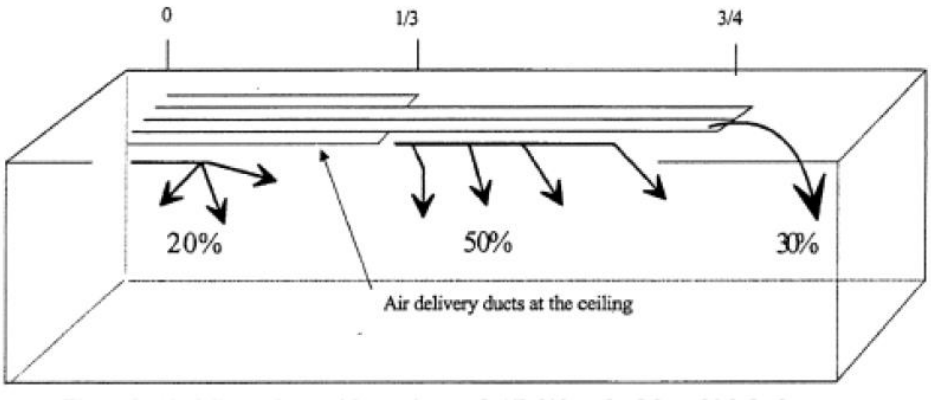

Figure 2.21 Air delivery ducts at 0, 1/3, ¾ length of the body of the vehicle (Cavalier, 2010).

Moureh at al. (2002), Moureh and Flick (2004), Moureh et at al. (2007) carried out a study with the aim of improving the air distribution systems inside the refrigerated vehicles. Authors experimentally and numerically assessed and characterized the airflow pattern inside a typical refrigerated vehicle loaded with pallets using a scale model (1:3:3) of semi-trailer. Two different

configurations, i.e., with and without air duct systems were analysed by the authors, which concluded that the presence of air-ducts systems:

- improves the overall homogeneity of the ventilation inside the vehicle;
- avoids the occurrence of stagnant zones;
- maintains the air velocities value in the rear part of the load at around 1 $m.s^{-1}$ instead of 0.1 $m.s^{-1}$, in case of air duct system absence.

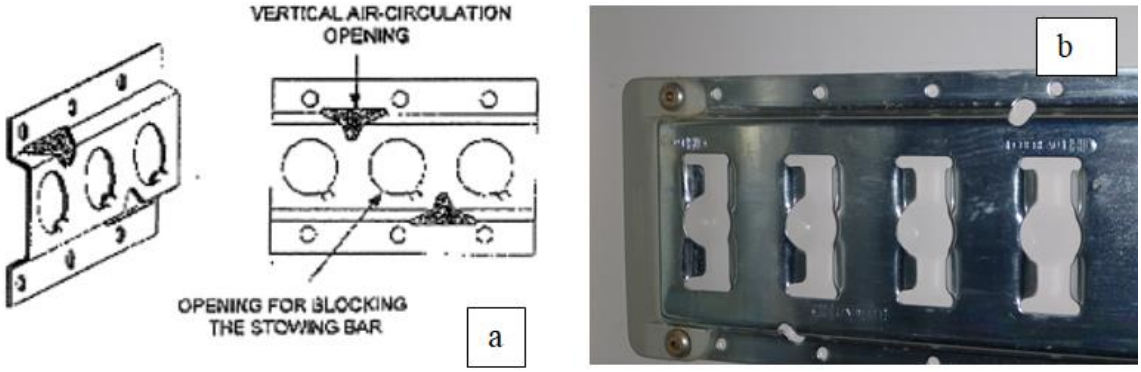

Figure 2.22 a) Scheme of lashing rails (Cavalier, 2010); b) example of lashing rails inside a truck.

2.1.2.4 Accessories

Depending on the type of realized transport, inside the vehicle there may be different accessories and special features, such as:

- rails for suspending products and plinths on the lateral walls (Figure 2.23),
- shelves (Figure 2.24),
- recessed and surface lighting (Figure 2.25a and Figure 2.25b).

These accessories, although useful, represent thermal bridges and can have an impact on the insulation performance. For example, the rails are very often installed in vehicles used for meat transport. Transport with hanging carcasses is very burdensome for the structure, as the rocking of the hanging carcasses itself causes dynamic and fatigue stress on the insulated enclosure in the direction of travel in acceleration or braking and laterally during curves.

Figure 2.23 Meat rails and plinths inside of a refrigerated vehicle.

Figure 2.24 Shelves inside of a refrigerated van.

Figure 2.25 Example of lightings inside of a refrigerated vehicle: a) recessed lighting; b) surface lighting

2.1.2.5 Type of doors and doors openings

The insulating performance of refrigerated vehicles is based not only on the thermal qualities of the walls and their assembly but also on the degree of airtightness of their enclosures and therefore the type of door mounted on the vehicle.

There are different types of doors for refrigerated vehicles:

- sliding shutter doors (Figure 2.26a and 2.26b)),
- total rear opening with two leaves (Figure 2.27),
- Single side openings, awning tailgate (2.28).

Doors should have the same insulation of all the other walls to not reduce the insulation performance of the vehicle. However, doors frames are generally reinforced in order to withstand shocks and this tends to create thermal bridges. The effect of these thermal bridges can be mitigated by placing insulation between two rows of joints. Therefore, some type of doors may be more or less performing than others in terms of insulation performance, influencing both the initial performance of the vehicle and the long-term performance depending of their use.

As pointed out be Cavalier (2010) door openings lead to significant losses of cold air and thus energy.The development of the distribution of fresh and frozen products has accentuated this phenomenon. The energy loss from the door is related to the type of door and size of the openings, the number of openings, duration of openings and those fittings used to limit the cold air outlets. Lafaye de Micheaux et al. (2015) carried out an experimental and numerical investigation of heat and mass infiltration rates during the opening of an empty refrigerated truck body. In this study, the authors showed that the volume flow rate increases progressively due the development of the doorway flow pattern, i.e. hot air entering at the top of the opening and cold air flowing outside at the bottom. In particular, Lafaye de Micheaux et al. (2015) pointed out the presence of two different mechanisms regarding heat and mass exchanges:

- an unsteady mass exchange between the inside and the outside air volumes which initially appears,called buoyancydriven flow. During this period, the density difference between the two volumes is the driving force. The volume flow rate reaches a peak value but quickly decays due to the temperature increase inside the truck body. For the tested body,

this first stage extends to about 20 s for the total door opening (aperture width is equal to the body width), and up to about 50 s for a 1/3 aperture ratio.

- A second kind of heat exchange between the outside air volume and the inner wall of the body occurring in a second time, called boundary layer flow. This is basically natural convection over the cold walls of the container. As pointed out by the authors; this phenomena appears once the inside air has roughly reached a ceiling temperature of a few Kelvin below the outside temperature. Then, a quasi-steady state heat transfer is observed until doors are closed, at a time that can reach 10 min in actual food deliveries.

The tightness of the insulated enclosure of the vehicle plays an important role during the opening of the doors, especially during deliveries, but also when the truck is moving due to the vacuum created by the speed on the rear frame of the body. In this regard, doors gaskets (see Figure 2.32) have to be installed to ensure the seal. However, in distribution, doors openings during the unloading phase of goods generate infiltration of a significant heat load into the insulated body, due to the humid air entry into the insulated enclosure. This additional load is responsible of several undesirable phenomena, such as the condensation of water vapor and the production of frost on the walls and within the evaporator of the refrigerating unit. The temperature inside the vehicle increases, differing from the required value for the proper transport of the perishable products and the cold chain may be compromised. Therefore, most of the refrigerated trucks use plastic strip curtains to reduce the mass transfer through the doorways during the periods of products unloading. A recent study carried out by Cemafroid (Reina et al., 2020**)** showed that the use of the plastic curtain may allow an energy savings up to 24 % for doors openings having a duration of 3 minutes, and 12 % for doors openings of 5, 10 and 15 minutes. Although this method is generally efficient, drivers often remove temporarily. Although this method is efficient, drivers often remove temporarily the strips air curtain because it blocks the access to refrigerated body. Another way to improve the stability of the temperature of the air during door openings is to use air curtains (Figure 2.30).

Clavier et al. (2011) presented an experimental investigation of the heat load through the doorway of a single compartment medium-size truck. This investigation was carried out under two different conditions, i.e. protecting or not the doorway by two types of air curtains (ambient single, or double with one being refrigerated). The double air curtain was found to be useful to improve the stability of the temperature of the indoor air and walls. As pointed by the authors; in the case of practical application, this would limit the temperature excursion sometimes experimented by the foodstuff in the trucks. Nevertheless, this protection system increases the infiltration heat load by 38% with respect to the unprotected doorway. Otherwise, the improvement in terms of temperature stability is lower for the single ambient air curtain, but using this system, as shown by this study, leads to a decrease of the infiltration heat load by 26 %.

Figure 2.26 Sling shutter door : a)view from the outside; b) view from the inside.

Figure 2.27 Total rear opening with two leaves a) without plastic curtains; b) with plastic strip curtains. (Cavalier, 2010).

Recently, Artuso (2019) and Artuso et al. (2019) developed a fully dynamic model of the insulated box of a refrigerated vehicle. The authors carried out simulations by choosing a delivery mission characterized by a total of twelve door opening operations where doors are kept completely opened and heat ingresses directly from the external environment. . Experimental data was collected during test of a vehicle following the ATP test . Simulation results gave input to insight on the correct dimensioning and sizing of a cooling unit and the analysis of the main heat fluxes that influence the thermal performance of the refrigerating system during operation. The model validation demonstrated the capability of the model to correctly predict the evolution of the internal box air temperature in both transient and steady-state conditions..

Figure 2.28 a) Awning tailgate; b) single openings on the lateral wall.

Figure 2.29 Door gaskets with four leaver joints.

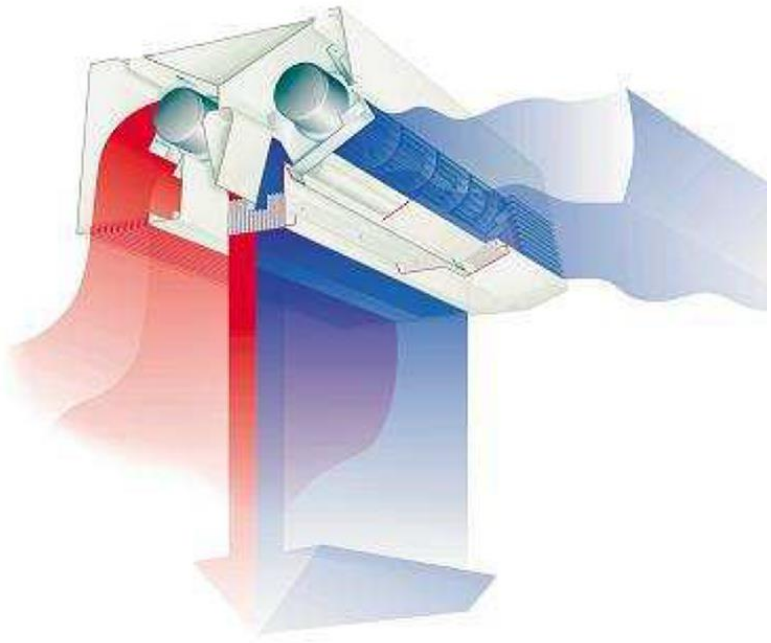

Figure 2.30 Principle scheme of the two air curtains system (Cavalier, 2010).

2.1.3 Regulation and Standards for refrigerated transport

Refrigerated transport is governed by various regulations and standards. Regulations may be divided in those regulations which impose obligations of means, e.g., for the transport equipment and those imposing performance obligations relating, e.g., transported products in both food and health cold chain.

This section provides an overview of the main regulations and standards currently in use for refrigerated transport, focusing in particular on ATP and its main specifications:

- the definition of the *K* coefficient and the equipment classification based on this coefficient;
- the inner heating method to measure the *K* coefficient in a climatic chamber of an ATP station;
- the ATP security coefficient introduced for the dimensioning of the refrigerating unit, strictly dependent on the insulation performance of the vehicle.

Finally, the process of ATP certificates used in France is also presented. This process has been implemented by Cemafroid since 1950 and has allowed the generation of a large amount of data recovered from the experiments carried out in its laboratories. Due to their close link with the process of certificates issuing certificates the two available databases in Cemafroid are therefore presented. All the data analyzed and used for the work of this thesis were extracted from these databases.

2.1.3.1 Overview of regulations and standards in refrigerated transport

As previously mentioned, regulations may be divided in those regulations which impose obligations of means, e.g., for the transport equipment and those imposing performance obligations relating, e.g., transported products in both food and health cold chain.

In the first category related to international or national obligations of means there are:

- the ATP which imposes the certification of refrigerated trucks for international transport in 51 countries,
- the European regulation (EU 37/2005) which requires the conformity of temperature recorders and their regular verification,
- WHO's PQS program requirements for vaccine transport.

Among the European regulations with performance requirements there are:

- The EU 852/2005 to ensure that temperatures of transported foods are maintained throughout the transport;
- The EU 2013/C343/01for pharmaceutical products within the framework of European Good Distribution Practices (GDP).

The main standards concerning temperature-controlled transport are:

- the EN378 concerning the Refrigeration equipment and its safety ;
- the EN 16440-1 March 2015 dealing with conformity of transport refrigeration units;

- the EN 17066-1 July 2019) on the dimensioning of transport units and bodies;

- EN 12830, EN 13485, EN 13486 on the conformity and verification of thermometers and temperature recorders.

In addition, there are a number of public testing and certification standards commonly used for temperature-controlled transport:

- PIEK and Quiet Truck standards for silent distribution equipment,
- Certicold Pharma certification standards for transport equipment for healthcare products;
- Certibruit benchmark for silent delivery in the city.

The presented regulations and standards applicable to temperature-controlled transport equipment can be summarised in Figure 2.31 where:

- black contour and black arrows indicate those relating to the refrigeration unit;
- the green ones identify those related to the insulated enclosure;
- the red ones highlight the ATP vehicle.

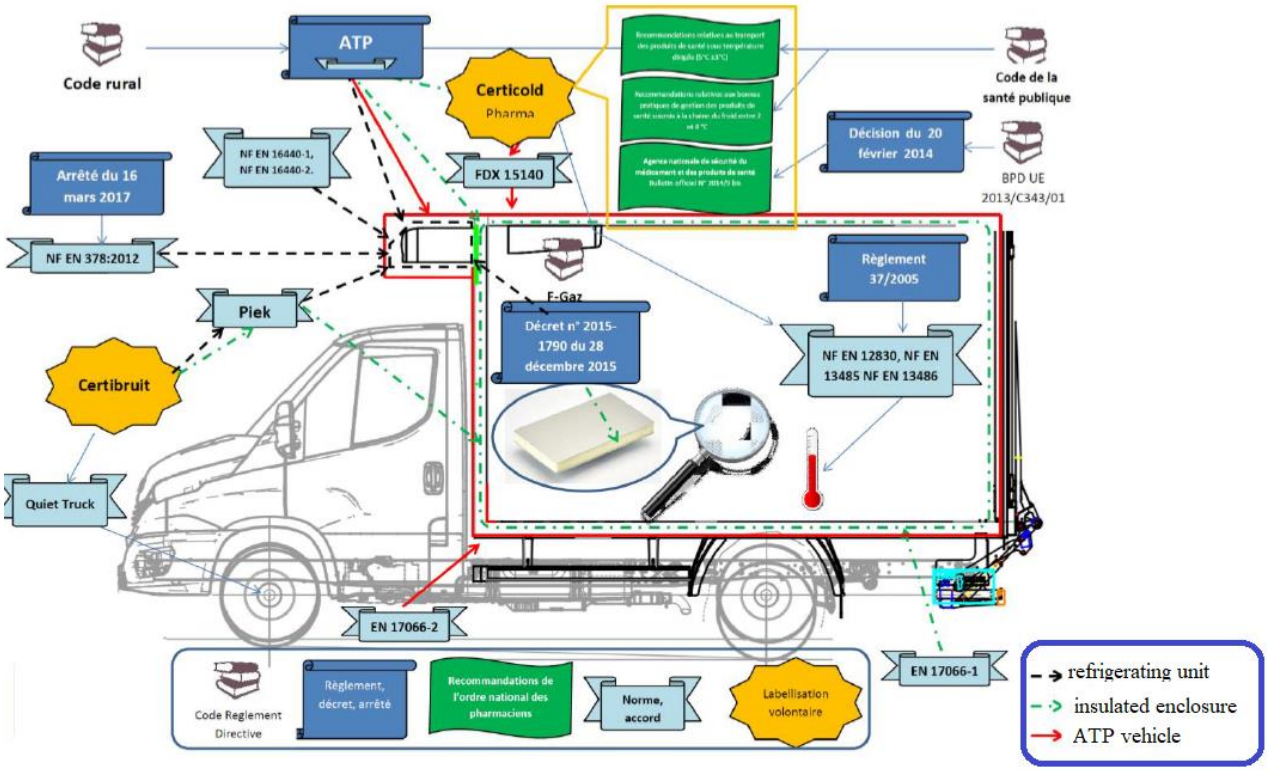

Figure 2.31 Overview of regulations and standards in refrigerated transport (Fertell and Cavalier, 2020).

The next subparagraph presents the general lines of ATP since this is the regulation applied in for international shipments as well as for national ones. This regulation provides the definitions for the different kind of equipment and those guidelines to test and periodically evaluate their performance from the point of view of the insulation of the enclosure and the cooling/heating capacity of the refrigerating unit.

2.1.3.2 ATP general lines

The consumption of products, in places and times other than those of collection or production and whose quality is highly dependent on the storage temperature, was made possible by the use of temperature controlled storage and even more thanks to the use of temperature-controlled means of transport. Refrigerated road transport saw his birth in the late 30s in USA and after the Second World War in Europe (Cavalier, 2016). Since then it continued to evolve, replacing the rail freight and recording an exponential growth all over the world in 1970. On this date the agreement on the International Carriage of Perishable Foodstuffs and on the Special Equipment to be used for such Carriage (ATP) was signed in the frame of UNECE. In 2019, 52 countries signed this agreement which is applied for operations carried out on the territory of at least two of the contracting parties. Some of these countries, such as, Russia, Italy, Spain, France and Portugal also apply ATP to the national refrigerated transport The aim of this regulation is to facilitate the international transport of perishable foodstuffs by harmonizing the relevant regulations and the administrative procedures and documentation requirements to which refrigerated transport is subject and setting common guidelines for testing and qualifying the refrigerated equipment. Carriers that adhere to ATP have to test refrigerated vehicles in terms of insulation capacity and the efficiency on the refrigeration unit. In this thesis, the focus is on the insulation capacity, also called "inner heating" method.

The basic notions and fundamental definitions to classify the vehicles used for the carriage of perishable foodstuff and the "inner heating" method used for testing them come from this regulation and are introduce below.

2.1.3.3 *K* Coefficient and equipment classification

The overall insulation coefficient is defined in the Annex I, appendix II of the ATP agreement as:

$$K = \frac{\dot{Q}}{\Delta T_{average}\, S} \qquad \text{Eq. (2.1)}$$

Where Q is the heating power or the cooling capacity, as the case may be, required to maintain a constant absolute temperature difference ΔT between the mean internal temperature T_{int} and the mean external temperature T_{ext}, during continuous operation, when the mean outside temperature T_{ext} is constant for an enclosure having a mean surface area, S. The mean surface area of the body is represented by the geometric mean of the internal surface area S_{int} and the external surface area S_{ext} of the body:

$$S = \sqrt{S_{ext}\, S_{int}} \qquad \text{Eq. (2.2)}$$

Referring to the K coefficient value the ATP regulation provides the following notion of insulated equipment.

Insulated equipment are thus defined as equipment of which the enclosures are built with rigid insulating walls, doors, floor and roof, by which heat exchanges between the inside and outside of

the body can be so limited that the K coefficient is such that the vehicle is assignable to one of the following two categories:

- Normally insulated equipment (IN) when $0.40 < K \leq 0.70$ W.m^{-2}. K^{-1}
- Heavily insulated equipment (IR) when $K \leq 0.40$ W.m^{-2}. K^{-1}.

ATP classifies equipment also on the basis of the type of device installed for the production of cold or heat inside the enclosure of the vehicle in the following categories:

Refrigerated equipment: insulated equipment which, using a source of cold, other than a mechanical or "absorption" unit (natural ice, with or without the addition of salt; eutectic plates, etc.) is capable, with a mean outside temperature, T_{ext}, equal to + 30 °C, of lowering the internal temperature T_{int} to, and thereafter maintaining it:

- at + 7 °C maximum, in the case of class A;
- at - 10 °C maximum, in the case of class B;
- at - 20 °C maximum, in the case of class C and
- at 0 °C maximum, in the case of class D.

  The K coefficient of refrigerated equipment of classes B and C shall in every case be equal to or less than 0.40 W.m^{-2}.K^{-1}.

Mechanically refrigerated equipment: insulated equipment either fitted with a mechanical compressor, or an absorption device which shall be capable, with a mean outside temperature, T_{ext}, equal to+ 30 °C, of lowering the mean inside temperature, T_{int} of the empty enclosure to, and thereafter maintaining it continuously in the following manner at:

- at a constant value that may be chosen between + 12 °C and 0 °C inclusive, in the case of class A;
- at a constant value that may be chosen between + 12 °C and - 10 °C inclusive , in the case of class B;
- at a constant value that may be chosen between + 12 °C and - 20 °C inclusive, for class C.
- at a constant value that is equal to or less than 0 °C, in the case of class D;
- at a constant value equal to or less than – 10 °C, in the case of class E;
- at a constant value equal to or less than – 20 °C, in the case of class F.

The K coefficient of equipment of classes B, C, E and F shall in every case be equal to or less than 0.40 W.m^{-2}.K^{-1}.

Heated equipment: insulated equipment, which is capable of raising the mean inside temperature of the empty enclosure to, and thereafter maintaining it for not less than 12 hours without renewal of supply at a practically constant value of not less than + 12 °C when the mean outside temperature, is as indicated

- : – 10 °C in the case of class A heat equipment;
- – 20 °C in the case of class B heated equipment;
- –30° C in the case of class C heated equipment;
- – 40° C in the case of class D heated equipment.

  The K coefficient of equipment of classes B, C and D shall in every case be equal to or less than 0.40 W.m^{-2}.K^{-}

Mechanically refrigerated and heated equipment: insulated equipment either fitted with its own refrigerating appliance, or served jointly with other units of transport equipment by such an

appliance (fitted with either a mechanical compressor, or an 'absorption' device, etc.), and heating (fitted with electric heaters, etc.) or refrigerating-heating units capable both of lowering the temperature T_{int} inside the empty body and thereafter maintaining it continuously, and of raising the temperature and the thereafter maintaining it for not less than 12 hours without renewal of supply at a practically constant value, as indicated below.

- Class A: T_{int} may be chosen between + 12 °C and 0 °C inclusive at a mean outside temperature between – 10 ºC and + 30 ºC.
- Class B: T_{int} may be chosen between + 12 °C and 0 °C inclusive at a mean outside temperature between – 20 ºC and + 30 ºC.
- Class C: T_{int} may be chosen between + 12 °C and 0 °C inclusive at a mean outside temperature between – 30 ºC and +30 ºC.
- Class D: T_{int} may be chosen between + 12 °C and 0 °C inclusive at a mean outside temperature between – 40 ºC and +30 ºC.
- Class E: T_{int} may be chosen between + 12 °C and – 10 °C inclusive at a mean outside temperature between – 10 ºC and + 30 ºC.
- Class F: T_{int} may be chosen between + 12 °C and – 10 °C inclusive at a mean outside temperature between – 20 ºC and +30 ºC.
- Class G: T_{int} may be chosen between + 12 °C and -10 °C inclusive at a mean outside temperature between – 30 ºC and +30 ºC.
- Class H: T_{int} may be chosen between + 12 °C and – 10 °C inclusive at a mean outside temperature between – 40 ºC and +30 ºC.
- Class I: T_{int} may be chosen between + 12 °C and -20 °C inclusive at a mean outside temperature between –10 ºC and +30 ºC.
- Class J: T_{int} may be chosen between + 12 °C and – 20 °C inclusive at a mean outside temperature between – 20 ºC and +30 ºC.
- Class K: T_{int} may be chosen between + 12 °C and – 20 °C inclusive at a mean outside temperature between – 30 ºC and +30 ºC.
- Class L: T_{int} may be chosen between + 12 °C and – 20 °C inclusive at a mean outside temperature between – 40 ºC and +30 ºC.

The K coefficient of equipment of classes B, C, D, E, F, G, H, I, J, K and L shall in every case be equal to or less than 0.40 W. m^{-2}. K^{-1}.

After dealing with the classification given by ATP for the vehicles, the next subparagraph presents the method proposed by the regulation to measure the K coefficient.

2.1.3.4 ATP internal heating method to measure the insulating performance in a climatic chamber of an ATP test station

The K coefficient may be measured either by using the "internal heating method" or the "internal cooling method". In either case, the empty vehicle must be placed in an insulated chamber and the test must take more than twelve hours of stabilization. During the test, whether by the internal cooling method or by the internal heating method, the mass of air in the chamber shall be made to circulate continuously so that the speed of movement of the air 10 cm from the walls is maintained at between l and 2 $m.s^{-1}$. In the present study, for the K coefficient measurement, the internal heating method is considered and described in this subparagraph. This method includes the measurement of twenty-four temperatures owing to as many probes, twelve of which are placed inside the vehicle and twelve on the outside. For parallelepiped shaped vehicles, these temperatures are measured 10 cm from the walls at the following twelve points (see Figure 2.32):

- the eight corners, on the inside for internal temperatures and on the outside for the external ones;
- the centers of the four faces having the largest area on the inside for internal temperatures and on the outside for the external ones.

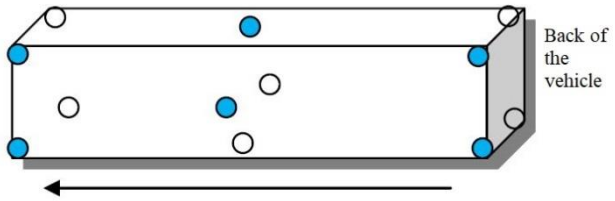

Figure 2.32 Example of temperature sensors positioning in a parallelepiped insulated enclosure.

If the shape of the vehicle is not parallelepiped, the twelve points of measurement shall be distributed as satisfactorily as possible having regard to the shape of the body.

With the measured temperatures, the internal and external arithmetic means, T_{int} and T_{ext} are then calculated. The test is carried out under steady state conditions, requiring that:

- T_{int} and T_{ext}, taken over a steady period of not less than 12 hours, shall not vary by more than ± 0.3 K, and shall not vary by more than ± 1.0 K during the preceding 6 hours.
- The difference between the heating power or cooling capacity measured over two periods of not less than 3 hours at the start and at the end of the steady state period, and separated by at least 6 hours, shall be less than 3 %.
- T_{int} and T_{ext}, and the mean values of heating or cooling capacity over at least the last 6 hours of the steady state period will be used in K coefficient calculation.
- T_{int} and T_{ext} at the beginning and the end of the calculation period of at least 6 hours shall not differ by more than 0.2

T_{int} and T_{ext} used to calculate the mean temperature of the walls of the body as follows:

$$T_w = \frac{T_{int}+T_{ext}}{2} \quad \text{Eq. (2.3)}$$

The presence of some electric heaters inside the vehicle's enclosure is needed to reach a temperature difference between the inside of the enclosure of the vehicle and the test chamber equal to 25°C ± 2 K. Furthermore, the average temperature of the walls of the body has to maintained at + 20 °C ± 0.5 K. The electric heaters placed inside the enclosure shall be fitted with fans having a delivery rate sufficient to obtain 40 to 70 air charges per hour related to the empty volume of the tested enclosure, and the air distribution around all inside surfaces of the tested body shall be sufficient to ensure that the maximum difference between the temperatures of any two of the twelve points does not exceed 2 K when continuous operation has been established. For the heat balance to be satisfied, the total required cooling power, $\dot{Q}$, which is used in Eq.(2.1), is the sum of the total heating power and ventilating power of the devices placed inside the enclosure. The heat dissipated by the electrical resistance fan heaters shall not exceed a flux of 1 W.cm^{-2} and the heater units shall be protected by a casing of low emissivity.

2.1.3.5 ATP Security Coefficient for the dimensioning of the refrigerating unit

The importance of the K coefficient is also found in the dimensioning of the refrigerating units. Paragraph 3 of the first annex of the ATP deals with the efficiency of the thermal devices of means of transport (i.e. also of refrigeration units) and provides a test procedure to determine the effectiveness of the operation of the refrigeration unit installed on a vehicle. A derogation from this procedure is indicated in paragraph 3.4.7 as follows: 'If the cooling device and all its accessories have individually undergone a test to determine the effective cooling capacity at the prescribed reference temperatures, with the favorable judgement of the competent authority, the means of transport may be recognized as a means of refrigerated transport, without any efficiency test, if the effective cooling capacity of the device is greater than the heat losses permanently through the walls for the class considered multiplied by a factor of 1.75. Therefore, the condition specified in the ATP to evaluate the nominal power value necessary for the correct operation of the unit is the following:

$$P_{nom} > 1.75 \text{ K S } \Delta T \quad \text{Eq. (2.4)}$$

Hence, the dimensioning within the framework of the ATP through Eq.(2.4) does not take into account the door openings in distribution but only the losses through the body increased by a security coefficient (k) equal to 1.75. This dimensioning corresponds well to long-distance transport without load breakage (intermediate door opening).

Actually, manufacturers when sizing refrigerated transport units, tend to take precautions and the refrigerating units are sized to take into account the other uses of the vehicles and in particular the

constraints of urban distribution. Figure 2.33 and Figure 2.34 show the distribution of the real dimensioning coefficients, calculated taking into account the nominal power at - 20°C of the refrigerating units . While there is a wide dispersion of design factors within the same type of equipment (Figure 2.33), the graph of Figure 2.34 clearly shows that the safety factors are homogeneous between the different types of equipment, with an average value of the French fleet approximately equal to 3, which is therefore well above the minimum value prescribed by the ATP agreement.

The correct sizing of the refrigerating unit is an energy performance factor that could be more strongly integrated in the choice of equipment.

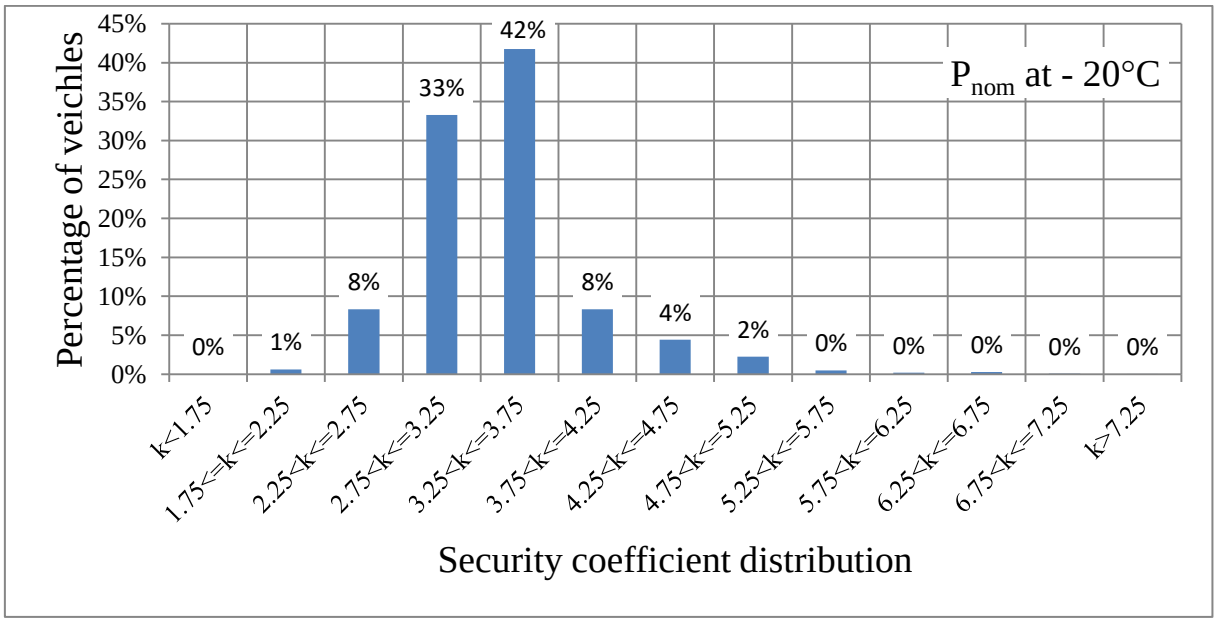

Figure 2.33 Security coefficient for class C single-temperature equipment with nominal power (Pnom) at – 20°C on the French market in 2019 (DATAFRIG© - Cemafroid 2020).

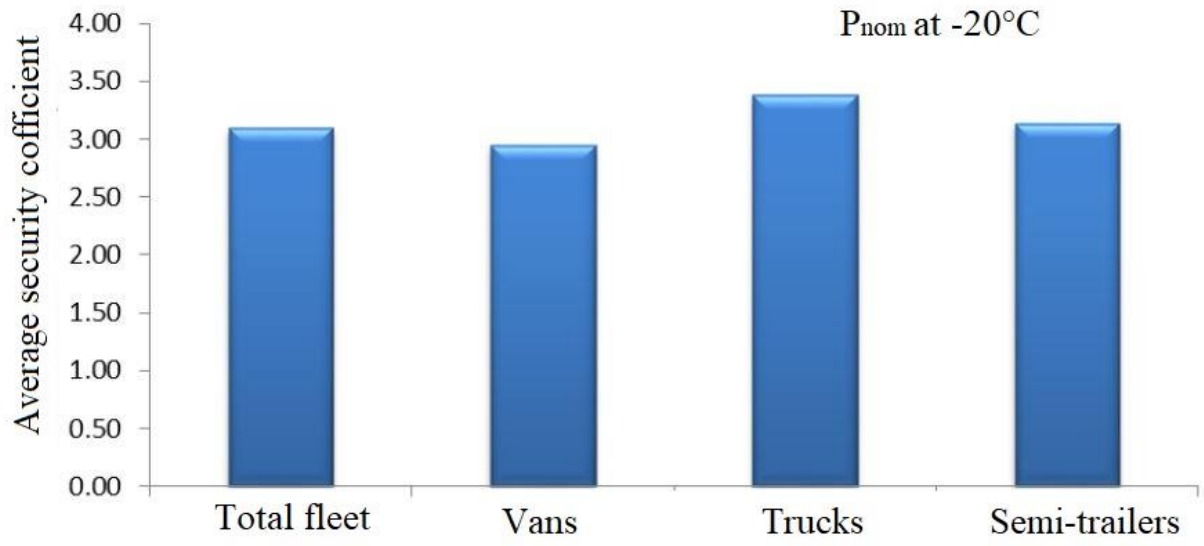

Figure 2.34 Average security coefficient of refrigeration units for the French fleet at the end of 2019 (DATAFRIG© - Cemafroid 2020).

2.1.3.6 Pull down test

The “inner heating” method (described in subparagraph 2.1.3.4) used to measure the K coefficient is well adapted to certificate the initial performance levels of the vehicles as well as to realize a long term performance evaluation at 12 years of each equipment but it cannot be used periodically for equipment in service. For this reason, the “pull down” test procedure had been developed and introduce in ATP as an alternative to check the compliance of equipment in service at six and nine years. The purpose of this test is to obtain a recording of the temperature-lowering process which is representative of the equipment’s refrigerating unit performance. The empty equipment shall be placed in an insulated chamber whose mean temperature shall be kept uniform, and constant to within ± 0.5 °C, at + 30 °C (see Figure 2.35). The objective of this test is to start from an equilibrium condition and to check if the unit is able to cool down. The mass of air in the chamber shall be made to circulate continuously so that the speed of movement of the air 10 cm from the walls is maintained at between l and 2 $m.s^{-1}$. Temperature measuring instruments protected against radiation shall be placed inside and outside the body at the points already swhon in subparagraph 2.1.3.4 (see Figure 2.32).When the mean inside temperature of the body, T_{int} reaches the outside temperature (+ 30 °C), the doors, hatches and other openings shall be closed and the refrigerating appliance and the inside ventilating appliances (if any) shall be started up at maximum capacity.

In addition, in the case of new equipment, a heating appliance with a heating capacity equal to 35% of the heat exchanged through the walls in continuous operation shall be started up inside the body when the temperature prescribed for the class to which the equipment is presumed to belong has been reached.

The mean outside temperature and the mean inside temperature of the body shall each be read at least every 5 minutes and the test shall be continued for twelve hours after the mean inside temperature of the body has reached the lower limit prescribed for the class to which the equipment is presumed to belong:

- Class A requires T = 0°C;
- Class B requires T = – 10°C;
- Class C requires T = – 20°C.

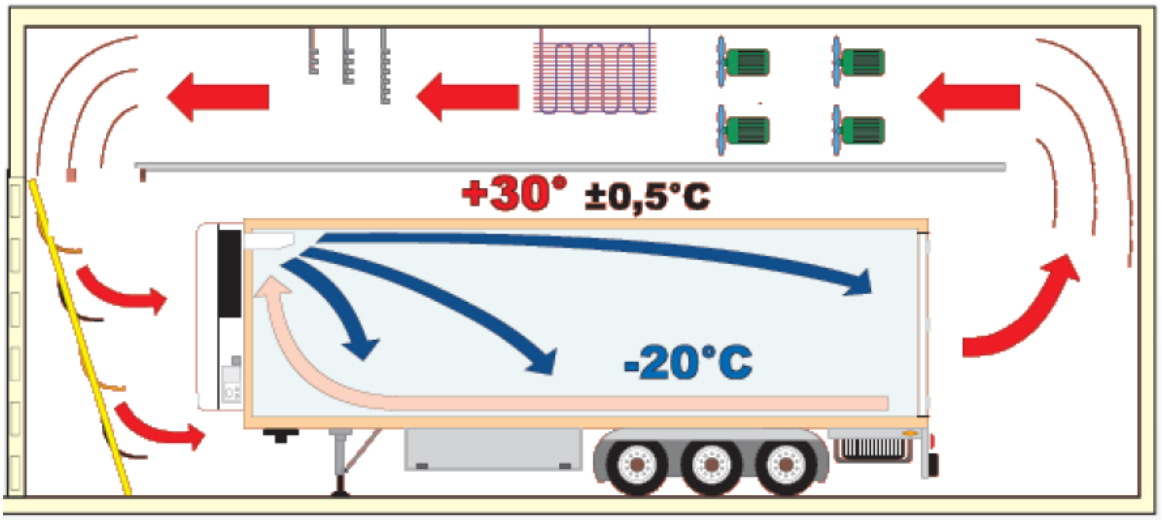

Figure 2.35 Pull down test procedure.

2.1.3.7 ATP certificate issuing in France and data production

The ATP agreement, ratified today by 52 countries, sets the requirements for the means necessary for the international or cross-border transport of perishable foodstuffs and defines the provisions for checking the conformity of temperature-controlled transport equipment. A number of countries, including France, also apply the ATP to transport on national territory. A certificate of technical conformity valid for six years, and renewable, is assigned to each piece of equipment, together with a regulatory marking. For the application of these regulations, France has had a database since 2002 which allows all temperature-controlled transport equipment to be managed and monitored in a dematerialized manner. Since 2009, as part of a public service delegation, Cemafroid has been designated as the Competent Authority to issue, on behalf of the Ministry of Agriculture, technical compliance certificates for temperature-controlled transport equipment. The process for issuing the certificates is structured and composed of different stages.

Firstly, the manufacturers integrate into the database all the information relating to each new piece of equipment. This information concerns the owner of the equipment, the insulated body and its accessories, the refrigeration system and the chassis if applicable. Each piece of equipment shall be identified by a serial number, for both the insulated enclosure and the refrigerating unit, and the reference of the respective test reports shall also be indicated. Subsequently, in order to obtain the initial certificate of technical conformity, the manufacturer shall submit an application via the database. Figure 2.36 shows the ATP certification scheme as implemented in France in 2019.

Immediately after the manufacturing, identified with “0” in Figure 2.38, each new prototype vehicle, refrigerating unit or cold production device, shall be tested in an official ATP test station. In particular, the insulated enclosure is submitted to the *K* coefficient test to check the insulation performance, while the refrigerating unit or cold production device or to a pull down test (introduced in subparagraph 2.1.3.6) , to verify its ability to drop and maintain the temperature at the desired value. Manufacturers of equipment after the test receive an official test report defining the required thermal characteristics. Based on this report they shall be authorized to prove the conformity of their series production to the prototypes. All declared information is automatically checked by the Datafrig® management system. A comparison is made between the equipment entered and its certified type in order to check its conformity.

At 6 years and then at 9 years, all the in-service refrigerated vehicles of the series must pass a pull down test in a test center approved by Cemafroid on the basis of a reference system. After 12 years, the in-service vehicle must pass an official ATP station to be subjected to the *K* coefficient test in addition to the pulldown test. In this way the vehicle can get an additional renewal, of six years which may be carried out in batches. The certificate can then be renewed every six years.

As indicated in the Cemafroid manufacturer's approval reference manual, all equipment with an ATP certificate of conformity, whether or not it is used on the public highway, must be fitted with:

- an identification plate manufactured and affixed by the manufacturer, also known as a nameplate or manufacturer's plate, and,
- a marking specific to ATP issued by the competent authority, consisting of : identification marks consisting of two stickers (classification mark and expiry date of validity of the certificate issued for the equipment); and a certificate of conformity plate, the latter being optional.

The identification plate (data plate or manufacturer's plate) shall contain at least the following information: name or business name of the manufacturer, country of manufacturer (or letters used in international road traffic), type/model (numbers and/or letters), number in the series and month and year of manufacturing. No inscription shall be affixed to the identification plate which could give reason to believe that the equipment complies with ATP, such as "ATP", "approved for the carriage of perishable foodstuffs", etc. Identification marks (classification mark and expiry date) shall be affixedhhhy externally on both sides of the vehicle, in the upper corners at the front of the vehicle. Only valid identification marks must be affixed. Figure 2.37 illustrates the correct positioning of the markings.

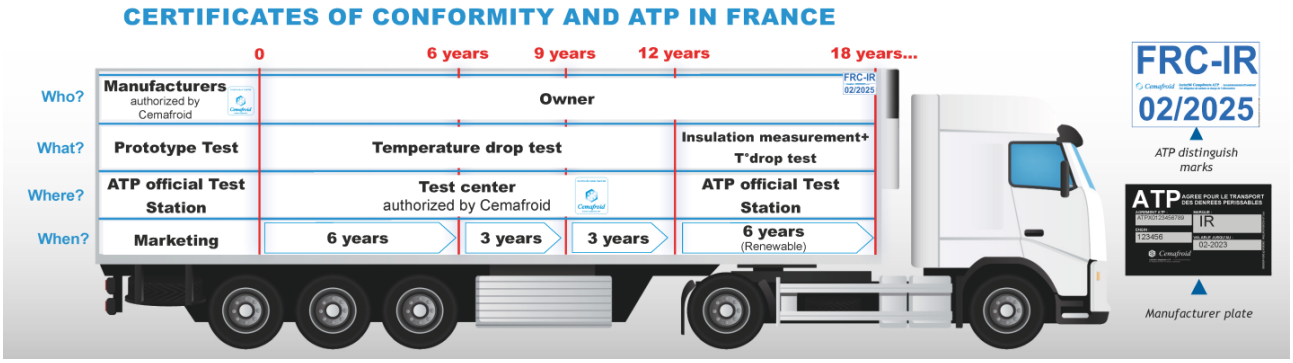

Figure 2.36 Actual ATP certification scheme implemented in France (Cemafroid, 2020).

Figure 2.37 Correct application of the ATP identification mark.

The issuing of certificates according to the scheme presented in Figure 2.36 allows generating a large amount of data which are collected in the Datafrig® management system.

Datafrig® is an ATP certificate management tool offering:

- a dematerialized procedure,
- the possibility of making a direct request via Internet,
- an electronic processing of the files.

This system allows the issuing of more than 30 000 certificates per year, including 15 000 certificates per year, issued at six and nine years, through tests carried out by about 200 authorized test centers.

Datafrig® is an ATP management software on top of a relational database containing tables where data is recorded. The database records, in fact, the data in more than 30 tables of the entire fleet of 350 000 temperature controlled equipment registered in France, of which approximately 120 000 hold an ATP certificate. The relational scheme of this database is presented in Figure 2.38. This relational scheme:

- identifies the data stored in the database;
- represents the relationships between the different data elements

In particular, each rectangle represents a table in the database and the arrows, the links between them.

For example the table called “Cellule” refers to the table of the insulated enclosure. In this table it is possible to find the following information:

- insulated enclosure model,

- serial number,
- date of manufacturing,
- mean surface area (m^2),
- internal surface area (m^2).

This table is connected to other tables such as the one related to the brand (identified on the scheme as “Marque Cellule”), the one related to the manufacturer (“Fabricant” on the scheme) and the one on the nature of the insulated enclosure (identified as “Nature Cellule”).

Globally Datafrig® database includes thirty-two tables, allowing the storage of a large amount of vehicle information, such as the type of vehicle, the accessories and the type of openings, the chassis, the refrigerating unit, the compartments and their position, etc.

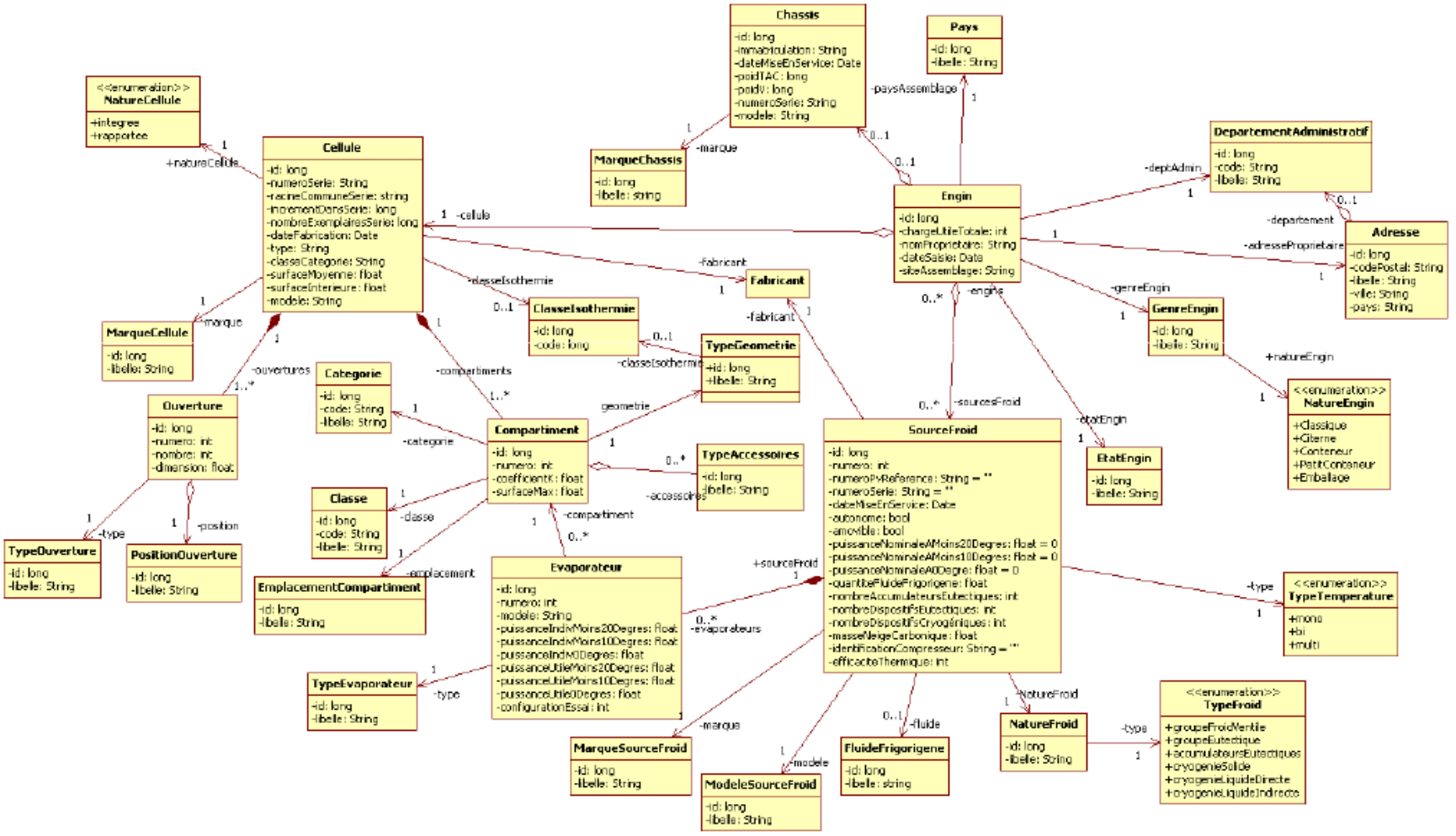

Figure 2.38 Datafrig® relational scheme.

In addition to Datafrig® database, Cemafroid also has another relational database recording and archiving only the results of the experiments carried out in its climatic chambers since 1999. Every year about two hundred and fifty *K* coefficient tests are carried out on different types of vehicles (Figure 2.39). The results of these tests together with other vehicle information are recorded in this second database. The vehicles registered in this database can also be found in Datafrig®. This second database with a simpler relational scheme than Datafrig®, allows collecting a lot of data, some of which are not recorded on Datafrig®. As example, some of the data collected through the table called "Intervention" are shown in Table 2.6. Information on the blowing agents used in the vehicle manufacturing process and their densities are examples of data missing on Datafrig®, but very useful for the study of the ageing phenomenon of refrigerated vehicles. In this thesis data from both these databases are used for the study of the ageing of refrigerated vehicles. However, these two databases differ in their structures. In order to be able to use the data from both of them a manual work of cleaning, processing and joining of data has to be performed first of all. The theoretical basis on how to interact with these databases are discussed in section 2.4 while the actual work carried out on the data is presented in Chapter 4.

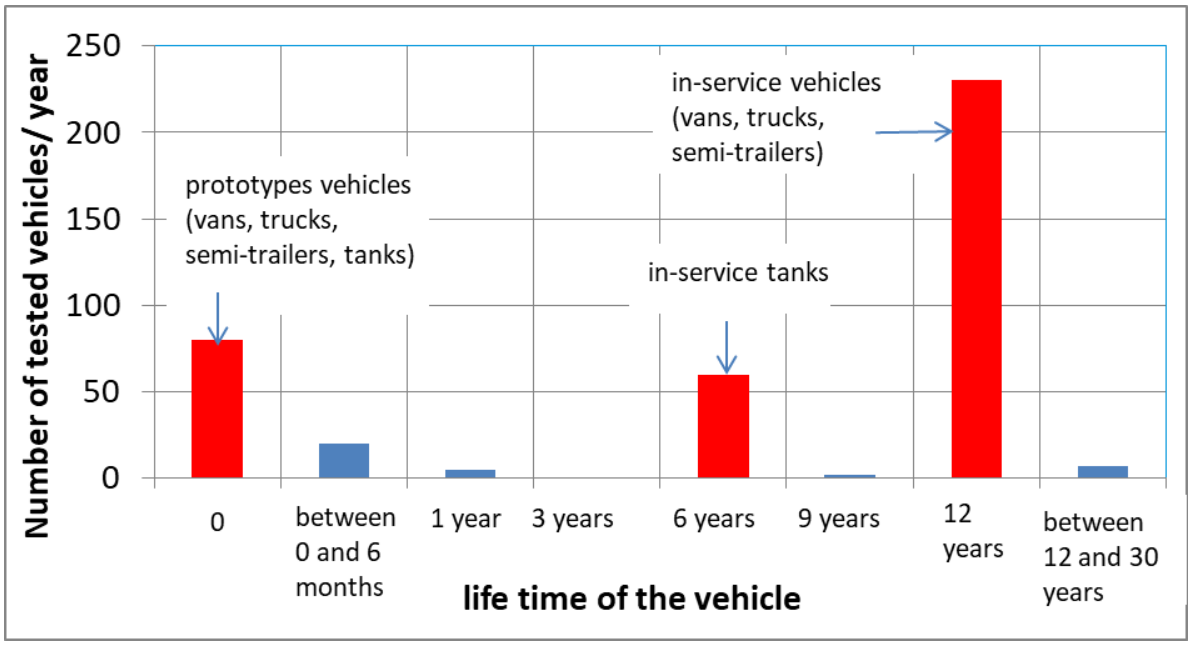

Figure 2.39 Number of experiments per years carried out in the Cemafroid climatic chambers as a function of the life time of the vehicle.

Table 2.6 Example of data extracted from the database of the Cemafroid climatic chambers

Recorded data	Type	Description
ID simple	numeric	primary key of the Intervention table
Intervention ID	numeric	link to the Client table
Int. Length	numeric	internal length of the enclosure in meters
Int. Width	numeric	internal width of the enclosure in meters
Int. Height	numeric	internal height of the enclosure in meters
Ext. Length	numeric	external length of the enclosure in meters
Ext. Width	numeric	external width of the enclosure in meters
Ext. Height	numeric	external height of the enclosure in meters
Ceiling thickness	numeric	total thickness of the ceiling in millimeters
Floor thickness	numeric	total thickness of the floor in millimeters
Lat. walls thickness	numeric	total thickness of side walls in millimeters
Rear door thickness	numeric	total thickness of the rear door in millimeters
Front wall thickness	numeric	total thickness of the front wall in millimeters
Ceiling insulation	text	nature of the ceiling insulation
Floor insulation	text	nature of floor insulation
Lat. wall insulation	text	nature of the lateral walls insulation
Rear door insulation	text	nature of the rear door insulation
Front wall insulation	text	nature of the front wall insulation

2.2 Evolution of materials and construction technologies

In order to understand the ageing of refrigerated transport vehicles, it is useful, first of all, to study the manufacturing technologies and their evolution over time. This evolution has, in fact, modified the design and the insulation performance of refrigerated vehicles.The goal of body manufacturers has always been to construct a lightweight body, having sufficient strength, in which the insulation could stay dry and maintain its original insulating value. As shown in Figure 2.40 over the time, different technologies and materials have been used for the construction of insulated vehicles. From vehicles made with natural materials in the 1940s to those made of polyurethane sandwich panels introduced in the 1970s and still in use today, to witness the recent introduction of new materials and technologies combined in hybrid solution with polyurethane panels, such as vacuum insulation and aerogel.

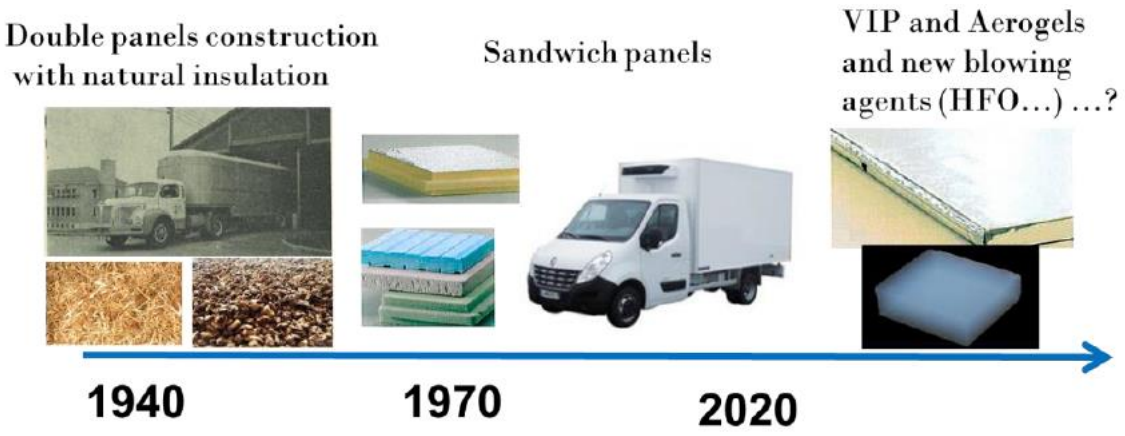

Figure 2.40 Evolution of insulating materials used in refrigerated vehicles since the 1940s.

Each of these materials has different characteristics, among which the most important to identify the insulation performance is thermal conductivity. Casillo (2011) presented a review of the materials used over the years for manufacturing insulated vehicles used in refrigerated transport. Figure 2.41 summarizes this review indicating, for each material, the associated thermal conductivity, λ.

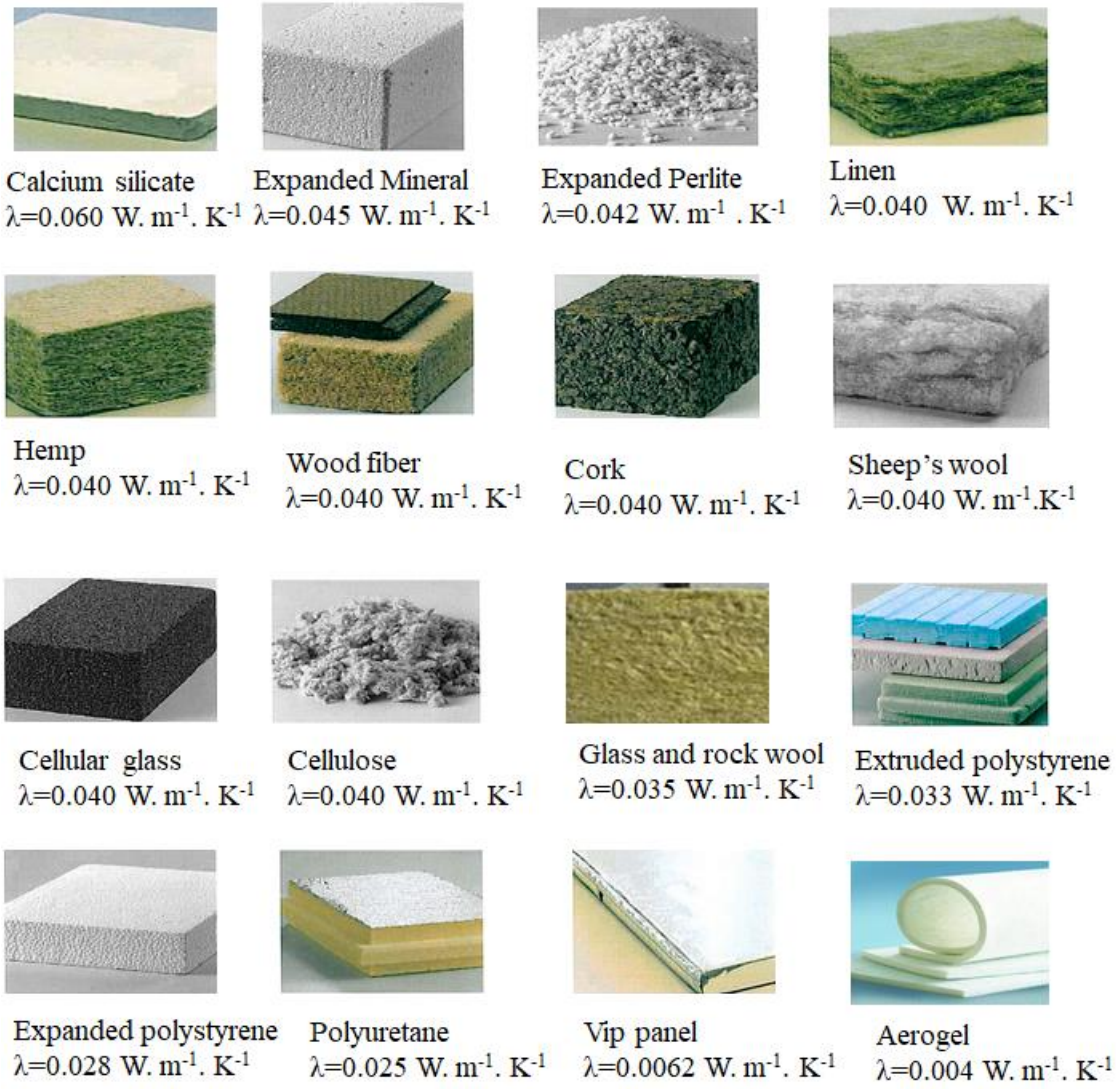

Figure 2.41 Review of materials used over the years in for manufacturing insulated vehicles transport (Casillo, 2011).

Nowadays in Europe it is possible to identify two major manufacturing techniques, quite strongly opposed and having distinct performances:

- sandwich panels with polyester skin, an historical solution implemented since the 1970s to replace the cork. Polyester combined with polyurethane (PU) or expanded polystyrene (EPS) insulating foams is an excellent insulation compromise with materials with low thermal conductivity, waterproof, mechanically elastic and easily repairable. It has proven itself for more than 50 years in all types of refrigerated transport. It offers flexibility, adaptability and personalization. It is the common solution for French, Italian and Spanish manufacturers;
- injected metal skin panels, developed more recently mainly by German manufacturers with PU foam injection technologies. If this solution offers good resistance to mechanical shocks, it combines highly thermally conductive materials with good insulation. The repair of these panels is more delicate and expensive in general.

These two technologies involve significantly different tools and manufacturing processes. They also lead to different performance and product qualities. The ageing of the vehicles and the maintenance of performance over time also depends on the technology chosen and its implementation.

An excursus of the construction technologies and materials used from the appearance of the first refrigerated vehicles until today is presented in the next subparagraph of this section. New materials already available on the market, those under test and future developments, are also presented.

2.2.1 The double panel framework and the first insulating materials

Since the first refrigerated transport by the French engineer Charles Tellier in 1876 (Tellier, 1910) the transport body insulation was a major issue. For insulating the cold room of the boat named "Frigorifique" and used to transport of fresh meat, Charles Tellier selected cork for its qualities, which at the time was not used as an insulating material. Cork has an important capacity of air storage, it is also waterproof which is an important quality for insulation in a boat and its thermal conductivity is around 0.040 $W.m^{-1}.K^{-1}$. Nevertheless the production of cork is rare and to insulate the "Frigorifique", Tellier was obliged to complete the insulating material by filling it with about 30 m^3 of chopped straw cut at 1 cm long. Chopped straw presented also good insulation properties but not so high than cork with its thermal conductivity around 0.070 $W.m^{-1}.K^{-1}$, which is nearly twice than the thermal conductivity of cork. Cork has been used for many years to insulate refrigerated boats, refrigerated rail-coaches and also the first refrigerated trucks appeared in the mid-thirties in United States and in the mid-forties in Europe; it was abandoned in the 50s to be replaced with other insulating materials. The first insulated trucks were built using the double panel bodywork scheme consisting in two bodies nested one inside the other whose interlayer was filled with insulating materials, such as glass or rock wool, polystyrene, etc. These materials have no mechanical resistance and are sensible to humidity. They can absorb water in large quantity and totally lose their insulation performances. As stated by Bogrow (1982), in such a system, even with an insulating material with a thermal conductivity of 0.035 $W.\ m^{-1}.K^{-1}$, the overall insulation coefficient could not be lower than 2.25 $W.m^2.K^{-1}$, a very high value compared with those of today. Some example of the first refrigerated vehciles are representd in Figure 2.42.

Figure 2.42 Examples of first refrigerated vehicles.

2.2.2 The technique of sandwich panels

The first vehicles used for refrigerated transport had walls with a thickness between 150 mm and 200 mm, reducing the useful transport volume and payload of the truck or trailer. The used materials were predominantly natural materials such as cork, rock wool or glass wool. The French regulation of 1952 and the United Nations economic commission for Europe ATP agreement of 1970 impacted the construction of transport equipment. With the introduction on the market of new insulating materials in the 60s, a new conception of the insulated vehicles was developed in Europe. The technique of sandwich panels appeared. Slices of insulating foam are inserted in between still plates or polyester coverage reinforced with fiberglass. These insulating foams offer a new characteristic with a rather good mechanical resistance offering new assembling possibilities. They are also far lighter than cork and not sensible to humidity than wools.

This section presents the principles behind this technology, the used materials and an example of refrigerated truck manufacturing process.

2.2.2.1 Sandwich panels materials

Sandwich panels are used to lend mechanical strength to insulated and mechanically refrigerated vehicles. A sandwich panel, which scheme is presented in Figure 2.43, is obtained by assembling two main elements:

- the sheathings, having good tensile and compressive strength. They are generally made of 1 mm steel or aluminum-alloy sheet or of a 2 or 3 mm fiberglass reinforced polyester-resin sheet ;
- the core which serves as a brace and is generally made of rigid closed-cell insulating foam with mechanical qualities that is sufficient but quite inferior of those of sheathings.

As regards the materials used for the sandwich panels, first appeared polyvinyl, then polyurethane and polystyrene. Their thermal performance is far higher than the one of cork, rock or glass wools.

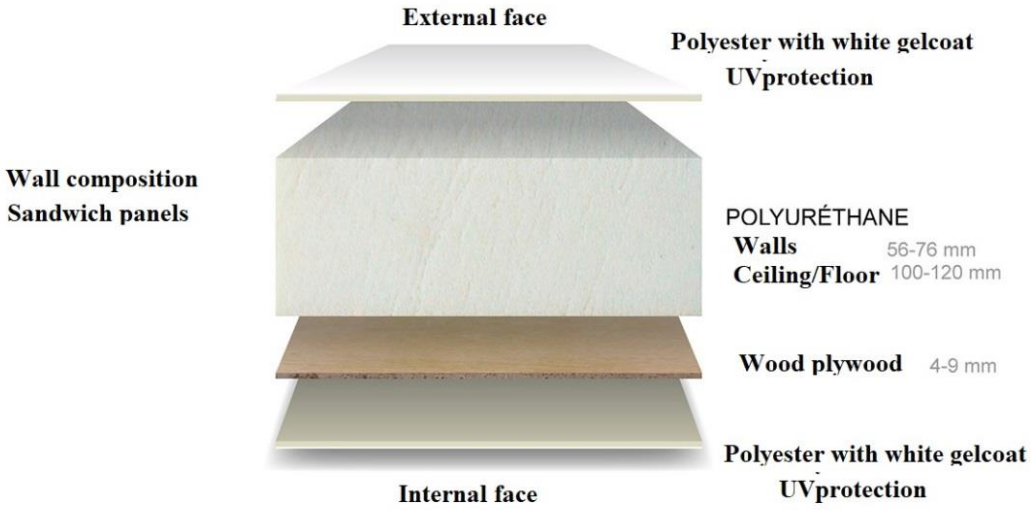

Figure 2.43 Sandwich panel scheme.

The term polyurethane stands for a family of insulating materials that in addition to the polyurethane (PU) also includes polyisocyanurate foams (PIR). Rigid polyurethane foams are produced through a chemical reaction between an isocyanate and a polyol both in liquid form and a blowing gas with a low-boiling point. The isocyanate and the polyol react directly on mixing, creating the polyurethane solid matrix.

The exothermic reaction between the isocyanate and the polyol is presented in Figure 2.44.

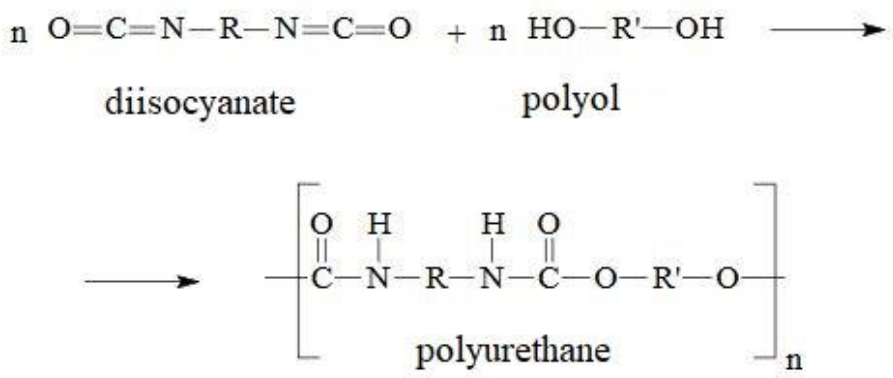

Figure 2.44 Reaction leading to the formation of polyurethane.

The heat released through this reaction lets the blowing agent evaporating and foaming the polymer matrix. The closed cell structure of polyurethane foams, thanks to its low permeability, allows the gas remaining in the insulation material over the long term. Furthermore, to remain inside the close cells, the blowing agents are characterized by a low diffusivity. The absence of these properties and characteristics would cause gases leakages into the atmosphere.

Sometimes vehicles are also realized with expanded polystyrene (EPS) or extruded polystyrene (XPS). The thermal conductivity of polystyrene is higher than PU foam but in floor and roof construction where there are fewer constraints for overall thickness, body builders can offset thermal losses by using thicker panels. In side walls, the insulation thickness is constrained by the maximum permissible insulated vehicle width of 2.60 m and euro pallet dimensions. A euro pallet is 1.0 m deep by 1.20 m wide and the need to accommodate 2 euro pallets side by side means that the insulation thickness can rarely be more than 45–50 mm (Tassou et al., 2009).

Excellent insulation properties are obtained through the use of blowing agents. Nowadays, depending on the blowing agent, the thermal conductivity of polyurethane foam is between 0.022 and 0.028 $W.m^{-1}.K^{-1}$, twice lower than those of cork and wools. From the 1970s to the mid-1980s, polyurethane foams were expanded with chlorofluorocarbons (CFCs), such as R-11. These blowing agents had a good insulation capacity thanks to their low value of thermal conductivity. However, they had a strong impact on the environment due to their high Ozone Depletion Potential value (ODP). Searching for new environmentally friendly fluids, to be used as working fluids in refrigeration systems and as blowing agents in insulating foams, became a matter of global concern after 1987, date of finalization of the Montreal Protocol. In 1995, manufacturers started realizing their insulated enclosure using the hydro chlorofluorocarbons (HCFCs) as blowing agents (R-141b and R-22). Hydro chlorofluorocarbons were less harmful to the environment than chlorofluorocarbons but they still had not a negligible impact on the ozone layer. In 2005, hydrocarbons (HCs) such as CO_2, cyclopentane and n-pentane and hydro fluorocarbons (HFCs) replaced HCFCs

Nowadays developed countries only use cyclopentane and CO_2 whereas developing ones still use HFCs and in same cases even HCFCs. The phase out limits of the blowing agents with their

corresponding thermal conductivity are summarized in Table 2.7. HFCs are still in use with a gradual phase-out to a total elimination foreseen for 2022.

As shown in Figure 2.45, it is possible to see that with the change from CFCs and HCFCs to the blowing agents used nowadays, manufacturers are constrained to use gases having a greater thermal conductivity.

Table 2.7 Evolution of blowing agents and their thermal properties.

Blowing agent	Thermal conductivity ($W.m^{-1}.K^{-1}$)	Phase out limit
R11 (CFC)	0.017	1/01/1995
R141B (HCFC)	0.019	1/01/2004
R22 (HCFC)	0.020	1/01/2004
R134a (HFC)	0.022	1/01/2022 (Regulation EU n°517/2014 compulsory from 1/01/2015)
Cyclopentane	0.021	Without limits
CO_2	0.027	Without limits

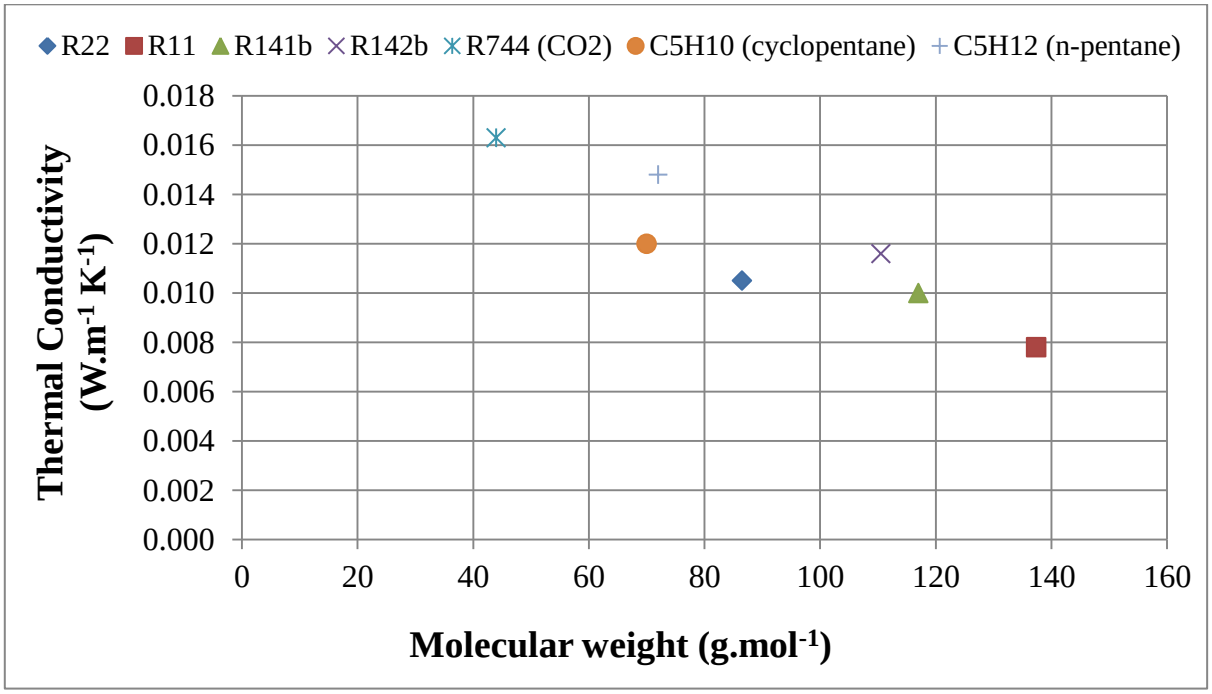

Figure 2.45 Thermal conductivity as a function of the molecular weight of the blowing agents.

2.2.2.2 Refrigerated truck manufacturing process

To realize the sandwich structure of the insulated enclosure, the PU foam is lined with a skink, playing also a major role in the performance of the panel. Most of the fleet is built with Glass reinforced Plastic (GRP) skin but also steal or aluminium plates are used. Different techniques may be used to realize the panels which could be made of bricks of foam blown in blocks and cut in slices and assembled together with the skin and inserts with resin or glue on tables or directly injected between skins with the blowing agent.

The "glueing method" is the technology currently most used for manufacturing insulated vehicles. This technique consists in tight glueing (in a vacuum or using a press) of sheathings to a prefabricated insulating core. This technique makes it possible to glue Z or omega shaped stiffeners into the sandwich panels (see Figure 2.46). These stiffeners unfortunately acts as thermal bridges but they are useful to to obtain the desired mechanical properties, if properly spread around. As presented in Figure 2.47a stresses are transferred from wall to wall, including doors, by glueing or riveting internal and external corners brackets (Heap, 2010). Concerning the doors assembly, the seals should be able to accommodate the deformations occurring on the road or when the temperature is brought down. Figure 2.47b and Figure 2.47c show the most common types of seals respectively multi-lip compressed seal and lap joints. The first kind is effective only on molded doors whereas the second type is used for larger sandwich-type doors.

Cadet (2004) presented the steps of the manufacturing process for a refrigerated truck. This process requires that the lateral walls, the ceiling and the floor are generally produced in a mold, the bottom of which is a stainless steel plate. The quality of this surface and its uniformity allow for smooth panels. Gelcoat, resin, and then the core of insulating material, the inserts and reinforcements are deposited on the stainless steel plate. After realizing the deburring of the contours, the panels are extracted from the mold. In the case of floor some holes are made to make the subsequent fixing to the frame. The front face is also made in a mold but an opening is made to allow the installation of the refrigerating unit. All the walls thus made are arranged on a special structure for gluing and assembling one to the other. Finally, the insulated enclosure is anchored on the frame, as shown in Figure 2.48.

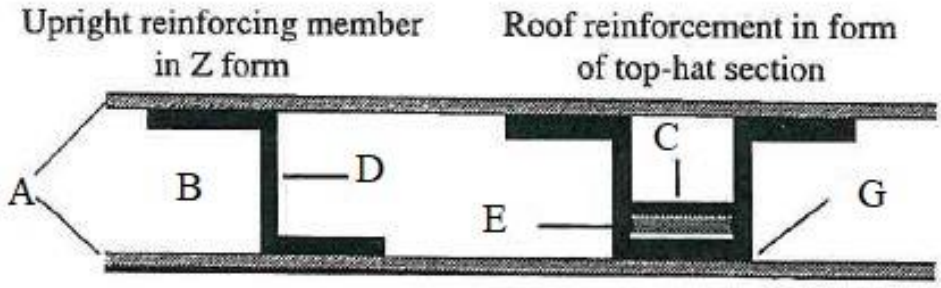

Figure 2.46 Internal reinforcement of sandwich panels (Heap, 2010).

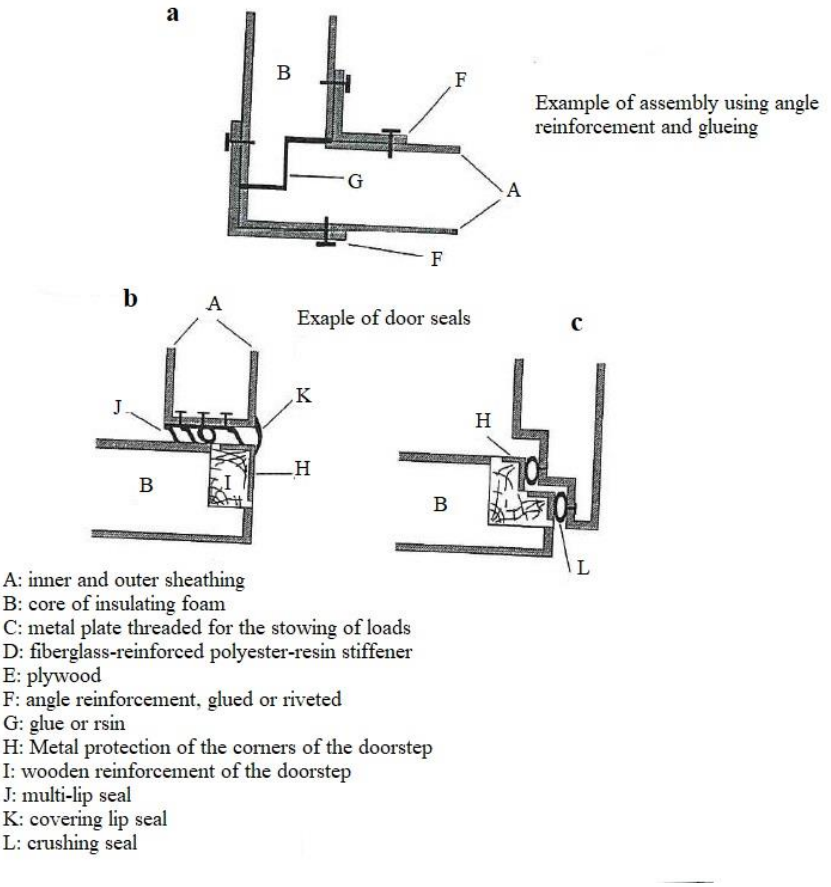

Figure 2.47 a) Example of assembly using angle reinforcement and glueing; b) multi-lip compressed seals; c) lap joints (Heap, 2010).

Figure 2.48 Anchoring of the insulated enclosure on the frame of the vehicle (Cadet, 2004).

Where it was hardly possible to reach a K value of 0.50 $W.m^{-2}K^{-1}$ in the 50s with 150 to 180 mm of insulating material, it became possible to reach K values of 0.25 $W.m^{-2}K^{-1}$ with only 80 to 100 mm of insulation: a tremendous progress in insulation performances. The use of sandwich panels took over the former double bodywork insulation and from nothing in 1952 reached 65% of the fleet in the 70s and 80s. The ATP regulation, requesting for high insulation performances with a maximum K value equal to 0.40 $W.m^{-2}.K^{-1}$ for frozen products, helped to switch from the old technology to the sandwich panels one .This technology made it possible to achieve good performance good ageing performances of the equipment such as those presented by the truck shown in Figure 2.49, tested at 30 years in Cemafroid and presenting a K value equal to 0.46 $W.m^{-2}.K^{-1}$.

Figure 2.49 Insulated enclosure built with a double panel system. 30 years old French refrigerated truck in Cemafroid ATP test laboratory in 2016.

European body manufacturers have also developed injection technologies. The insulating polyurethane foam is injected in between two skins in a mold. The skin may be made of steel or polyester. The full body may be made of injected panels or only some components most of the time doors and openings. Since 1970, all the European production is built with sandwich panels or injected panels either with polyester or metal skins. Sandwich panels allow very high thermal performances with a large variety of options and adaptations of the refrigerated transport body.

2.2.3 New insulating materials and technologies

Facing the challenge of insulation performance and also sustainability, insulating material manufacturers are developing new products and different arrangements and materials for manufacturing the insulated enclosures. The reduction of energy consumption and environmental impact of refrigerated transport systems can be achieved by the increase of insulation enclosure performance and energy efficiency of the refrigeration units.

Polystyrene manufacturers must replace R134a as blowing agents in extruded polystyrene (PSE). They have proposed new PSE versions introducing graphite in the foam with a reduced quantity of R134a or without. They are replacing it with CO_2 or hydrocarbons. This allows to keep the same insulating performances or to increase them while reducing the environmental impact. Polyurethane manufacturers have been producing HFCs free foam for 15 years; nevertheless they

are trying to improve the insulation performances. They are testing new chemical mix for the foam but also new blowing agents such as hydrofluorooloeines (HFO). They are announcing higher thermal performances with thermal conductivity lower of ten percent. Insulating material manufacturers have also introduced products such as vacuum insulated panels (VIPs). VIPs consists of an open cell foam slab enclosed in a barrier film (Brown et al., 2007) which ensures the insulated core to be sealed against air and moisture diffusion. A gas absorber, also known as getter, absorbs water vapour, atmospheric gases and gases emitted by the slab during the life of the panel to maintain the vacuum.

The main benefit of the VIPs is that the thermal conductivity of such a system is much less than the one of polyurethane or standard silica aerogel. Hammond and Evans (2014) presented a paper to study the viability of the use of vacuum insulating panels in the refrigeration sector. As reported in Figure 2.50, the thermal conductivity of such a system is much less than the thermal conductivity of polyurethane or standard silica aerogel. In their study, they demonstrated that the economical convenience (based on the assumed prices for a non-conventional technology) is possible, if the life of the component is long enough to recover the extra cost via the energy consumption reduction.

Nevertheless, vacuum insulation still represents a niche on the market due to its expensive cost and time-consuming process. Another disadvantage of VIPs is their vulnerability during manufacturing, during application and in use since the barrier film is very easily punctured. A simple puncture may immediately deteriorate the insulation of the panel. In the case of refrigerated transport, the mechanical stress due to load and unload of the goods and the vibrations, is a factor which can compromise the vacuum causing damage to the sealing or contamination of the goods with aerogels which are toxic. For this reason, because of their weak mechanical seal, manufacturers may adopt this technology in the form of hybrid solution (Panozzo, 1999), containing vacuum insulation inserted in the polyurethane structure.

With regard to aerogels, they derive from silicate materials and also present very high insulation performances but with very low mechanical resistance alone.

The thermal conductivity of the monolithic aerogels is around 0.018 $W.m^{-1}K^{-1}$ at ambient pressure (1.01 bar). They represent a structural morphology (amorphous, open-celled nanofoams) rather than a particular chemical constituency and are already used in some insulated parcels for distribution of very high value products. Their principal benefits are higher insulation properties when compared to PU foams and, contrary to traditional materials, a possible absence of ageing. However, the use of such materials will prevent challenges as it does not have the structural strength that foam has especially when incorporated into a sandwich panel that many structures now rely on (Lawton and Marshall, 2007).

Glouannec et al. (2014) presented an experimental and numerical design study of an insulation wall for refrigerated integral panel van, taking into account the thermal properties of the insulating multilayer panel, the impact of the external environment (solar irradiation, temperature) and durability. The different experimental and numerical tools developed allowed the dynamic characterization of the thermal transfer within several multilayer insulation walls. The interest of increasing the wall insulation was highlighted. In particular, reflective multi-foil insulation and aerogel layers gave good results, especially for limiting peak heat transfer and energy consumption during the daytime period. Thus, increasing the multilayer panel thickness by 20% led to a 36% reduction of energy compared to a reference case. Moreover, this study showed that the evaluation of the wall heat transfer coefficient according to the ATP criteria is insufficient due

to the considerable influence of solar irradiation was highlighted. This can increase the peak heat transfer by up to 43%.

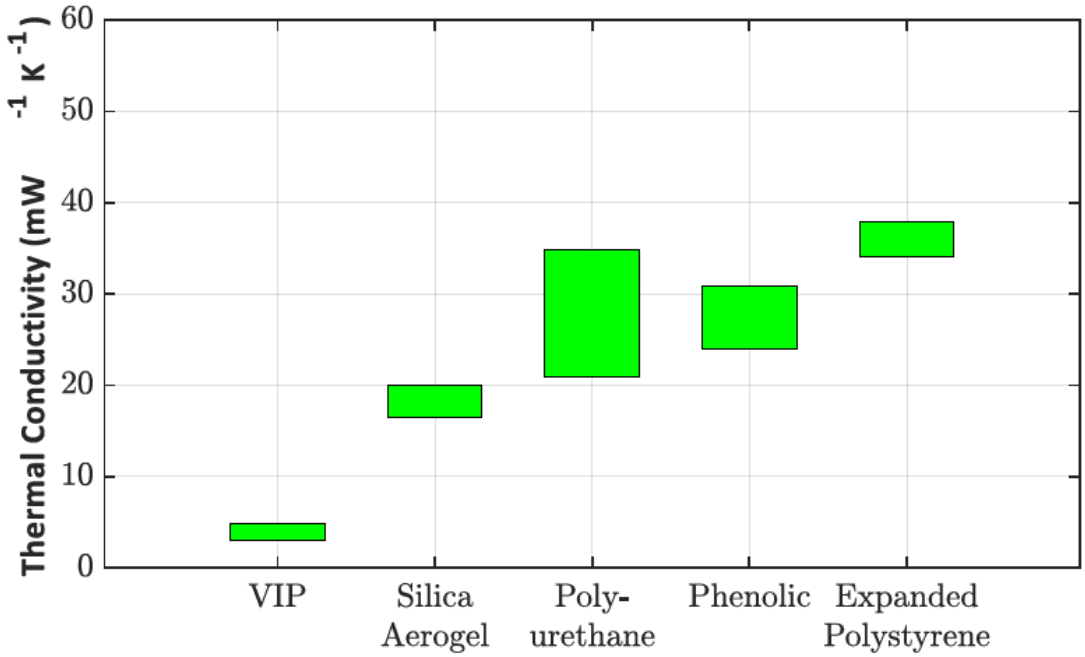

Figure 2.50 Comparison of thermal conductivities of insulating materials (Hammond and Evans, 2014).

An advanced energy technology that is attracting the interest in cold-chain systems concerns the thermal energy storage based on phase change materials (PCMs). PCMs are substances characterized by a high heat of fusion, capable of storing and releasing large amounts of energy, thereby producing the cooling effect necessary to maintain a constant temperature throughout the journey.

The combination of PU foams and micro-encapsulated phase change materials i.e. PU–PCM foam is an interesting way to combine the advantage of thermal insulation and thermal energy storage capacity. In such composite foams, PCM micro-capsules are dispersed in a polyurethane foam matrix during the production process, i.e. directly during the mixing stage of the liquid reaction components. In recent years, several papers have investigated the incorporation of PCM in a PU matrix (Borreguero et al., 2010, Tinti et al. 2014, Copertaro et al., 2016). Most of these studies focused on synthesis methods and the thermal energy storage

capacity of the composite but few studies have dealt with thermal evaluation of PU-PCM foams in use. Moreover, all these studies focused on composites with a low PCM mass content (< 25%) (Yang et al., 2015). Promising results have been obtained, especially for refrigerated transport applications. Thus the feasibility of the incorporation process has been demonstrated though no significant evolution of thermal conductivity has been observed for a PCM mass content from 4.5% to 13.2% (Tinti et al., 2014)

Great improvements could be achieved by changing the manufacturing technology and selecting new materials. A better insulation performance may be obtained also by reducing thermal bridges or using rare gases (Kripton and Xenon, whose thermal conductivity is very close to that of R11

and the use of foams whose cells shall have nano-dimensions). As example see the study presented by Panozzo et al. (2011). However, as much as it may be useful, intervening on the insulating material alone is not enough to improve the insulation performance of refrigerated vehicles suitable for the transport of perishable products. As a matter of fact, these undergo to the ageing phenomenon which depends on several factors. Evidence of this is shown in Figure 2.51, confirming that the insulating materials are not the only factor of the ageing: the K values of all the vehicles become worse regardless of the type of insulation material used, with open cells or even in fibrous shape (Boldrin et al., 1990). The next section therefore deals with the studies already present in the literature on the ageing phenomenon.

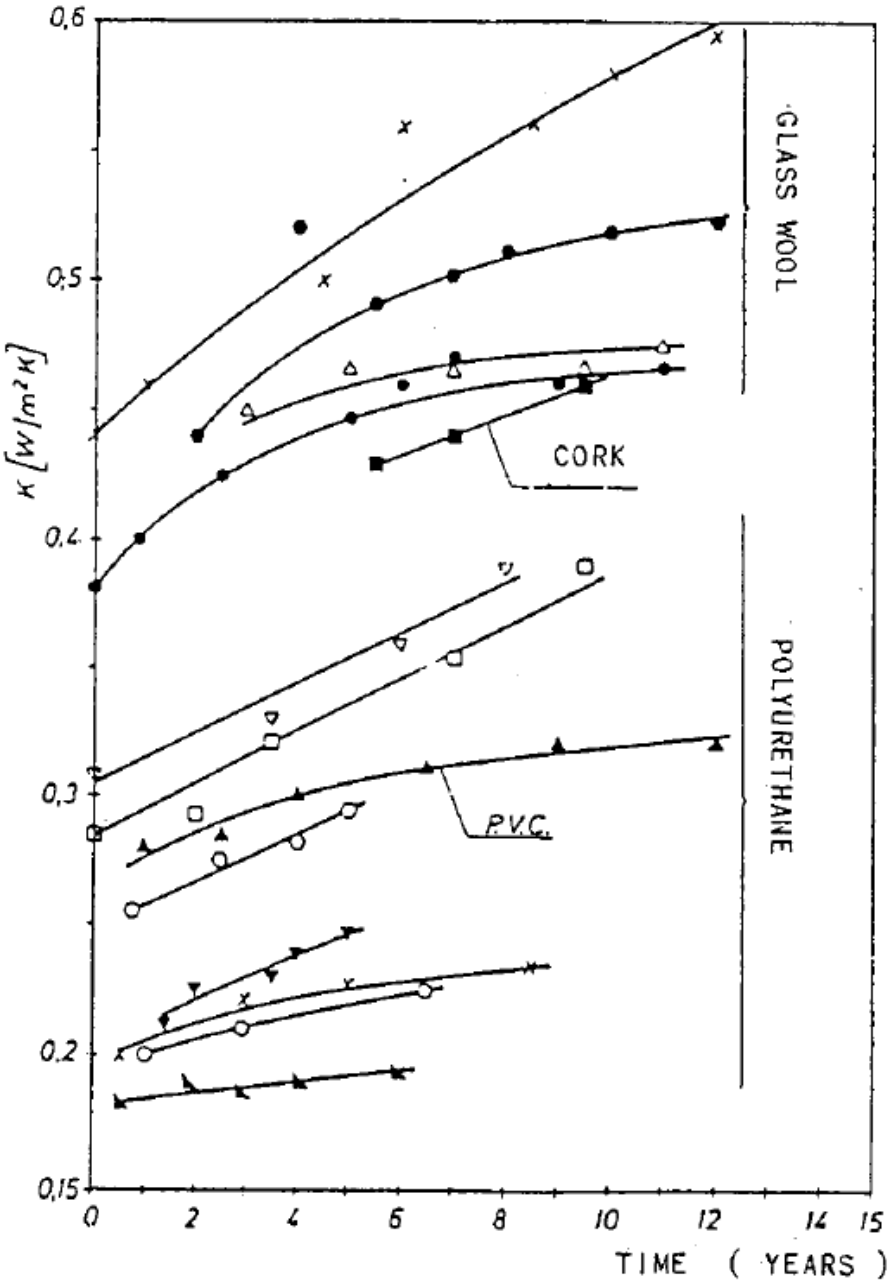

Figure 2.51 Experimental data about K coefficient evolution during the time of different railway cars realized with different insulating materials (PU, PVC, natural insulant such as cork, fibrous insulant like glass wool). (Boldrin et al., 1990).

2.3 Ageing of refrigerated transport vehicles

An important concern for refrigerated vehicles is the "ageing" of the insulation material: after the foaming, the gas trapped into the foam cells tends to migrate due to concentration difference with the environment, mechanical vibration, damages and environmental effects (Mastrullo et al., 2019). The performance of insulated enclosures of refrigerated vehicles is usually characterized by their overall insulation coefficient ("K coefficient") and a parameter measuring the percentage increase of the K value over the time is defined as a possible measure of the ageing. The increase of K with the time may lead to excessive temperature ranges in the cargo space and faster warming in the absence of refrigeration (Lawton and Marshall, 2007). The oversizing of the cooling power of the refrigeration unit counteracts the excessive temperature ranges due to the increasingly ageing but results in greater energy consumption and environmental pollution through GHG emissions.

Considering that the refrigerated road transport fleet amounts to some four million pieces of equipment in service worldwide (Cavalier and Tassou, 2011), the effect of refrigerated transportation on the environment is not negligible. In the perspective of reducing food losses and limiting the contribution of refrigerated transport to pollution, it is of major importance to understand the phenomena involved in the ageing process of insulated enclosures of refrigerated vehicles in order to find ways to prevent it.

The various definitions of ageing used by other authors will be introduced in the first section of this paragraph. Then, recent studies on the ageing are reviewed highlighting the studies that discriminated the factors having an influence on the ageing process including those which tried to model it.

2.3.1 Definitions of ageing

The ageing of a refrigerated vehicle used in the carriage of perishable foodstuffs may be quantified through the evolution over the time of the K coefficient. The French regulation requires that this coefficient is measured for all the in-service vehicles after twelve years from their purchase whereas immediately after the manufacturing only the K coefficient of the prototype, K_p, is measured to certify the whole series. The K coefficient measurement at twelve years allows renewing the ATP certificate for other six years, after which the K coefficient test must be repeated for a renewal of a further six additional years. According to this rule for renewal, the ageing evaluation may be made by comparing the K coefficient value of the in-service vehicle at the twelfth year of life, K_{12} to the initial K value of the prototype equipment, K_p , through their ratio, A_{12}:

$$A_{12} = \frac{K_{12}}{K_p} \qquad \text{Eq. (2.5)}$$

Another way to evaluate the ageing rate is through the average annual ageing coefficient introduced by Boldrin et al. (1993):

$$C.I.A. = \frac{K_n - K_p}{K_p\, N} \qquad \text{Eq. (2.6)}$$

Where, K_n is the coefficient value of the in-service vehicle at the n-th year and N is the number of year of the vehicle's life.

Panozzo et al. (1999) also introduced a parameter called "Quality coefficient", defined as:

$$QC = \frac{K_{theoretical}}{K_{measured}} \qquad \text{Eq. (2.7)}$$

This parameter was introduced to calculate the ageing of a single vehicle, when its K value was measured only after some years of service and the initial value is unknown.

The $K_{theoretical}$ is a computed value which assumes that the thermal resistance of the whole body is related only to the insulating foam and gives an ideal reference value that neglects the thermal bridges due to geometric singularities. It is defined as follows:

$$K_{theoretical} = \lambda \frac{\sum \frac{S_i}{\delta_i}}{\sum_i^n S_i} \qquad \text{Eq. (2.8)}$$

Where, λ is the initial thermal conductivity of the foam, while S_i and δ_i are respectively, the mean surface and the thickness of the i-th wall of the insulated body. Previous studies (Boldrin et al., 1990) concluded on a statistical basis that the contribution of bridges and singularities can reach up to 30-35% of the theoretical value.

2.3.2 Factors affecting the ageing of refrigerated transport equipment

The evolution of K coefficient with time can be very different from one vehicle to another due to many factors, whose analysis and modelling has been previously treated by several studies. Boldrin et al. (1990) Boldrin et al. (1993), Panozzo et al. (1995) and Panozzo et al. (1999) presented an amount of data statistically relevant related to the ageing of different categories of vehicles for the refrigerated transport working under different conditions (types of goods, working temperatures). The analysis of the data collected at the ITC-CNR of Padova allowed isolating the causes of the ageing over the time and classifying them in two main categories:

- physical-chemical factors and,
- mechanical factors.

It is necessary to underline that in these studies, the ageing was evaluated by comparing the K value measured at twelve years of life and the initial K value which had not been measured but calculated. As already mentioned, the ATP regulation does not require the initial K coefficient test on all vehicles produced in the series, but only on a prototype vehicle.

2.3.2.1 Physical-chemical factors

Panozzo et al. (1999) defined the ageing as a degradation of the thermal insulation properties of the insulated enclosure which main causes are related to:

- permeability of the foams to the gases (air and blowing agents),
- condensation of water into the foam cells,
- increasing of the percentage of the open broken cells.

These causes explain the ageing from a physio-chemical point of view and primarily concern the panels used to build the insulated enclosure and the insulation materials itself.

The first point, the permeability of the foams to the gases, is due to the fact that partial pressures of the gases inside the cells of the polyurethane foam constituting the sandwich panels change over the time altering the contributions of each individual gas to the overall conductivity of the mixture. Therefore the gas molecules are able to migrate through the solid material in a long time even if it is apparently impermeable.

This phenomenon was analyzed and modeled by Panozzo et al. (1995) considering a standard sandwich panel, composed by polyurethane foam (density of 32 $kg.m^{-3}$, thickness of 95 mm) foamed with R11 as blowing agent and by an external and internal cover sheets, (thickness of 2.5 mm), made of polyester resin reinforced by glass wool (GRP).

From the results presented by these authors it emerges that:

- the carbon dioxide produced by the polymerization comes out relatively quickly and after 30 days its partial pressure is about a tenth of the initial pressure;
- the direct influence of the water vapour (in gas phase) is negligible in the ageing phenomena: the partial pressure, due to diffusion is very low in comparison with the partial pressures of air and R11.
- the permeability of the wall to the air is higher than that of halogenated hydrocarbons by almost an order of magnitude, so the phenomenon initially implies a substantial entry of air into the cells (where its initial partial pressure is close to zero) with reduced reduction of the partial pressure of the blowing agent. The total pressure increases compared to the initial pressure and the cells “swell”, a thing that may cause serious problems to the insulated enclosures;
- the blowing agent comes out more slowly and therefore there is a long phase in which the total pressure increases and the air concentration increases: having air a conductivity 78 higher than R11 (or similar), the apparent conductivity increases. Subsequently, the blowing agent begins to come out from the polyurethane foam: the total pressure decreases and the percentage of air increases even faster, with a consequent increase in conductivity.

Corain et al. (2010) modeled these phenomena and proposed the shape of the theoretical ageing curve for bare polyurethane panels, shown in Figure 2.52a and 2.50b, where the percentage ageing ($100\ \frac{K_n - K_p}{K_p}$) is plotted as a function of the years of life of the vehicle. Figure 2.52a represents the theoretical ageing curve in logarithmic scale for a refrigerated vehicle. The first inflection point, close to the origin, is due to the phenomenon of air inlet in the polyurethane cells composing the sandwich panels of the vehicle. The second inflection point models the loss of blowing agent from the cells. The useful part of the curve arrives to 30 years (see Figure 2.52b). This shape of the

ageing curve reflects the assumption that the major effect on the ageing is due the migration of the air from the environment into the closed cells of the foam (the opposite migration of the blowing agent to the environment is too slow due to the larger dimensions of the blowing agents molecules in comparison with the molecules of the air, like O_2, N_2, CO_2, H_2O).

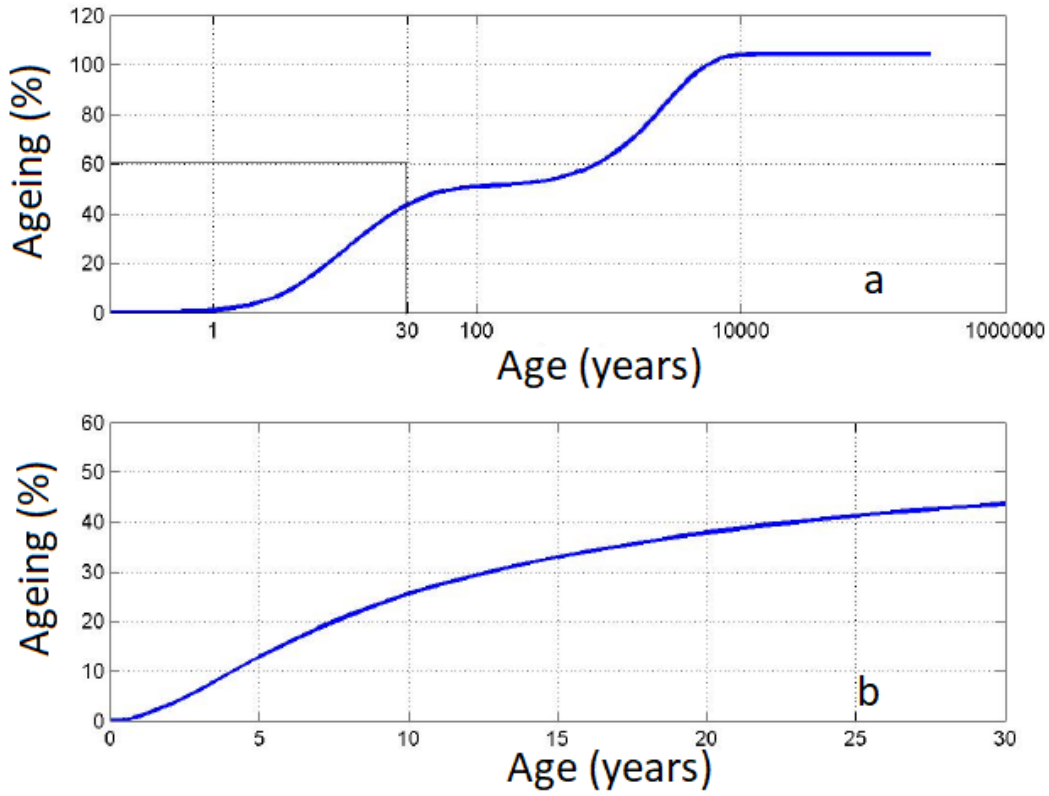

Figure 2.52 a) the theoretical ageing curve in logarithmic scale for a refrigerated vehicle; b) curve in linear scale time showing the useful period for the ageing (Corain et al., 2010).

2.3.2.2 Mechanical factors

Ageing of refrigerated vehicles also has a mechanical component due to the movements on the road, the routes covered and the payload. The effect of only some of these factors was analysed in previous studies. The statistical analysis carried out by Panozzo et al. (1999) highlighted the influence in the ageing rate due to the meat rails and to the refrigerating units As pointed out by the authors, in presence of these accessories, the mechanical stresses are signficantly increased. The meats, for example, left hanging and free to move during transport stress structurally the load compartment until compromising its insulating capacity.

These aspects are highlighted in Figure 2.53a and 2.53b, showing respectively the ageing rate as a function of the years for vehicles in presence or absence of the refrigerating unit and in presence or absence of meat rails. The populations of these vehicles were selected in such a way that the composition should be homogeneous for the parameters: thickness of the walls, number of the doors and also type of use. Panozzo et al. (1999) pointed out that in the first case (Figure 2.53a) the difference of the ageing curves is appreciable only when the vehicle is aged (after more than

12 years of service that is a limit of normal use for some European markets); in the second case (Figure 2.53b) the difference is evident since the beginning of the useful life and increases with the service time.

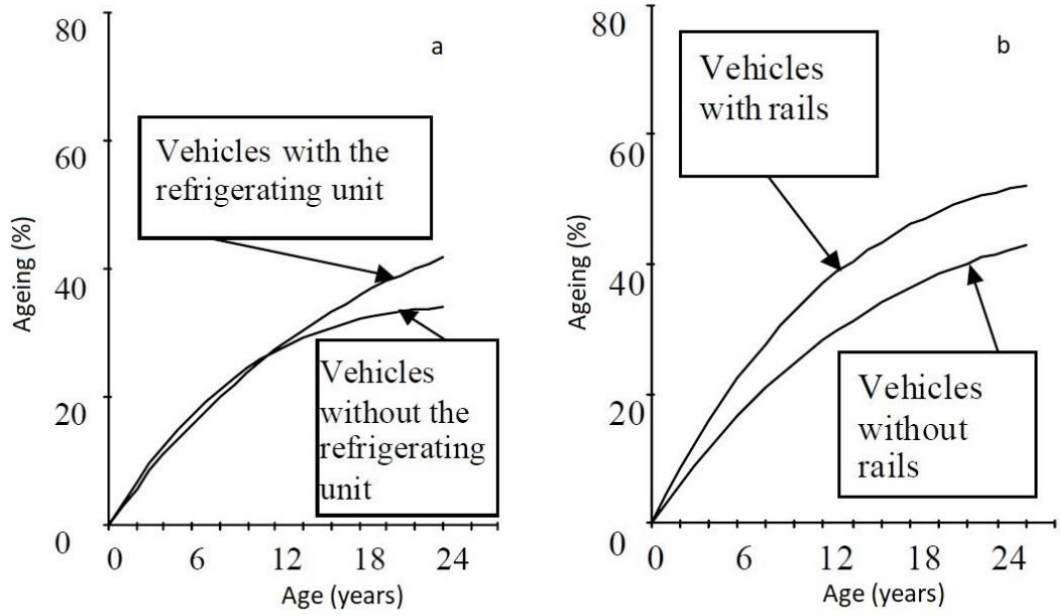

Figure 2.53 a) influence of the refrigerating units on the ageing rate; b) influence of rails for meat suspending on the ageing rate (Panozzo et al., 1999).

Another mechanical factor analyzed by Boldrin et al. (1993) concerns the type of transported foods. As shown in Figure 2.54 the average annual ageing coefficient (see Eq.2.6) is greater for those vehicles used for general and meat transport.

Corain et al. (2010) proposed a mathematical formulation of the ageing curve which is able to take into consideration both the effects of structural characteristics, operation and maintenance practices, and those resulting from the physical processes involved in the heat transfer within the insulating panel. That model has been calibrated with respect to the data available through the ATP database (for details, see Panozzo, 2009). As main results, authors stated that many structural factors, i.e. the presence of rails and refrigerating unit significantly affect the ageing process. The curve resulting from this model is plotted with experimental results in Figure 2.55 and it is possible to see that there is an immense data dispersion and that only few data are following the theoretical trend.

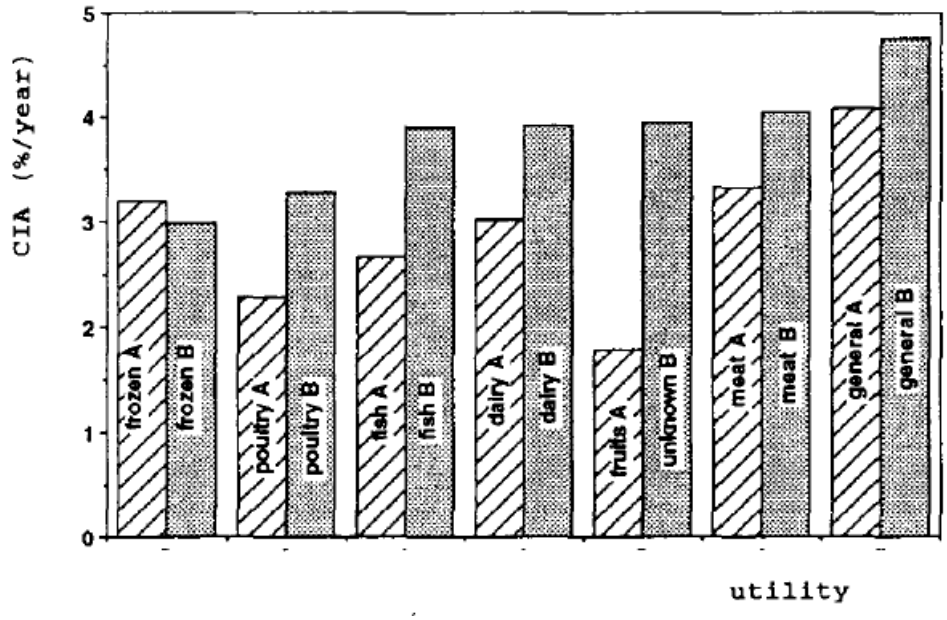

Figure 2.54 Average ageing coefficient, subdivided in function of the type of transported foods for the sample A containing 150 vehicles and for sample B containing 458 (Boldrin et al., 1993).

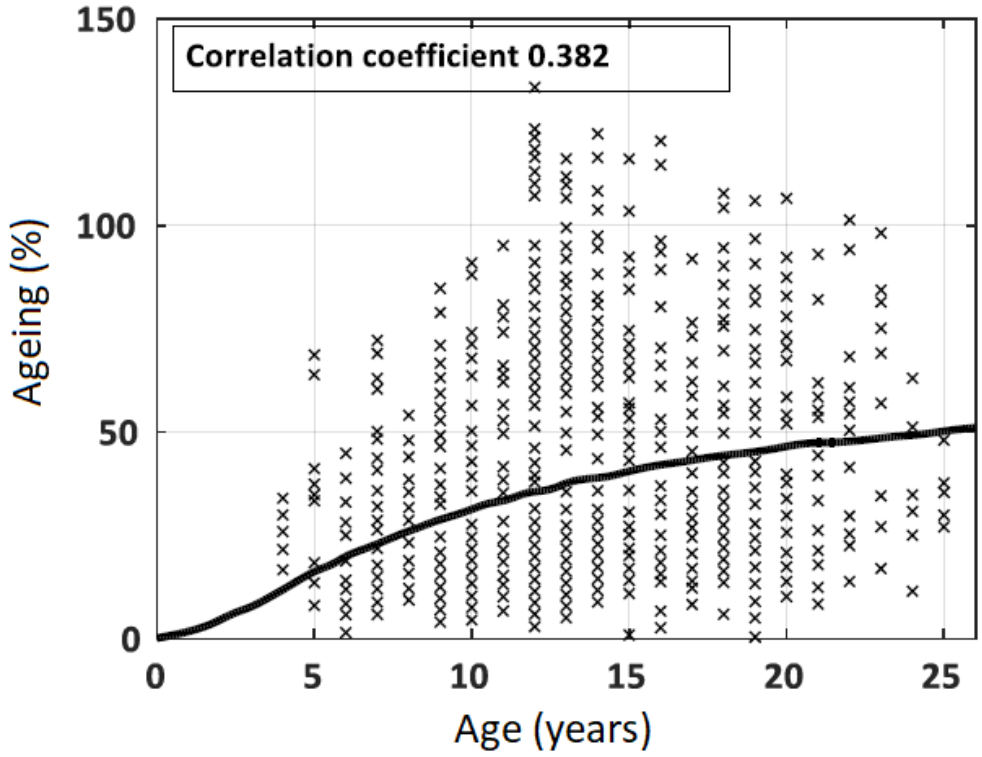

Figure 2.55 Ageing percentage variation over the time. Black, continuous line: theoretical curve based on diffusion of gases trapped in the cells under certain conditions typical for a class of refrigerated vehicles. (Corain et al., 2010)

2.4 Introduction to Big Data and Machine Learning

The development of the IoT (internet of things) and Artificial Intelligence (AI) markets offers an potential opportunities for temperature-controlled transport. It is a market that is expected to generate close to 90 billion USD in 2025, with developments expected to take place mainly in the United States, Europe and Asia-Pacific, as shown in Figure 2.56. As highlighted in a recent study carried out by Cemafroid (Fertel and Cavalier, 2020), this rapidly expanding market will influence temperature-controlled transport because for its "hardware" deployment it requires temperature-sensitive electronic components that require specific, well-controlled transport conditions. Moreover, as the miniaturization of Internet of things (IoT) devices increases, voluminous amounts of data have been produced. However, such data is not useful without analytic power. This also occurs in the refrigerated transport and cold chain sector where huge amounts of data are generated and need to be processed and analyzed. The quantitative explosion of digital data has forced researchers to find new ways of seeing and analyzing the world. It is about discovering new orders of magnitude in the capture, retrieval, sharing, storage, analysis and presentation of data. Thus was born the concept of "Big Data".

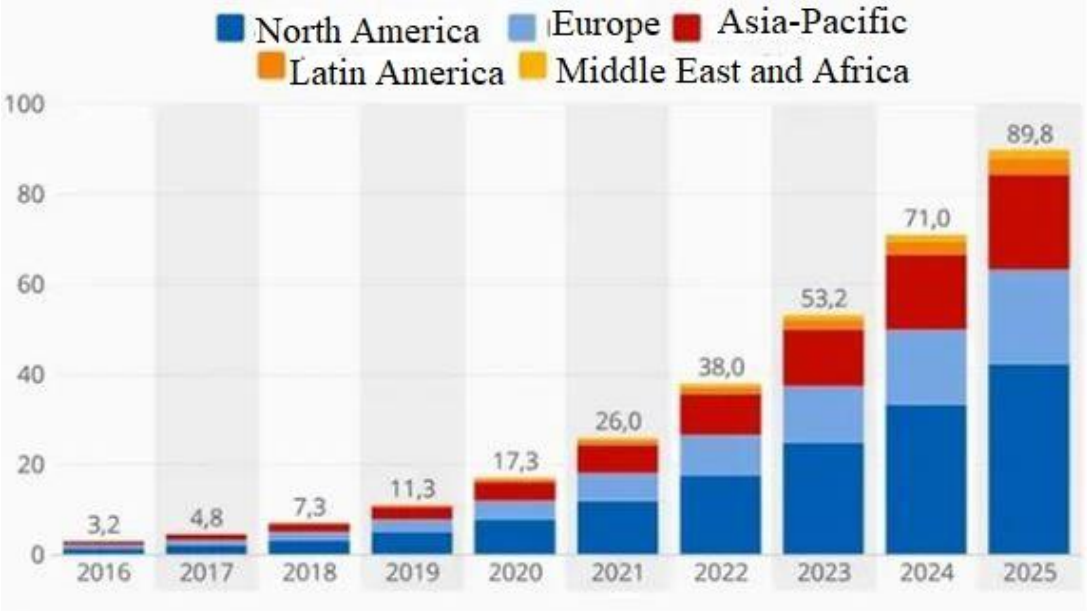

Figure 2.56 Projected growth (in billion of USD) of the AI market between 2016 and 2025 (Boittiaux, 2018).

Nowadays, most small size to large size organizations use a Data Base Management System technology (DBMS), which is a system responsible for the efficient storage and retrieval of the data in databases. The cardinal point is therefore the existence of a database, an organized collection of logically inter-connected data items. Today every field of study, be it Basic Sciences, Applied Sciences, Engineering, Social Sciences, Bio-Medical Sciences and so on, are dealing with Large Scale datasets and lot of work is being carried out to better harness and process Big Data, using domains like Machine Learning (ML) which holds tremendous potential in handling modern data challenges.

The topic of Big Data and Machine Learning is contextualized within this thesis because, as already seen in subparagraph 2.1.3.7, Cemafroid has a large amount of data accumulated over the years through two DBMS. From these data, the objective is to efficiently obtain the information necessary to study the ageing of vehicles used in the cold chain. The following paragraphs aim at introducing those techniques of Big Data and Machine Learning that will be applied to the Cemafroid databases. The results of such analyses will be presented in Chapter 4.

First of all, what is big data and what is machine learning, then the main definitions used for data pre-processing and data analysis are recalled. Finally the techniques of regression and classification in machine learning are discussed. These are, in fact, the techniques applied in Chapter 4 to the available databases to study the ageing of refrigerated transport equipment through a numerical approach.

2.4.1 Big data and Machine Learning concepts

Big data is a relatively new concept but the storage and analysis of data is a branch of applied computer science that existed for several years.

Laney (2001) defined Big Data has with the '5V's' concept:

Volume: until 2010, an estimated 13 000 exabytes of data was generated where 1 exabyte equals 1 Billion Gigabyte. The volume of the current Big Data datasets is a significant attribute as such datasets are considered out-of-scope in terms of prevailing traditional Database Management Techniques.

Velocity: velocity is the rate at which the data is being collected. With the increase in the accessibility of Internet over the globe and integration of machines and processes with Internet and centralized data collection techniques, the speed at which data is collected increases continuously.

Variety: Along with the volume and the rate of data generation, the type of data is also an important attribute in defining Big Data. Data collected can be structured or unstructured. Structured data is the systematic data collected from sources such as sales or financial transactions, reservation systems. Unstructured Data is the data generated from sources such as social media, emails, and communications.

In addition to the traditional definition of Laney, Big Data can be explained with two additional 'V's' with the 5V's concept (see Figure 2.57). The additional two 'V's' being:

Veracity: veracity is often defined as the quality or trustworthiness of the collected data. Considering the accuracy of the collected data and analyzing it, is important. Thus, when it comes to Big Data, quality is always preferred over quantity. To focus on quality, it is important to set metrics around the type of data that is collected and its sources.

Value: Acquiring datasets of the Big Data scale involves substantial investment. The value of a dataset can be determined by estimating the insights that can be generated from the dataset post-analytics **(**XSNET, 2017**).**

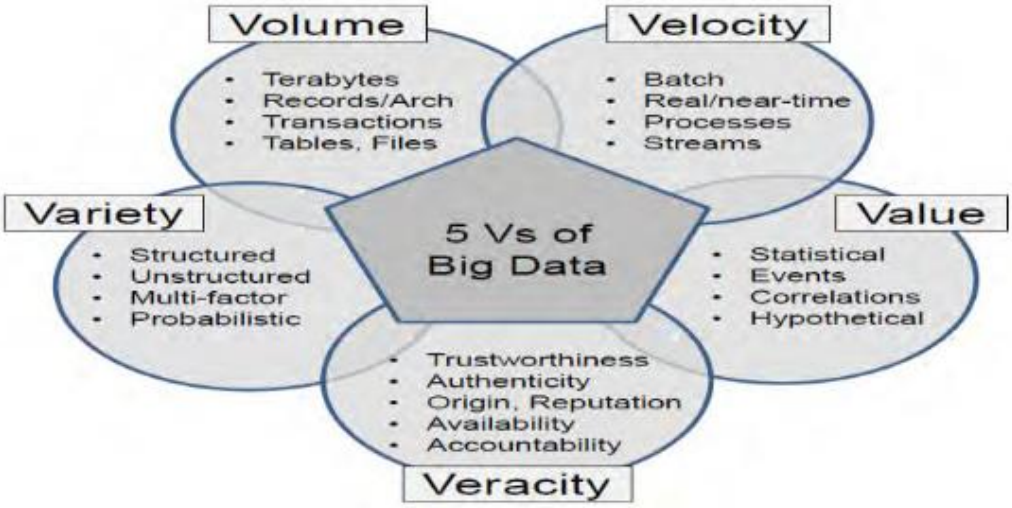

Figure 2.57 5Vs of Big Data (Ishwarappa and Anuradha, 2015).

Organizations and companies today have more data at their disposal than ever. Few would argue that it is necessary lifeblood of their business. As pointed out by Herjolfsson (2019), this is especially true in the cold chain, a temperature-controlled segment of the supply chain for products that require an uninterrupted series of refrigerated production, storage, and distribution activities to maintain a strict low-temperature range end-to-end. Over time, data and information collected in real time may help companies to ensure product delivery, reduce delivery times, improve product shelf life, and accelerate the shipping and quality review process. Data-based insights can also be used to improve supplier and partner relationships and eliminate bad players in the supply chain. As highlighted in a recent study realized by Accenture (Awwad et al., 2018), companies with a disciplined strategy of utilizing Big Data Analytics had bigger returns for their respective investments in Big Data Analytics. These returns are shown in Figure 2.58. At the top of these returns there are 46% improvement in customer service and 41% faster and more effective reaction time to supply chain issues.

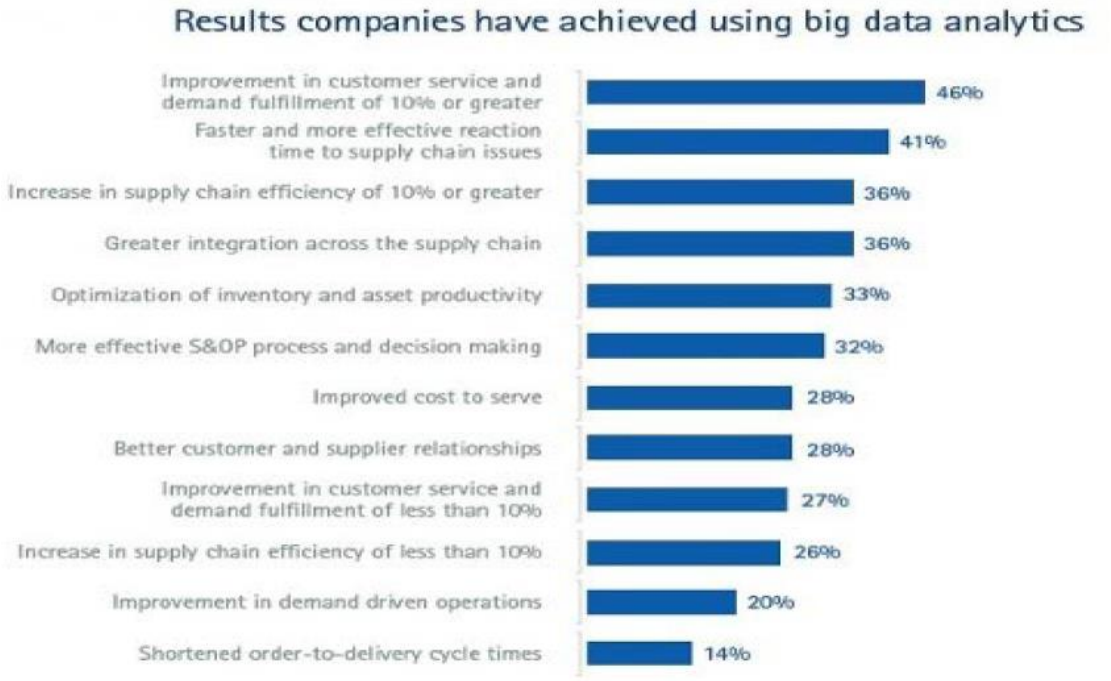

Figure 2.58 Results achieved using Big Data (Miguel and Gómez, 2016).

IoT and cloud technology now enables enterprises to collect data and reverse it quickly and intelligently. The most important benefit of IoT in cold chain logistics is increased efficiency and productivity. The traditional processes involved in cold chain logistics are time-consuming and involve excessive human intervention. For example, a standard temperature monitoring process currently involves manual readings that need to be monitored and analyzed constantly. The data then needs to be manually entered into a system and then analyzed to get a complete overview of the logistics cycle. This proves to be a very time consuming and inefficient process. However, with an IoT enabled supply chain management system, the temperature readings can be done in real-time and be automatically updated in the system. In the field of refrigerated transport, transport companies may acquire information regarding their shipping lanes (ocean, air, road, and rail), packaging, products shipped, suppliers and logistics partners and can thus make targeted decisions that can improve efficiency and reduce product waste and operations.

While data collection is important, it is only a part of the story, as it is only as useful as the quality of actionable insights that it provides. Incomplete or inaccurate data capture, or focusing on the wrong data altogether, leads to bad analysis and poor decision-making. This is made worse when data collection is a manual or ad hoc process that is prone to error and therefore increases costs and risks, as has been the case in the cold chain until relatively recently.

Once it has been clarified that the concept of Big Data refers to the possibility of having information, Machine Learning describes one particular method to analyze the data and then use the information that can be extracted from them.

Machine Learning is therefore a field of AI (Artificial Intelligence) that can be broadly defined as computational methods using experience to improve performance or to make efficient and accurate predictions starting from existing data.

Samuel (1959) defined Machine Learning as the field of study that gives computers the ability to learn without being explicitly programmed.

As stated by Géron (2017), Machine Learning may be helpful for:

- problems for which existing solutions require a lot of hand-tuning or long lists of rules: one Machine Learning algorithm can often simplify code and perform better;
- complex problems for which there is no good solution at all using a traditional approach: the best machine learning techniques can find a solution;
- fluctuating environments: a machine learning system can adapt to new data;
- getting insights about complex problems and large amounts of data.

The two relational databases available at Cemafroid (introduced in subparagraph 2.1.3.7) encourage to take the advantages of Big Data and Machine Learning techniques into account for their analysis. The information to be extracted from these data is how vehicles subjected to refrigerated transport are ageing and the main factors that determine this ageing phenomenon. The final objective, through this information, is to create a predictive ageing model.

2.4.2 Main definitions

Basic notations and definitions used in this thesis to study the available database and then look at the problem of ageing from a numerical point of view are recalled in this section. It is important to point out that terminology often changes depending on the field of application of informatics and mathematics (Big Bata, Machine Learning, and statistics). The main definitions used in this thesis are the following ones (see Levene et al., (1999) and Mohri et al., (2012) for further details).

Dataset: a dataset is a collection of data. In the case of tabular data, a dataset corresponds to one or more tables extracted from a database, where every column of a table represents a particular variable, and each row corresponds to a given record of the dataset in question. Several characteristics define the structure and properties of a dataset. These include the number and types of features and labels, defined below.The data used to build the final model usually comes from multiple datasets. In particular, the three following datasets are commonly used in different stages of the creation of a model and will also be used in Chapter 4:

1. ***Training sample****:* it is a set of examples used to fit the parameters of a model. The model learns from these data. In practice, training data help the machine to connect the patterns in the data to the right answer.
2. ***Validation sample***: the sample of data used to provide an unbiased evaluation of a model fit on the training dataset while tuning model hyper-parameters, where a hyper parameter is a parameter whose value is used to control the learning process. The evaluation becomes more biased as skill on the validation dataset is incorporated into the model configuration. The validation set is used to evaluate a given model, but this is for frequent evaluation.
3. ***Test sample***: a test sample is a dataset that is independent of the training dataset, but that follows the same probability distribution as the training dataset. The sample of data used to provide an unbiased evaluation of a final model fit on the training dataset. The test sample is only used once a model is completely trained (using the train and validation sets).

Features*:* as definedby Bishop (2006) a feature is an individual measurable property or characteristic of a phenomenon being observed.

Consider the training dataset as the one in Table 2.8: the average surface of the insulated enclosure, the type of vehicle and the issued ATP class are the features (or features) which are often represented as a vector, associated to an example.

Table 2.8Example of features of a dataset.

Average Surface of the insulated enclosure (m^2)	Type of vehicle	Issued ATP class
70	Truck	FRC
23	Van	FRAX
155	Semi-trailer	FRC
35	Van	IN

Labels*:* they are the final output. When data scientists speak of labeled data, they mean groups of samples that have been tagged to one or more labels. In the dataset of Table 2.1, the different type of vehicles such as van, truck or semi-trailer is called label.

After introducing the basic notations of a database, the existing Machine Learning algorithms useful for their study have to be introduced.

Machine Learning systems can be classified according to the amount and type of supervision they get during training (Géron, 2017). There are three major categories: supervised learning, unsupervised learning and reinforcement learning.

Supervised learning is where there are input variables and an output variable, and it is possible to use an algorithm to learn the mapping function from the input to the output. The goal is to be able to classify new and unknown values given known observations of other variables. Hence, supervised learning develops predictive models based on both input and output data.

Unsupervised learning consists in having only input data and no corresponding output variables. The aim of unsupervised learning is to find patterns in the data in order to learn more about the data. Therefore, data are grouped and interpreted based only on the input data.

Reinforcement leaning focuses on regimented learning processes, where a Machine Learning algorithm is provided with a set of actions, parameters and end values. By defining the rules, the machine learning algorithm then tries to explore different options and possibilities, monitoring and evaluating each result to determine which one is optimal (Makkar et al., 2019)

As the main goal of the thesis is to study and predict the ageing of refrigerated transport vehicles, the type of Machine Learning used is the supervised one

The predictive modeling is divided into two main types of problems: the regression problem and the classification problem which implies to this thesis. In particular, some of the most important supervised learning algorithms are:

- k-Nearest Neighbors;
- linear regression;
- logistic regression;
- support vector machines (SVMs);
- decision trees and random forests;
- neural network.

Decision trees and random forests algorithms are used in this thesis and applied to the available data for the study of the ageing of refrigerated vehicles. Decision tree is quite easy to understand and interpret, however, a single tree is not sufficient for producing effective results:for this reason a random forest of 2000 decision trees was used to build the prediction model. Before presenting these algorithms, it is important to consider that in order to solve a given problem of supervised learning; one has to perform the following steps:

- selection of the data
- data pre-processing
- choose an algorithm
- training , testing and fitting a model;
- validating the model method.

Each of these steps is briefly introduced in the following subparagraphs to be then applied to the available databases in Chapter 4.

2.4.3 Data selection

One of the most important goals of any machine learning study is to obtain good quality data from the available databases. This primary objective requires several steps, of which, the first one is the data selection phase. The selection of the dataset needs an accurate knowledge of the database from which the data is taken. This accurate knowledge of the database and its relational scheme allows realizing the request for data extraction from the database in the most appropriate way possible. A properly executed extraction lays the basis for continuing the study of the data in the most correct way. In order to interact with databases and therefore to perform a data extraction there is, today, a standardized language called SQL (an acronym that stands for Structured Query Language). This language has been used in this thesis for the extraction of data from the two available databases (already presented in Chapter 2, subparagraph 2.1.3.7) both by the external provider that manages the Datafrig® database and internally for the extraction of data from the second available and directly accessible database in Cemafroid (the one collecting results of experiments carried out in Cemafroid since 1999). It is important to have an idea of what are the tuples the user is looking for, and more importantly what distinguishes them from the other tuples in the database: being able to separate the desired tuples from the others is what makes it possible to later write a SQL query, with selection conditions that capture the desired characteristics

The main components of SQL queries are the following.

- **SELECT**: it is the essential command that initiates every SQL query and is called the projection clause establishing which columns are to be reported in the final result;
- **FROM**: it is the keyword that allows defining which tables, views, or subqueries will be used as data sources. It is also in the FROM clause that it is possible to define junctions between tables.
- **WHERE**: this command in a SQL query allows extracting the rows from a database that respect a condition. This ensures obtaining only the desired information.

For example, let us imagine making an extraction from the Cemafroid database (the one recording the results of the experiments carried out in its climatic chambers) introduced in subparagraph 2.1.3.7. Let us also imagine one wants to extract the information about the nature of the walls insulation and, in particular, to extract only those vehicles whose blowing agent is the

cyclopentane. This information is recorded in the table of the database called “Intervention” (see Table 2.6).

The extraction will therefore be carried out in this way:

SELECT Nature of side walls insulation, Nature of floor insulation, Nature of ceiling insulation, Nature of rear wall insulation, Nature of front wall insulation.

FROM Intervention.

WHERE Nature of side walls insulation=“cyclopentane”, Nature of floor insulation= “cyclopentane”, Nature of ceiling insulation=“cyclopentane”, Nature of rear wall insulation= “cyclopentane”, Nature of front wall insulation=“cyclopentane”.

By executing these commands it is possible to extract the desired information from the available databases.

2.4.4 Data pre-processing

Data pre-processing phase is the first crucial step, since it leads to better data sets, cleaner and more manageable. During pre-processing the raw data is transformed in a form that can support effective ML applications (Bengio et al., 2013).

Using Excel and SQL Management Studio, both available databases in Cemafroid were analysed and linked together. Data were then cleaned and pre-processed.

The following is an introduction to the concepts of data pre-processing applied to the available data in Chapter 4.

Data pre-processing includes cleaning, instance selection, normalization, transformation, feature extraction and selection, etc. The product of data pre-processing is the final training set. This phase as pointed out by Olivieri et al. (2019) may affect the way in which outcomes of the final data processing can be interpreted. Kotsiantis et al. (2006) reviewed most important data pre-processing actions, presenting the know algorithms for each one of these steps. Some of these steps are listed below.

Incomplete data is an unavoidable problem in dealing with most of the real world data sources. The topic has been discussed and analysed by several researchers in the field of ML (Bruha and Franek, 2006; Guyon and Elisseeff, 2003). Generally, there are some important factors to be taken into account when processing unknown feature values. One of the most important ones is the source of ‘unknowingness’, which is worth to be considered because it is found in the available databases of this thesis. This source of unknowingness may be generated as follows:

- a value is missing because it was forgotten or lost;
- a certain feature is not applicable for a given instance, e.g., it does not exist for a given instance;
- for a given observation, the designer of a training set does not care about the value of a certain feature (so-called “don’t-care value”).

Analogically with the case, the expert may choose from a number of methods for handling missing data. Some of these methods (Lakshminarayan et al., 1999) are the following:

- ***Method of ignoring rows with unknown feature values****:* this method is the simplest: just ignore the instances, which have at least one unknown feature value;

- ***Most common feature***: the value of the feature that occurs most often is selected to be the value for all the unknown values of the feature;
- ***Mean substitution***: substitute a feature's mean value computed from available cases to fill in missing data values on the remaining cases. A smarter solution than using the "general" feature mean is to use the feature mean for all samples belonging to the same class to fill in the missing value ;
- ***Regression or classification methods***: develop a regression or classification model based on complete case data for a given feature, treating it as the outcome and using all other relevant features as predictors;
- ***Hot deck imputation***: identify the most similar case to the case with a missing value and substitute the most similar case's Y value for the missing case's Y value;
- ***Method of Treating Missing Feature Values as Special Values***: treating "unknown" itself as a new value for the features that contain missing values.

Noisy Data: missing or incorrect values of data are one of the primary sources of noise in data, which may severely hamper the outcome of applying analytics over the data set containing noise. Traditional mechanisms of removing noise from the data set fails in case of Big Data Processing due to their lack of scalability and it is not possible to simply discard noisy data by deleting them as some very interesting insights may be part of them. Efforts are made to increase scalability of outlier detection for effectively exploring anomalies in large data sets (Singh and Provan, 1996). Outliers are data that appear anomalous or outside the range of expected values.

***Heterogeneous Nature of Data*:** it is the Variety characteristics of Big Data that gather and present data collected from various sources, in different formats and are thus essentially heterogeneous in nature. These heterogeneous data in different formats e.g. unstructured, text, audio and video data formats poses challenges to ML algorithms with regard to their learning rate. It is not possible to treat all the features of a dataset equally important and concatenate them into one as this will not result in an optimal learning outcome and optimal performance. Big Data is seen as an opportunity to learn from multiple viewsin parallel and then learn the importance of feature views with respect to the task to be accomplished. Thus, it will be robust to the data outliers to address optimization and data convergence issues (Cai et al., 2013). The heterogeneous mixture data i.e. the collection and storage of mixed data based on different patterns or rules can be challenging in analysis of large scale data. The solution to deal with such data has been proposed by Ryohei and Satoshi (2012), where authors make a mention of 'heterogeneous mixture learning' an advanced form of analysis technology developed by NEC.

***Discretization of Data*:** it is the process of translating the quantitative data into qualitative data resulting in a non-overlapping division of continuous domain. Decision Trees and Naive Bayes are the examples of some ML algorithms which can only deal with discrete data. Attribute discretization leads to categorization of data which are effective for learning task. However, when dealing with Big Data such traditional approaches are not efficient. The solution is parallelization of standard discretization methods by developing a distributed version of the Entropy Minimization Discretizer based on Minimum Description Length Principle in big data platforms, boosting performance as well as accuracy (Ramirez-Gallego et al., 2015**)**. Another solution is where the data are first sorted based on the values of numerical features and then split into fragments of original class features (Zhang and Cheung, 2014).

***Data Labelling*:** annotations are important in data understanding but the process is quite tedious as data increase in size/dimension. Alternative methods have been proposed for data labelling when dealing with Big Data e.g. Online Crowd-generated repositories which can serve as a source for free annotated training data (Nguyen-Dinh et al., 2013). Probabilistic program induction is another approach to address human-level concept learning. User-specific context is another issue that must be addressed properly; otherwise it will result in diminished performance.

***Feature Representation and Feature Selection*:** the way the data is represented or features are selected (prominent feature identification) affects the performance of ML algorithms (Bengio et al., 2013).

Feature subset selection is the process of identifying and removing as much irrelevant and redundant features as possible (see Figure 2.59). This reduces the dimensionality of the data and enables learning algorithms to operate faster and more effectively. Generally, features are characterized as:

- relevant: these are features have an influence on the output and their role cannot be assumed by the rest;
- irrelevant: irrelevant features are defined as those features not having any influence on the output, and whose values are generated at random for each example;
- redundant: a redundancy exists whenever a feature can take the role of another (perhaps the simplest way to model redundancy).

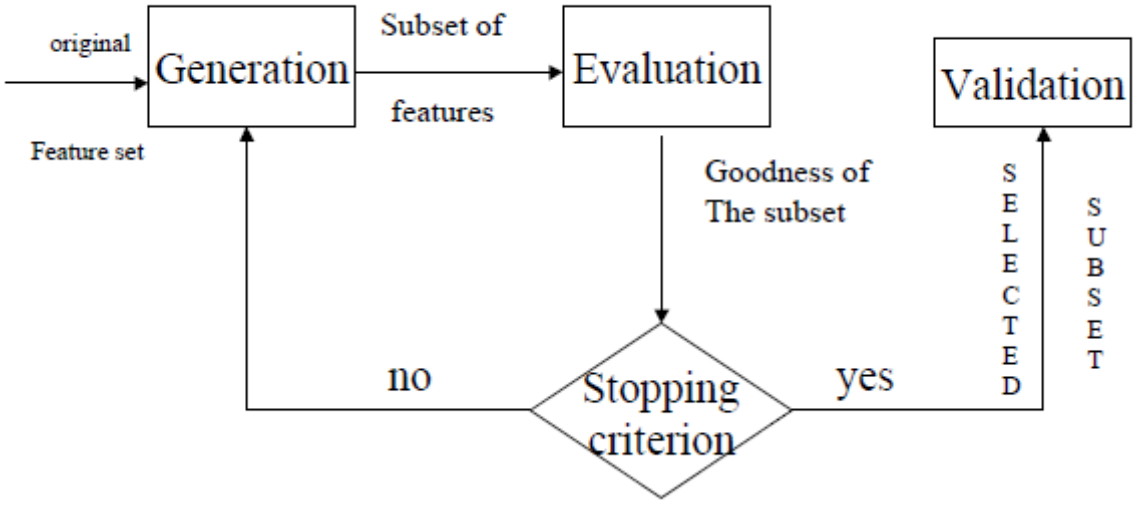

Figure 2.59 Results achieved using Big Data (Miguel & Gómez, 2016).

2.4.5 Choose an Algorithm

After selecting, understanding and cleaning the data, the next milestone consists in identifying the right algorithm based on the categorized problem which in the case of this thesis concerns the study of the ageing of vehicles used in the cold chain. Some of the elements affecting the choice of a model are:

- the accuracy of the model;
- the interpretability of the model.
- the complexity of the model;
- the scalability of the model;
- how long does it take to build, train, and test the model?
- how long does it take to make predictions using the model?
- does the model meet the prefixed goal?

After the due considerations in a supervised learning problem it is possible to choose, between classification and regression models.

In this thesis both these types of algorithms are considered for the study of the ageing of refrigerated vehicles. These two types of algorithms are described in the next subparagraphs and then put into practice using the available data in Chapter 4.

2.4.5.1 Classification and Regression in Machine Learning: main differences

Mohri et al. (2012) reviewed the major classes of learning problems. Among these, there are problems related to classification and regression. Regression and Classification algorithms are Supervised Learning algorithms. Both algorithms are used for prediction in Machine Learning and work with labeled datasets. With the help of supervised learning, the algorithm analyzes the training data (set of training examples) and produces a correct outcome from labeled data.

Supervised learning implies the existence of input variables (X) and an output variable (Y) and the possibility of using an algorithm to learn the mapping function, f, from the input to the output:

$$Y = f(X) \qquad \text{Eq. (2.9)}$$

The function f is therefore defined as a mapping of each element x of a set X (the domain of the function), to a unique element y of another set Y (the codomain of the function).

As a results, if $x_1 = x_2$, then $f(x_1) = f(x_2)$.

Therefore, it is possible to say that all supervised learning methods start with an input data matrix, usually called X here. Each row of X represents one observation. Each column of X represents a feature.

The main difference between classification and regression problems is that the output variable in regression is numerical (or continuous) while that for classification is categorical (or discrete). For

regression, *Y* must be a numeric vector with the same number of elements as the number of rows of *X*. For classification, *Y* can be any of these data types:

- numeric vector;
- categorical vector;
- character array;
- string array;
- cell array of character vectors;
- logical vector.

It is possible to summarize the main objectives of these two different approaches in the following way:

- in classification, the goal is to assign a class (or label) from a finite set of classes to an observation. In other words the answers are categorical variables. Examples of applications are: predicting if the emails received are spam or not spam, predicting if a patient will have a heart attack within a year, image and speech recognition problems and all the other cases where the possible classes are true and false. In the specific case of this thesis the problem of classification, studied in Chapter 4 (section 4.3, paragraph 4.3.1) concerns the prediction of ageing of refrigerated vehicles in classes such as weak, medium and strong.
- regression algorithms attempt to estimate the mapping function (f) from the input variables (x) to numerical or continuous output variables (y). In this case, y is a real value, which can be an integer or a floating point value. Therefore, regression prediction problems are usually quantities or sizes. The purpose of a prediction model is to be able, given an input feature vector of fixed size, to predict the value of the output. To this end, the model needs to be trained on a significant number of examples for which the output is known, in order to learn how the features can be used to predict the output. Applications include forecasting stock prices, energy consumption, or disease incidence. In this thesis the goal is to predict, from the data available on the refrigerated vehicle fleet, an exact numerical value of the coefficient A_{12} (see Eq. 2.5 in subparagraph 2.3.1). This is dealt with in Chapter 4 (subparagraph 4.3.2).

2.4.5.2 Relationship between classification problem and functional dependencies

A classification problem is concerned with building models that separate data into distinct classes. These models are built by inputting a set of training data for which the classes are pre-labelled in order for the algorithm to learn from. The model is then used by inputting a different dataset for which the classes are withheld, allowing the model to predict their class membership based on what it has learned from the training set.

A supervised classification problem (Mohri et al., 2012), consists in a set of *N* training examples, of the form $\{(x_1,y_1), ..., (x_N , y_N)\}$ where x_i is the feature vector of the i-th example and y_i its label. Given this training set, classification is the task of learning a target function *g* that maps each example *x* to one of the *k* classes. The function *f*, known as a classifier is an element of some space of possible functions *F*, usually called the hypothesis space. The objective of a learning algorithm is to output the classifier with the lowest possible error rate, which is the portion of

misclassified examples according to their ground truth label. This process relies on a strong hypothesis, which is the existence of a function from the features to the labels, and only seeks to determine such a function. In a complementary way to look at functional dependency (FD) could be a way to determine if such a function even exists.

To understand this relationship, it is necessary to recall that when a function (see Eq. 2.9) from a feature vector X to a label Y exists, it follows that the FD ($X \rightarrow Y$) should be satisfied. A functional dependency is denoted by $X \rightarrow Y$: it is a constraint that describes the relationship between features in a relation from a database. In relational database theory, functional dependencies help to maintain the quality of data in the database. They play a vital role in Data Base design to find the difference between good and bad databases.

Thus, it seems logical to first verify the existence of a function using functional dependency, before determining one of them with a classification algorithm. Strictly speaking, it is only possible for a relation to satisfy entirely a FD: otherwise, the dependency is not satisfied, there is no middle ground. When dealing with real life data, it is very likely that the FD will not be satisfied, even though a classification model might then be built with satisfying performances. However, understanding what tuples prevent the FD from being satisfied can then lead to improve the results, if the identified blockages can be explained and fixed through the knowledge acquired on the field. Such tuples are called counterexamples, and are defined as follows:

Let *r* be a relation over *R* and $X \rightarrow Y$ a FD on *R;* the set of counterexamples of *f* over r is denoted *CE* ($X \rightarrow Y$) and defined as follows:

$$CE\ (X\ \rightarrow\ Y, r) = \{(t_1, t_2) | t_1, t_2 \epsilon\ r, t_1[X] = t_2\ [X] and\ t_1[Y] \neq t_2[Y]\} \qquad \text{Eq. (2.10)}$$

Counterexamples identify pairs of tuples for which the classifier will never be able to perform correctly, as for the same input it will always predict the same output. These pairs are therefore very important, as their number directly impacts the quality of the classification. As a result, in order to evaluate the impact of counterexamples on classification, it is necessary to know their proportion in the dataset. Indeed, if a classifier only contains a few counterexamples, the impact on the classification will be marginal. On the opposite, a large counterexample set will significantly impact the accuracy results. Evaluating the impact of counterexamples can be a little subtle. Indeed, a single tuple might cause many counterexamples, if it is in conflict with many other tuples that agree between them. On the opposite, on other relations, the counterexamples might be all due to many different tuples that each are in conflict with only a few other tuples.

This problem is actually equivalent to estimating the error of the FD in a relation, a problem addressed by Kivinen and Mannila (1995), in which three measures are presented, given a FD $X\ \rightarrow\ Y$ and a relation *r*.

The first one, G_1, gives the proportion of counterexamples in the relation:

$$G_1(X\ \rightarrow\ Y, r) = \frac{|\{(u,v) | u,v\ \epsilon\ r, u\ [X] = v\ [Y], u\ [X] \neq v\ [Y]\}\ |}{|r^2|} \qquad \text{Eq. (2.11)}$$

Following this first measure, it is also possible to determine the proportion of tuples involved in counterexamples. This measure, G_2, is given as follows:

$$G_2(X \rightarrow Y, r) = \frac{\{|u \in r,\ \exists v \in r: u[X]=v[Y],\ u[X]\neq v[Y]\}|}{|r|} \quad \text{Eq. (2.12)}$$

These two metrics are designed to evaluate the importance of counterexamples in the relation. Similarly, measure G_3 computes the size of the set of tuples in r to obtain a maximal new relation s satisfying $X \rightarrow Y$.

Contrary to Kivinen and Mannila (1995) which present this measure as an error, in this thesis, it is proposed as follows:

$$G_3(X \rightarrow Y, r) = \frac{\max[(|s||s\subseteq r, s \models X \rightarrow Y)]}{|r|} \quad \text{Eq. (2.13)}$$

Le Guilly et al. (2019) underlined that G_3 is a direct upper bound for the accuracy of a classifier trained on the considered data, when the between the features and the class in considered, exactly as for the application to the available Cemafroid data in Chapter 4.

Hence, the practical application of these concepts is presented in Chapter 4 (paragraph 4.6) where the existence of a function on the ageing of refrigerated vehicles is studied. The knowledge on refrigerated transport and ageing acquired during the three years of the thesis, combined to those in data science of the experts of LIRIS allowed generating a fruitful discussion through which it has been possible to identify the counterexamples from the available dataset and then to model the phenomenon through classification and regression algorithms. The identified counterexamples are presented in Chapter 4 and the possible reason of their existence will be explained as possible solution to improve the implemented classification model.

2.4.5.3 Decisions trees

Decision Trees are a non-parametric supervised learning method used for classification and regression. The goal is to create a model that predicts the value of a target variable by learning simple decision rules inferred from the data features. Practically, a decision tree is a flowchart-like tree structure where an internal node represents a feature (or attribute), the branch represents a decision rule, and each leaf node represents the outcome. This flowchart-like structure helps in the decision to be made. The topmost node in a decision tree is known as the root node. The tree is built from the root (first splitting condition) to the leaves (predictions) and conditions are chosen in such a manner that they are the ones dividing the best the training data with respect to the value to predict. For each incoming vector, the tree starts from its root and follows the only possible root given the features of the vector, until it reaches one of the tree leaves that contains the prediction for the given value. Each node in the tree is based on a condition that is satisfied or not: for a given input there is therefore only one possible output. For learning models, decision trees are usually binary, meaning that each node in the tree gives exactly two branches. The final goal

is to have leaf nodes as pure as possible – each leaf only represents records within the same class –with the discrimination between classes (Larose and Larose, 2014). Decision tree can also be represented as sets of if-then rules to simplify the understandability (Maimon and Rokach, 2010).

2.4.5.4 Random Forest algorithm

Random forests are based on a "forest" of decision trees, in the sense that many different trees are trained in parallel and used to make the prediction with the use of multiple decision trees and a technique called Bootstrap Aggregation, commonly known as "bagging". The basic idea behind this is to combine multiple decision trees in determining the final output rather than relying on individual decision trees. The initial training dataset is sampled so that each tree learns from a slightly different dataset: this is done to avoid bias coming from the data, and to produce different trees that might identify different relevant patterns in the data. Similarly, only partial sets of features can be given to each tree (as long as all features are represented in the forest); thus, a chance is given to all features to appear, as they might sometimes be outshone by other features when considering the entire dataset. To make a prediction, the output of each tree is used: in the case of regression, an average is calculated over the forest, to form the final prediction. In the case of classification, a majority vote is performed to from the final decision.Figure 2.60 shows an example of a random forest used in this thesis for the ageing prediction.

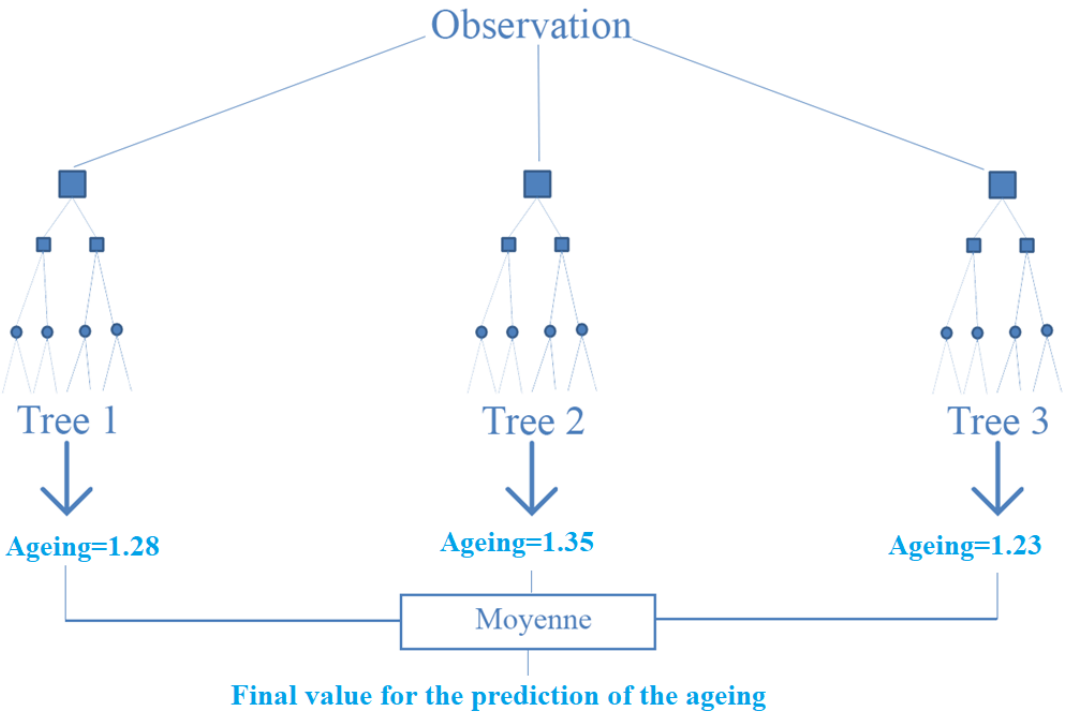

Figure 2.60 Example of random forest to predict the ageing of refrigerated vehicles.

2.4.6 Training, testing and fitting a predictive model

The goal of a machine learning model is to generalize well from the training data to any data from the problem domain. This allows making predictions in the future on data never seen by the model.

Hence, when the final model has been chosen, the next steps are to train, test and fit it so that it can make good predictions. To do this the dataset may be separate in almost two parts: 80% of it going into a training set and the last 20% going into a test set

There is a terminology used in machine learning when talking about how well a machine learning model learns and generalizes to new data, namely overfitting and underfitting.

Over-fitting and under-fitting are the two biggest causes for poor performance of machine learning algorithms.

Over-fitting means that the model performs well on the training data, but it does not generalize well. This happens when the model is too complex relative to the amount and noisiness of the training data. The possible solutions to this problem identified by Géron (2017) are:

- to simplify the model by selecting one with fewer parameters (e.g., a linear model rather than a high-degree polynomial model), by reducing the number of features in the training data or by constraining the model;
- to gather more training data
- to reduce the noise in the training data (e.g., fix data errors and remove outliers).

Under-fitting is the opposite of overfitting: it occurs when the model is too simple to learn the structure of the data. The main options to fix this problem are (Géron, 2017):

- selecting a more powerful model, with more parameters
- feeding better features to the learning algorithm (feature engineering);
- reducing the constraints on the model (e.g., reducing the regularization hyper-parameter).

2.4.7 Evaluate a model

In Machine Learning, performance measurement is an essential task. To check or visualize the performance of a model different measurements are available for that purpose such as the Receiver Operating Characteristic (ROC) Curves, Recall measurement, Precision measurement and accuracy measurement. Some of these measurements are introduced in the nest subparagraphs.

2.4.7.1 Confusion matrix

The performance of a classification model can be summarized in a so-called contingency table or confusion matrix where the general idea is to count the number of times instances of class A are classified as class B. For example, one of the goals of this thesis is to produce a model that is able to classify vehicles as subject to “low ageing” and vehicles subject to “high ageing”. The matrix confusion of such a model is presented in Figure 2.61. The results of this matrix are expressed as follows:

- True Positive (TP) : the prediction is correct and the actual value is positive (i.e. the value of actual class is “low ageing” and the value of predicted class is also “low ageing”).
- False Positive (FP) : the prediction is wrong and the actual value is positive; actual class says that the vehicles are subject to high ageing whereas the predicted one says the inverse. .
- True Negative (TN): the prediction is correct and the actual value is negative (i.e. the value of actual class is “high ageing” and value of predicted class is also “high ageing”).
- False Negative (FN): the prediction is wrong and the actual value is negative (i.e. the value of the actual class is “high ageing” and the predicted one is “low ageing”.

A perfect model would only produce ‘true positives’ and ‘true negatives’, and not include any ‘false positives’ or ‘false negatives’.

	Predicted class		
Actual class		Class= low ageing	Class= high ageing
	Class= low ageing	True Positive	False Negative
	Class= high ageing	False Positive	True Negative

Figure 2.61 Confusion matrix for the discretization of the ageing of refrigerated vehicles in two classes: low ageing and high ageing.

2.4.7.2 Precision, Recall and F_1 score

Once True Positive, False Positive, True Negative and False Negative have been introduced it is possible to evaluate a model through other metrics such as: the Precision, the Recall and the F1 score, introduced as follows:

- Precision is the ratio of correctly predicted positive observations to the total predicted positive observations:

$$Precision = \frac{True\ positives}{True\ positives + False\ Positive} \quad \text{Eq. (2.14)}$$

- Recall (also called Sensitivity or True Positive Rate,TPR) is the ratio of correctly predicted positive observations to the all observations in actual class “slow ageing”:

$$Recall = TPR = \frac{True\ Positives}{True\ Positives + False\ Negatives} \quad \text{Eq. (2.15)}$$

A Precision equal to 1 does mean 100% success: all vehicles classified as subject to “slow ageing” are indeed subject to slow ageing, but this does not mean that all “slow ageing” vehicles have been found.

On the other hand, a Recall of 1 means that all vehicles subject to slow ageing have been detected, but not that no legitimate "slow ageing" vehicle have been classified as "slow ageing" vehicle.

- F_1 score is the weighted average of Precision and Recall. Therefore, this score takes both false positives and false negatives into account:

$$F_1 = \frac{2\,(Recall.\ Precision)}{Recall+Precision} \qquad \text{Eq. (2.16)}$$

2.4.7.3 ROC curve

A receiver operating characteristic curve, or ROC curve, is a graphical plot that illustrates the diagnostic ability of a binary classifier system as its discrimination threshold is varied.

ROC curve is widely used to measure the performance of supervised classification rules (Hand and Till, 2001) and is a technique for visualizing, organizing and selecting classifiers based on their performance (Fawcett, 2006).

The ROC curve (Figure 2.62) is plotted with True Positive Rate (TPR) against the False Positive Rate (FPR) where TPR is defined by Eq. (2.15) and FPR, also known as Specificity, Fall-out or False alarm ratio is defined as:

$$FPR = \frac{False\ Positives}{False\ Positives + True\ Positives} \qquad \text{Eq. (2.17)}$$

The area under the ROC curve (AUC) represents how well a parameter can distinguish between two classes. The larger is the area, the better is the model.

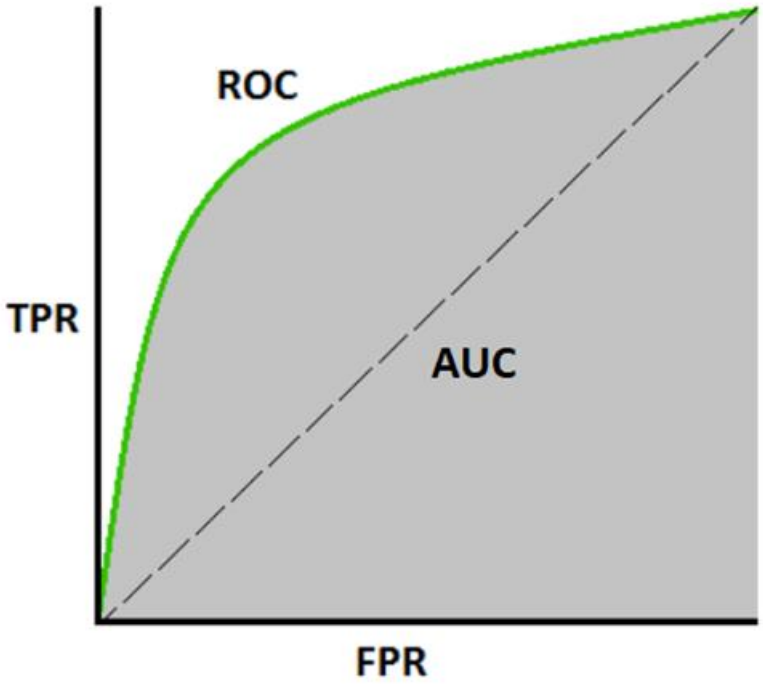

Figure 2.62 Example of ROC curve.

2.4.7.4 Mean absolute percentage error (MAPE) and root-mean squared error (RMSE)

To assess the performance of a regression model it is possible for those data for which the output is known, to compare the predicted values to the actual ones. With this purpose, the mean absolute percentage error (MAPE) is a widely used metric in regression scenarios. It is formally defined as follows:

$$MAPE = \frac{100\%}{n}\sum_{i=1}^{n}\left|\frac{A_{t_i}-P_{t_i}}{A_{t_i}}\right| \qquad \text{Eq. (2.18)}$$

Where n is the number of rows used for testing, A_{t_i} refers to the actual value and P_{t_i} to the predicted one. It is clearly a percentage error, and should be as close as possible to 0%. Another metric, called the root-mean squared error ($RMSE$) is also commonly used. It is defined as follows:

$$RMSE = \sqrt{\frac{1}{n}\sum_{i=1}^{n}\left(A_{t_i} - P_{t_i}\right)^2} \qquad \text{Eq. (2.19)}$$

2.5 Conclusions and main issues

This section presents :

- The main conclusions that can be drawn from the state-of-the-art review ;
- The objectives of the present study.

2.5.1 Main conclusions from the state-of-the-art

This Chapter laid the fundamental background for the study of the ageing of refrigerated vehicles in four different parts, the conclusions of which are set out below.

The first topic dealt with concerns refrigerated transport and cold chain logistics: these represent the context of the study and therefore need to be analyzed in more detail. Refrigerated transport and cold chain logistics are closely interconnected. As a matter of fact, refrigerated transport plays a key role in the continuity of the logistic steps of the cold chain. For this reason, the different logistic schemes in which a refrigerated vehicle can be involved were introduced. All these logistic schemes are still used today but it has been seen as the current trend concerns the development of e-commerce that tends to encourage the scheme concerning the door-to-door distribution. In this first part, a refrigerated vehicle was described in all its components and the necessary definitions and concepts from the ATP regulation for vehicle classification and K coefficient tests implementation were also introduced. When the general lines of the ATP regulation were addressed, the certificate issuing process implemented in France was also introduced as well as the data generation process that follows. In this regard, the databases available to Cemafroid, the ATP authority competent in France, were introduced. All the concepts presented in this first part as well as data extracted from the described databases are the fundamentals which are then applied both in Chapters 3 and 4, respectively dedicated to the experimental activities and the implementation of learning problem to study the ageing phenomenon from such data.

Secondly, the materials and technologies used in the manufacturing process of the insulated enclosures were reviewed. It was important to devote an entire section to their evolution because the insulation performance of refrigerated vehicles and therefore the way they age over time change according to them. It was pointed out that the construction of insulated enclosures has not changed significantly since the 1970s and the advent of sandwich panels based on insulating foam and polyester, introduced on the market to replace insulated enclosures built with natural materials, especially cork. The insulation performance of new enclosures has even deteriorated due to the banning of halogenated foam blowing agents since the early 1990s. The overall isothermal coefficient of isothermal bodies has thus lost around 25% over the last thirty years after having been halved between 1950 and 1970. This development is the opposite of what has happened in history at a time of energy savings. Manufacturers must therefore reverse the trend. The use of new insulation and technologies such as aerogels and VIPs are essential to meet this challenge.

The third part of this chapter was dedicated to the review of the studies on the ageing of refrigerated vehicles, already present in the literature. These works provided a definition of the ageing as well as the most important factors involved in this process. It is worth pointing out that in all these studies, the ageing is studied by comparing a K coefficient measured at twelve years

of life with an initial calculated K coefficient. The exactitude of the K values at the beginning of the life of the vehicles is not certain since these values do not come from direct measurements. The absence of direct measurements of the K coefficient at the beginning of the life of a vehicle comes from the ATP regulation. As a matter of fact, as seen in the process of certificates issuing introduced in subparagraph 2.1.3.6, this regulation, immediately after the manufacturing, imposes tests only on prototype vehicles and not on vehicles produced in the series.

The ageing has been defined by Panozzo et al. (1999) as the degradation of the thermal insulation properties of the insulated enclosure. The factors highlighted by the various studies can be summarized in two categories i.e., the physical-chemical factors and the mechanical ones. Among the factors belonging to the first category there are the permeability of the foams to the air and blowing agents, the condensation of water into the foam cells and the increasing of the percentage of the open broken cells. On the other hand, among the mechanical factors, the presence of some accessories, such as meat rails and refrigerating unit, were highlighted. Corain et al. (2010) developed a model which takes into account both the physical processes involved in the heat transfer within the insulating panel and the effects of structural characteristics, as well as operation and maintenance practices on the life of refrigerated transport vehicles. However when the curve resulting from this model is plotted with experimental results it was found that only few data follow the theoretical trend.

The last part of this chapter dealt with Big Data and Machine Learning fundamentals for the study of the ageing of refrigerated vehicles. All the steps of such a learning problem were approached: from the selection of the data and their pre-treatment and pre-processing to the validation of the produced model through the use of a chosen algorithm. The theoretical foundations presented here are then put into practice in Chapter 4 on the Cemafroid available data.

2.5.2 Objectives of the study

The present work aims at providing new elements in the study of the ageing of refrigerated vehicles used in the cold chain, trying to fill some of those gaps of the literature studies. The numerous factors that influence the ageing phenomenon are analyzed through different approaches and solutions to improve the insulation performance of vehicles are also proposed. The ultimate goal is to predict the ageing of refrigerated vehicles.

Thus, the main objectives of this thesis can be summarized as follows:

- to study the the insulation performance of a vehicle during key periods of its life which have never been studied before, such as immediately after its manufacturing.: i.e., the first months of its use.
- to study the impact of installing the refrigeration unit and other accessories on the insulated enclosure of the vehicle ;
- to experimentally assess the difference between new prototype vehicles and real new series-produced vehicles. A vehicle produced in a series, even if based on its prototype, may be very different from the latter. Thus, the initial K coefficient of a real vehicle, K_0 could be greater or lower than the K coefficient of a prototype vehicle, K_p. To date, as evidenced by the state of the art review, no study has ever proved the inconsistency (and consequent lack of accuracy about ageing) induced by the practice yet authorized by the

regulation. Hence, one of the main objectives of this study is to fill this gap by providing exact values of the initial K coefficient, K_0 of several refrigerated vehicles of different type;

- to assess the benefits that the addition of new materials, such as VIPs, may have in the manufacturing process of refrigerated vehicles;
- from thousands of cases of refrigerated vehicles stored in Datafrig© database, to develop a data-centric approach to confirm known factors for the ageing process but also to infer new ones using state of the art machine learning and intelligence artificial techniques;
- to predict the ageing by building a numerical model, using supervised machine learning techniques, i.e. classification and regression algorithms;
- to predict the initial K coefficient value, K_0, of a vehicle from a purely thermal-physical point of view and based on this calculation, to try to predict also its ageing at twelve years of life.

2.6 References

Amr, M., Ezat, M., Kassen, S., 2019. Logistics 4.0: Definitions and Historical Background. Novel Intelligent and Leading Emerging Sciences Conference 2019, Nile University, Giza, Egypt.

Artuso, P., 2019 Theoretical and experimental analysis of the transient behavior of refrigerated transport systems. PhD thesis, University of Padova, Italy.

Artuso P., Rossetti A., Minetto S., Marinetti S., Moro L., Del Col D., 2019. Dynamic modeling and thermal performance of a refrigerated truck body during operation. International Journal of Refrigeration, 99 (288-299).

Awwad, M., Kulkarni, P., Bapna, R., Marathe, A., 2018. Big Data Analytics in Supply Chain: A Literature Review. Proceedings of the International Conference on Industrial Engineering and Operations Management Washington DC, USA.

Barreto, L., Amarala, A., Pereiraa,T., 2017. Industry 4.0 implications in logistics: an overview. Procedia Manufacturing 13, (1245–1252).

Bartodziej, C. J., 2017. The Concept Industry 4.0. Technical University of Berlin and Tongji University in Shanghai.

Borreguero, A. M., Valverde, J. L., Peijs, T., Rodríguez, J. F., Carmona, M., 2010. Characterization of rigid polyurethane foams containing microencapsulated Rubitherm® RT27. Part I, Journal of Material Science; 45, (4462–4469).

Brecht, P. E., 1992. Shipping Special Commodities. American President Lines, Oakland, CA.

Bruha, I., Franek, F, 1996. Comparison of various routines for unknown attribute value processing: covering paradigm. International Journal of Pattern Recognition and Artificial Intelligence, 10 (8), (939–955).

Bengio, Y., Courville, A., Vincent, P., 2013. Representation learning: a review and new perspectives. IEEE Transaction on Patterns Analysis and Machine Intelligence. 35 (8), (1798–1828).

Bishop, C., 2006. Pattern recognition and machine learning. Information Science and Statistics. Springer.

Boittiaux, P., 2018. L'intelligence artificielle, un marché qui vaut des milliards. Technologie et télécommunications. Online source: https://fr.statista.com/infographie/13385/lintelligence-artificielle-un-marche-qui-vaut-des-milliards/.

Bogrow, A., 1982. Evolution technique des véhicules à température dirigée. Génie Rural Janvier-Février 1982, (21–27).

Boldrin, B., Minotto G., Panozzo, G., Toniolo, B., Varotto, G., 1990. Ageing of insulated vehicles: statistical elaboration of test result. Proceedings of Commissions B2, C2, D1, D2/3, Dresden, Germany, IIF/IIR, (839–845).

Boldrin, B., Minotto., G., Panozzo, G., Toniolo, B., Lanza, W., Florio, G., Jacobini, A., Sallusti, L., 1993. New data about ageing of insulated vehicles in service: a statistical analysis. Proceedings of Commissions. B1, B2, D1, D2/3, Palmerston North, New Zealand, IIF/IIR, (555–564).

Brown, T., Evans, J. A., , Swain, M. V.L. , 2007.Use of vacuum insulation panels to improuve perfromance of refrigerators and insulated shipping containers. Proceedings of 22nd International Congress of Refrigeration, Beijing, China.

Cadet, E., 2004. La naissance d'un fourgon frigorifique. L'officiel des transporteurs magazine. Mars-2004.

Cai, X., Nie, F., Huang, H., 2013 Multi-view k-means clustering on Big Data. International Joint Conferences on Artificial Intelligence (2598–2604).

Casillo, V., 2011. Nuove tecnologie e materiali per casse isolate. Tesi di laurea, Università deli Studi di Napoli Fedrico II.

Cavalier, G., 2010. 26 Challenges facing refrigerated trucks for sustainable development. Industria & formazione, suppl. 1 n. 341.

Cavalier, G., Tassou, S. A., 2011. Sustainable refrigerated road transport. 21st Informatory Note on Refrigerating Technologies, International Institute of Refrigeration.

Cavalier, G., 2016. Sustainability in Transport Refrigeration Systems..Reference Module in Food Science, First Edition. Elsevier Inc. http://dx.doi.org/10.1016/B978-0-08-100596-5.03176-0.

Chamikara, M. A. P., Bertok, P., Liu, D., Camtepe, S., Khalil, I., 2019. Efficient privacy preservation of big data for accurate data mining. Information Sciences. In press .

Clavier, F., Sartre, V., Bonjour, J., 2011. Infiltration heat load through the doorway of a refrigerated truck protected with an air curtain. Proceedings of the 23rd International Congress of Refrigeration. Prague, Czech Republic.

Corain, L., Panozzo, G., Pepelyshev, A., Rossi, S., Salmaso, L., 2010. Estimating and testing for influence of specific structural factors on aging of refrigerated vehicles. Publication de l'Institut de statistique de l'Université de Paris, Livre, fascicule 3, (25–40).

Copertaro, B., Principi, P., Fioretti, R., 2016. Thermal performance analysis of PCM in refrigerated container envelopes in the Italian context –Numerical modeling and validation. Applied Thermal Engineering, 102, (873–881).

Corain, L., Mattiello, F., Panozzo, G., Rossi, S., Salmaso, L., 2011. Effect of structural factors on aging curve of refrigerated vehicles. Proceedings of the 23rd International Congress of Refrigeration. Prague, Czech Republic.

Derens, E., Guilpart, J., Palagos, B., 2004. Données chiffrées sur la chaîne du froid des produits réfrigérés. Revue général du froid, juillet-août 2014, (27–32).

Fawcett, T., 2006. Introduction to ROC analysis. Pattern Recognition Letters 27 (861–874).

Fertel, C., Cavalier, G., 2020. L'innovation sur le marché des engins de transport sous température dirigée .Étude technico économique (Cemafroid Confidential study).

Gandomi, A., Haider, M., 2015. Beyond the hype: Big Data concepts, methods, and analytics. International Journal Informatics Management. 35(2), (137–144).

Gantz, J., Reinsel, D., 2010: The Digital Universe Decade - Are You Ready?. Basic Books.

Gantz, J., Reinsel, D., 2011: Extracting value from chaos technical report white paper. International Data Corporation (IDC) Sponsored by EMC Corporation.

Géron, A., 2017. Hands-On Machine Learning With Scikit-Learn and Tensorflow: Concepts, Tools, and Techniques to Build Intelligent Systems. O'Reilly Media, Inc., 1005 Gravenstein Highway North, Sebastopol, CA 9547.

Glouannec, P., Michel, B., Delamarre, G., Grohens., Y., 2014. Experimental and numerical study of heat transfer across insulation wall of a refrigerated integral panel van. Applied Thermal Engineering, Elsevier, 73, (196 – 204).

Guyon, I., Elisseeff, A., 2003. An Introduction to Variable and Feature Selection. The Journal of Machine Learning Research, 3, (1157–1182).

Hammond, E.C., Evans, J.A., 2014. Application of Vacuum Insulation Panels in the cold chain - Analysis of viability. Interantional Journal of Refrigeration 47, (58–65).

Heap, R.D., 2010; Guide to Refrigerated Transport , 2nd Edition, 2010. International Institute of Refrigeration.

Herjolfsson, G., 2019. How Real-Time Data is Automating the Temperature-Controlled Supply Chain. Online source: https://www.rtinsights.com/how-real-time-data-is-automating-the-temperature-controlled-supply-chain./

Ishwarappa, Anuradha, J., 2015. A brief introduction on Big Data 5Vs Characteristics and Hadoop Technology. Procedia Computer Science 48, (319–324).

Kivinen, J., Mannila, H, 1995. Approximate inference of functional dependencies from relations. Theoretical Computer Science 149, (129–149) .

Kotsiantis, S.B., Kanellopoulos, D., P. E. Pintelas, 2006. Data Preprocessing for Supervised Leaning. International journal of computer science.Volume I number 1.

Lafaye de Micheaux, T., Ducoulombier, M., Moureh, J., Sartre, V., Bonjour, J, 2015. Experimental and numerical investigation of the infiltration heat load during the opening of a refrigerated truck body. International journal of refrigeration 54, (170– 189).

Lakshminarayan K., Harp, S., Samad, T., 1999. Imputation of Missing Data in Industrial Databases, Applied Intelligence 11, (259–275).

Laney, D., 2001. 3D Data Management: Controlling Data Volume, Velocity and Variety. Gartner file No.949. Online source: http://blogs.gartner.com/doug-laney/files/2012/01/ad949-3D-Data-Management-Controlling-Data-Volume-Velocity-and-Variety.pdf.

Larose, D.T., Larose, C.D., 2014. Discovering Knowledge in Data: An Introduction to Data Mining. Wiley, 336 pages.

Laundrie, J.F., 1986. Unitizing goods on pallets and slipsheets. General Technical Report FPL-GTR-52. Madison, WI: U.S. Department of Agriculture, Forest Service, Forest Products Laboratory; 1986. 45pages.

Lawton, A.R., Marshall, R.E., 2007. Developments in refrigerated transport insulation since the phase of CFC and HCFC refrigerants. Proceedings of 22nd International Congress of Refrigeration, Beijing, China.

Le Guilly, M., Petit, J.M., Scuturici, V.M., 2019. Evaluating classification feasibility over datasets using functional dependencies. BDA 2019 35e Conference sur la Gestion de Données: Principes, Technologies et Applications. Lyon, France.

LesEchos, 2019 « Le e-commerce alimentaire en plein essor ».

Levene, M., Loizou, G., 1999. A Guided Tour of Relational Databases and Beyond. Springer-Verlag, Berlin, Heidelberg .

Maimon, O., Rokac, L., 2010. Data Mining and KnowledgeDiscovery Handbook. Spinger.

Makkar S., Devi G.N.R., Solanki V.K., 2020. Applications of Machine Learning Techniques in Supply Chain Optimization. In: Gunjan V., Garcia Diaz V., Cardona M., Solanki V., Sunitha K. (eds) ICICCT 2019 – System Reliability, Quality Control, Safety, Maintenance and Management. Springer, Singapore.

Markovitch, S., Rosenstein, D., 2002. Feature Generation Using General Constructor Functions, Machine Learning, 49, (59–98).

Mastrullo, R., Mauro, A.W., Panozzo, G., 2019. Factors affecting energy consumptions and carbon footprint in refrigerated road transport: a brief review of recent advances in technology, materials and methods. Proceedings of the. 25th IIR International Congress on Refrigeration, Montréal, Québec, Canada.

Miguel, J., Gómez, F., 2016. Top Challenges for Big Data in the Supply Chain Management Process.

Mohri, M., Rostamizadeh, A.,Talwalkar, A., 2012. Foundations of machine learning. MIT press.

Moureh, J., Menia, N., Flick, D., 2002. Numerical and experimental study of airflow in a typical refrigerated truck configuration loaded with pallets.

Moureh, J., Flick, D., 2004. Airflow pattern and temperature distribution in a typical refrigerated truck configuration loaded with pallets. International Journal of Refrigeration

Moureh, J., Tapsoba, S., Flick., D., 2007. Influence of air ducts on airflow characteristics in a typical refrigerated truck configuration loaded with vented pallets. Proceedings of 22nd International Congress of Refrigeration, Beijing, China.

Nguyen-Dinh, L.V., Rossi, M., Blanke, U., Tr¨oster, G., 2013: Combining crowd-generated media and personal data: semi-supervised learning for context recognition. In: Proceedings of the 1st ACM International Workshop on Personal Data Meets Distributed Multimedia, (35–38).

Oliveri, P.; Malegori, C.; Simonetti, R.; Casale, M., 2019. The impact of signal pre-processing on the final interpretation of analytical outcomes – A tutorial. Anal Chim Acta 1058, (9-17).

Panozzo, G., Boldrin B., Minotto, G., Toniolo, B., Biancardi, N., 1995. Ageing of insulated vehicles: theoretical model and experimental analysis. Proceedings of the 19th Internatinal Congress of Refrigeration, Den Hague, Netherlands.

Panozzo, G., 1999. Parameters affecting the ageing of the insulated vehicles. Proceedings of the 20th International Congress of Refrigeration, Sydney, Australia.

Panozzo, G., Minotto, G., Barizza, A., 1999. Transport et distribution de produits alimentaires: situation actuelle et tendances futures. International Journal of Refrigeration 22, (625–639).

Panozzo, G., 2009. Frozen Food Transport. Frozen Food Science and Technology, (276–302).

Panozzo, G., Rossi, S., Cuogo, G., Cuccato, G., Franceschi, M., 2011. News solutions for insulated boxes. Proceedings of the 23rd International Congress of Refrigeration, Praha, Czech Republic.

Rai, A., Tassou, S.A., 2017. Energy Demand and Environmental Impacts of Alternative Food Transport Refrigeration. 1st International Conference on Sustainable Energy and Resource Use in Food Chains, Berkshire, UK.

Ramírez-Gallego, S., García, S., Mouriño-Talín, H., Martínez-Rego, D., Bolón-Canedo, V., Alonso-Betanzos, A., Manuel Benítez, J., Herrera, F., 2015. Data discretization: taxonomy and big data challenge. WIREs Data Mining and Knowledge Discover, 24 pages.

Reina, A., Suquet, T., Capo, C., Latchan, F., Mauro, A.W., Cavalier, G., 2020. Proposal of a method to determine the effects of doors opening to size equipment of delivery trucks. Proceedings of the 6th IIR Conference on Sustainability and the Cold Chain, Nantes, France.

Ryohei, F., Satoshi, M., 2012. The most advanced data mining of the big data era. NEC Technical Journal 7(2), (91–95).

Samuel, A. L., 1959. Some Studies in Machine Learning using the Game of Checkers. IBM Journal on Research and Development 3, (211–229).

Singh, M., Provan, G. M., 1996. Efficient learning of selective Bayesian network classifiers. In Machine Learning: Proceedings of the 13th International Conference on Machine Learning. Morgan Kaufmann.

Somol, P.and Pudil, P., 2002. Feature Selection Toolbox. Pattern Recognition 35, (2749–2759).

Tassou, S.A., De-Lille, G., Ge, Y.T., 2009; Food transport refrigeration – Approaches to reduce energy consumption and environmental impacts of road transport. Applied Thermal Engineering 29, (1467–1477).

Tellier, C., 1910.Histoire d'une invention moderne, le frigorifique. 1 vol. (XI-456 p.), Édition Ch. Delagrave Paris, DL 1910, Préface de Jacques Arsène d'Arsonval (1851–1940) membre de l'institut et fondateur de l'AFF.

Tinti, A., Tarzia, A., Passaro, A., Angiuli, R., 2014. Thermographic analysis of polyurethane foams integrated with phase change materials designed for dynamic thermal insulation in refrigerated transport. Applied Thermal Engineering.

Tole, A. A., 2013. Big data challenges. Database Systems Journal, 4(3), (31–40).

Vesco, A., 2015. Analisi degli effetti di invecchiamento delle caratteristiche termiche dei veicoli isolati. Tesi di laurea Università degli Studi di Padova.

Vigneault, C., Thompson, J., Wu, S., 2009. Designing container for handling fresh horticultural produce. In N. Benkeblia (Ed.),Postharvest Technologies for Horticultural Crops, 2 (25–47). Kerale, India: Research Signpost.

XSNET, 2017. Updated for 2017: The V's of Big Data: Velocity, Volume, Value, Variety, and Veracity.

Yang, C., Fischer, L., Maranda, S., Worlitschek, J., 2015. Rigid polyurethane foams incorporated with phase change materials: a state-of-the-art review and future research pathways, Energy Build. 87 (25–36).

Chapter 3

Experimental activities

Nomenclature of Chapter 3

Abbreviations

ATP	Agreement on the International Carriage of Perishable Foodstuffs and on the Special Equipment to be Used for such Carriage
DGAl	Directorate-General for Food
$Fuel\ cons$	Fuel consumption
IN	Normally insulated equipment
IR	Heavely insulated equipment
VIP	Vacuum insulation panel

Greek

Δ	Variation	
δ	Thickness	[m]
$\lambda.$	Thermal conductivity,	[$W.m^{-1}.K^{-1}$]
ρ	Resititivity	[$\Omega.m$]

Roman

h	Height	[m]
I	Current	[A]
K	Overall heat transfer coefficient	[$W.m^{-2}\ K^{-1}$]
L	Lenght	[m]
l	Width	[m]
P	Power losses	[W]
R^2	Coefficient of determination	
S	Mean surface area	[m^2]
s	Speed	[$m.s^{-1}$]
$\sigma(\overline{x_j})$	Standard deviation of $\overline{x_j}$	[same of $\overline{x_j}$]
T	Temperature	[K]
$U(\overline{x_j})$	Expanded uncertainty of $\overline{x_j}$	[same of $\overline{x_j}$]
$u(\overline{x_j})$	Composed uncertainity of $\overline{x_j}$	[same of $\overline{x_j}$]
W	Power	[W]

Subrscripts

0	Initial/immediately after manufacturing (refferd to the real vehicle)
ambient	Ambient
app	Apparent
average	Average
B	Type B uncertainity
$calculated\ for\ all\ vehicles$	Calculated for all vehicles
$calculated\ for\ semi-trailers$	Calculated for semi-trailers
$calculated\ for\ trucks$	Calculated for trucks
$calculated\ for\ vans$	Calculated for vans
ext	External
i	i-th
int	Internal
n	n-th year of life
p	Prototype
$self-heating$	Self heating
$st-semitrailer$	Semi-trailer having standard sandwich polyurethane panels.
$VIP-semitrailer$	Semi-trailer with VIP insertions
th	Theoretical

3. Experimental activities

In this work the following experimental activities were carried out:

- K coefficient tests of prototype vehicles after their manufacturing and K coefficient tests of in-service vehicles after 12 years of use;
- K coefficient tests realized several times at key periods in the life of some refrigerated vehicles;
- experimental assessment of the refrigerating unit impact;
- experimental assessment of the difference between new refrigerated vehicles and their corresponding prototypes;
- the evaluation of the thermal and energy performance of a new type of vehicles built with sandwich panels having vacuum inserts inside their walls;

The main purpose of these activities was to understand some of the factors (i.e. the manufacturing process, the interventions that can be made on the vehicle in the first months of life and the presence on the vehicle of some accessories and special features) having an influence in the ageing process; not only in the long terms but also at the beginning of the of the vehicle. As a matter of fact, the ageing of a refrigerated vehicle may depend on the initial performance of the vehicles. However, the initial performances of the vehicles in the series may differ from those of the corresponding prototypes. Therefore, the reasons for these differences were sought and analyzed.

Among the objectives of the experimental activities, there was also to study new types of vehicles having better thermal and energy performances. A manufacturer of refrigerated vehicles lent itself to this experimental assessment allowing tests on a new type of refrigerated vehicles having VIP insertions inside the walls.

All these experimental activities require the measurement of K coefficient. Different vehicles were subject to this kind of test following the ATP "inner heating" method introduced in chapter 2 (subparagraph 2.1.3.3). The K coefficient measurements were carried out in the Cemafroid climatic chambers. This chapter begins with a detailed description of the experimental apparatus, giving particular attention to the measurement equipment and to the uncertainty of measured and derived parameters. The different experimental activities carried out are then described with the presentation and the discussion of the obtained results.

3.1 Cemafroid experimental apparatus

Cemafroid has four climatic chambers (indicated in Figure 3.1 as Tunnel 1, Tunnel 2, Tunnel 3, Tunnel 4) whose performances are those imposed by the ATP:

- temporal temperature stability of 2 K when the steady-state conditions are established;
- spatial homogeneity of the average temperature resulting from the twelve ATP measurement points equal to 2 K;
- accuracy of the control system of 0.2 K;
- air speed around the walls of a vehicle between 1 and 2 m. s^{-1}.

This implantation takes into account the strictest environmental regulations with a cold production system using ammonia (NH_3) and carbon dioxide (CO_2), i.e. natural fluids with low

environmental impact as working fluids, guarantying a long service life of the system as well as an optimal response in terms of achievable power and transient duration.

The main refrigeration unit, serving the four tunnels in the plant, uses ammonia as working fluid. It was produced by the Artic Company with an ammonia charge of 40 kg for a power output of 300 kW when the evaporation temperature is equal to -8°C.

This refrigerating unit mainly consists of a compression station consisting of 4 Bitzer brand screw compressors, a plate condenser (NH_3/MEG 30%) and a flooded evaporator (NH_3/MEG 30% were, MEG 30% is a 30% ethylene glycol solution). The NH_3 unit is completed by a CO_2 unit to guarantee the achievement of negative air temperatures in tunnel 2. The distribution of the cold is carried out by two circuits: a first loop in which circulates the glycol cooled by the NH_3 unit and a second one in which circulates Temper 55 (a ready-to-use heating carrier on a base of acetate and potassium formiate in a water solution, without glycol, which is non-toxic and non-polluting) cooled by the CO_2 unit.

The software used to control the operation of each climatic chamber is Spiral VS, it allows controlling the following parameters related to the internal conditions:

- temperature,
- speed of the air blown by the ventilation system,
- humidity,
- overpressure,
- fresh air intake and,
- exhaust gas extraction.

The control system acts on cooling and heating with the help of pneumatic valves powered by a specific compressor and power relays.

Figure 3.1 Plan of the climatic chambers in Cemafroid.

It is important to underline that during the design of the experimental plant, to reduce the noise generated by the tests and refrigeration machines, an acoustic study was carried out. This study led to the adoption of technical solutions which are able to guarantee good working conditions and limit the noise in the area adjacent to the plant. These solutions include:

- insertion of diaphragms and silencers on air circuits,
- insulation to dampen machine vibrations,
- use of low noise impact fans in tunnels,
- oversized heat exchange batteries to allow a reduction in fan rotation speed,
- location of the noisiest machinery in special soundproofed machine rooms.

The next subparagraph introduces the specific test facility used to realize the *K* coefficient of the vehicles studied in this thesis.

3.1.1 Test facility and *K* coefficient measurement

Five independent benches are available to carry out the tests on temperature-controlled transport vehicles. Located in the larger tunnel, T_1 (Figure 3.2), benches 1, 2 and 3 (Figure 3.3) are designed predominantly for the implementation of *K* coefficient tests on vehicles having parallelepiped shapes. These benches were used for the experiments carried out in this thesis. The dimensions and characteristics of tunnel 1, T_1, are summarized in Table 3.1. All the *K* coefficient tests presented in this chapter were realized in this tunnel using the internal heating method in the standardized (i.e. ATP), steady-state conditions previously introduced (see paragraph 2.1.3.4) and resumed in Table 3.1. A scheme of the measurement principle in the climatic chamber is also

represented in Figure 3.4a) whereas Figure 3.4b) shows an example of instrumented vehicle. The presence of some ventilated electric heaters is needed to reach the temperature difference between the inside of the body and the test chamber equal to 25°C ± 2 K. For the heat balance to be satisfied, the total required cooling power, Q, which is used in Eq. (2.1), is the sum of the total heating power W_1 and ventilating power W_2 of the devices placed inside the enclosure. Figure 3.5 illustrates the establishment of the steady state conditions during the K coefficient test for a semi-trailer having a mean surface area, S equal to 155 m^2.

The steady state conditions are those prescribed by the ATP :

- the mean outside temperatures and the mean inside temperatures of the body, taken over a steady period of not less than 12 hours, shall not vary by more than ± 0.3 K, and these temperatures shall not vary by more than ± 1.0 K during the preceding 6 hours;
- the difference between the heating power or cooling capacity measured over two periods of not less than 3 hours at the start and at the end of the steady state period, and separated by at least 6 hours, shall be less than 3 %;
- the mean values of the temperatures and heating or cooling capacity over at least the last 6 hours of the steady state period will be used in K coefficient calculation;
- the mean inside and outside temperatures at the beginning and the end of the calculation period of at least 6 hours shall not differ by more than 0.2 K.

Figure 3.2 Entrance of the Cemafroid test tunnel, T_1.

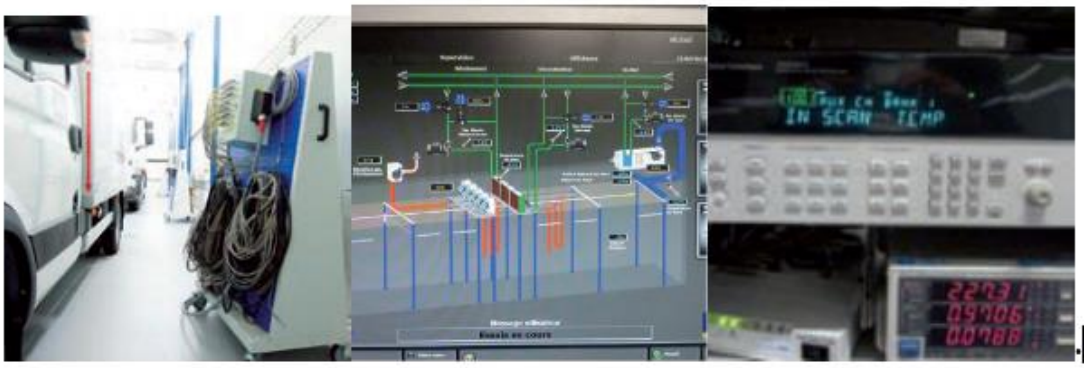

Figure 3.3Test benches of Cemafroid tunnel T1.

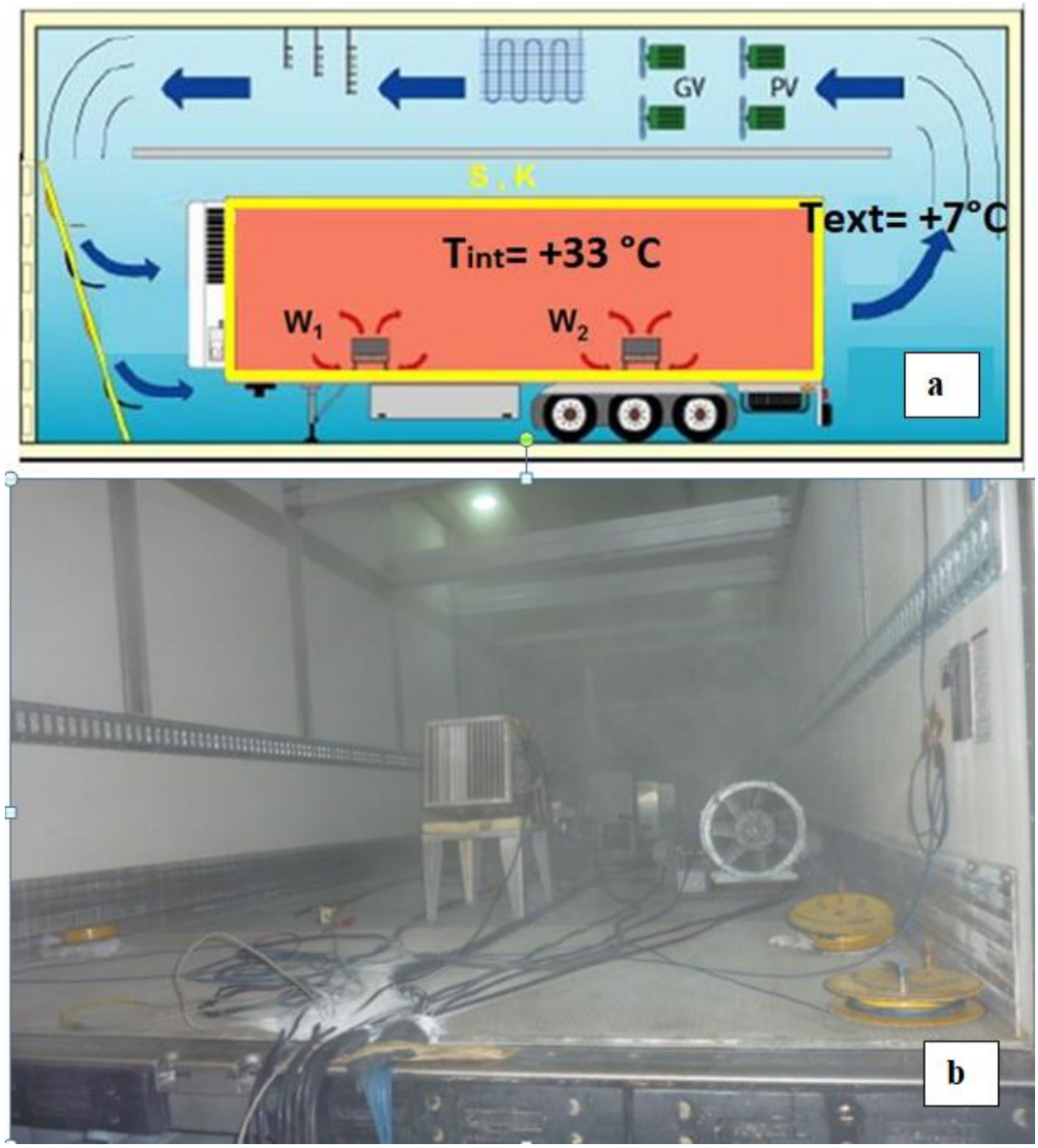

Figure 3.4 a) Measurement principle of the *K* coefficient; b) example of instrumented vehicle.

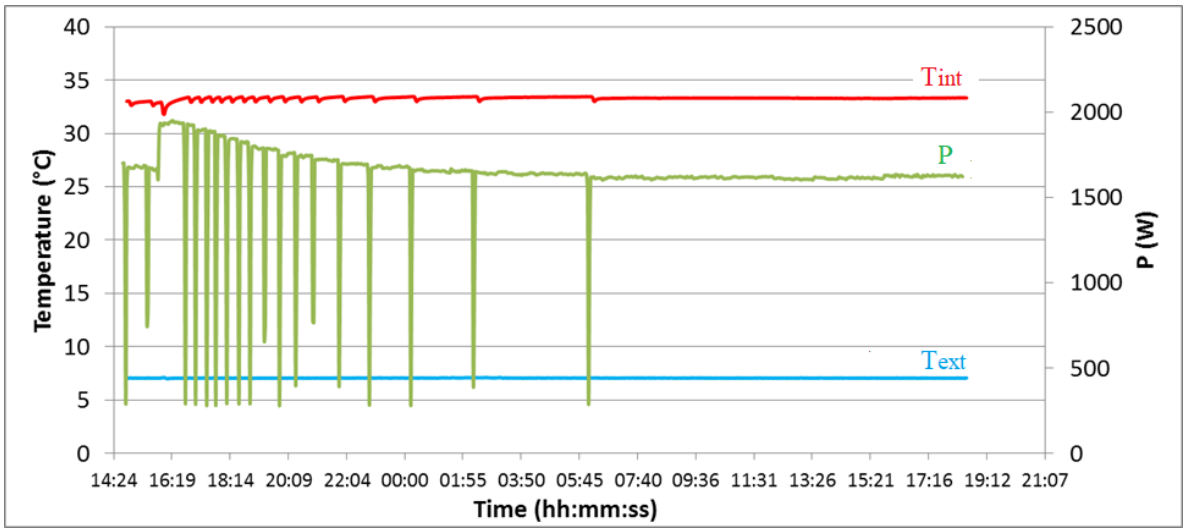

Figure 3.5 Establishment of the steady state conditions during K coefficient test.

Table 3.1Tunnel T1: dimensions and characteristics.

Volume (m^3)	620
Height (m)	5.2
Width (m)	5.2
Length (m)	23
Temperature setting (°C)	0-55
Rate of temperature change (°C/min)	2
Available Power at 30°C (kW)	100

Table 3.2 ATP standardized steady-state conditions for K coefficient tests.

Speed of external air, s	1 to 2 $m.s^{-1}$
Average wall temperature	20°C±0.5 K
Difference between outside and inside temperatures	25°C±2 K
Duration of establishment of steady state	at least 12 h

The next subparagraphs deal with the description of data acquisition system and the measured quantities during *K* coefficient tests:

- temperature measurement,
- surface measurement and,
- power measurement.

The procedure for calculating the measurement uncertainties of these quantities is also presented. From their combination, the measurement uncertainty of the *K* coefficient is then determined.

3.1.2 Data acquisition system and user interface

In order to determine the K coefficient, the test bench designed and developed by Cemafroid includes a part related to the entire technical infrastructure (measuring instruments, cables and communication boxes, etc.) and a software part consisting of three applications shown in the graph of Figure 3.6

The functionalities of the first two programs (Confeol and Gestion Centrale) are presented below; the third one (F75220) is simply responsible for the final reports editing in DOC format.

The "Confeol" program manages the different experiment configurations (K coefficient experiment, pull down experiment, etc.). In the case of the K coefficient experiment the main functions performed by this program are:

- defining the parameters useful to start a K coefficient experiment for parallelepipedic boxes and cylindrical tanks with a maximum of 8 compartments (i.e. the temperature acquisition system, the temperature probes and their position inside the insulated enclosure and the power meter, the different components of measurement uncertainties to take into account…)
- writing a backup file with the startup defined parameters;
- reading a backup file with the existing startup settings.

The "Gestion Centrale" program (whose initialization page is presented in Figure 3.7) is responsible both for continuous measurement readings and storage of calculation results on the PC hard disk in a measurement file in DAT format. It allows:

- defining the useful parameters to start a K coefficient experiment for parallelepipedic and cylindrical tanks with a maximum of 8 compartments,
- writing a measurement file and saving it on the local server;
- calculating the averages, maximums and minimums values of the inside and outside temperatures, the ambient temperature and the power dissipated in the insulated enclosure during the test,
- calculating the components of measurement uncertainties
- displaying measurements and calculation results in real time.

The "Gestion Centrale" program operates in the following environment:

- A PC for data collection monitored through the LABVIEW software, and a connection to the instrument database (metroAcces.dsn) The PC is connected to the Cemafroid local network via an Ethernet port.
- A temperature measurement unit type: Ni 9148, NI9149 with 4-channel RTD Ni 9217 modules, an Agilent 34970A temperature acquisition system communicating with the PC via Ethernet;.
- A power meter, YOKOGAWA WT 200, with digital output type GPIB,
- A 0-10 V or 4-20 mA analog transmitter for pressure or flow measurements connected to the Agilent data logger's acquisition card or to the NI9148 or NI9149 extension chassis.

For the beginning of the experiment the operator, must fill in a form and define the following information:

- time and date;

- the type of insulated enclosure (i.e., single or multiple compartment);
- the name of the costumer;
- the identification number of the test report;
- the name of the test bench (bench 1, bench 2,bench 3).

The temperature acquisition is done every 10 seconds and then the raw measurements are

- corrected;
- organized according to the labels of the measuring chains.

The average temperatures and the associated measurement uncertainties are then calculated every two minutes.

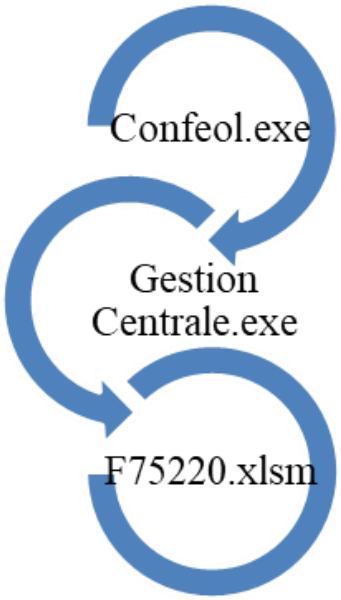

Figure 3.6 Applications of the software part of the test bench.

Figure 3.7 Labview interface of the inizialization page of the "Gestion Centrale"program

3.1.3 Measurement of main quantities and associated measurement uncertainties

This subparagraph presents the quantities measured in the K coefficient test:

- the average temperature inside the body (12 probes);
- the average temperature outside the body (12 probes);
- the internal heating power;
- the dimensions of the insulated enclosure.

The procedure used to calculate the uncertainities associated to the measurement is also presented. This procedure is applied to every experiment carried out. Therefore the result of the measurement uncertainties changes depending to the experiment.

Hence, it is considered appropriate, first of all, to recall what is meant by uncertainty of measurement.

3.1.3.1 Preliminaries on measurement uncertainties

The result of a measurement consists of three equally important elements: the measured value, the unit of measurement, and the measurement uncertainty. The measured value provides a quantitative data, which takes on meaning once the unit of measurement with which to relate it has been specified. The measurement uncertainty has a no less important meaning, as it expresses the extent of the possible deviation between the measurement result and the actual value of the measurand. Hence, the uncertainty is the expression of the statistical dispersion of the values attributed to a measured quantity. All measurements are subject to uncertainty and a measurement result is complete only when it is accompanied by a statement of the associated uncertainty. Uncertainties can be divided into two evaluation categories, marked by the letters A and B. Category A refers to random uncertainties, category B to systematic uncertainties.

The type A uncertainty can be estimated as the standard deviation from the mean value defined by the T-Student distribution for a measured quantity a sufficient number of times (at least 30 times) as will be shown practically below.

For systematic type B uncertainties there are no statistical or deterministic relations, they are estimated according to criteria such as the upper limit of the maximum fixed error that can reasonably be expected. Furthermore, the type B uncertainty assessment is not composed of multiple observations and the uncertainty distribution is assessed 'a priori' based on previous measurement data, operator experience, technical specifications of the manufacturer or data provided in calibration certificates or similar reports and assigned uncertainties taken from manuals. The uncertainties associated with the Type B assessment can often be considered to be independent of each other, which make it possible to apply the root-sum square (RSS) method to obtain the total uncertainty of Type B.

Also the two uncertainty assessments, A and B, can be considered independent of each other, according to ISO standards and in the same way, the composed uncertainty may also be calculated using the RSS method as:

$$u(\bar{x}_j) = \sqrt{{u_A}^2 + {u_B}^2} \qquad \text{Eq. (3.1)}$$

In order to increase the probability that the real value is within the uncertainty range considered, the composed uncertainty is multiplied by a factor, k_1, called "enlargment" factor:

$$U(\overline{x_j}) = k_1\, u(\overline{x_j}) \qquad \text{Eq. (3.2)}$$

For examples k_1 =2 defines a confidence interval of approximately 95.45%, while for k_1 =3 the confidence interval is greater than 99%. In other words, a value of k_1 =2 gives the confidence that reasonably about 95% of the true value of the measurand is within the estimated extended range. For the measurement uncertainties calculated in this thesis, a k factor equal to 2 is taken into account.

3.1.3.2 Temperature Measurement and associated measurement uncertainty

The measuring temperature probes used in the Cemafroid Tunnel laboratory are the four-wire platinum resistance thermometers type Pt100, shown in Figure 3.9 (see in Appendix, "Annex A: calibration certificate of four-wire platinum resistance thermometers type Pt100"). These probes can be used in a temperature range between - 80°C and + 250°C. As already shown when describing the K coefficient test procedure (see Chapter 2, subparagraph 2.1.3.4), twelve of them are placed inside the enclosure and, in a specular way, twelve others are placed outside the enclosure.

The procedure to calculate the uncertainty of connection of a measurement chain to a central temperature measurement station is first presented. When calibrating these measuring chains by comparison with the standard thermometer, the components taken into account in the estimation of the uncertainty due to this connection are the following ones:

- A: dispersion of calibration results;
- B_{1U}: uncertainty of use of the standard thermometer;
- B_4: homogeneity of the comparison medium;
- B_5: stability of the comparison medium;
- B_6: uncertainty related to the resolution of the instrument.

These components are calculated as follows.

A: for each calibration point (temperature step), the calibration result (accuracy error or correction) is an average $x_{\bar{j}}$ of n measurements. The standard uncertainty on this result is estimated by the standard deviation of the n measurements. For the connection uncertainty balance, the type A component, $u_A(x_i)$, is estimated by the maximum standard deviation σ:

$$\sigma(\overline{x_j}) = \sqrt{\frac{\sum_{i=1}^{n}(x_{ji}-\overline{x_j})^2}{n-1}} \quad \text{with } \overline{x_j} = \sum_{i=1}^{n}\frac{x_{ji}}{n} \qquad \text{Eq. (3.3)}$$

$$u_A = \max\left(\sigma(\overline{x_j})\right) \qquad \text{Eq. (3.4)}$$

Where:

- i is the number of the measurement $i \in (1...n)$;
- j is the temperature step number $j \in (1...M)$ with M, the number of temperature stages;
- n is the number of measurements per step.

B_{1U}: when a calibration is performed, the uncertainty components related to the standard thermometer (drift, connection, modeling residuals and resolution) are grouped into a single term entitled "uncertainty of use of the standard thermometer". The standard thermometer is used in a controlled environment and maintained between +23°C and +/- 3°C. The calibration is carried out in a liquid bath under the same conditions as calibration at the reference metrology laboratory (LNE). The connection uncertainty is estimated by considering the uncertainty of use as a standard deviation.

$$u_{B1} = u\,(\text{use of the standard thermometer}) \qquad \text{Eq. (3.5)}$$

B_4: the measurement uncertainty due to the temperature non-homogeneity of the comparison medium used during calibration is calculated as the the maximum of non-homogeneity of the medium, assuming that the non-homogeneity is a random variable with a rectangular distribution:

$$u_{B4}\left(\overline{x_j}\right) = \frac{max|\text{non}-\text{homogeneity}|}{2\sqrt{3}} \qquad \text{Eq. (3.6)}$$

B5: the measurement uncertainty due to the lack of stability over time of the temperature of the comparison medium used during calibration is equal to the maximum value of the stability standard deviation:

$$u_{B5}\left(\overline{x_j}\right) = \max(\text{standard deviation}) \qquad \text{Eq. (3.7)}$$

B6: the measurement uncertainty related to the resolution of the measuring chain in calibration (digital display) is calculated by assuming that for any displayed measurement the resolution error is at most half the resolution and applying a rectangular law:

$$u_{B6}\left(\overline{x_j}\right) = \frac{\text{resolution}}{2\sqrt{3}} \qquad \text{Eq. (3.8)}$$

By composing the standard uncertainties, it is possible to calculate the combined standard uncertainty, ($\overline{xj}$) (see Eq. 3.1). This uncertainity is also called uncertainty of the connection of the temperature measurement chain,($\overline{xj}$) and is computed as follows:

$$u_{connection}(\bar{x_j}) = \sqrt{u_A^2(\bar{x_j}) + u_{B1}^2(\bar{x_j}) + u_{B4}^2(\bar{x_j}) + u_{B5}^2(\bar{x_j}) + u_{B6}^2(\bar{x_j})} \quad \text{Eq. (3.9)}$$

And the enlarged uncertainty (see Eq. 3.2) is equal to:

$$U(\text{connection}) = 2\, u_{connection}(\bar{x_j}) \quad \text{Eq. (3.10)}$$

The best uncertainty obtained in Cemafroid with these means is U = 0.039°C.

The components from the measurement chain have to be added to this value of uncertainity. Therefore, when using such a temperature measurement chain, the different components to be taken into account are:

- B_{1R} :uncertainty of connection;
- B_2: drift of the measuring chain;
- B_6: uncertainty related to the resolution of the measurement chain;
- B_7: uncertainty related to modeling residuals from corrections applied to the value read by the measurement chain;
- B_8: uncertainty due to the influence of the ambient temperature on the probes.
- B_9: self-heating uncertainty (residual deviation due to the difference in self-heating of Pt100 in air and alcohol);
- B_{11}: uncertainty related to the influence of radiation (negligible in the presence of radiation protection).

These components are calculated as follows.

B_{1R}: the uncertainty components related to the calibration of each temperature measurement chain, *X*, are grouped into a single term entitled "instrument connection uncertainty", previously presented (see Eq.3.9).

The standard uncertainty of the connection is half the enlareged uncertainty U (connection):

$$u_{B1R}(X) = u\,(connection) = \frac{U(\text{connection})_{k_1=2}}{2} \quad \text{Eq. (3.11)}$$

Where k_1 = 2 is the “enlargement” factor introduced through Eq. 3.2.

B_2: the measurement uncertainty due to the drift of measurement chain of the temperature, X is derived from the maximum of the absolute value of the drift calculated for all years of use and temperature steps, to which a rectangular law is applied:

$$u_{B2}(X) = \frac{2\,(\max|drift|)}{2\sqrt{3}} \quad \text{Eq. (3.12)}$$

In the case of a first use and without a history which allows determining the drift of the instrument, the connection uncertainty of the instrument is taken into account:

$$u_{B2}(X) = u(connection) \quad \text{Eq. (3.13)}$$

B_6: the measurement uncertainty associated with the resolution of the measurement chain for a temperature X is calculated by assuming that for any displayed measurement the resolution error is at most half the resolution and applying a rectangular law:

$$u_{B6}(X) = \frac{\text{resolution}}{2\sqrt{3}} \quad \text{Eq. (3.14)}$$

B_7: the application of a fitting function (minus square fitting) leads to consider the modelling error as an uncertainty component on the temperature X. The modelling uncertainty is deduced from the maximum of the absolute value of the modelling residuals of the last correction applied, by applying a rectangular law. The maximum obtained over all temperature steps at the last adjustment is taken:

$$u_{B7}(X) = \frac{2(\max|\text{modelling residuals}|)}{2\sqrt{3}} \quad \text{Eq. (3.15)}$$

B_8:

$$u_{B8}(X) = \frac{\delta_{Tambient}}{\sqrt{3}} \quad \text{Eq. (3.16)}$$

Where $\delta_{Tambient}$takes into account a variation from the temperature at which the probe is etallonated (T=23°C).

B_9:

$$u_{B9}(X) = \frac{\delta_{T_{self-heating}}}{\sqrt{3}} \quad \text{Eq. (3.17)}$$

$B_{11:}$ is negligible since some devices ensuring the protection to the radiation are used.

By composing the presented uncertainties, the combined standard uncertainty (X) is obtained. This uncertainity represents the best uncertainty for the use of the temperature measurement chain:

$$u(\bar{x_j}) = \sqrt{u_{B1R}^2(X) + u_{B2}^2(X) + u_{B6}^2(X) + u_{B7}^2(X) + u_{B8}^2(X) + u_{B9}^2(X)} \quad \text{Eq. (3.18)}$$

The temperature measurement to be considered results from the arithmetic mean of the temperature measured by twelve sensors placed according to the prescriptions of the ATP. The internal and external temperatures are therefore calculated as follows:

$$T_{int,average} = \frac{1}{12}\sum_{i=1}^{12} T_{int,i} \quad \text{Eq. (3.19)}$$

$$T_{ext,average} = \frac{1}{12}\sum_{i=1}^{12} T_{ext,i} \quad \text{Eq. (3.20)}$$

Where *i* indicates the generic i-th probe.

The average temperature difference between the inside and the outside of the equipment is given by the formula:

$$\Delta T_{average} = \left|T_{int,average} - T_{ext,average}\right| \quad \text{Eq. (3.21)}$$

The respective measurement uncertainty is assessed as:

$$u^2\left(\Delta T_{average}\right) = \left(u\left(T_{ext,average}\right) - u\left(T_{int,average}\right)\right)^2 \quad \text{Eq. (3.22)}$$

The measurement uncertainty of the internal average temperature, $u\left(T_{int,average}\right)$ is calculated as follows:

$$u^2\left(T_{int,average}\right) = u^2_{T_{int}} + u^2_{reproducibilityT_{int}} \quad \text{Eq. (3.23)}$$

$$u^2_{T_{int}} = \max(u^2_{T_{int}}) \quad \text{Eq. (3.24)}$$

where $u_{T_{int}}$ is computed by using eq. (3.18) whereas $u^2_{reproducibilityT_{int}}$ is calculated as follow:

$$u^2_{reproducibility\ T_{int}} = \left(\sigma^2_{spatial\ dispersion}\right) + \frac{N-1}{N}\,\sigma^2_{temporal\ repeatability} \quad \text{Eq. (3.25)}$$

In the above equation , $\sigma_{spatial\ dispersion}$ is calculated as:

$$\sigma_{spatial\ dispersion} = \sqrt[2]{\frac{1}{11}\sum_{i=1}^{12}(T_{int,i} - T_{int,average})^2} \quad \text{Eq. (3.26)}$$

and $\sigma_{temporal\ repetability}$:

$$\sigma_{temporal\ repetability} = \max\left[\sqrt[2]{\frac{1}{11}\sum_{j=1}^{12}(T_{int,j} - T_{int,i})^2}\right] \text{ where } i = 1, \ldots.12 \quad \text{Eq.(3.27)}$$

The measurement uncertainty for the mean outside temperature, $u(T_{ext,average})$, is evaluated using the same procedure:

$$u^2(T_{ext,average}) = u^2_{T_{ext}} + u^2_{reproducibilityT_{ext}} \quad \text{Eq. (3.28)}$$

$$u^2_{T_{ext}} = \max(u^2_{T_{ext}}) \quad \text{Eq. (3.29)}$$

$$u^2_{reproducibilityT_{ext}} = (\sigma^2_{spatial\ dispersion}) + \frac{N-1}{N}\sigma^2_{temporal\ repeatability} \quad \text{Eq. (3.30)}$$

$$\sigma_{spatial\ dispersion} = \sqrt[2]{\frac{1}{11}\sum_{i=1}^{12}(T_{ext,i} - T_{ext,average})^2} \quad \text{Eq.(3.31)}$$

$$\sigma_{temporal\ repeatability} = \max\left[\sqrt[2]{\frac{1}{11}\sum_{j=1}^{12}(T_{ext,j} - T_{ext,i})^2}\right] \text{ where } i = 1, \ldots.12 \quad \text{Eq. (3.32)}$$

Figure 3.8 Four wire platinum resistance thermometers type Pt100 used in Cemafroid.

3.1.3.3 Measurement of the heating power and associated measurement uncertainties

The power measuring chain is a WT 200 power meter which consists of two main components:

- a digital display;
- a IEEE 488.2 digital output.

The Wattmeter is externally calibrated by a COFRAC accredited laboratory (see in Appendix, "Annex B:Wattmeter calibration certificate"). The values displayed by the Wattmeter are corrected by applying a correction function f_1 (slope a_1 and intercept b_1) which is a function of the electrical current rating of the device.

In the "Gestion Centrale" acquisition software, the measured powers are directly corrected for each "current" rating. The uncertainty of use of the wattmeter or uncertainty on the corrected power of the wattmeter is known.

When using the wattmeter (displayed values), the different components to be taken into account are:

- B_{1R}: Power meter connection uncertainty;
- B_2: Power meter drift;
- B_6: uncertainty related to the resolution of the wattmeter;
- B_7:uncertainty related to modelling residuals from applied corrections (function f_1)
- B_{11}: line losses due to the length of connecting cables.

The influence of the ambient temperature is neglected because the wattmeter is used in a controlled environment under the same calibration conditions.

The calculation of each of these components is presented below.

B_{1R}: when a wattmeter is used to measure a "X" value of power, the uncertainty components related to calibration are grouped into a single term called "instrument connection uncertainty". This term is derived from the wattmeter calibration certificate (see in Appendix, Annexe B). The connection uncertainty is derived from the expanded uncertainty given on the calibration certificate by dividing it by the expansion factor k_1=2 (introduced through Eq. 3.2):

$$u_{B1R}(X) = \frac{U_{connection}}{2} \quad \text{Eq. (3.33)}$$

B_2: the uncertainty related to the drift of the wattmeter is deduced from the maximum of the absolute value of the drift calculated for all years and all power ratings, to which a rectangular law is applied:

$$u_{B2}(X) = \frac{2(max|drift|)}{2\sqrt{3}} \quad \text{Eq. (3.34)}$$

B_6: the uncertainty related to the resolution of the (numerical) instrument is calculated by applying a rectangular law.

$$u_{B6}(X) = \frac{resolution}{2\sqrt{3}} \quad \text{Eq. (3.35)}$$

B_7: the application of a fitting function (minus squares adjustment) leads to consider the modelling error as an uncertainty component on the calculated X power. The modelling uncertainty is obtained from the maximum of the absolute value of the modelling residuals of the last correction applied (function f_1), to which a rectangular law is applied. The maximum obtained over all power steps at the last adjustment is taken:

$$u_{B7}(X) = \frac{2\ (\max|\text{modelling residuals}|)}{2\sqrt{3}} \quad \text{Eq. (3.36)}$$

B11: the installation of the automatic heating power control system was designed to reduce the length of the cable between the power meter and the heating resistors. These losses are calculated as follows:

$$P(line\ losses) = RI^2 = \rho\frac{L}{S}I^2 \quad \text{Eq. (3.37)}$$

Where ρ is the resistivity of the cable (for hardened copper, $\rho=1.8.10^{-8}$ Ω.m), L is the length of the cable (in meters) and S is its cross-section (in m²). For I, the maximum value of the current is taken according to the chosen rating (0.2A, 0.5A, 1A, 2A, 5A, 10A or 20A).

The uncertainty related to line losses is calculated from the absolute value of the maximum line loss for each size, to which a rectangular law is applied:

$$u_{B11}(X) = \frac{\max|\text{line losses}|.2}{2\sqrt{3}} \quad \text{Eq. (3.38)}$$

Compounding the standard uncertainties presented above it is possible to obtain the combined standard uncertainty (see Eq. 3.1), which is the best uncertainty in the use of the wattmeter:

$$u_{c,wattmeter} = \sqrt{(u_{B1R}^2(X) + u_{B2}^2(X) + u_{B6}^2(X) + u_{B7}^2(X) + u_{B11}^2(X)} \quad \text{Eq. (3.39)}$$

In steady state, the average power is calculated as follows:

$$W_m = \frac{1}{n}\sum_{i=1}^{n} W_i \quad \text{Eq. (3.40)}$$

Where :

- i is the number of measurement, $i \in (1...n)$,
- n is the number of measurements per step.

The instantaneous powers are measured with the same wattmeter for which the uncertainty of use is known and the standard uncertainty of the steady-state mean power is determined from the variance of W_m. :

$$u(W_m) = \sqrt[2]{\sigma_{repeatability}^2 + u_{c,wattmeter}^2(X)} \quad \text{Eq. (3.41)}$$

In the above equation $\sigma_{epeatability}^2$ is calculated as:

$$\sigma_{repeatability}^2 = \frac{\sum_{i=1}^{n}(W_i - W_m)}{n-1} \quad \text{Eq. (3.42)}$$

3.1.3.4 Length and Surface Measurement and associated measurement uncertainties

Lengths measurements are carried out by various means:

- class II tape measure,
- double decametre class II,
- laser meter

No environment correction is applied to the length values. The external dimensions are measured using wood shims which allow the distances between the flat parts of the walls to be measured and eliminate the problems associated with external corner angles or reliefs in the door closing devices.

The uncertainty related to the measuring Class II equipment, is calculated using the following law for determining the maximum permissible deviation: m.p.d. = 0.2 L + 0.3. Where L is the length rounded up to the nearest whole metre. Hence, the estimated standard deviation is $B_{l1} = 3\ 10^{-3}$ m.

With regard to the laser metr, according to the calibration carried out by LNE laboratory, the expanded measurement uncertainty on the accuracy error is 1.2mm + 2.10^{-6} L. For measurements of long lengths (13m), the uncertainty calculated is $B_{l5} = (1.2 + 2.10^{-6}13.10^{3})/2 = 0.613mm= 0.613.10^{-3}$ m

The components of uncertainty related to the method of operation are:

- the uncertainty from reading: the length is read at 1 mm, i.e. 0.001 m. Hence, the estimated standard deviation is $B_{l2} = 0.001/3 = 0.577\ 10^{-3}$ m
- the uncertainty arising from the use of chocks: the positioning of the shims can lead to a random error of 3mm.
  Hence, the estimated standard deviation is $B_{l3} = 0.003/3 = 1.732\ 10^{-3}$ m.

The surface calculation is based on a parallelepiped insulated enclosure (Figure 3.9). Both for internal and external surfaces, i.e., S_{int} and S_{ext} the following formula is used:

$$S_{int\,(ext)} = 2\left(L_{int(ext)}l_{int(ext)}\right) + 2\left(h_{int(ext)}l_{int(ext)}\right) + 2\left(L_{int(ext)}h_{int(ext)}\right) \qquad \text{Eq. (3.43)}$$

Where: L is the length, l the width and h the height of the insulated enclosure. Subscripts int and ext refer respectively to the internal and external part on which the surface calculations are carried out .

The surface area, S, used in the K coefficient formula, is the mean surface area of the insulated enclosure, already defined by Eq. (2.2) and the associated measurement uncertainity is calculated as follows:

$$u^2(S) = \left(\frac{dS}{dS_{int}}\right)^2 u^2(S_{int}) + \left(\frac{dS}{dS_{ext}}\right)^2 u^2(S_{ext}) \qquad \text{Eq. (3.44)}$$

$$u^2(S) = \left(\frac{1}{2}\frac{S_{ext}}{\sqrt{S_{int}S_{ext}}}\right)^2 u^2(S_{int}) + \left(\frac{1}{2}\frac{S_{int}}{\sqrt{S_{int}S_{ext}}}\right)^2 u^2(S_{ext}) \quad \text{Eq. (3.45)}$$

$$u^2(S) = \left(\frac{1}{4}\frac{S_{ext}^2}{S_{int}S_{ext}}\right) u^2(S_{int}) + \left(\frac{1}{4}\frac{S_{int}^2}{S_{int}S_{ext}}\right)^2 u^2(S_{ext}) \quad \text{Eq. (3.46)}$$

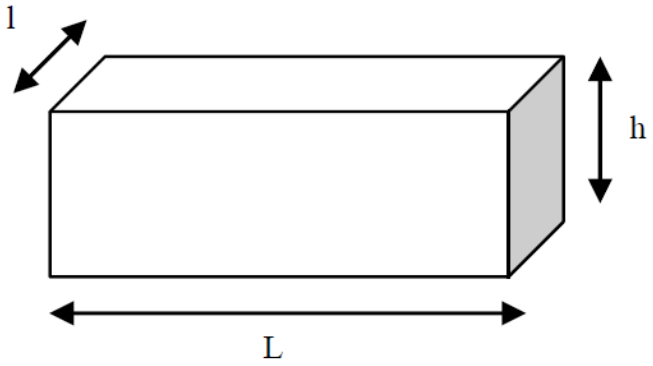

Figure 3.9 Parallelepiped insulated enclosure schema for lengths measurements

3.1.3.5 Measurement uncertainty of K coefficient

The procedures explained in the previous subparagraphs (3.1.3.2, 3.1.3.3, 3.1.3.4) are combined here because the uncertainty of each K coefficient measurement is calculated taking into account the several sources of uncertainty:

- the steady-state mean heating power, W_m,
- the temperature difference, $\Delta T_{average}$, between the mean internal temperature $T_{int,average}$ and the mean external temperature, $T_{ext,average}$, and,
- the surface area of the body, S.

The combined uncertainty for the K coefficient measurement is therefore evaluated as:

$$u^2(K) = \left(\frac{1}{S\Delta T_{average}}\right)^2 u^2(W_m) + \left(\frac{W_m\,\Delta T_{average}}{(S\Delta T_{average})^2}\right)^2 u^2(S) + \left(\frac{W_m S}{(S\Delta T_{average})}\right)^2 u^2(\Delta T_{average}) \quad \text{Eq. (3.47)}$$

The expanded relative uncertainty, $U(K)$ is twice the relative standard uncertainty, $u(K)$.

3.2 Real ageing at key moments on the life of a refrigerated vehicle

This section provides the results of *K* coefficient tests realized several times at key periods in the life of some refrigerated vehicles. These tests were realized in the climatic chamber of Cemafroid ATP test station.

For the first time, *K* values at instants other than those imposed by ATP (i.e. after manufacturing for the prototype vehicle and after twelve years for all vehicles in the series) are provided. Furthermore these measurements are realized on the same vehicles and allow making a real estimation of the ageing over the time of these vehicles. The results of the following experimental assessments are therefore presented:

- measurement of the *K* coefficient during the first months of a semi-trailer;
- measurement of the *K* coefficient even after twelve years of use (i.e.: at eighteen, twenty-four and thirty years after the manufacture) for a small sample of trucks.

3.2.1 *K* Coefficient tests during the first months of the life of a refrigerated semi-trailer

At the beginning of its life, the refrigerated vehicle may undergo various interventions which can impact on the *K* coefficient value. With the aim of assessing the impact of these interventions on the insulation performance of the vehicle as well as the ageing during its first months of life, a refrigerated semi-trailer with a mean surface of 155 m^2 was tested at different moments and under different conditions, i.e. in presence or absence of the refrigeration unit and of the door inserts. When removing the refrigeration unit from the semi-trailer, a shutter buffer takes its place. The tested semi-trailer was built based on a prototype that was also tested at time t_0 = 0: its *K* coefficient was found to be equal to 0.39 Wm^{-2} K^{-1}.

The following subparagraphs present:

- the tested vehicle;
- test followed test protocol and the conditions of the experiments;
- the results of the experimental assessment.

3.2.1.1 Tested vehicle

The vehicle chosen for the test is a semi-trailer (see Figure 3.10) having an average surface area equal to 155 m^2 and an internal volume of 86 m^3. The door type is a total rear opening with two leaves having four lever joints. The walls of the vehicle are made of polyurethane sandwich panels coated with polyester and whose blowing agent is cyclopentane for the side walls, ceiling and floor, and CO_2 for the front face and the door.

Figure 3.10 Tested semi-trailer.

3.2.1.2 Test protocol and ATP standardized test conditions

The measurement of the *K* coefficient on the semi-trailer was performed at different times and under different conditions. These tests conditions can be grouped in two phases, explained below.

Phase one consists of several interventions on the insulated enclosure to assess the incidence of certain accessories. In particular, the refrigeration unit and the rear door inserts are removed. In this first phase three *K* coefficient tests were carried out as follows:

- t_0 = 0: at the exit of the manufacturing chain, with the refrigerating unit and door inserts on the insulated enclosure.
- t_1 = 6 days after removing the refrigerating unit and positioning the shutter buffer;
- t_2 = 14 days, with shutter buffer and removing the doors inserts.

After these interventions, phase two aims at assessing the ageing of the insulated enclosure during the first months of the vehicle's life. In fact, after the removal of the refrigeration unit and door inserts, the insulated enclosure underwent no further modifications and the *K* coefficient experiments only served to assess the ageing of the insulated enclosure over the time.

This phase groups the following experiments in the same configuration, i.e. without the refrigeration unit and without the inserts of the back frame of the door:

- t_2 = 14 days
- t_3 = 30 days,;
- t_4 = 125 days.

3.2.1.3 Results of the experimental assessment

For the *K* coefficient tests carried out in both phases, the value of the maximum measured uncertainty obtained, equal to ± 3.7% was considered. The *K* coefficient obtained from the tests of

the three different steps of the first phase (i.e. t_0 = 0, t_1 = 6 days and t_2 = 14 days) are shown in Figure 3.11.

The removal of the refrigerating unit and the positioning of the shutter buffer, six days after the manufacturing of the vehicle, result in a reduction of the K coefficient $\left(\frac{K_{t1}-K_{t0}}{K_{t0}}100\right)$ by 2.5%. Fourteen days after , the door inserts were removed, which causes a further decrease of the K coefficient by 2.8 %. Overall, these removal interventions result in a decrease of the K coefficient (therefore an improvement of the insulation performance) by 5.3%.

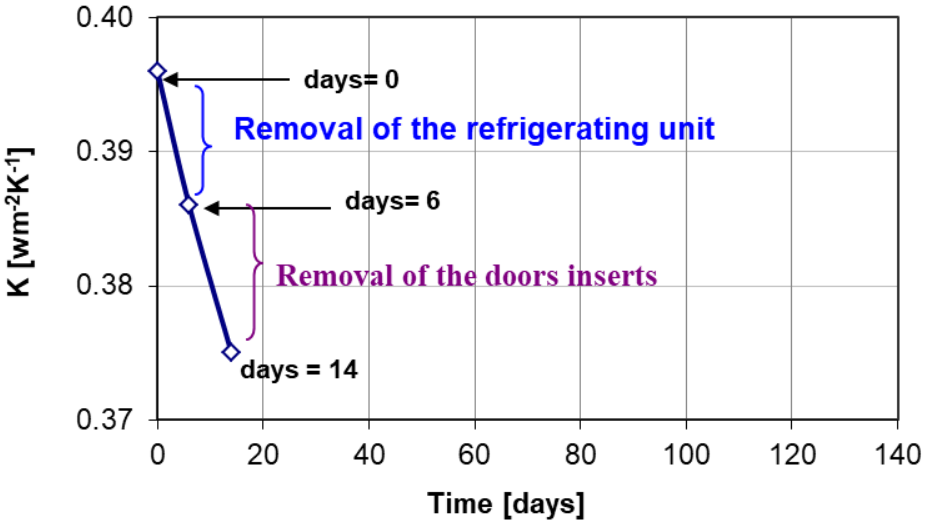

Figure 3.11 Results of the first phase.

The results of the second phase are shown in Figure 3.12.

The absence of a reference point at t_0 = 0 does not allow analysing the ageing over the whole period but only from the 14th day. The ageing rate $(\frac{K_{t4}-K_{t2}}{K_{t2}}100)$ observed for the period is equal to 1.3% over 111 days. Although this result is interesting because it allows having measures of K not prescribed by ATP, it is not yet sufficient to conclude about ageing. Other measurements are required.

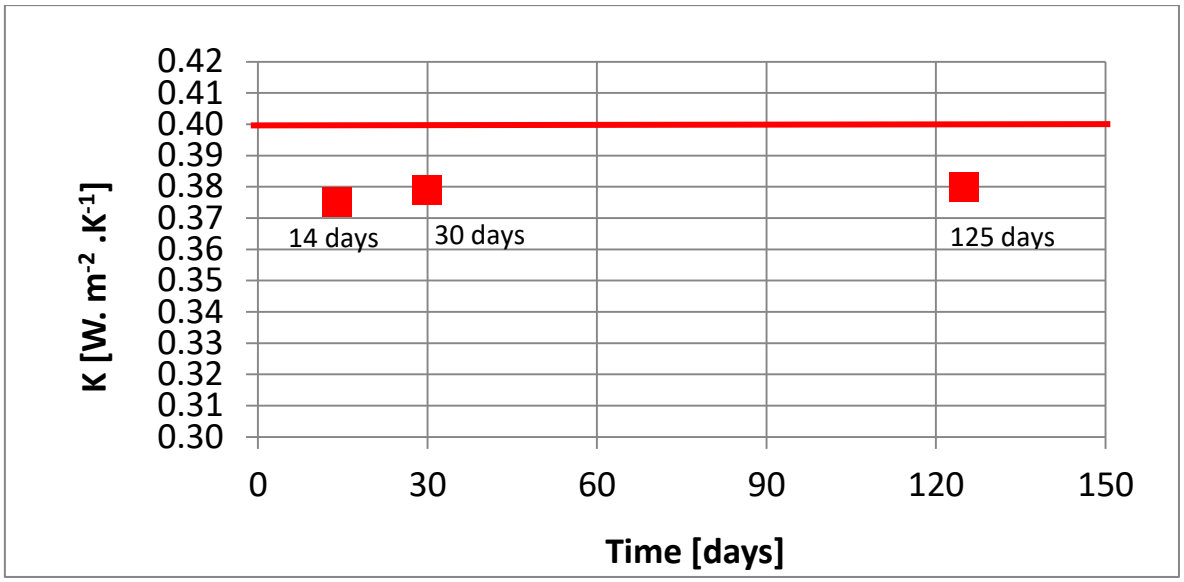

Figure 3.12 Results of the second phase. Red line represents the ATP threshold value for reinforced insulation (K≤0.40W.m^{-2}.K^{-1}).

3.2.2 K Coefficient tests during the last years of the life of a refrigerated truck

Data of ten in-service refrigerated trucks of different firms, whose tests were repeated even after twelve years of life, were extracted from the Datafrig® database.

The time evolution of their K coefficient is plotted on Figure 3.13. For all the values of K coefficient a measurement uncertainty, u (K) calculated by using Eq. (3.47), equal to ±3.7% was considered. In this Figure the square-shaped markers represent the measured K values of the in-service vehicles and the triangle-shaped markers the initial K values of the, corresponding prototypes. The evolution of K can be very different from one vehicle to another. This may be mainly due to the different usages of the vehicles (type of transported products), as well as to the different manufacturing technology used to build the vehicle, leading to different performances over the time (see Table 3.3). Also, in the period 0-12 years the variation of K is larger than in the period 12-18 years with a mean relative difference between K_{12} and K_p (i.e.,$\frac{K_{12}-K_P}{K_p}$) equal to 66 % whereas between K_{18} and K_{12} this difference (i.e., $\frac{K_{18}-K_{12}}{K_{12}}$) reaches a mean value equal to 5 %. Only one vehicle has been tested at twenty-four and thirty years and in this period of time the K coefficient is growing faster than in the period 12-18. This vehicle was presented in Chapter 2 (Figure 2.49) and it is an example of a vehicle where the construction technology and a good maintenance allowed its use over a period of 30 years.

Concerning the first portion of the curves, related to period 0-12 (with the K_P as reference point at instant 0) the ageing may be different (greater or lower) from the measured value (66 %) since, actual vehicles realized in the series could deviate from their reference prototypes. For this reason, this part of the curves has been represented in the graph by dotted lines. The concern about the existing difference between prototypes vehicles and actual vehicles realized is deepened in the next section.

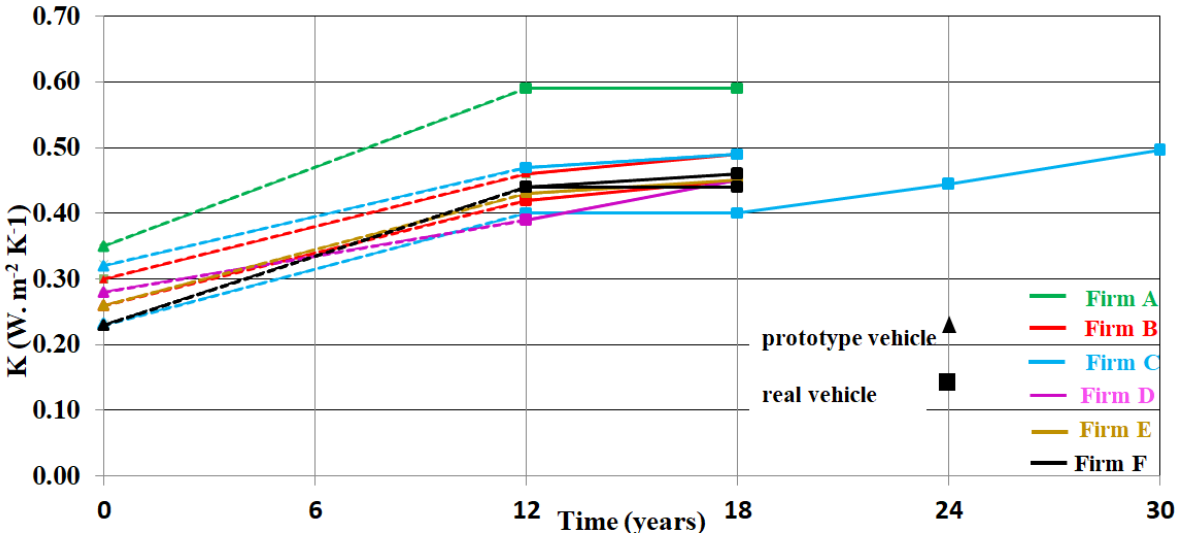

Figure 3.13 Time evolution of *K* coefficient of ten in-service refrigerated trucks.

Table 3.3 Type of transported products, manufacturers and K coefficient values of the eleven trucks

Type of transported products	**Manufacturer**	K_p [W.m^{-2}.K^{-1}]	K_{12} [W.m^{-2}. K^{-1}]	K_{18} [W.m^{-2}. K^{-1}]	K_{24} [W.m^{-2}. K^{-1}]	K_{30} [W.m^{-2}. K^{-1}]
Meat transport	Manufacturer A	0.35	0.59	0.59	/	
Local freight	Manufacturer C	0.32	0.47	0.49	/	
Mixed products	Manufacturer B	0.30	0.46	0.49	/	
Dairy products	Manufacturer D	0.28	0.39	0.45	/	
Meat transport	Manufacturer C	0.27	0.44	0.47	/	
Meat transport	Manufacturer E	0.26	0.43	0.45	/	
Mixed products	Manufacturer B	0.26	0.42	0.45	/	
Mixed products	Manufacturer C	0.40	0.40	0.40	0.45	0.50
Frozen food	Manufacturer F	0.23	0.44	0.44	/	
Mixed products	Manufacturer F	0.23	0.44	0.46	/	
Mixed products	Manufacturer D	0.22	0.38	0.40	/	

3.2.3 Conclusion of the experimental assessments

This section presented K values measured for the first time at instants other than those prescribed by the ATP regulation.

With regard to the semi-trailer tested in the first months of its life, it was also possible to highlight the impact of the addition/removal of the refrigerating unit and the door inserts on the evolution of the K coefficient. The semi-trailer was tested in both situations: in the presence of these accessories and then in their absence. The pipes and fixings of the refrigeration unit on the insulated enclosure of the semi-trailer as well as the inserts used to fix the door frames represent thermal bridges which penalize the value of the K coefficient. In particular, it was found that the removal of these components caused a decrease of the K coefficient by 5.3%. After assessing the impact of these accessories, the insulated enclosure of the semi-trailer underwent three K coefficient tests at different moments of its life. It was found that in a period of 111 days after the manufacturing, the ageing rate was 1.33 %. This section also highlighted the ageing of a small sample of vehicles in the last years of their life. In particular it has been pointed out that in the period between the manufacturing and the following twelve years of use, the average ageing on the basis of this sample can be estimated at 66 %. In the successive period of life between eighteen and twenty-four years of life, the relative increase of K coefficient is only 5 %. However, if the increase of 5 % between twelve years and eighteen years is a certain increase (because it is calculated on the basis of measurements made on the same real vehicle), the same does not happen in the period between the manufacture and the first twelve years of use. In this case, the ageing is assessed by taking a prototype vehicle as a reference and the ageing rate could be therefore greater or lower than 66 %. In the next section, some of the aspects highlighted here will be more investigated. In particular, the impact of the refrigeration unit will be further investigated and new production vehicles will be tested to compare them to the respective prototypes. This will allow having an estimation of the error that is made when the prototype vehicle is taken as a reference in the ageing assessment.

3.3 Impact of the refrigerating unit

In the previous paragraph the impact that the mounting on the vehicle of the refrigerating unit may have on the insulation performance of the vehicle was analyzed for a single semi-trailer. The refrigerating unit and the positioning of the shutter buffer were realized six days after the manufacturing of the vehicle. In this paragraph this kind of experiment is carried out for four semi-trailers of different firms. However, these semi-trailers were all built with sandwich panels whose blowing agent is cyclopentane, do not have any special accessories inside them and all have an average surface area of 158 m^2.

The realized analysis consisted of K coefficient tests on each of these four vehicles in two different conditions: in the presence and in the absence of the refrigerating unit. The tests were carried out in the climatic chamber of the Cemafroid and for each obtained K value a measurement uncertainty of ± 3.6 % was considered.

As described for the first phase in this case, when removing the refrigeration unit from the semi-trailer, a shutter buffer was placed. The results of this experimental assessment are shown in Figure 3.14, where the non–colored parts of the bars having defined contours represent the measured K_0 values in absence of refrigerating unit. In any case, when mounting the refrigerating unit the K_0 values increase. For these fours semi-trailers, the average value of the difference between K measured in these two conditions, i.e. in presence or absence of the refrigerating unit, is equal to 0.02 W. $m^{-2}.K^{-1}$. A sample of only four vehicles is still a small sample and further measurements are needed to achieve better representativeness. However, given the uniqueness of the measurements, it is decided to take them into account.

This value equal to 0.02 W. $m^{-2}.K^{-1}$will be used in the next section when presenting the tests carried out on new production vehicles to compare their initial K values (K_0) to the K values of the respective prototypes (K_p). The prototypes are tested in the absence of a refrigerating unit, therefore in order to make the comparison between K_0 and K_p, the K_p coefficient values will be increased by a factor equal to the estimated value (0.02 W. $m^{-2}.K^{-1}$)

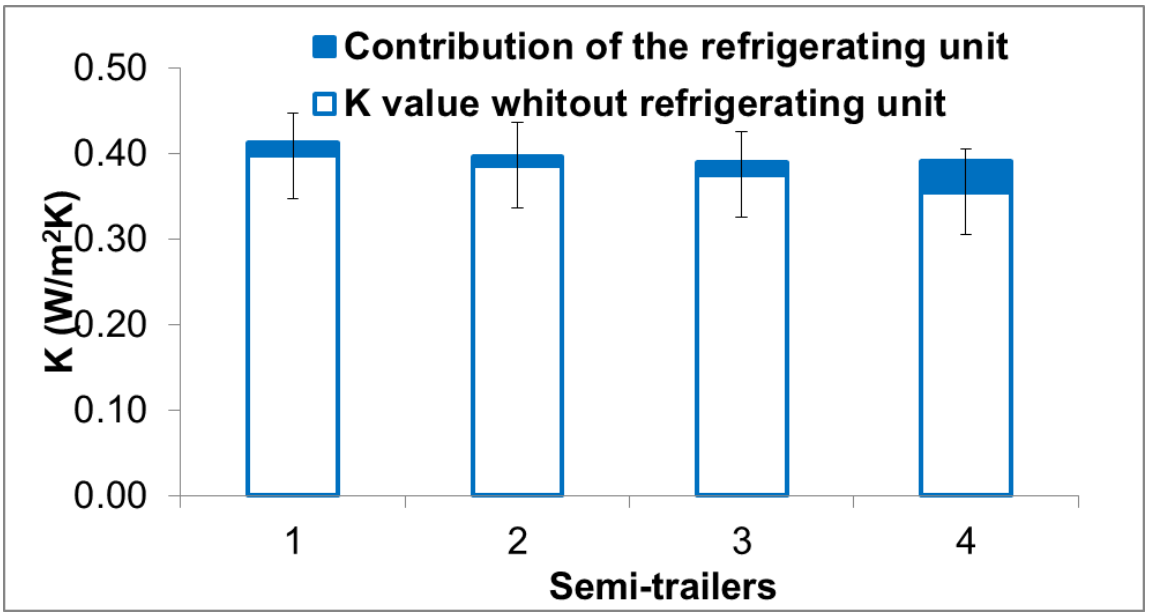

Figure 3.14 Measured *K* values for four semi-trailers in presence and absence of the refrigeration unit.

3.4 Experimental assessment of the difference between new refrigerated vehicles and their corresponding prototypes

As discussed in the section 3.2, series-produced vehicles may differentiate themselves from their respective prototypes and may also undergo some interventions in the first moments of their life.

In May 2017, the French Directorate-General for Food (DGAl) commissioned Cemafroid to carry out an insulation performance monitoring programme of new series-produced vehicles, subject to the provisions of Article R 231-59 of the Rural and Maritime Fishing Code and paragraph 1c of Appendix 1 of Annex 1 of the ATP.

The main objective of this control programme was to verify that these series-produced vehicles could comply with their corresponding prototypes.

This programme was carried out over a period of three years and involved three series of vehicles, i.e., fourteen vans, fourteen trucks and thirteen semi-trailers, all being built with reported insulated enclosures and used for the transport of perishable foodstuffs under the ATP Agreement. All these vehicles were subjected to the K coefficient test, realized in the Cemafroid test chamber of Tunnel T_1.

The results of this insulation monitoring programme were analyzed in the context of this thesis because, for the first time, it was possible to compare the insulation performance of new series-produced vehicles to the insulation performance of their corresponding porotypes. This comparison represents a first fundamental step in the study of the ageing of refrigerated vehicles. As a matter of fact, according to the rule for renewal, provided by the ATP regulation, the assessment of the ageing of refrigerated vehicles has always been realized by comparing the K coefficient value of the in-service vehicle at the n-th year (twelve in France, nine in Italy), K_n to the initial K value of the prototype equipment, K_p, being, usually, the only one available after manufacturing.

In accordance with ATP, however, this evaluation may include some biases in that sense that the real vehicle produced in the series with the same design of the prototype, may vary in terms of surface and number of accessories, with the tolerance allowed by the current regulation. Its internal surface, for example, may vary by ±20 % compared to the prototype and the real equipment could present less accessories or openings. Furthermore, there are also some reasons intrinsic to the production process that could alter the real K coefficient value. For instance, the curing of the insulant foam before manufacturing may be quite different from one case to another. The reference prototype may have small differences in size and geometry, and hence a different initial K value (K_p) compared to the initial K value of the vehicle realized in the series, K_0. This circumstance may affect the assessment of the real ageing.

This chapter first presents the criteria imposed by the monitoring programme for the selection of vehicles and for deciding whether they are compliant or not with the ATP. Then, the

experimental results obtained by testing the three series of newly manufactured vehicles are presented. The reasons for the existing difference between the real K coefficient values, K_0 and the corresponding reference prototypes, K_p are investgated.

3.4.1 Criteria imposed by the monitoring progamme

3.4.1.1 Selection criteria of tested vehicles

Each vehicle subjected to this experimental study was selected on the basis of the ATP certificate obtained on the basis of the K the coefficient test realized earlier on the corresponding prototype vehicle. Furthermore each vehicle was selected to meet the following three criteria:

- built or having applied for an ATP certificate in France for less than six month;
- mono or multi temperature;
- belonging to the category of mechanically refrigerated equipment of class C, which should also imply the occurrence of the notion of heavily insulated equipment ($K \leq 0.40$ W.m^{-2}.K^{-1}).

3.4.1.2 ATP compliance criteria

The main purpose of the monitoring programme was to check that the K_0 coefficient of the series-produced vehicles complied with the two criteria presented below:

- with regard to the maximum authorized value of class C ($K \leq 0.40$ W.m^{-2}.K^{-1});
- with regard to the value of the K_p coefficient of the reference prototype vehicle as given in the official test report, taking into account the uncertainty in the determination of the K coefficient value and applying a further correction to the measured due to the impact of the refrigeration unit. This correction was considered equal to 0.02 W.m^{-2}.K^{-1} on the basis of the experience gained in the field through the realization of several testes carried out on vehicles before and after mounting the refrigeration unit (some of these tests have been presented in section 3.3)

3.4.2 Comparison between the K_0 value of newly manufactured vehicles and the K_p value of their reference prototype

Each one of the forty-four new vehicles tested in the context of this experimental analysis corresponds to a prototype vehicle, previously subject to the K coefficient test. The results of these tests are shown in Figure 3.15 where the vehicles are distributed as follows:

- the first fourteen vehicles (from number 1 to number 14) represent the series of vans;
- vehicles from number 15 to 28 represent the series of trucks;
- the last fourteen vehicles (from number 29 to 41) are the series of semi-trailers.

Moreover, the results of Figure 3.16 are represented as follows:

- the coloured (blue) bars represent the K_0 coefficients of the new vehicles produced in the series while,
- the non-coloured bars represent the K_p coefficients of the corresponding prototype vehicles.

For each experimental result, both for prototypes and new vehicles, the associated measurement uncertainty, calculated using Eq. (3.47) is also represented on the graph. Minimum and maximum values of these measurement uncertainties, for each series of vehicles are summarized in Table 3.4. For each case, the measurement uncertainties of K_p and K_0, are less than the maximum value of uncertainty required by the ATP, equal to ±5 %.

Table 3.4 Minimum and maximum values of the calculated measurement uncertainties for the K_0 of the forty-one vehicles under the experimental assessment and for the corresponding K_p of prototypes vehicles.

	Minimum measurement uncertainty	**Maximum measurement uncertainty**
$K_p$vans	±1.6 %	±3.7 %
K_0 vans	± 1.7%	± 4.5 %
K_p trucks	±1.6 %	± 3.7 %
K_0 trucks	±1.2 %	± 3.8%
K_p semi-trailers	± 1.6 %	± 3.7%
K_0 semi-trailers	±1.3 %	± 3.7%

Among the forty-one new vehicles tested, fifteen were built in such a way that the insulation performance was very close to the insulation performance of the prototype vehicles and in some cases even better.

Vehicles number 2, 8, 12, 13, 22, 36 are examples of vehicles faithfully built with respect to their prototype: in fact the K_p and K_0 coefficients are almost equal.

Vehicles number 3, 4, 7, 11, 14, 19, 25, 26, 30 were conceived better than the reference prototypes: their K_0 are lower than the corresponding K_p. All the other measured K_0values of the new vehicles are greater than the measured values of the prototypes, K_p. Also, vehicles number 5, 9, 16, 17, 18, 23, 24, 27, 33, 35, 37, 38, 40 and 41 results show to what extends the difference between $K_0$and K_p can have an impact on the real performance of the vehicles actually circulating on the road. Taking as reference their K_0, which are greater than 0.40 $W.m^{-2} K^{-1}$, these vehicles would have obtained a different insulation class (IN) compared to that obtained based on the corresponding K_p (IR). As a matter of fact, as shown in Figure 3.15, their K_0 measured value exceeds the red line on the graph representing the ATP threshold between reinforced insulation, IR (when $K \leq 0.40$), and normal insulation, IN (when$0.40 > K \geq 0.70$). The difference between K_0 and K_p on the set of forty-two vehicles which, in relative terms (i. e. $\frac{K_0 - K_p}{K_p}$ %) reaches an average value of 6% and a maximum of 31%, has an impact on the evaluation of the real ageing of the vehicles. Considering the three different sets of vehicles (vans,

trucks, semi-trailers), the minimum value of this difference is associated with semi-trailers (see Table 3.5). This could be due to the fact that this kind of vehicles is built in a more standardized and homogeneous way, compared to smaller vehicles.

Table 3.5 Relative difference between K_0 and K_p for the three sets of vehicles.

	$\frac{K_0 - K_p}{K_p}$ %		
	Minimum	**Average**	**Maximum**
Vans	- 20%	2%	23%
Trucks	- 10%	8%	31%
Semi-trailers	- 8%	11%	22%
All vehicles	- 26%	6%	31%

Taking into account the criteria imposed by the monitoring programme, it is pointed out that:

- 49% of the vehicles (i.e. vehicles number 1, 2, 4, 6, 8, 10, 12, 13, 15, 20, 21, 22, 26, 28, 29, 31, 32, 34, 39) are fully compliant with the criteria of reinforced insulation imposed by ATP ($K_0 \leq 0.40$ W.m^{-2}.K^{-1}). These vehicles are represented by the dark green bars in Figure 3.16.
- 17% of the vehicles (i.e. vehicles number 3, 7, 11, 14, 19, 25, 30) have a lower K coefficient, i.e. a higher insulation performance, even lower than the 7% tolerance imposed by the monitoring programme. These vehicles are represented in Figure 3.16 by light green bars.
- vehicle number 17 represented by the orange bar in Figure 3.16 does not comply with ATP criteria but nevertheless has a K coefficient within the tolerance of 7% set by the monitoring programme.
- 32% of the vehicles (i. e. vehicles number 5, 9, 16, 18, 23, 24, 33, 35, 37, 38, 40, 41) do not does meet the criterion of class C ($K \leq 0.40$ W.m^{-2}.K^{-1}). In this case the vehicles are represented by red bars in Figure 3.16.

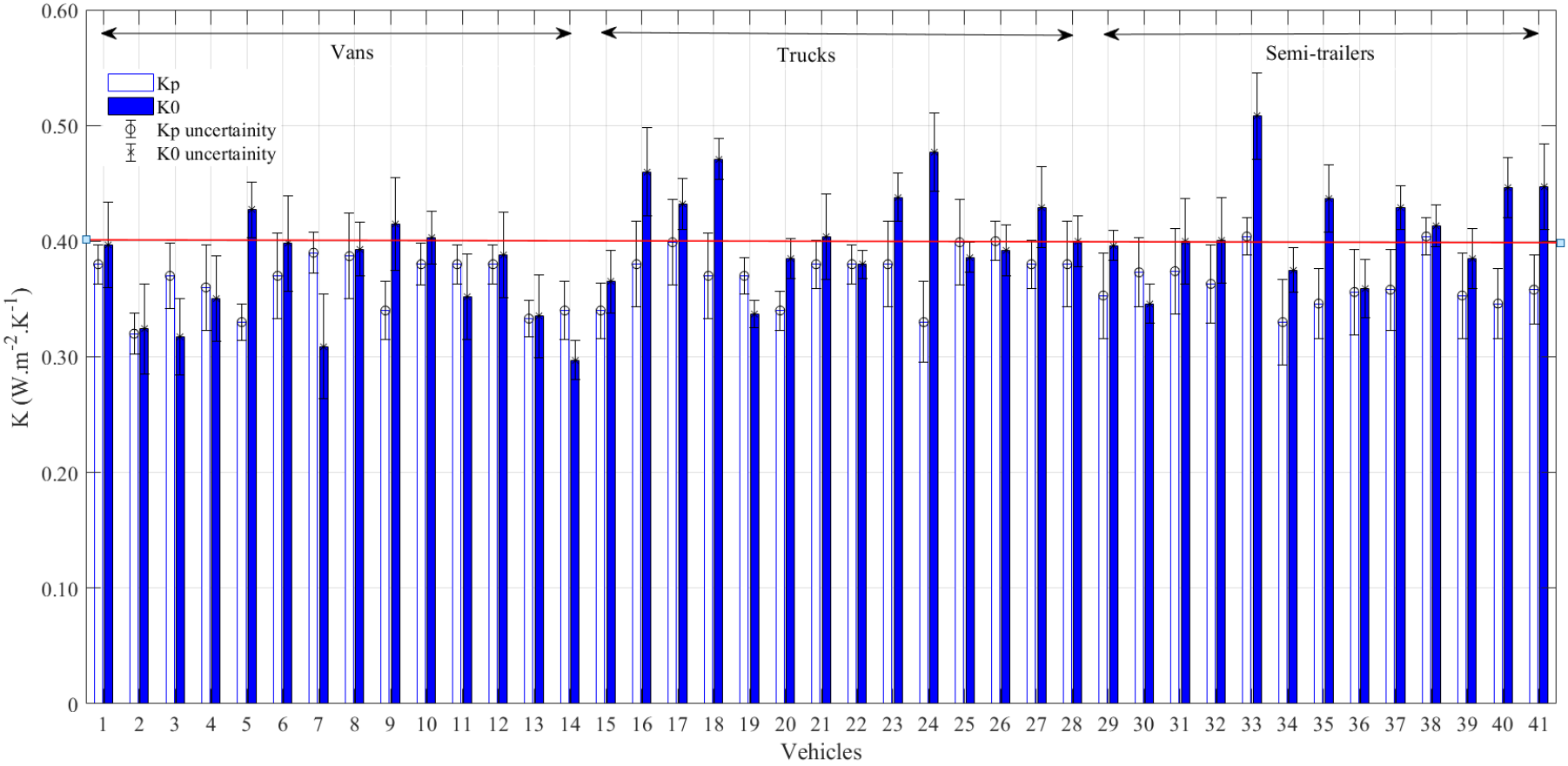

Figure 3.15 K_0 coefficient of tested vehicles (represented by the colored bars) andK_P values (non-colored bars) associated to the corresponding reference prototype vehicles. Red line represents the ATP threshold value between reinforced insulation, IR and normal insulation, IN.

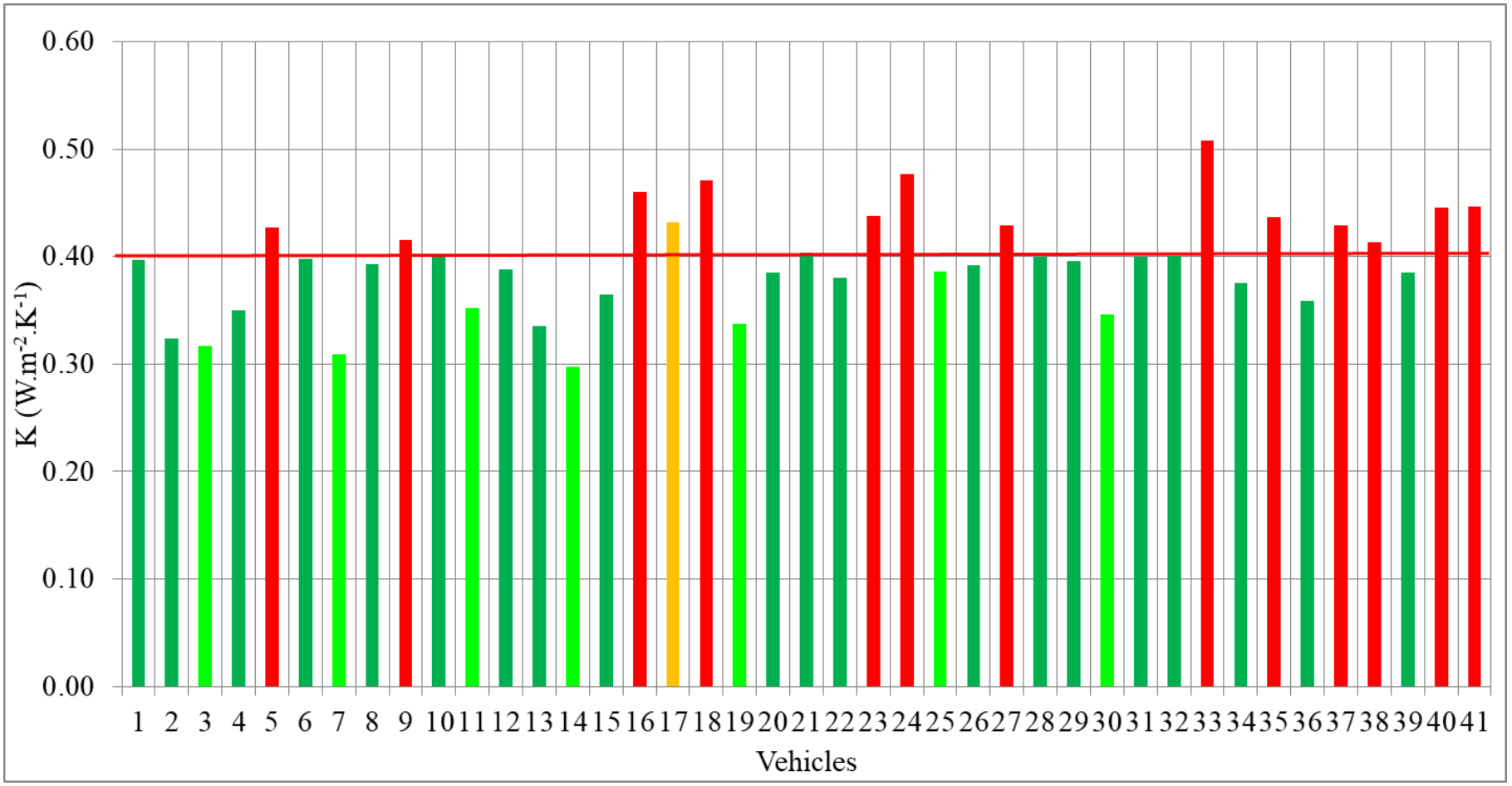

Figure 3.16 Compliance to ATP of the forty-one new vehicles taking into account the criteria imposed in the control programme; Red line represents the ATP threshold value between reinforced insulation, IR and normal insulation, IN.

3.4.3 Possible reasons for the existing differences between new vehicles and their corresponding prototypes

3.4.3.1 Surface influence

The ATP regulation allows the comparison of the actual insulation performance of a refrigerated vehicle to that of a reference prototype. This reference prototype may have small differences in size and geometry. As a matter of fact the ATP regulation allows the construction of series production vehicles with a surface area that differs from that of the prototype by more or less 20%. Figure 3.17 shows the percentage variation of the surface area for the forty-one tested vehicles compared to the surface of the corresponding prototype vehicles. This surface variation is calculated as follows:

$$\frac{S_0 - S_p}{S_p} \% \qquad \text{Eq. (3.48)}$$

Where S_0 is the mean surface area of the real vehicle built in the series and S_p the one associated with the reference prototype vehicle.

For the forty-one vehicles under study, as shown in the graph of Figure 3.18, this percentage change in surface area varies from a minimum value of -15% to a maximum value of 17%, respecting the criterion set by the ATP regulation.

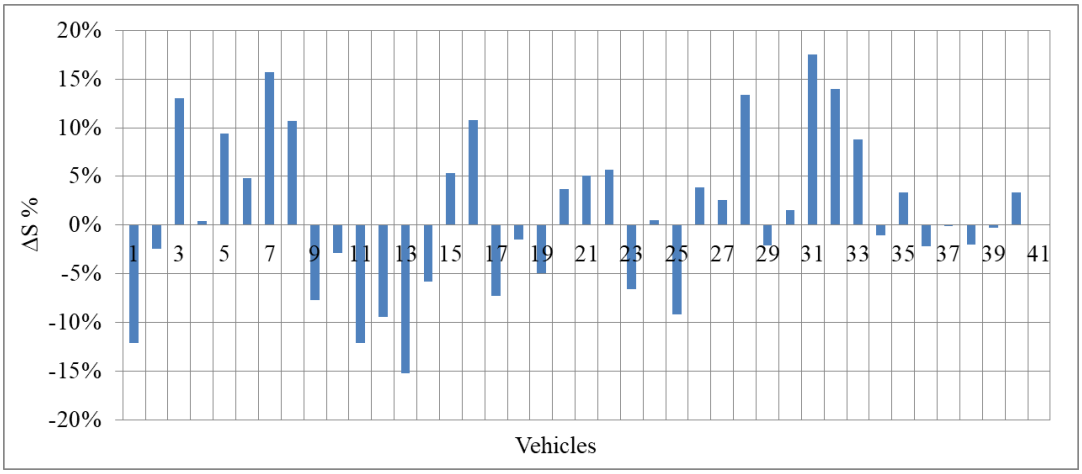

Figure 3.17 Percentage variation in surface area between the new vehicle and the corresponding prototype vehicle.

To understand the impact of this surface variation on the existing variation between K_p and K_0, the theoretical K coefficients for real vehicles and their prototype vehicles have been calculated using Eq. (2.8). This equation assumes that the thermal resistance of the whole body is related only to the insulating foam and gives an ideal reference value that neglects the thermal bridges due to geometric singularities.

To calculate these theoretical K values, an average value of initial thermal conductivity equal to 0.023 $W.m^{-1}.K^{-1}$ was used. This value comes from the data available in the literature provided by the manufacturers (see Table 3.6) and it was chosen because the density value of the polyurethane walls for all the vehicles tested has a value between 30 and 50 $kg.m^{-3}$.

The graph of Figure 3.18 shows the calculated theoretical K values. The non-colored bars on the inside that only have a purple outline represent the theoretical K values for the prototypes vehicles ($K_{p,th}$) whereas the purple colored ones the theoretical K values for new vehicles ($K_{0,th}$). Note that for prototypes number 24 and 41, it was not possible to carry out the calculation due to a lack of data.

For all the vehicles, the $K_{p,th}$ and $K_{0\text{-}th}$ are nearly the same. In this case, one can thus suppose that the geometry does not affect the variation between the measured K values, K_p and K_0. The existing differences between the measured values may therefore be due to all the changes carried out on the new vehicles including the assembling of the refrigeration unit on them.

Table 3.6 Initial thermal conductivity of polyurethane foam measured at 10°C for polyurethane foams having different value of density (Commisione Tecnica ANPE, 2011).

Density of the polyurethane foam ($kg.\ m^{-3}$)	Initial thermal conductivity of polyurethane foam measured at 10°C ($W.\ m^{-1}K^{-1}$)
>30 ; <50	0.022 - 0.024
>50	0.023 - 0.025

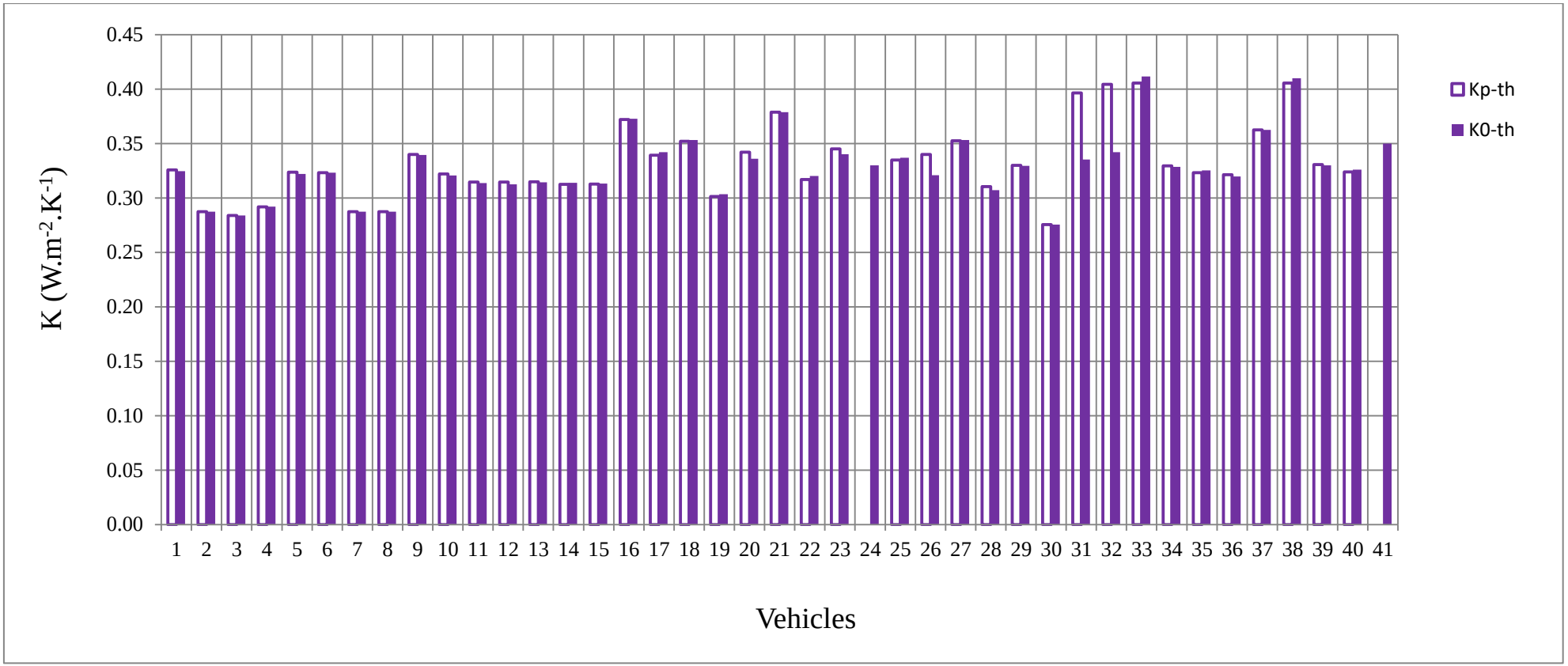

Figure 3.18 Theoretical K values of newly manufactured vehicles $K_{0,th}$, compared to the respective theoretical K values of the corresponding prototypes, $K_{p,th}$

3.4.3.2 Influence of the solid matrix of the vehicle structure

In the previous subparagraph, to assess the influence of the change in the average surface area, it was assumed that the vehicle structure was composed only of insulating material. Conversely, in order to resist to cracking, crumbling, shifting, and packing from the shock, vibration, and flexing of the body structure, but also in order to prevent from breakdown at extreme temperatures, the real vehicles are not made only of polyurethane foam but include a solid matrix. Using the values of the measured K_0 of the forty-one tested new vehicles, it is possible to define an apparent thermal conductivity (λ_{app}) which takes into account the presence of the solid matrix as follows:

$$\lambda_{app} = K_0 \delta_{average} \quad \text{Eq. (3.49)}$$

Where $\delta_{average}$ is the average thickness of the vehicle's walls, calculated as follow:

$$\delta_{average} = \frac{\sum \delta_i S_i}{\sum S_i} \quad \text{Eq. (3.50)}$$

A linear regression was performed separately for each series of vehicles in order to identify the apparent conductivity that is the slope of the line. The equations and the coefficients of determination obtained separately for each series of vehicles are the following:

$$K_{0,calculated\ for\ vans} = 0.028 \left(\frac{1}{\delta_{average}}\right) \qquad R^2 = 0.55 \quad \text{Eq. (3.51)}$$

i.e. λ_{app} is equal to 0.028 W.m^{-1}.K^{-1},

$$K_{0,calculated\ for\ trucks} = 0.032 \left(\frac{1}{\delta_{average}}\right) \quad \text{avec } R^2 = 0.14 \quad \text{Eq.(3.52)}$$

i.e. λ_{app} is equal to 0.032 W.m^{-1}.K^{-1},

$$K_{0,\ calculated\ for\ semi-trailers} = 0.0294 \left(\frac{1}{\delta_{average}}\right) \quad \text{avec } R^2 = 0.52 \quad \text{Eq. (3.53)}$$

i.e. λ_{app} = 0.0294 W.m^{-1}.K^{-1}.

To identify the average apparent conductivity taking into account the presence of this new series of vehicles, the results of K_0 of the three series of vehicles were gathered together and the same

kind of linear trend was discovered. The relationship for all the dataset of vehicles between K_0 and $\frac{1}{\delta_{average}}$ is presented in Figure 3.19 where the slope of the line represents the average thermal conductivity of the forty-one vehicles considered as a unique series:

$$K_{0,calcutaed\ for\ all\ vehicles} = 0.030\left(\frac{1}{\delta_{\text{average}}}\right) \qquad R^2 = 0.25 \qquad \text{Eq. (3.54)}$$

By looking at Eq. (3.51), Eq. (3.52) and Eq.(3.53) it is possible to see that the R^2 coefficient varies from 0.014 (case of truck) to 0.55 (case of vans). The coefficient of determination, R^2, is an indicator that allows judging the quality of a simple linear regression. It measures how well the model fits the observed data or how well the regression equation fits to describe the distribution of points. This coefficient can vary between 0 and 1, i.e. between low and high predictive power. It is possible to see that in the case of semi-trailers and vans, with R^2, equal to 0.55 and 0.50 respectively, the quality of the linear regression is better than in the case of trucks.

The apparent thermal conductivity, λ_{app} for all vehicles considered as unique series is equal to 0.030 W.m^{-2}.K^{-1} (see Eq. 3.54) highlighting that the presence of the solid matrix causes an increase between 20 and 30% compared to the initial values of the thermal conductivity of the polyurethane foam declared by the manufacturers (see Table 3.5).

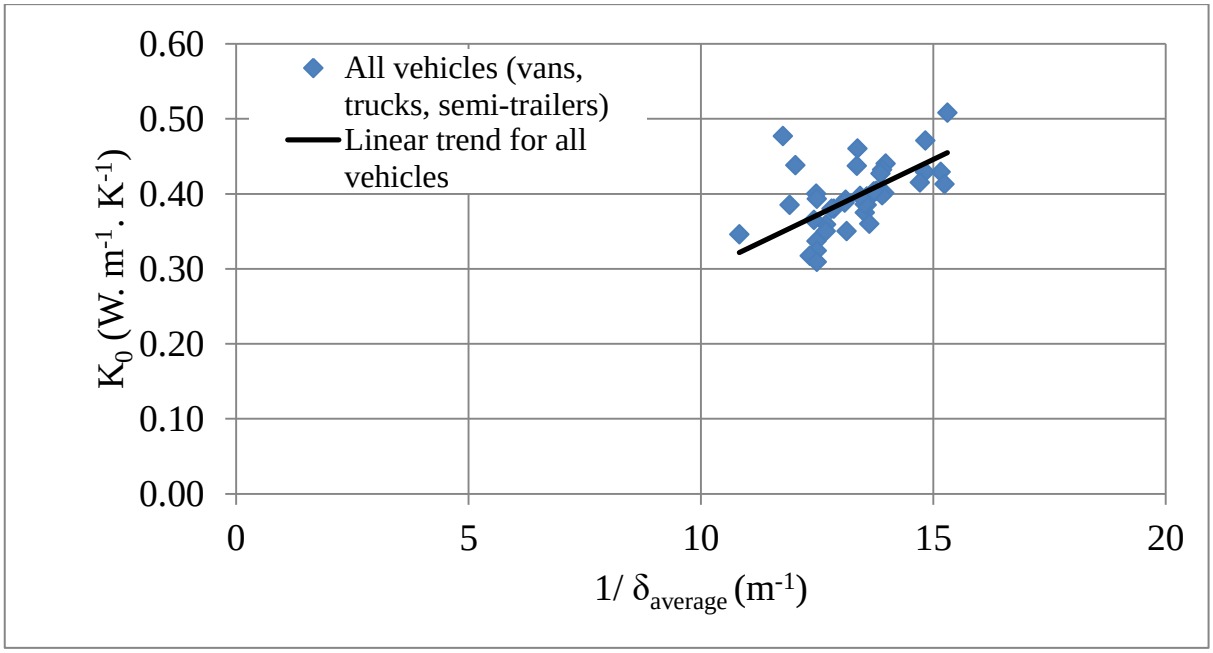

Figure 3.19 Measured Measured K_0 values of forty-one newly manufactured vehicles as a function of $1/\delta_{average}$.

3.4.3.3 Impact of doors and some accessories

The insulation performance depends primarily on the construction techniques and insulation materials used which allow the manufacturers to get closer to the theoretical performances but it also depends on the tightness of the insulated enclosure. The tightness of the insulated enclosures is above all linked to the seals and rubber gaskets, their design and installation on the doors. Door gaskets may be poor insulators as they deteriorate with time. However heat leakages may also occur in refrigerated vehicles with new seals, due to the pressure difference between the internal (cargo) space and the external environment. This pressure differences between external and internal environment can lead to an increase of air infiltration through door seals. The tightness of the body plays an important role during deliveries when the doors are frequently open, but also when the truck is driven and the depression is created by the speed on the rear frame of the body. It also concerns the overall thermal insulation of the enclosure (Estrada Flores and Eddy, 2006). There are different types of doors for refrigerated vehicles: sliding shutter doors, total rear opening with two leaves, singles side openings, awning tailgate. Depending on the type of door, the tightness can be more or less effective and have an impact on the long term ageing as well as on the initial value of the K coefficient. At the beginning of its life, the refrigerated vehicle may undergo various interventions which could differently impact on the K coefficient value. This may happen by replacing one type of door with another one or even by removing one or more doors in the real vehicle. This is what is found on vans number 3, 7 and 11. As a matter of fact, as shown in Figure 3.15 these vehicles are characterized by lower values of K_0 than K_p of their corresponding prototype vehicles. This difference may be due to the change of doors and in the absence of some of them on the new vehicles of the series. The absence or the presence of some accessories on the real vehicle may also contribute to impact on the K_0 coefficient value. Table 3.7 summarizes the differences between prototype vehicles and real vehicles. In absence of two single side openings, the inserts for all type of meat suspension, the two recessed plugs, the seven recessed pins and the full-length recessed lashing rail, the real van number 3 performs better than its prototype (K_0 = 0.32 whereas K_p = 0.37). The same thing happens for the van number 4: the real vehicle is built in the absence of the single side opening and without inserts, therefore showing a better K_0 coefficient, equal to 0.35 W. $K^{-1}.m^{-2}$ against K_p equal to 0.36. For van number 7 the main difference between the real vehicle and the prototype vehicle is to be found in the type of doors. Whereas the prototype has an awning tailgate and a shutter sliding door on the right side, the real van of the series was built with a total rear opening with two leaves and one single side opening. Aluminum and steel plates for fixing all option were also removed. These changes meant that the K coefficient passed from 0.39 for the prototype to 0.31 for the new van.

Table 3.7 Differences between prototype vehicles and real vehicles number 3, 4, 7 and 11.

Vans	Prototype	Real vehicle of the series
	Enclosure description	Enclosure description
Number 3	Doors: total rear opening with two leaves, two single side openings. Others: surface lighting, presence of inserts for all types of meat suspension; 2 recessed plugs, 7 recessed pins; 2 liquid drain holes, full-length recessed lashing rail	Doors: total rear opening with two leaves; Others: surface lighting, 2 liquid drain holes,
Number 4	Doors: total rear opening with two leaves, one single side opening. Others: 2 liquid drain holes, recessed switch to the ceiling, 1 non-recessed lighting on the ceiling, 4 ceiling inserts for meat suspension; 2 inserts on the floor.	Doors: total rear opening with two leaves. Others: 2 liquid drain holes, recessed switch to the ceiling, 1 non-recessed lighting on the ceiling.
Number 7	Doors: Awning Tailgate, shutter sliding door on the right side, Others: 6 aluminium plates for installation of all options, 11 steel plates for fixing all options, ceiling light wall lamp, 1 liquid drain hole.	Doors: total rear opening with two leaves, one single side opening. Others: 1 liquid drain hole
Number 11	Doors: total rear opening with two leaves, shutter sliding door on the right side, shutter sliding door on the left side. Others: 2 surface lightings, 2 bars for meat suspension fixed on the ceiling	Doors: total rear opening with two leaves. Others: 1 surface lighting.

3.4.4 Conclusion of the experimental assessment

This section mainly reports on experimental results concerning the difference existing between forty one vehicles for refrigerated transport and their corresponding prototypes. These results allow concluding that K_p is not the best reference point for the assessment of ageing. As a matter of fact, at the moment of their construction, real vehicles exhibit K coefficients (K_0) deviating up to 31% from the K values of the corresponding prototypes (K_p). Considering the K value of the prototype (K_p) as the reference measurement, some of the vans realized in the series, would have received a wrong insulation class according to the ATP Agreement. Combining the results of K_0 of the three series of vehicles as a unique series, an apparent thermal conductivity λ_{app} was calculated and found to be equal to 0.030 $W.m^{-1}.K^{-1}$. This parameter takes into account the presence of the solid matrix that improves the mechanical robustness to the structure of the vehicle. This value of λ_{app} is greater, by 20 to 30%, than the conductivity of polyurethane foam

declared by the manufacturers. The role of accessories that may differ in the prototypes and in the in-service vehicles was also highlighted. Finally, this experimental assessment was useful to apprehend the importance of the doors in the insulation efficiency. Removing doors or changing their type (which is common practice when building real vehicles after their prototypes) affects significantly the value of the K coefficient. Thus, improving the choice of the doors as well as their tightness appears to be a useful challenge to enhance the insulation performance of the vehicles realized on the series.

This study was part of the monitoring program launched by DGAl and supervised by Cemafroid. This monitoring program had a real impact on the production of the participating manufacturers who, by modifying certain elements, were able to achieve better performance over the three years.

With respect to the criteria introduced in this programme among the forty one tested vehicles :

- 49% are fully compliant with the ATP criteria and the objectives proposed by the control plan;
- 15% of the vehicles have a lower insulation performance outside the 7% tolerance level.
- 2% do not meet ATP criteria but have an insulation performance within the 7% tolerances;
- 34% of the equipment is not in compliance with the ATP and have an insulation capacity greater than the tolerances envisaged in the control plan protocol.

3.5 Experimental assessment of the benefit of vacuum insulation in refrigerated vehicles

This section presents the results of K coefficient tests carried out on two refrigerated semi-trailers made by integrating the VIP system in some of their walls. These semi-trailers were built by CHEREAU which is a French reefer body manufacturer created in 1953 in Normandy. First, the technical description of these two semi-trailers is introduced and then, the K coefficient results for both semi-trailers are presented. The semitrailers involved in this experimental assessment are prototypes vehicles, hence the K values initially measured coincide with the K_p

Moreover, the assessment of the reduction of fuel consumption obtained with a semi-trailer having VIPs insertions was realized comparing the semi-trailer with VIP insertion having the lower K_p coefficient to a third semi-trailer built with standard polyurethane sandwich panels.

3.5.1 Design of the new insulating enclosure

The two prototype semi-trailers submitted to the present experimental assessment were realized with polyurethane sandwich panels adding VIP in some of their walls.

Figure 3.20a shows the VIP section used for the semi-trailers of the present study, Figure 3.20b presents a piece of sandwich wall where it is possible to see the VIP insertion and Figure 3.20c one of the two tested vehicles of the present study.

The detailed composition of the walls and the mean surface area, S of the semi-trailers with VIP insertions are presented in Table 3.8. Semi-trailer n.1 has VIP insertions in the ceiling and in the lateral walls whereas semi-trailer n.2 only has VIP insertions in lateral walls.

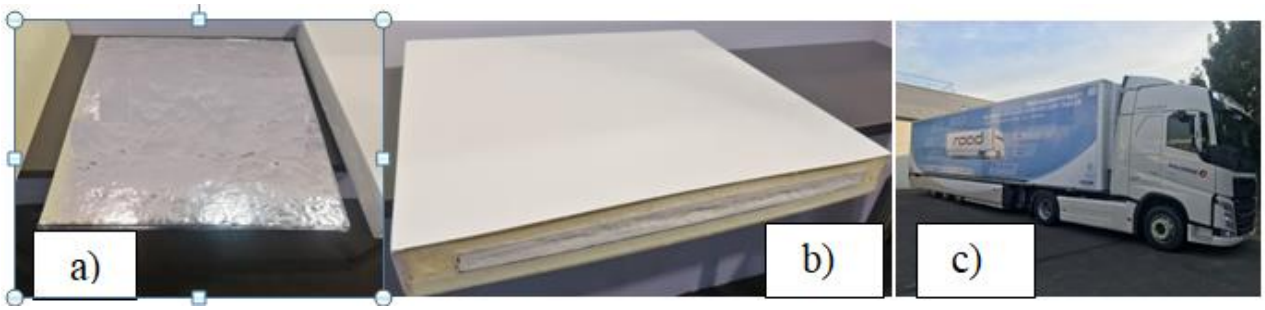

Figure 3.20 a) VIP insertion used in the construction of the semi-trailers presented in this study; b) sandwich wall with VIP insertion of semi-trailers of the present Study; c) one of the semi-trailers of present study with VIP insertions.

Table 3.8 Composition of the walls of the two tested semi-trailers.

Semi-trailer n.1 CHEREAU ($S = 157$ m^2)					
Wall	**Ceiling**	**Floor**	**Lateral walls**	**Front wall**	**Rear wall/door**
Composition	Polyester, polyurethane foamed with cyclopentane and VIP insertion , polyester	Aluminum and plywood, polyurethane foamed with cyclopentane, plywood and polyester	Polyester, polyurethane foamed with cyclopentane and VIP insertion , polyester	Polyester, polyurethane foamed with cyclopentane, polyester	Polyester, polyurethane foamed with cyclopentane, polyester
Thickness of each component of the wall (mm)	3+102+3= 108	24+105+9=138	2.5+58+2.5=63	2.5+80+2.5=85	3+70+3=76
Semi-trailer n.2 CHEREAU ($S = 156\ m^2$)					
Wall	**Ceiling**	**Floor**	**Lateral walls**	**Front wall**	**Rear wall/door**
Composition	Polyester, polyurethane foamed with cyclopentane , polyester	Aluminum and plywood, polyurethane foamed with cyclopentane, plywood and polyester	Polyester, polyurethane foamed with HFC and VIP insertion, polyester	Polyester, polyurethane foamed with cyclopentane, polyester	Polyester, polyurethane foamed with HFC, polyester
Thickness of each component of the wall (mm)	2+76+2= 80	24+105+9=138	2.5+58+2.5=63	2.5+80+2.5=85	3+70+3=76

3.5.2 K coefficient assessment

The assessment of the K_p coefficient was realized for the two semi-trailers, whose design and wall composition are presented in Table 3.8, following the ATP "internal heating" method (see Chapter 2, subparagraph 2.1.3.4). From this experimental assessment it was found that semi-trailer n. 1 has a value of K_p coefficient equal to 0.27 W. m^{-2}. K^{-1}, whereas the value of K_p of semi-trailer n. 2 is greater, equal to 0.32 W. m^{-2}.K^{-1}. This is probably due to the fact that in the case of semi-trailer n. 2, the VIP is only inserted in lateral walls.

The insertion of VIPs both in the lateral walls and in the ceiling, as in the case of semi-trailer n. 1, allows obtaining an initial K coefficient 33% lower than the average initial K coefficient usually obtained for semi-trailers built with standard polyurethane sandwich panels foamed with cyclopentane and 15% lower than the average K_p coefficient obtained for semi-trailers built with standard polyurethane sandwich panels foamed with R141b (see Figure 3.21). However, even

with the inclusion of VIPs only in the side walls, there is a decrease of K_p of 13% compared to the average value obtained for vehicles made only with polyurethane sandwich panels foamed with cyclopentane.

Figure 3.21 shows the minimum, average and maximum values of K_p for three series of semi-trailers extracted from Datafrig® database and the measured K_p value of semi-trailer number 1 with VIPs insertions in both lateral walls and ceiling. Minimum values are represented by white bars, average values by the gray ones and maximum values by black bars.

The three series of vehicles on which the minimum, average and maximum values were obtained include respectively 265 semitrailers having sandwich panels foamed with cyclopentane, 367 semi-trailers having sandwich panels foamed with R141b and 58 semi-trailers having sandwich panels foamed using R11. Standard deviation (σ) of K_p coefficients for these three series of vehicles is equal to 0.024 for semi-trailers foamed with cyclopentane, 0.027 for those foamed using R141b and, 0.022 for semi-trailers with R11 as blowing agent. As shown in Figure 3.21, VIP insertions in the ceiling and lateral walls allow obtaining initial performances comparable to the average performance obtained by using R11 as blowing agent. R11, as explained in Chapter 2 (subparagraph 2.2.2.1) is no loger used due to its high Ozone Depletion Potential but it was the blowing agent with the lowest thermal conductivity, therefore allowing the best initial insulation performance (see Table 2.7).

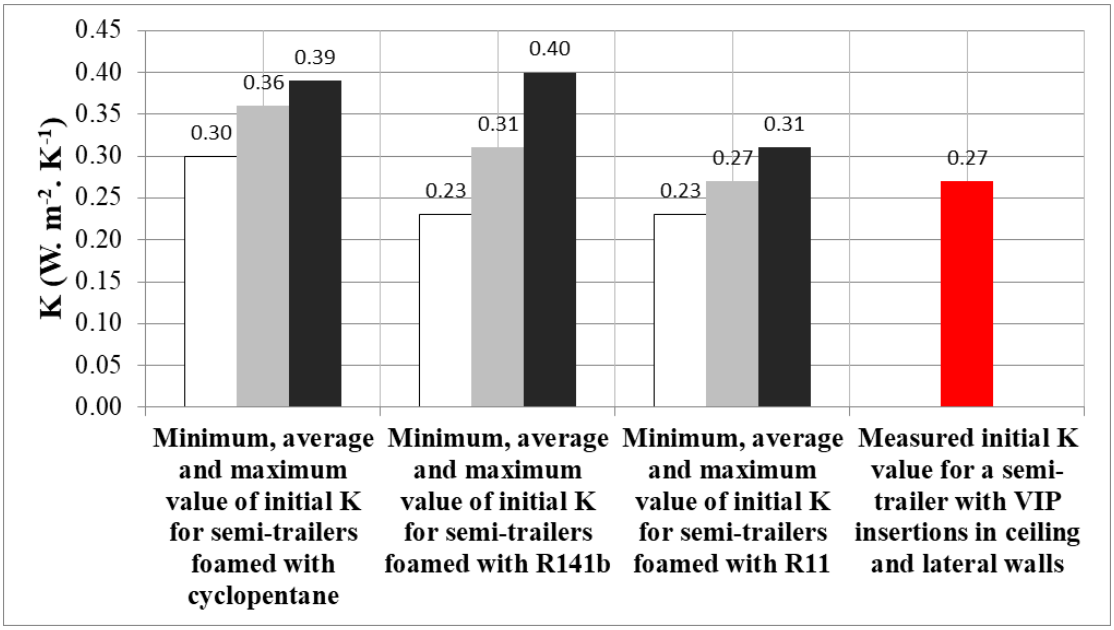

Figure 3.21 Measured K_p value of semi-trailer n.1 with VIP insertions in ceiling and lateral walls compared to the maximum, average and minimum $K_p$values of different samples of vehicles having a different blowing agent.

3.5.3 Fuel consumption assessment

The consumption of diesel fuel of semi-trailer n.1 was compared to that of a conventional semi-trailer of the same manufacturer, having same dimensions but different insulation performance. As a matter of fact, this third semi-trailer is built with standard polyurethane sandwich panels foamed with cyclopentane without VIP insertions.

This semi-trailer initially underwent the K coefficient test, whose value was found to be 0.37 $W.m^{-2}.K^{-1}$. This value is 28% higher than the K_p of semi-trailer n.1. For both semi-trailers a pull down test (introduced in Chapter 2, subparagraph 2.1.3.6) was carried out with the simultaneous measurement of the spent diesel fuel. This test requires the vehicle to be placed in the test chamber ensuring its rear part to be at least four meters from the bottom of the climatic chamber. During the test, the external temperature of the tunnel is set at + 30 ± 0.5°C while the refrigerating unit is set at temperature value equal to - 20°C. The pull down test was carried out in the two operating modes in which the refrigeration unit can operate, i.e., the continuous mode and the on-off mode. Note that the same refrigerating unit was used for this assessment by replacing it from one semi-trailer to the other one. Table 3.9 summarizes the instrumentation used for these pull down tests.

An example of data acquisition during pulls down test in the start and stop mode for the semi-trailer with VIP insertion is shown in Figure 3.22. For this semi-trailer, the refrigeration unit manages to bring the internal temperature at -20 ° C within four hours and twenty minutes.

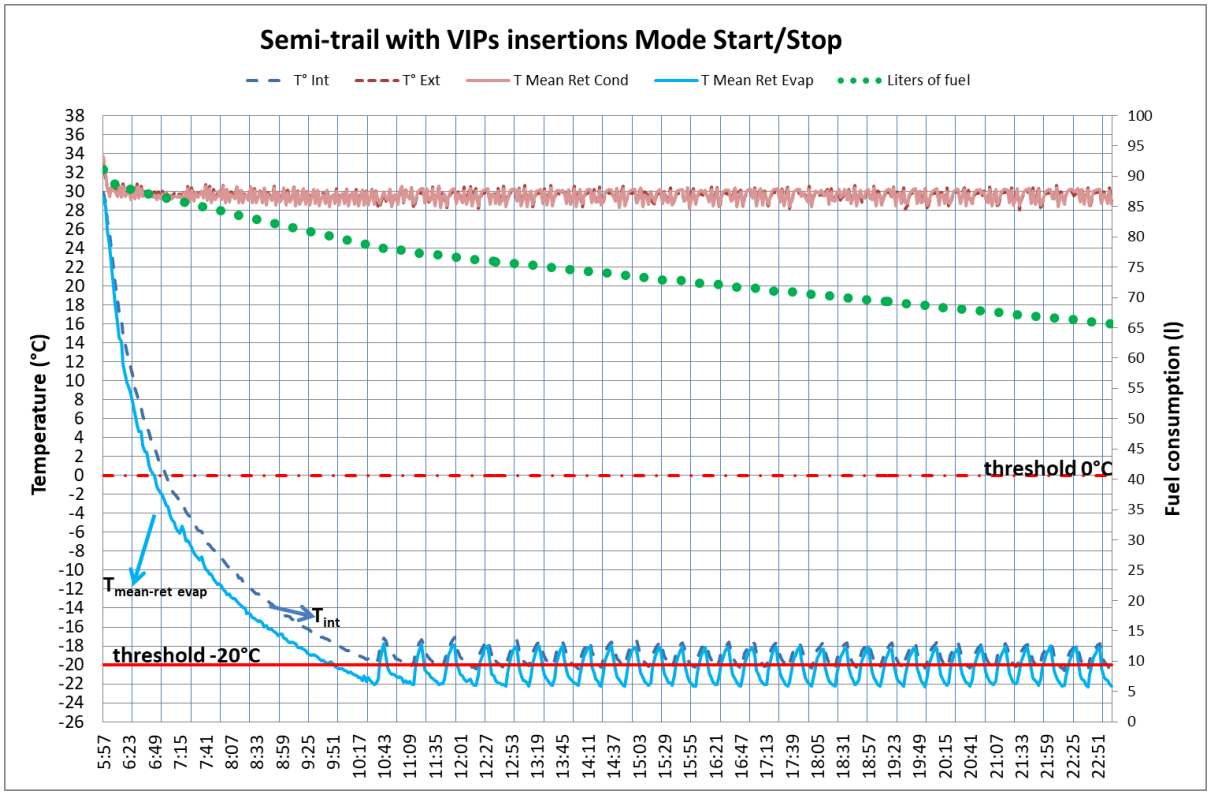

Figure 3.22 Pull down test for semi-trail with VIP insertions.

To measure the diesel fuel consumption a remote diesel tank was connected to the pump of the refrigerating unit. This diesel tank was placed on a precision scale and connected to a computer. This method allowed having the instantaneous measurement of the diesel fuel mass.

Table 3.9 Instrumentation for the pulldown tests.

Used temperature probes	Position of the probes
12 internal probes	at the four corners of the front and rear faces and in the center of lateral walls , ceiling and floor.
12 external probes	at the four corners of the front and rear faces and in the center of lateral walls , ceiling and floor.
4 probes at the evaporator suction	arranged to grid the surface
4 probes at the condenser suction	arranged to grid the surface

The results of the energy consumption assessment are summarized in Table 3.10 Semi-trailer n.1 having VIP insertions has lower consumption than the conventional semi-trailer having standard sandwich polyurethane panels. This reduction is calculated as:

$$\frac{Fuel\ cons_{st-semitrailer} - Fuel\ cons_{VIP-semitrailer}}{Fuel\ cons_{st-semitrailer}}\ 100 \qquad \text{Eq. (3.55)}$$

Where $Fuel\ cons_{st-semitrailer}$ is the fuel consumption of the standard semi-trailer, whereas $Fuel\ cons_{VIP-semitrailer}$ is that of semitrailer with VIP insertions.

Using Eq.(3.55) the energy saving is quantified to be equal to 23% in continuous mode and 34% in the start and stop mode. As a matter of fact, in the continuous mode 1.76 liters of fuel per hour are spent in the case of semi-trailer with VIP insertions compared to 2.29 liters per hour the case of conventional semi-trailer. The fuel consumption is slightly lower for the start and stop mode: 1.49 liters per hour for semi-trailer with VIP insertion and 2.25 liters per hour for conventional semi-trailer. These energy savings cannot be generalized to all types of vehicle but only refer to the comparison of semi-trailers presented in this study whose K_0 coefficients are respectively equal to 0.37 and 0.27 $W.m^{-2}.K^{-1}$ ad are obtained following the specific operating conditions presented in the previous paragraph.

Table 3.10 Energy consumption assessment

Operating mode	Semi-trailer CHEREAU	Fuel consumption (l/h)	Energy saving
Start and stop	Standard semi-trailer	2.25	34%
	Semi-trailer with VIP insertion	1.49	
Continuous mode	Standard semi-trailer	2.29	23%
	Semi-trailer with VIP insertion	1.76	

3.5.4 Conclusions of the experimental assessment

This section reported on experimental results of K coefficient for a new type of semi-trailers including VIP insertions inside some of their walls. These two semi-trailers were built by CHEREAU and tested in the Cemafroid test station. Tests were realized following the ATP test procedure for K coefficient measurements. Semi-trailer n. 1 has VIPs insertions in its ceiling and in its lateral walls, whereas the semi-trailer n. 2 has VIPs only in its lateral walls.

The presence of VIPs in the ceiling and in the lateral walls of semi-trailer number 1 allows obtaining an initial K value, K_p equal to 0.27 $W.m^{-2}.K^{-1}$, 33% lower than the average initial coefficient usually obtained for vehicles built with polyurethane standard sandwich panels foamed with cyclopentane and comparable to the average performance obtained by using R11 as blowing agent.

Semi-trailer n. 2 has a greater initial K_p value, equal to 0.32 $W.m^{-2}.K^{-1}$. This greater value is probably due to the fact that VIPs are only inserted in lateral walls for this semi-trailer. The results of this study demonstrate that despite its vulnerability to mechanical stress, when VIP system is inserted in a foam matrix there is an improvement of the thermal insulation of the vehicle from the first moments of the life of the vehicle.

An energy assessment was also realized comparing the fuel consumption of semi-trailer number 1 having VIPs insertions in the ceiling and in the lateral walls with a standard semi-trailer of similar dimensions built with standard polyurethane sandwich panels foamed with cyclopentane (having K_p= 0.37 $W.m^{-2}.K^{-1}$) . This assessment pointed out energy savings when introducing VIPs in the walls of the semi-trailer equal to 34% in start and stop mode and 23% in the continuous mode. The introduction of VIPs proves to be a real challenge for manufacturers of refrigerated vehicles to enhance the insulation performance of their vehicles and consequently reduce the energy consumption and the environmental impact.

3.6 Conclusions

In this chapter the experimental facilities available at Cemafroid were first introduced then, the measured quantities involved in the K coefficient test were detailed as well as the methodology used for the calculation of the relative measurement uncertainty dealt with all the experimental activities carried out in this thesis. Lastly, the results of a series of experimental campaigns allowing to study the early life ageing of refrigerated trucks and the sensitivity of ageing to various manufacturer characteristics were reported. The main conclusions arising from these activities are:

- by testing a semi-trailer several times at the beginning of its life, it was possible to find out that over a period of one hundred and eleven days the ageing of the insulated enclosure was equal to 1.3%. This result is not yet sufficient to conclude about the ageing and others measurements are required during the lifetime of the vehicle.
- The addition or removal of accessories has an impact on the evolution of the K coefficient. Removing the door inserts and the refrigeration unit from the same semi-trailer of previous point, a relative decrease of 5.3% on the K coefficient was found.
- The impact of the refrigeration unit was deepened: four semi-trailers were tested under two different conditions, i.e. in presence or absence of the refrigerating unit, and the mean value of the difference between K measured in these two conditions was found to be equal to 0.02 $W.m^{-2}.K^{-1}$. Improving the mounting technique and the insulation of the refrigerating unit thus appear to be two useful tracks to enhance the insulation performance of the vehicles realized on the series;
- The K coefficients of ten trucks measured after twelve years of life were analyzed and it was possible to find that in the period between 12 -18 years the relative increase of the K coefficient is equal to 5% whereas in the period 0-12 this amounted to 66%. However, as pointed out, the aging between 0 and 12 years could be larger or smaller due to the fact that it refers to the K coefficient of the prototype vehicle and not to that of the real one.
- To assess the difference between the real vehicle and the prototype one (which may be a source of a wrong assessment of the ageing) forty-one new vehicles of different categories underwent the K coefficient test and compared with their respective prototypes. This experimental campaign allowed, for the first time, to have information not yet available before: the K_0 coefficient of newly produced vehicles. This assessment allowed pointing out that K_p is not the best reference point for the ageing assessment. As a matter of fact, at the moment of their construction, real vehicles, depending on their type (vans, trucks, semi-trailers) exhibit real K coefficients (K_0) deviating up to 31% from the K values of the corresponding prototypes (K_p). Considering the K value of the prototype (K_p) as the reference measurement, some of the vehicle realized in the series, would have received a wrong insulation class according to the ATP Agreement.
- The experimentation carried out on these forty-one new vehicles also made it possible to calculate an apparent thermal conductivity, λ_{app}. Thus, the results of K_0 of the three series of vehicles were combined as a unique series of vehicles and λ_{app} was found to be equal to 0.030 $W.m^{-1}.K^{-1}$. This parameter takes into account the presence of the solid matrix that improves the mechanical robustness to the structure of the vehicle. This value of λ_{app} is greater, by 20 to 30%, than the conductivity of polyurethane foam declared by the manufacturers.

- On the series of trucks of the forty-one vehicles it was possible to apprehend the importance of the doors in the insulation efficiency. Removing doors or changing their type (which is common practice when building real vans after their prototype) affects significantly the value of the K coefficient. Thus, improving the choice of the doors as well as their tightness appears to be a useful challenge to enhance the insulation performance of the vehicles realized on the series.
- Two semi-trailers with VIP insertions in some of the walls were subjected to the K coefficient test and an improvement in insulation performance was found in both vehicles. This new technology of VIP insertions in hybrid form in the classic sandwich panels is one of the solutions for the short-term future in terms of energy savings in refrigerated transport. In fact, the vehicle with the largest VIP insertion has an initial K value, K_p equal to 0.27 $W.m^{-2}.K^{-1}$, which is comparable to the average value obtained in the past when R11 was used as blowing agent. In addition, there was also a reduction in energy consumption on this vehicle compared to a vehicle with standard sandwich panels with cyclopentane as blowing agent. These energy savings are equal to 34% in start and stop mode and 23% in the continuous mode.

3.7 References

Estrada Flores, S., Eddy, A, 2006. The use of thermography to aid design of refrigerated road vehicles. Conference on Innovative Equipment and Systems for Comfort and Food Preservation, Auckland, NZ.

Chapter 4

Implementation of a Data learning problem to study the ageing phenomenon

Nomenclature of Chapter 4

Abbreviations

ATP	Agreement on the International Carriage of Perishable Foodstuffs and on the Special Equipment to be Used for such Carriage
CE	Counterexamples
CETHIL	Centre d'Energétique et de THermIque de Lyon
CFC	Chlorofluorocarbon
C.I.A.	Annual ageing coefficient
DGAl	Direction générale de l'Alimentation
FD	Funcitional dependency
HCFC	Hydrochlorofluorocarbon
HFC	Hydrofluorocarbon
INSA Lyon.	Institut National des Sciences appliquée de Lyon
LIRIS	Laboratoire d'Informatique en Image et Systèmes d'Information
MAPE	Mean absolute percentage error
ML	Machine Learning
ODP	Ozone depletion potential
RMSE	Root-mean squared error
SQL	Structured Query language

Greek

Δ	Variation	
σ(x)	Standard deviation of x	[the same of x]

Roman

A_{12}	Ageing coefficent	
F	Coefficient F	[kWh]
K	Overall heat transfer coefficient	[W.m^{-2} K^{-1}]
G_1	Proportion of counterexamples	[kg]
G_2	Proportion of tuples involved in counterexamples	[W]
G_3	Size of the set of tuples in r to obtain a maximal new relation s satisfying $X \rightarrow Y$	[hours]

Subscripts

12	12^{th} year of the vehicle's life
enclosures arranged on the frame	Enclosure arranged on the frame
i	i-th
integrated enclosures	Integrated enclosure
Manuf1	Manufacturer number 1
Manuf2	Manufacturer number 2
Manuf3	Manufacturer number 3
Manuf4	Manufacturer number 4
monobloc units	Monobloc units
p	Prototype
semi-trailers	Semi-trailers
split units	Spits units
trucks	Trucks
vans	Vans

4. Implementation of a Data learning problem to study the ageing phenomenon

This chapter deals with the implementation of all the phases of a machine learning problem. These steps were presented in Chapter 2 (subparagraph 2.4) in a purely abstract way and are applied here to the study of the ageing of refrigerated transport vehicles. Thus, this chapter presents:

- the available databases in Cemafroid;
- the selection of the data and the creation of the final dataset used for the study;
- the treatment of data for both statistical analysis and machine learning algorithm;
- a first statistical analysis of the data that allowed to discover, visualize and get insights from them;
- the study of the existence of a first classification model;
- the selection, the training and the final results of a regression model.

The detailed study of the available data, their preparation and pre-treatment and the numerical modelling were made possible and carried out through the fruitful support of the experts of the LIRIS laboratory, associated with this thesis work.

4.1 Databases in Cemafroid

The two available databases and their relational scheme are described in Chapter 2 (subparagraph 2.1.3.6) when dealing with the issuing process of ATP certificates and the production of the data existing behind this process.

The first database, Datafrig®, records the data and the information of the entire fleet of 350 000 temperature controlled equipment registered in France, of which approximately 120 000 hold an ATP certificate. The second one is the database containing the results of all the K coefficient tests realized in the Cemafroid test chambers since 1999.

The first database is managed by an external service provider, while the second is accessible and manageable directly from the Cemafroid.

The cleaning and pre-processing phase of the data was a rather long and challenging part of the thesis. Using Excel, Matlab and SQL Management Studio, both databases were analyzed and then linked together. After having established and realized the junction of the two databases, several transformations on the features were necessary especially on the categorical ones. The selection of data and the pre-processing phase that led to the creation of the final datasets used in this thesis are presented in the next paragraph.

4.2 Data Selection

The selection of the data was realized starting from the two available databases in different steps. In the case of Datafrig®, the external supplier that manages the database provided a SQL extraction on the basis of an accurate request. On the other side, for the second database, the one recording the experimental results from Cemafroid test chambers, the extraction was done directly through a SQL code.

The Datafrig® data are first self-controlled by the body manufacturer, secondly automatically controlled and analyzed by the Datafrig® software, then checked by a first technician and finally validated by a supervisor. During the audit of the manufacturing of the refrigerated vehicle, an independent auditor verifies the quality of these data and compares them to the real equipment. This five-steps system of quality control has been devised to guarantee a high level of quality for the data recorded in the database.

The data on the second database (the one containing the results of the experiments carried out in Cemafroid) are manually recorded and directly controlled by the operator before starting the K coefficient test.

The data coming from these two databases are used this chapter for the study of the ageing of refrigerated transport vehicles but first they undergo a treatment process that includes the following steps:

- extraction,
- junction and,
- pre-processing phase.

These steps are presented in the following subparagraphs.

4.2.1 Data extractions

A dataset was firstly extracted by the external provider from Datafrig® through SQL. This dataset was obtained by selecting vehicles having received an ATP certificate between 2010 and 2017 and initially contained 300 000 lines (“tuples” in data sciences language). Generally, through a Datafrig® extraction, one tuple of the obtained dataset refers to a single vehicle. However, there are some exceptions since, in the case of multi-compartment vehicles; each compartment of the vehicle generates a single tuple on the dataset. However, not all the 300 000 tuples are useful for studying the ageing because among them there are also vehicles having six and nine years of life for which the certificate was delivered after a pull down test. For these vehicles only the initial K_p coefficient is known.

The vehicles to be considered for the study of the ageing are those having received a certificate after twelve years of life and for which it is possible to compare the K_p coefficient to the K_{12} coefficient. To this end, four filters presented in Table 4.1 were applied to this first dataset. Only with the application of the first filter (non-null value of K_{12}) the dataset was reduced from 300 000 tuples to 8083 tuples.

By applying these filters the dataset was reduced to 2347 tuples. The filter concerning the uniqueness on the serial number of the insulated enclosure and the license plate number are

introduced because this information serves as a link with the dataset extracted from the second database. As a matter of fact, through the use of these unique keys the 2347 vehicles extracted from Datafrig® were found on this second Camafroid database and another dataset was extracted through another SQL query.

Table 4.1Filters applied to the dataset extracted from Datafrig®.

Applied filter	Tuples of the database after applying the filter
Non-null value of K_{12}	8083
Non-null value of K_p	7500
K_{12} value different from K_p value	7179
Unique enclosure serial number and license plate	2347

4.2.2 Joining the two datasets

The two datasets generated through the extractions referred to the same vehicles and their integration was carried out with the aim of adding more important information to the data extracted from Datafrig®, such as the type of blowing agent used in the vehicle manufacturing process. As a matter of fact, this feature is recorded on the database of experiments carried out at the Cemafroid but it is not reported on Datafrig®. A third dataset containing 2000 tuples, integrating oth previous datasets has been built through a Matlab code. This dataset underwent a further phase of pre-processing, described in the next paragraph.

4.2.3 Data pre-processing and preparation

In order to obtain a good performance, both for statistical analysis and for building numerical models, it is important that the data are as complete and exact as possible.

To this end, duplicates rows as well as outliers were manually identified and removed from the final dataset resulting from the junction.

In addition, rows containing too many null values were not considered since they cannot be taken into account by a prediction model that needs values on all the features to make a prediction. In this regard it is important to note that in order not to exclude some important features from the analysis the final dataset was manually updated. This was done for example for the attribute “type of refrigerated transport performed”. The direct knowledge of the vehicle owner, acquired by Cemafroid, made it possible to trace this information considered important for the study of the ageing of refrigerated transport vehicles. Such a manual processing and updating has been a difficult and laborious aspect of the study.

For statistical analysis, as a result of this pre-processing phase, the final dataset was found to contain 1158 tuples. The same dataset is used is this thesis to create a first classification model. For the numerical regression model others data obtained with a further SQL extraction from the Datafrig® database (realized by the external provider) were added to the 1158 tuples. This new

extraction made it possible to select the vehicles having received an ATP certificate at twelve years of life in 2018 and 2019. With the new data, the dataset increased from 1158 to 2120 tuples. For these new data, the same pre-processing phase previously described was iterated.

In both datasets, each tuple describes a unique refrigerated over 117 features of both categorical and numerical nature. However, most numerical models can only operate with numerical values. For this reason, an additional transformation step was necessary to be able to use these datasets for the ageing prediction. As a result, categorical features listed in Table 4.2 were converted to numerical values, using one-hot-encoding (Garavaglia and Sharma, 1998) that consists in dividing one categorical feature, represented by a column of the dataset, into n columns, where n is the number of categories in the considered categorical feature. Each new column then consists in a category, and each row takes the value 1 if it belongs to the category and 0 otherwise. As example, in Figure 4.1 this transformation is explained for the categorical feature "type of vehicle". After this last transformation the data are ready to be used for the statistical analysis and to build a numerical model predicting the ageing of refrigerated transport vehicles.

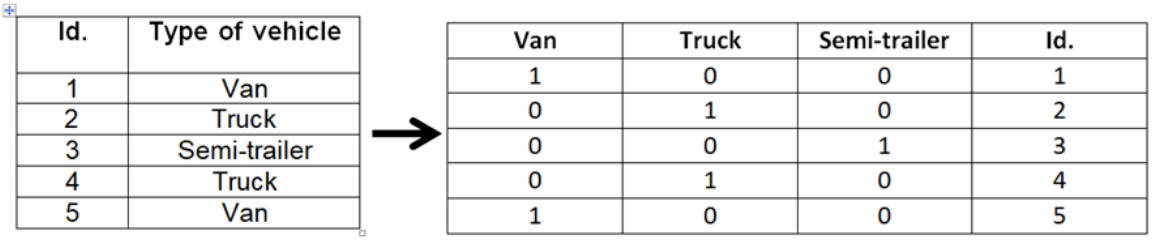

Id.	Type of vehicle
1	Van
2	Truck
3	Semi-trailer
4	Truck
5	Van

Van	Truck	Semi-trailer	Id.
1	0	0	1
0	1	0	2
0	0	1	3
0	1	0	4
1	0	0	5

Figure 4.1 One-hot-encoding for the categorical feature "type of vehicle".

Table 4.2 Categorical features considered for the study of the ageing of refrigerated vehicles and converted to numerical ones through the one-hot-encoding transformation.

Categorical feature of the dataset	Values of the categorical feature to convert in numerical ones
Type of vehicle	Van; truck; semi-trailer
Type of refrigerated transport carried out	Meat; fruits, mixed products; frozen products; dairy products…
Nature of the enclosure insulation	Integrated enclosure; arranged on the frame of the vehicle
Manufacturer	Manufacturer A; manufacturer B; manufacturer C…
Architecture of the refrigerating unit	Monobloc; split
Type of temperature of the refrigerating unit	Mono-temperaure, bi-temperature ; multi-temperature.
Type of blowing agent used in the manufacturing process of the refrigerated vehicle	Cyclopentane; R11; R141b.

4.3 Discover and visualize the data to gain insights: a statistical analysis of K coefficient test results

The main objective of the statistical analysis presented in this paragraph is to confirm already known ageing factors and to identify new ones. The conclusions will be then compared, in the next subparagraph of this section, to those obtained by studying the phenomenon with a different approach: that of numerical modeling using artificial intelligence techniques.

4.3.1 Methodology description of the statistical analysis

The main objective of this section is to study how the A_{12} coefficient (defined through Eq.(2.5) as the ratio between K_{12} and K_p) behaves from a statistical point of view in the obtained dataset containing 1158 tuples. Simple notions have been used, such as histograms and probability density functions, using classical smoothing techniques such as kernel density estimation (KDE). Those statistical techniques are known to deliver meaningful visualization allowing to better understand the studied ageing values of A_{12}.

The approach consists of two steps described as follows:

- First, six features (see the screenshot of the dataset in Figure 4.2) out of 117 available in the final dataset have been carefully selected, since they are considered important by domain experts. These features are:
    1. the type of vehicles,
    2. the nature of the insulated enclosure (with integrated insulation or assembled on the vehicle platforms);
    3. the blowing agent used in the manufacturing process;
    4. the manufacturer,
    5. the different architectures of refrigerating units,
    6. The usage of the vehicle on the type of performed transport.

These features are known to have a strong influence in practice on the ageing process. Moreover, each of them has only a few distinct values, allowing to see if one of them has a particular influence on A_{12};

- Second, the data distribution of A_{12} values have been visualized for each value of each selected feature, allowing to get quite easily the influence of that value on the ageing process and more importantly, to compare how those values influence the ageing process. When studying the effect of one feature, in order to isolate the effect of the other features, a sample of vehicles with characteristics as identical as possible was chosen. In this way the only variation was on the analysed feature.

B	C	D	E	F	G	H	I	J
Vehicles	**Kprototype**	**K12**	**Type of vehicle**	**Nature of insulation**	**Blowing agent**	**Manufacturer**	**Architecture of refrigerating unit**	**Usage of vehicle**
1	0.31	0.47	truck	assembled	cyclopentane	A	Monoblock	fruits and vegetables
2	0.36	0.49	semi-trailer	assembled	cyclopentane	B	Monoblock	meat transport
3	0.29	0.36	semi-trailer	assembled	R141b	C	Monoblock	diary products
4	0.29	0.35	van	integreated	R-141b	A	Monoblock	mixed transport
5	0.36	0.51	van	integreated	R-141b	A	Split	meat tranport
6	0.31	0.39	van	integreated	cyclopentane	B	Split	diary products
7	0.23	0.41	truck	integreated	R11	B	Split	meat transport
8	0.32	0.34	semi-trailer	assembled	cyclopentane	D	Monoblock	meat transport
....	...	....	....	....	....	...	...	....
1158	0.31	0.43	semitrailer	assembled	cyclopentane	E	Split	meat tranport

Figure 4.2 Selected features from the final dataset for the statistical analysis.

4.3.2 Results of the statistical analysis: factors affecting the ageing of refrigerated transport equipment

The analysis was carried out on the basis of the following criteria:

i) type of equipment and materials (this criterion includes the first three features identified in the previous subparagraph: the type of vehicle, the design of the insulated enclosure and the type of blowing agent used);
ii) influence of the body manufacturer,
iii) influence of the architecture of the refrigerating units,
iv) type of refrigerated transport realized.

The behavior of the A_{12} coefficient with respect to each of these criteria is presented in the following subparagraphs. When analyzing one feature at a time similar vehicles were chosen to isolate the effects of other features on the analysis.

4.3.2.1 Type of equipment and materials

Depending on the category of the vehicle (i. e. vans, trucks and semi-trailers), the performance may vary. Figure 4.3 shows the probability densities of A_{12} for three different samples of vehicles. These probability densities allow defining analytically the distribution of the variable A_{12} around the mean value, represented by the peak of the curve. The population covered by these curves is 227 vans, 470 trucks and 424 semi-trailers. The curve corresponding to the semi-trailers is located more to the right (i.e. to higher values of A_{12}) than the other curves. As a matter of fact, during their life, and because of their size, semi-trailers undergo more mechanical stress than trucks and vans. For this reason, after twelve years of life, semi-trailers generally have a Kvalue diverging more from the initial value of the prototype, than in the case of trucks and vans. However, the width of the curve corresponding to the semi-trailers is smaller than the widths of the other curves: the dispersion of the values of parameter A_{12} is less for semi-trailers. This is due to the fact that they are realized in a more standardized way than trucks and vans. This is quantified from the standard deviation for semitrailers, $\sigma_{\text{semi-trailers}}$,which is equal to 0.18, is the lower one.

Refrigerated vehicles presented in this section are made with sandwich panels in which the insulation is realized with polyurethane foam. Independently of the nature of the foam, the insulated enclosure of the vehicle may be designed in two different ways: i) with integrated

insulation or, ii) assembled on the vehicle platforms. The performance of the vehicle depends on the design of the insulated enclosure. The curves of Figure 4.4 highlights this aspect representing the probability densities of the parameter A_{12} for 52 refrigerated enclosures with integrated insulation and 149 refrigerated enclosures assembled on the vehicle platforms. The vehicles whose insulated enclosures are arranged on the vehicles platforms are represented by the curve whose shape is more regular and centered around the mean value. The width of this curve, in fact, is smaller than the width of the curve which refers to integrated enclosures, highlighting that the dispersion of the values of A_{12} is less for vehicles with insulated enclosures assembled on the vehicle platforms than for vehicles with integrated insulation.

As a matter of fact the standard deviation, σ, is lower for the enclosures arranged on the frame than for the integrated ones: $\sigma_{\text{enclosures arranged on the frame}}$=0.18 whereas $\sigma_{\text{integrated enclosures}}$= 0.21

The origin of this difference is to be found in the different designs of the two types of insulated enclosures. Insulated enclosures assembled on the vehicle platforms are made in series through repeatable and mastered industrial process, which allow more standardized performances than single and handicraft production of enclosures with integrated insulation.

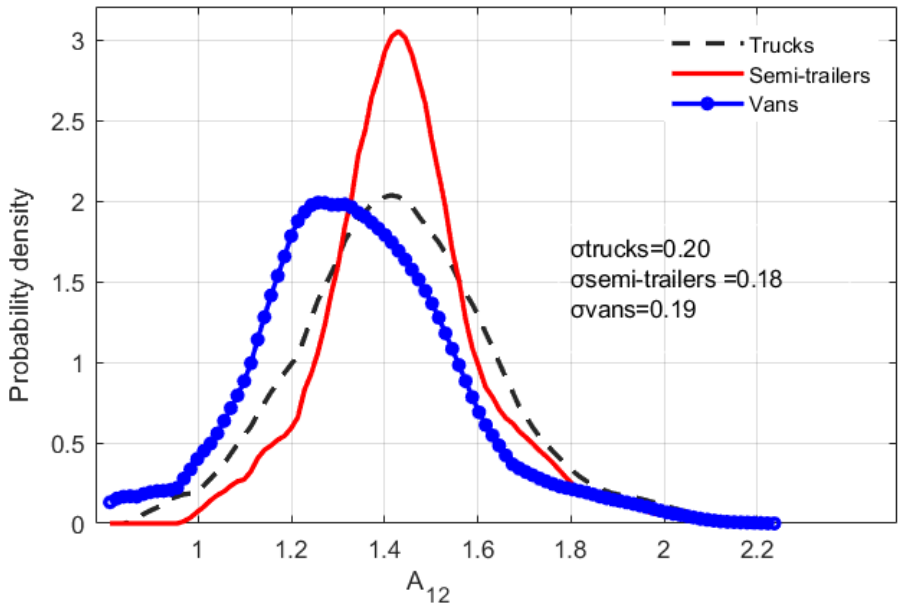

Figure 4.3 Probability densities of A_{12} for vans, trucks and semi-trailers.

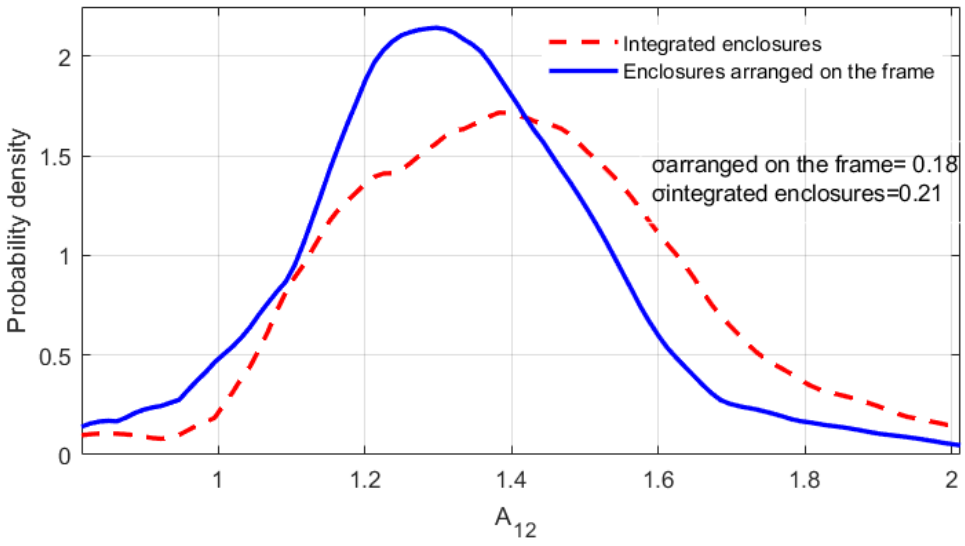

Figure 4.4 Probability densities of A_{12} for vehicles with integrated insulation and assembled on the vehicle platforms.

The gases used as blowing agents have undergone a process of evolution since 1970, when chlorofluorocarbons (CFCs), such as R11, were used for the construction of insulated vehicles. These blowing agents had a good insulation capacity thanks to their low value of thermal conductivity. However, they had a strong impact on the environment due to their high Ozone Depletion Potential value (ODP). Searching for new environmentally friendly fluids, to be used as working fluids in refrigeration systems and as blowing agents in insulating foams, became a matter of global concern after 1987, date of finalization of the Montreal Protocol. As already discussed in Chapter 2 (subparagraph 2.2.2.1), this research led to a first shift from CFCs to HCFCs, then to HFCs, which will be definitively expelled from 1 January 2022 (see Table 2.7). Today, insulated enclosures are generally made with polyurethane foam expanded to cyclopentane. The insulation performance of the insulated enclosure varies depending on the used blowing agent. Three samples of semi-trailers, each one referring to a different blowing agent, are compared in Figure 4.5, through the probability densities of A_{12}. Counterintuitively, the curve which refers to the sample of 46 semi-trailers foamed with cyclopentane has a peak at smaller values of A_{12} than the one referred to a sample of 108 semi-trailers foamed with R-141 and the one referred to a sample of 47 foamed with R11. Even if, cyclopentane is the blowing agent with the poorest initial thermal conductivity (see Table 2.7), it seems to be the one which allows a better long-term preservation of the insulating properties. However, the lowest standard deviation is to be attributed to the R_{141b} ($\sigma_{R141b} = 0.09$)

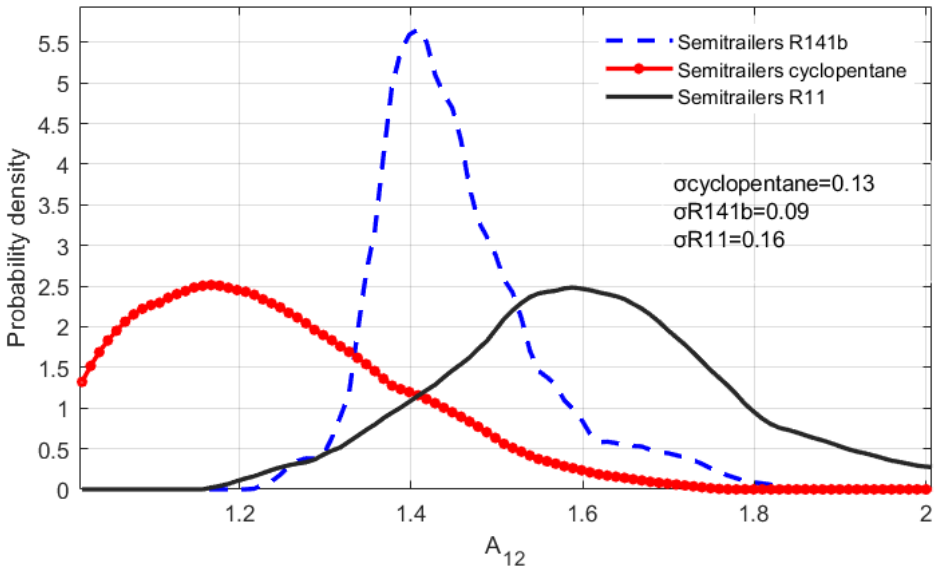

Figure 4.5 Probability densities of A_{12} for vehicles foamed with different blowing agents (cyclopentane, R141b and R11).

4.3.2.2 Influence of the body manufacturer

Manufacturing technology and assembly process vary from one body manufacturer to another and have an influence on the initial performance of the vehicle as well as on the long-term ageing. This aspect was already pointed out by Boldrin et al. (1990). The probability densities of A_{12} of different manufacturers of trucks are presented in Figure 4.6. The number of vehicles considered here varies from 30 to 140 vehicles. The peaks of the curves are located at different values of A_{12}, highlighting the fact that each manufacturer has a different performance at the initial time as well as in the long term. The body manufacturer presenting the smaller dispersion of the values of A_{12} is the manufacturer number two. This manufacturer has, in fact, a probability density represented by the curve having a more regular shape and with the smaller width. As a matter of fact it presents the lowest standard deviation (σ_{Manuf2}=0.15). Its manufacturing and assembly process appears to be more homogeneous than the others.

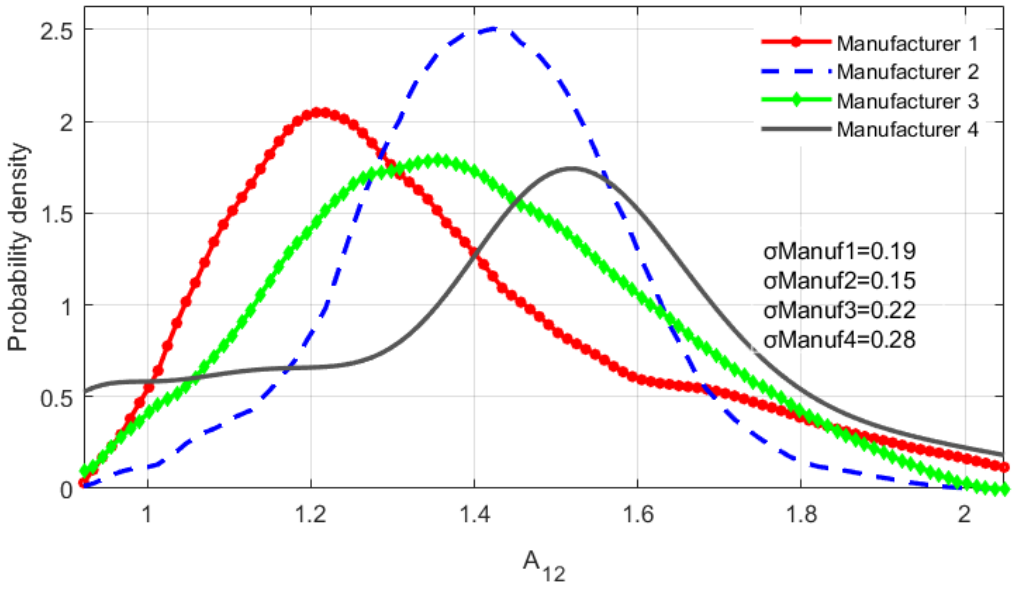

Figure 4.6 Probability densities of A_{12} for four different manufacturers of trucks

4.3.2.3 Influence of different architectures of refrigerating units

Previous studies (Panozzo et al., 1999 and Capo et al., 2018) pointed out that the presence of the refrigerating unit causes additional thermal losses and accelerates the ageing of the vehicle. In refrigerated transport it is possible to identify two different kinds of refrigerating units' architectures: the monobloc architecture and the split one. The first one provides a cabinet which encloses the refrigeration circuit, the compressor and the fan. This cabinet is installed through a protrusion realized on the entire wall (front side of the vehicle). The wall due to this perforation has a reduced insulating performance. The second one, the split system, is characterized by an internal unit and an external one connected through the passage of two pipes in the wall. It requires only the realization of holes for the passage of the pipes. Depending on the different architectures, performances may vary. The probability densities of A_{12} for 533 vehicles equipped of monobloc mono-temperature units and 252 split mono-temperature units are presented in Figure 4.7. The curve referring to monobloc units has a smaller width than the one referring to splits ones (i.e the standard deviation for monobloc units, $\sigma_{\text{monobloc units}}$ is smaller than the standard deviation of split ones, $\sigma_{\text{split units}}$). This is due to the fact that monobloc units are installed through a more repeatable and standardized process. As a matter of fact, the dispersion of the values of A_{12} is less for monobloc than for split units. The passage of the pipes through the walls and the refrigerating unit fixation may be responsible for the greater diversity in the installation of splits unit. An incorrect method to realize these actions could affect the insulation and therefore the ageing over the time. However, even if there is greater diversity in the installation on the vehicle of the split groups, this architecture has less influence on the long-term performance: the peak of the curve of split units is, for this reason, shifted to the right (i.e. at lower values of A_{12}).

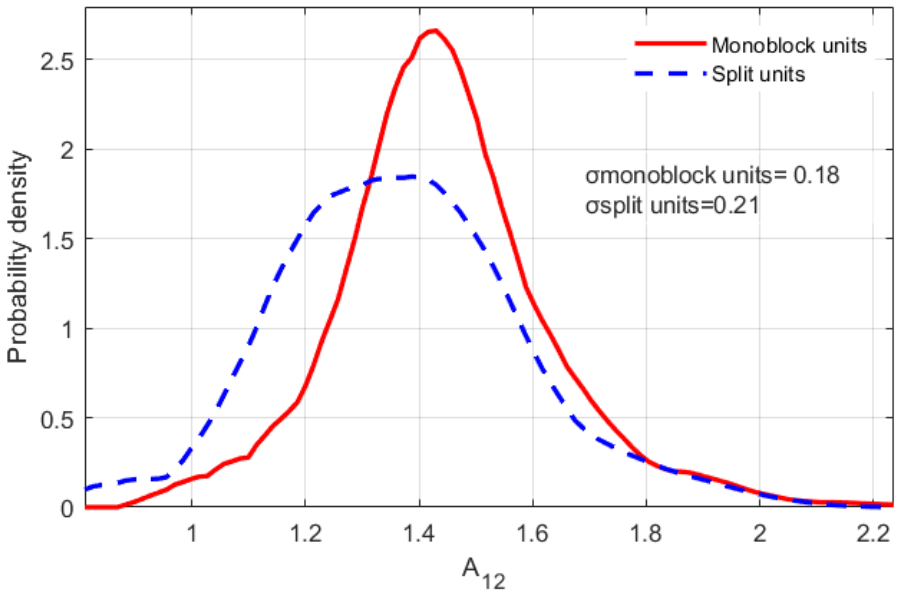

Figure 4.7 Probability densities of A_{12} for 533 vehicles equipped with monobloc units and 252 vehicles equipped with split units.

4.3.2.4 Usage of the vehicle: type of realized refrigerated transport

The usage of the vehicle is one of the factors which allow a better understanding of the ageing phenomenon (Boldrin et al., 1993). Different samples of vehicles dedicated to different kind of transport are presented in Figure 4.8. In order to compare the ageing of these vehicles to the ageing of the vehicles presented by the cited studies, the results of presented in this Figure are reported in terms of the annual ageing rate, through the $C.I.A.$ parameter calculated after twelfe years of use of the vehicle (see Eq. 2.5). These results are comparable to those presented by Boldrin et al. (1993). This confirms that the greater $C.I.A.$ corresponds to vehicles dedicated to the transport of meat. In this type of transport the presence of the rails for suspending the carcasses on the roof may cause increased mechanical stresses for the body of the vehicle.

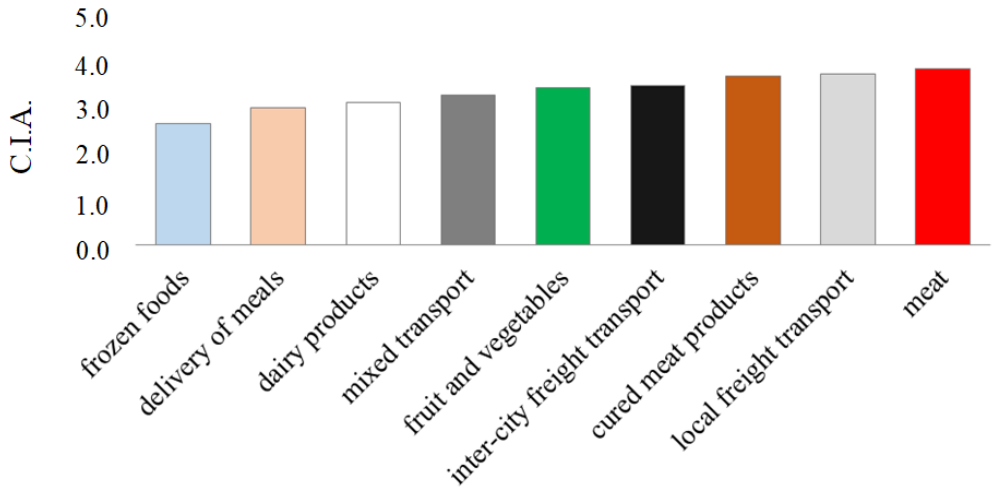

Figure 4.8 Average annual ageing coefficient, C.I.A. (B. Boldrin et al. 1993) for samples of vehicles dedicated to different types of transport.

4.3.3 Coefficient F

In order to rank the importance of the factors having an influence on the ageing phenomena, presented in subparagraph 4.3.2, a new weighting coefficient can be defined as follows:

$$F = \frac{MAX\ (C.I.A.)_i}{\min\ (C.I.A)_i} \qquad \text{Eq. (4.1)}$$

Where $C.I.A.$, the annual ageing coefficient, is calculated after twel years of use of the vehicle using Eq. 2.6 and the subscript i indicates the *i-th* factor. This factor gives an idea of the spread of population for each feature. Figure 4.9 shows the values of coefficient F calculated for each factor presented in subparagraph 4.3.2, showing their importance on the ageing process.

Based on the statistical analysis carried out the blowing agents and type of refrigerating units are the factors that more than all other factors have influence on the ageing of refrigerated transport equipment. The F coefficient allows ranking factors and thus provides a feature selection method. Such an approach is required to be able to predict K_{12} values using machine learning techniques.

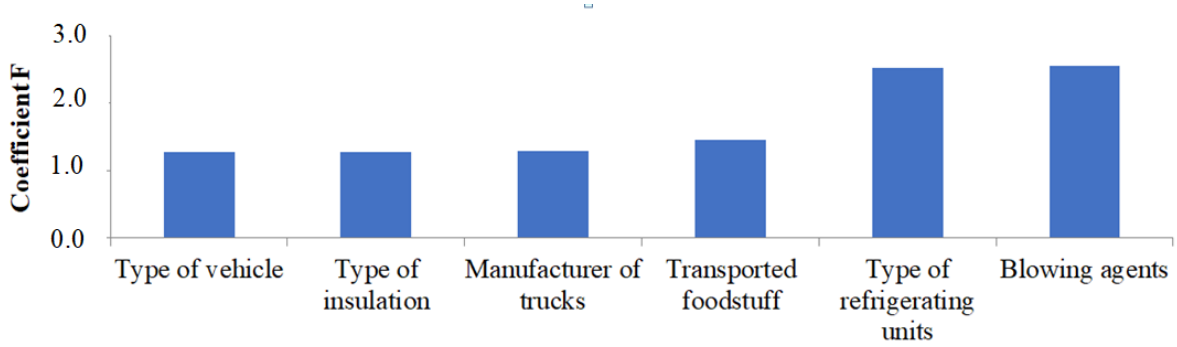

Figure 4.9 Coefficient F ranking the factors affecting the ageing of refrigerated equipment

4.3.4 Conclusions of the statistical analysis

Section 4.3 reports on the statistical analysis of the results of K coefficient tests realized in the laboratory of Cemafroid for a sample of 1158 in-service refrigerated vehicles. This analysis allowed confirming the influence of factors already studied: the type of vehicle, the influence of manufacturer and the type of transport realized. Other important factors not yet considered before were analyzed. The results highlighted that the performance in the long-term is higher for those refrigerated vehicles which insulated enclosures are assembled on their platforms than for vehicles with an integrated insulation. The influence of the refrigeration unit on the performance of the refrigerated vehicle was already treated in a previous study (Panozzo et al., 1999). Through this statistical analysis it was possible to put in evidence the influence of the architecture of the refrigerating unit. Monobloc units are installed through a more homogeneous technology than splits ones but cause a greater reduction of the insulating performance due to the perforation that must be realized on the wall for their installation. Another important aspect, relevant for understanding the ageing phenomena, highlighted by the present statistical analysis, concerns the influence of the blowing agent. Three samples of refrigerated semi-trailers foamed with different blowing agents were compared. This comparison showed that semi-trailers foamed with cyclopentane have better performance in the long period. It is important to point out that the analysis presented in this section is made by comparing the insulation performance of refrigerated vehicles at twelve years of life to the initial performance of their reference prototypes. As pointed out in Chapter 3 the K value of the reference prototype, K_p, is not the most correct indicator for the ageing evaluation due to the fact that reference prototype may have small differences in size and geometry, and hence a different initial K value compared to the initial K value of the vehicle realized in the series. Testing the vehicles realized in the series at the beginning of their life and following the evolution of their K coefficient during the whole life cycle is of primary importance for the study of the ageing phenomena.

After having analyzed the data from a purely statistical point of view, the next paragraphs focus on the numerical modelling of the ageing phenomenon using classification and regression algorithms.

4.4 Numerical Modelling of the ageing of refrigerated transport equipment

The statistical analysis carried out in previous section allowed to highlight the influence of important factors not yet considered before: the type of insulation, the blowing agent used in the foaming process and the influence of the architecture of the refrigerating unit. The ageing problem relied, up to this point, on experimental studies and statistical analysis. In the present paragraph the problem is approached from a different angle: a numerical approach. Such a numerical approach is possible thanks to the existence of the Datafrig® database and includes the development of:

- a first classification problem for the ageing of refrigerated transport vehicles,
- a regression model (Han and Kamber, 2006) to predict the ageing of refrigerated vehicles.

When modelling the ageing phenomena with a classification algorithm, the existence of a function using functional dependency (FD) and counterexample was also studied. Training a model is a task, verifying its goodeness is another issue. For this reason the notion of FD has been used. as, As seen in Chapter 2 (subparagraph 2.4.5.2), before creating a model FD first deals with the question of its existence .

4.4.1 Classification of the ageing problem

With the aim of discretizing ageing of refrigerated vehicles in two classes, i. e. suffering from “slow ageing” or “fast ageing”, a first classification was built following several steps performed with Microsoft Azure. As shown in this Figure 4.10, once the cleaned dataset containing 1158 refrigerated vehicles was obtained and after performing some transformation operations such as selecting the relevant features in the dataset, editing metadata and converting to indicator values, it was possible to proceed to a traditional classification workflow: the data was split in a training set (80% of data) and a testing set (the remaining 20%). It was decided to build a first classification model using a decision tree (Breiman, 2017). This model was chosen because decision trees are quite easy to understand and interpret. A decision tree is thus a classifier organized in a tree-like manner.This classifier has an immediate translation in terms of decision rules, mutually exclusive and ordered (if, then, otherwise). However, a single tree is not sufficient for producing effective result. To improve the results, a boosted version of the algorithm (Schapire, 1990) was used. The features chosen for the construction of this first model are as follows:

- manufacturer of vehicles,
- nature of insulated enclosure,
- type of vehicle,
- payload,
- empty weight ,
- mean surface area,
- number and type of door openings on the enclosure,
- architecture of refrigerating unit;

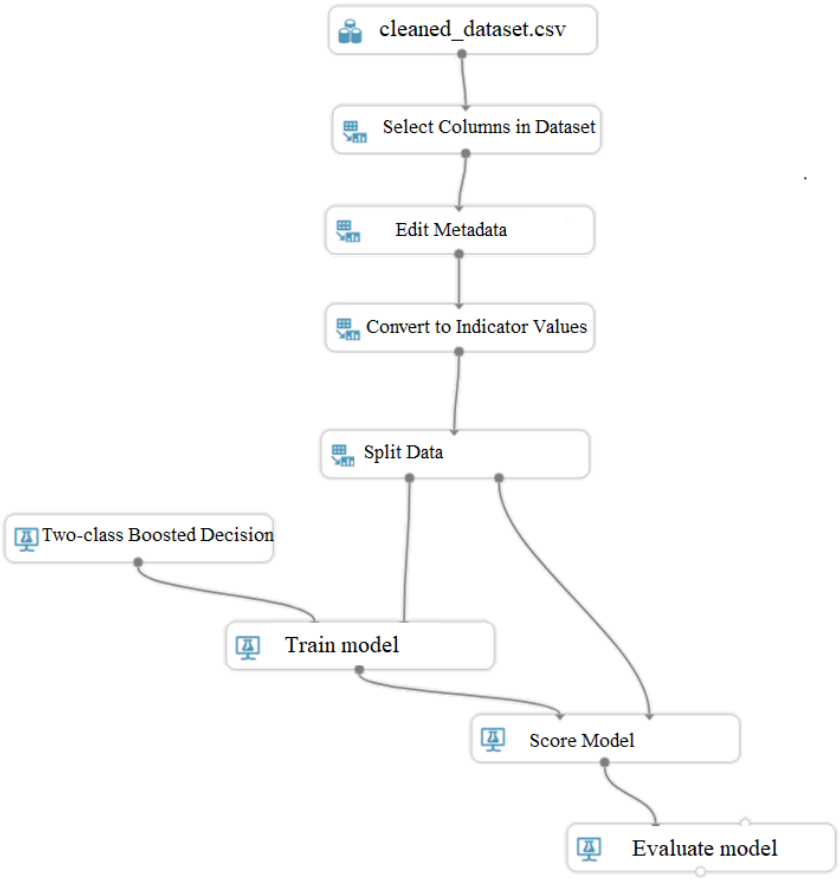

Figure 4.10 Steps of a classification model built for discretizing the ageing of refrigerated vehicles in slow ageing or fast ageing.

4.4.1.1 Result of the model

This first model discretizes the vehicles of the dataset in two classes:

- the first class includes those subject to low ageing while,
- the second class contains those subject to high ageing.

This discretization is done by referring to the average ageing value, where ageing has been assessed in relative terms ($\frac{K_{12}-K_p}{K_p}$). This average value for the dataset under study, containing 1158 refrigerated vehicles, is equal to 0.43. Hence, vehicles whose ageing is lower than 0.43 (see Figure 4.11) are included in the class of vehicles subject to low ageing; on the contrary, all those vehicles whose ageing is greater than 0.43 are classified as susceptible to high ageing.

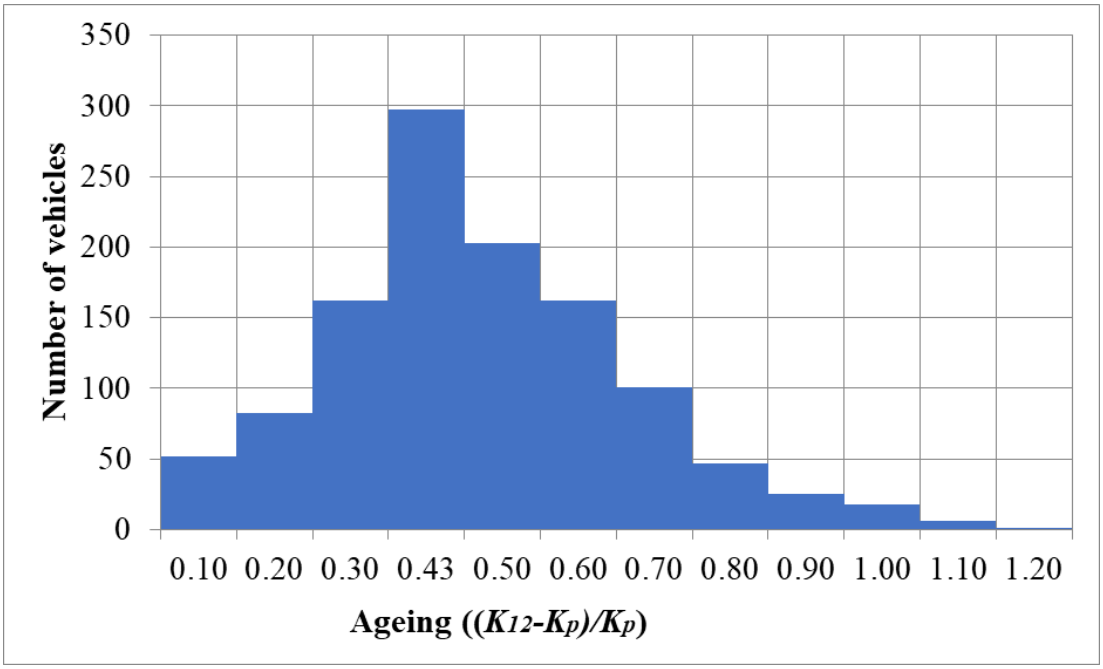

Figure 4.11 Gaussian distribution of the vehicles of the studied dataset.

The metrics of this model are: a Precision of 0.818 and a Recall of 0.783.The F_1 score is estimated at 0.800. The definitions of these metrics are given in Chapter 2, subparagraph 2.4.7.2 through Eq. (2.14), Eq. (2.15) and Eq. (2.16). In addition, a ROC curve (for its definition see Chapter 2, subparagraph 2.4.7.3) of the classifier is presented in Figure 4.12, also showing good performances for the ageing prediction. As a matter of fact, the area under the ROC curve (AUC) represents how well a parameter can distinguish between two groups. The larger is the area the better the model.

With this first model available, it was possible to understand what could be done to improve the results and what where the blocking points in the dataset itself. For example, some tuples might require additional cleaning, or some records in the database might cause problem for the learning process. As checking the data manually is very tiresome, even on a small dataset, it appeared that the notion of functional dependency could be extremely useful for this specific task. As a matter of fact, understanding which tuples prevent the functional dependency from being satisfied can then lead to improve the results. This is where the notion of counterexample is useful. Counterexamples identify pairs of tuples for which the classifier will never be able to perform correctly, as for the same input; it will always predict the same output. Understanding where these counterexamples come from, and what can be done to avoid having such tuples in the dataset, is then a crucial tool to improve the classification performances. In the next sub-section, counterexamples from the used dataset are presented as well as some possible reasons to explain them in order to find some solutions to improve the classification model.

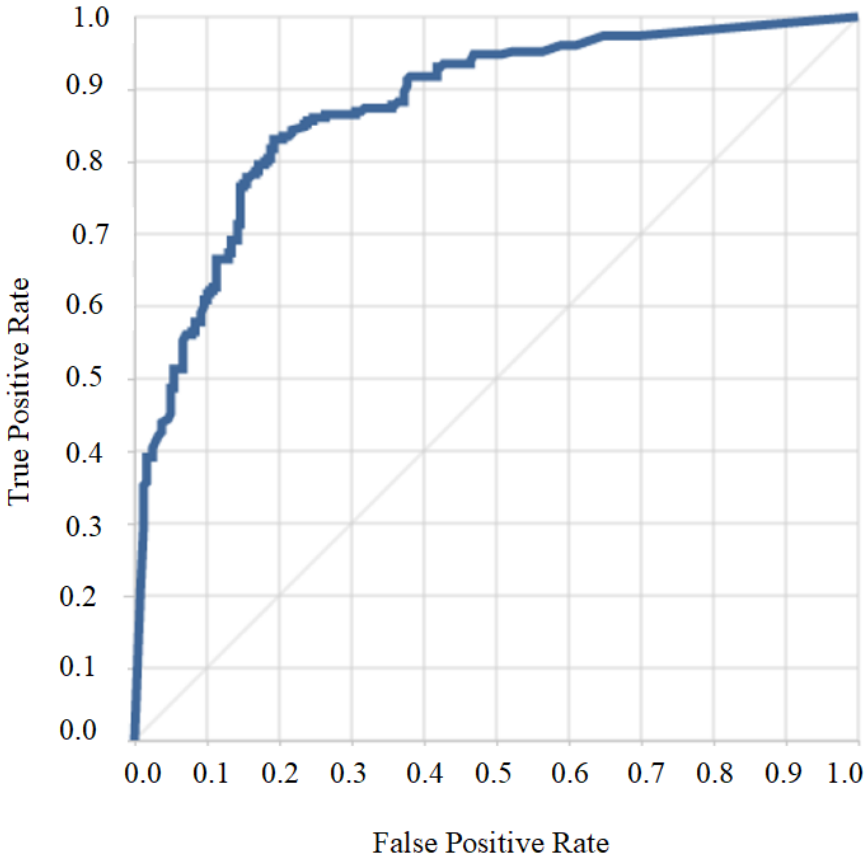

Figure 4.12 ROC curve for the prediction of refrigerated vehicles ageing classes.

4.4.1.2 Studying the existence of the classification model through the use of counterexamples

The existence of a function is assessed using the notions of functional dependencies and counterexamples introduced in Chapter 2, subparagraph 2.4.5.2.

Table 4.3 presents a sample of counterexample highlighting five features. Each line represents a counterexample, which is two tuples. As they both share the same values over the classification features, only the ageing column, on which they differ, is represented for both (Ageing $A_{12,1}$ and Ageing $A_{12,1}$). It appeared that several factors could explain the counterexamples, each having a different solution. Ultimately, these factors were divided into three main categories:

- ***Dirty data***: a considerable amount of time was spent on preparing and cleaning the dataset in order to use it for classification. However, when looking at counterexamples, it appeared that some tuples contained data that appeared to be incorrect. For counterexample 1 in Table 4.3, it appeared that the vehicle with a low ageing was actually a van instead of a truck. Similarly, for counterexample 2, the vehicle with a high ageing actually transported meat instead of vegetables. For this first category, once the data experts were aware of their existence, it was easy for them to identify these mistakes, based on the value of all the features. In addition, these counterexamples are easy to fix by correcting the wrong values.

- ***Missing information****:* for other counterexamples, it appeared that the features selected for classification were not enough to explain their existence. However, other features, which were not kept for classification, allowed discriminating between the two tuples involved in the counterexample. For instance, in Table 4.3, counterexample 3 can be removed if the number of food cases in the vehicle is taken into account. For counterexample 4, a specific characteristic of the cooling unit differed between the two tuples. As a result, taking those additional features, that at first had not been considered relevant for the classification, allowed removing counterexamples, which will then improve the classifier's performances.
- ***Human Factor***: finally, for a last group of counterexamples such as number 5 and 6 from Table 4.3, it appeared that the only possible explanation was the human factor, such as how the driver operates the vehicle. Indeed, this may influence the ageing of the vehicle, but it is also hard to quantify and poses critical and preserving issues. As a result, this last class of counterexamples is very difficult to fix, as data cannot be cleaned or completed. However, being aware that such counterexamples exist helps the data expert in understanding the limitations of the classification model to produce.

  Finally, it also indicates other values that could be interesting to record: in this case for example the average speeds of the vehicle and the kilometers travelled by the vehicle after twelve years of use but also previously, after six years and nine years when the vehicle passes through the test station for a pull down test. This information could be of great relevance to take into account of the human accident factor in the study of the ageing of refrigerated vehicles.

Table 4.3 Sample of counterexample found in the available dataset.

id	Manufacturer	Type of insulation of the enclosure	Insulation material and Blowing agent	Type of vehicle	Transported Products	Ageing $A_{12,1}$	Ageing $A_{12,2}$
1	Firm 1	Integrated	Polyurethane with cyclopentane	Truck	Meat	High	Low
2	Firm 2	Integrated	Polyurethane with cyclopentane	Van	Fruits	High	Low
3	Firm 3	Arranged on the frame	Polyurethane with cyclopentane	Truck	Frozen food	High	Low
4	Firm 4	Integrated	Polyurethane with cyclopentane	Semi-trailer	Vegetables	High	Low
5	Firm 5	Arranged on the frame	Polyurethane with cyclopentane	Truck	Cheese	High	Low
6	Firm 6	Arranged on the frame	Polyurethane with cyclopentane	Semi-trailer	Diary products	High	Low

4.4.1.3 Measuring the counterexamples rate

Three aforementioned metrics, G_1 , G_2 and G_3, were introduced in Chapter 2, subparagraph 2.4.5.2. They were computed over the refrigerated vehicles dataset. The proportion of counterexamples, $G_1 = 9.02\%$, is low, showing that the pairs of tuples in the dataset are not a big proportion. However, as $G_2 = 100\%$, all tuples from the dataset are involved in at least one counterexample: this is likely because a few tuples are in conflict with almost all the other. This is confirmed by measuring G_3 = 86.73%: this shows that to obtain a counterexamples-free dataset, the vast majority of the data can be saved. The counterexamples were found, using an interface developed by the experts of the LIRIS laboratory (for more details see Le Guilly, 2020). It is named LeaFF (Learning Feasibility with FDs), and can be used to query the data used for prediction, retrieve the counterexample, and obtain the metrics for FD satisfaction. A snapshot of this interface is presented on Figure 4.13, applied to the available Cemafroid data: it shows the part of the interface that can be used to enter the features and the class, so that the FD can be checked and counterexamples retrieved if necessary.

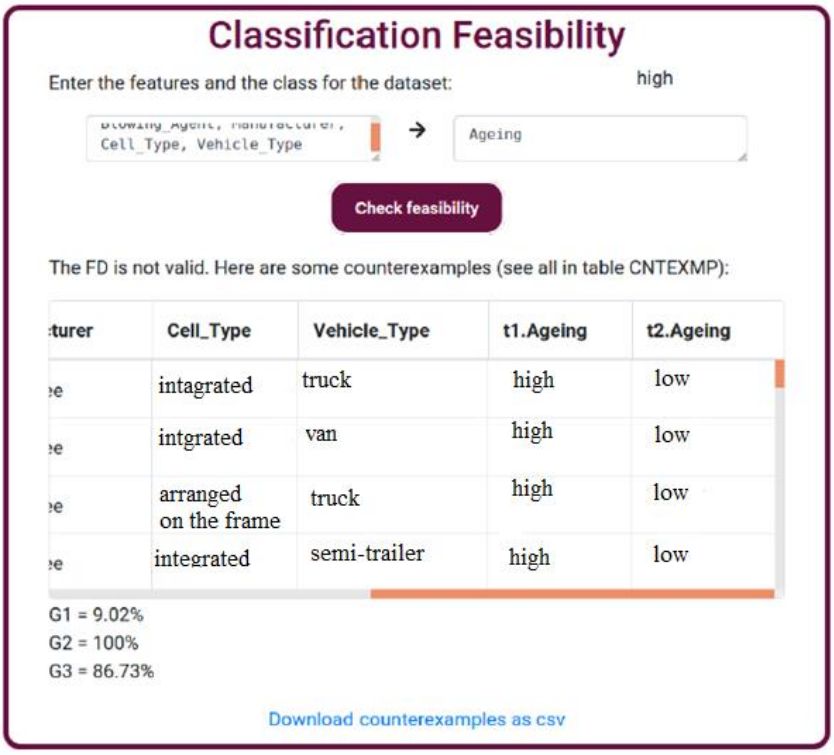

Figure 4.13 LeaFF interface developed by LIRIS laboratory (Le Guilly et al., 2020).

The identified counterexamples allowed to find limitations in the dataset, to take concrete actions to get higher quality data, and therefore to improve the results for a future new model. The counterexamples are inthat sense a perfect starting point for a discussion between data scientists and domain experts: while the first gain knowledge on data they are not expert on, the others can point out important information more easily. The counterexamples are for domain experts a way to read concrete information that have an impact on the day-to-day work by helping clean and improve the dataset and better understand the data used in the learning process. The study of the existence of a function through the use of counterexamples also shows that in classification, it is not possible to ignore the field reality, and to only see the problem as a matrix of data: the physical process is as important as the data itself, and bridges have to be built between physical and numerical models.

4.4.2 Regression ageing model

After discretizing the ageing into two classes, “low ageing” and “high ageing”, it was decided to determine an exact value of ageing (numerical and not categorical value), so it is no longer a problem of classification but of regression. The theoretical foundations put into practice in this section were presented in Chapter 2 (subparagraphs 2.4.5.3, 2.4.5.4, and 2.4.7.3).

4.4.2.1 Election of the model: random forest algorithm

As a result of careful comparisons, the random forest algorithm was chosen for its high-performance features, especially on small datasets (Fernández-Delgado et al., 2014) such as the ones considered here. Random forest builds multiple decision trees and merges them together to get a more accurate and stable prediction. The random forest algorithm randomly selects observations and features to build several decision trees and then averages the results. One big advantage of random forest is that it can be used for both classification and regression problems, which form the majority of current machine learning systems. Another great quality of the random forest algorithm is that it is very easy to measure the relative importance of each feature on the prediction. For the prediction of the ageing of refrigerated vehicles, a random forest of 2000 decision trees was used to build the prediction model (see Figure 4.14 as example of decision tree), using the following features:

- manufacturer,
- type of vehicle,
- average surface area of the insulated enclosure (m^2)
- payload (tons),
- empty weight (tons),
- total weight allowed in charge (tons)
- number and type of door openings on the enclosure,
- type of insulation of the enclosure
- insulation materials used to realize the enclosure,
- transported products,
- blowing agents used to foam the insulated body,
- type of refrigerating unit,
- presence of different features; recessed lighting control, bars or rails for the meat suspension, recessed lashing rails, liquid drain holes.

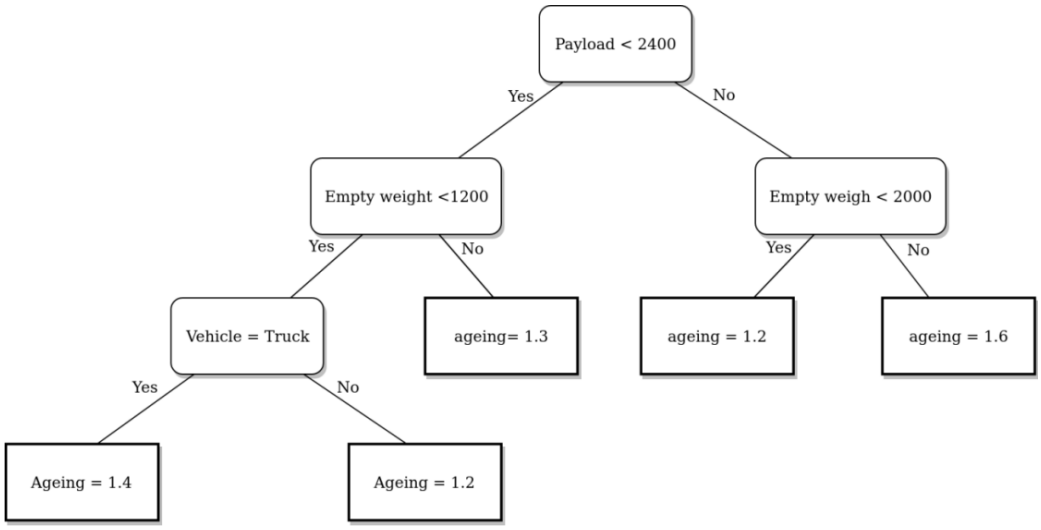

Figure 4.14 Example of a one of the 2000 binary decision trees of the random forest used to build the prediction model.

4.4.2.2 Training and Testing of the model

The data used for testing the regression model should be different from the one used to train it, to make sure that the model generalized correctly on data it has not "seen" before. To this end, 80% of the dataset was dedicated for training, with the remaining 20% left for testing.

4.4.2.3 Results and comparison with experimental data

A first model was built for 1092 vehicles and another one for a dataset containing 2120 vehicles. The difference between the two datasets lies in the fact that for the one containing 1092 vehicles, the blowing agent used in the manufacturing process is known. The performance of the model obtained on 20% of the data of these datasets is summarized in Table 4.4. The model was developed in Python 3, using the scikit-learn library (Pedregosa et al., 2011).The obtained performance underline the importance of the features taken into account for the numerical model: despite the lowest number of rows in the dataset, the prediction is better when the blowing agent is taken into account, which confirms the importance of this factor for the study of ageing as pointed out by Capo et al. (2019). Another way to apprehend the quality of the regression model referred to the 1092 data consists in plotting the predicted values of $\frac{K_{12}}{K_p}$ against the measured ones (see Figure 4.15). It appears that 95% of the available data points fall within a ±10% error band, which should qualify the model as efficient for predictions.

Table 4.4 Performance of the model with two different datasets, obtained on the 20% of data excluded from training

	1092 vehicles dataset with blowing agent information	**2120 vehicles dataset without blowing agent information**
RMSE	0.117	0.132
MAPE	5.76%	6.73%

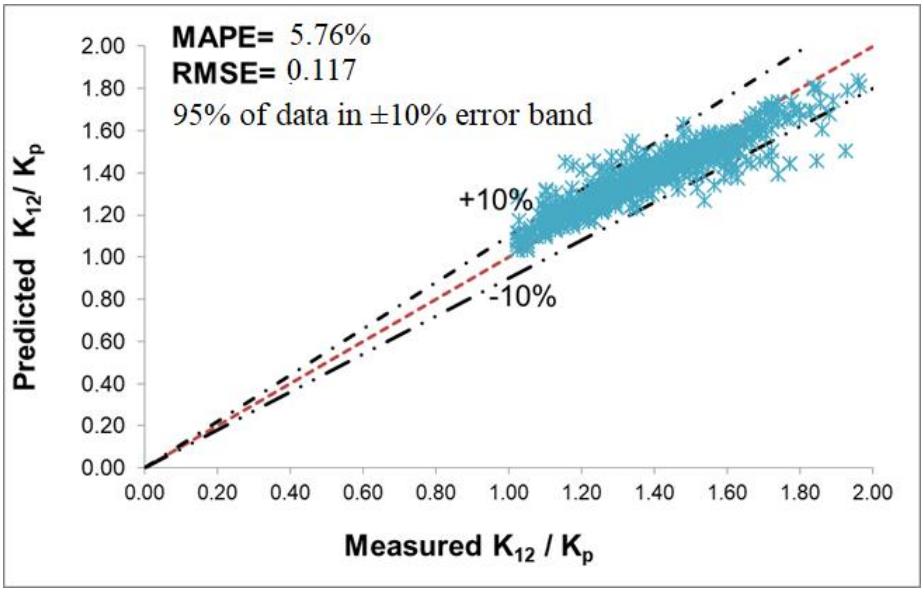

Figure 4.15 Comparison of $\frac{K_{12}}{K_p}$ values predicted by the model referred to 1092 data with measured ones.

4.4.2.4 Analysis of the importance of the features

In order to trust the numerical model, it is necessary to be able to deploy it in real scenarios: if the decisions of the algorithms cannot be understood on the basis of knowledge acquired on the field of refrigerated transport, then it will be hard to trust the prediction made by the numerical model, as they appear to contradict the physical observations. For this purpose the most important features in the random forest construction were analyzed. This investigation was made by analyzing how discriminative a feature is for the construction of each node of each tree. The result consists in the ranking of each feature used for the study, from the most to the least important. The importance of each feature is quantified by a percentage, such that the sum over all features is equal to 100%. Table 4.5 presents the sixteen most important features for the dataset of 1092 vehicles with their corresponding coefficient. To relate the most important features presented in this Table to the knowledge acquired on the field of refrigerated transport as well as to the results of the previous statistical analysis, some of these features can be grouped together. This makes sense as they belong to the same kind of attribute, often identified in a specific way on the field of refrigerated transport.

As a matter of fact, the three features related to weight, i.e. feature 1, 2 and 6 of Table 4.5, are connected to each other and represent another way to describe the attribute already known as "type of vehicle". Describing the type of vehicle through the use of weight-related features allows obtaining an even finer level of details, as the vehicle type usually consists in a few categories (i.e. vans, trucks and semi-trailers) while the weights can take many different values expressed in tons. In the vehicle type category it is also possible to include the average surface area of the insulated enclosure, this is in third place in the ranking with a coefficient of 9%. This choice is made because the average surface as well as the weights, varies according to the type of vehicle. The position in the table of these four features and the value of their coefficient allow confirming that the type of vehicle plays an important role in the present model for the ageing prediction, which is a clue to confirm its validity with respect to the domain knowledge.

The blowing agent, with a coefficient equal to 8%, appears to be of high importance for the quality of the ageing prediction. This clearly explains the difference of performance when the model is applied to the two different datasets. The identification of the blowing agent as important feature for the ageing prediction also confirms the statistical analysis presented in chapter 4.

Other features of Table 4.5 that may be grouped together are features 7, 8, 9, 10: they all belong to the family of features called by the domain experts as "accessories of the insulated enclosure". Therefore, the model highlights that the contribution of some accessories (e.g. the bars or the rails for the meat suspension) may be discriminating in the ageing prediction. This is in line with previous studies: the presence of the rails for suspending the carcasses on the roof was already investigated by Boldrin et al. (1993) who pointed out that this kind of accessories may cause an increased mechanical stress for the body of the vehicle, and finally influence its ageing. However, the model also highlights the influence of other accessories: the recessed lighting controls, the recessed lights and the recessed lashing rails.

With a coefficient equal to 3%, the manufacturers also appear among the most important features identified by the model for the ageing prediction (see features 11, 12 and 14 of Table 4.5), which confirms previous studies (Boldrin et al., 1990). Manufacturing technology and assembly process vary from one manufacturer to another and have an influence on the initial performance of the vehicle as well as on the long-term ageing.

A new element not yet highlighted by any previous study concerns the presence of liquid drain holes. This feature is in Table 4.5 at position 13 with a coefficient of 3%. Liquid drain holes, as their name suggests, allows draining liquids and water that otherwise would stagnate inside the enclosure. However, they represent openings and therefore deteriorate the insulation of the enclosures. This deterioration may influence the ageing process.

Finally, the model puts in evidence something previously discussed: the presence of the refrigerating unit (Panozzo et al., 1999) and the influence of the refrigerating unit architecture (monobloc or split) highlighted through the statistical analysis The presence of the refrigerating unit causes further thermal losses and accelerates the ageing of the vehicle. Regarding the architecture, a monobloc unit consists in a cabinet which contains the refrigeration circuit, the compressor and the fan. This cabinet is installed through a protrusion on the front of the vehicle, which results in a reduced insulating performance. Split systems are characterized by an internal unit and an external unit connected through the passage of two pipes in the wall. It requires only the realization of holes for the passage of the pipes. Although monobloc units are installed through a more homogeneous technology than splits, they cause a greater reduction of the insulating performance due to the perforation realized on the wall for their installation. The model highlights these concepts by showing (positions 15 and 16 in Table 4.5) that the presence or absence of the refrigerating unit plays a role in the ageing and that the monobloc architecture is discriminating for this purpose. Conclusions arising from the analysis of the importance of the various features are interestingly pertinent with the previous statistical analysis (see paragraph 4.3.2) whose scope was restricted to a few features, as identified thanks to the knowledge acquired on the ground.

Table 4.5 Most important features identified by the model for the dataset containing 1092 vehicles.

Feature	Coeff.	Feature	Coeff.
1. Payload (tons)	11%	9. Bars or rails for the meat suspension	4%
2. Empty weight (tons)	11%	10. Recessed lashing rails	3%
3. Average Surface area of the insulated enclosure (m^2)	9%	11. Manufacturer A	3%
4. Blowing agent R141b	8%	12. Manufacturer B	3%
5. Blowing agent Cyclopentane	8%	13. Liquid drain holes	3%
6. Total weight allowed in charge (tons)	5%	14. Manufacturer C	3%
7. Recessed lighting control	4%	15. Presence or absence of the refrigerating unit	2%
8. Recessed lights	4%	16. Type of refrigerating unit:	1%

		monobloc architecture	

4.4.2.5 Comparison with statistical analysis

Table 4.6 summarizes all the considerations made on the most important features identified by the model, comparing them to the factors playing a role in the ageing process as highlighted by the statistical study presented in paragraph 4.3. The left column of Table 4.6 lists the features identified by the model, of which some have been grouped together based on the knowledge acquired on the ground. As a result of the experience gained on the ground by carrying out numerous tests and K coefficient experiments makes it possible to intuitively understand which features most influence the ageing process and therefore to order them in order of importance. From first to sixth according to the value of the coefficient of importance presented in Table 4.5. The right column of Table 4.6 reports the most important factors in the ageing process previously identified by the statistical analysis. Even if they are presented in a different order and are not exactly the same, the features revealed by the use of a random forest algorithm agree well with the conclusion from the statistical study presented in the above section. In this setting, the analysis of the numerical model realized through the interpretation of the importance of the different features helped trust the model and better understands its decisions.

Table 4.6 Most important features selected by the model compared to the factors identified by the statistical analysis.

Features selected by the present model according the knowledge of domain expert	Factors affecting the ageing identified by the statistical analysis
1. Type of vehicle: payload, empty weight, total weight allowed in charge, average surface area	a. Blowing agent (R11, R141b, cyclopentane)
2. Blowing agent : R141b or cyclopentane	b. Type of refrigerating unit (monobloc or split)
3. Accessories: recessed lighting control, recessed lights, bars or rails for meat suspension, recessed lashing rails	c. Transported foodstuff (meat, meals, dairy products, frozen foods,…)
4. Manufacturer (A, B, C)	d. Manufacturer (A, B, C,..)
5. Particularities of the insulated enclosure: presence of liquid drain holes on the floor	e. Type of insulation
6. Refrigerating unit: absence or presence of monobloc one	f. Type of vehicle: van, truck, semi-trailers

4.4.2.6 Conclusions of the numerical modelling

This section reported on the numerical modelling for the prediction of ageing of refrigerated vehicles. A first classification model was built using standard classification methods. It showed very promising results, but also raised interrogations. In order to understand the dataset and to demystify the classifier, the classification model was studied from the features to the class to be predicted as a functional dependency, FD. The counterexamples to this FD are direct clues to apprehend the limitations of the classifier. The counterexamples were analyzed, and various causes for their existence were discovered, as well as potential solutions to remove them. This first step allowed further improving the dataset under study, which was then analyzed from the regression point of view. This regression model was built using a random forest algorithm that is efficient for small databases like the one considered for the present study, containing 2120 rows corresponding to as many vehicles having more than one hundred features. An additional feature was recovered for 1092 of these vehicles: the type of blowing agent used in the sandwich panels during the foaming process of the sandwich panels constituting the body of the insulated enclosures. It was then decided to apply the chosen algorithm to two different databases: the first one containing all the 2120 extracted vehicles without information on the blowing agent, the second one containing only the 1092 having the information of the blowing agent. The model results show higher prediction efficiency when applied to the 1092 vehicle dataset containing the blowing agent information. MAPE and RMSE are, in this case, respectively equal to 5.76% and 0.117 whereas for the 2120 vehicles dataset, their value reaches 6.73% and 0.132. Based on the obtained results, the model is considered as efficient enough to be tested in real scenarios. It could be used to predict values for which the ageing is not known. To understand the produced model, a study was carried out on the most important features used for the construction of each node of the trees. The features ranking process made it possible to confirm already know factors and to discover new ones influencing the ageing process, namely the presence of some accessories not yet taken into consideration (recessed lighting control, recessed lights and lashing rails) as well as the presence of liquid drain holes. The analysis of the feature ranking also showed that the

numerical model relies on mechanisms that make sense with respect with the domain knowledge and the statistical analysis carried out upstream of the numerical modelling process.

4.5 Conclusions

In this Chapter all the implementation steps of a machine learning problem were applied to the available data in order to understand, study and model the ageing phenomenon to which vehicles suitable for refrigerated transport are subjected over the time. This study was carried out in synergy with the data science experts of the LIRIS laboratory of INSA Lyon.

The available Cemafroid data were initially subjected to a meticulous pre-treatment process in order to improve their quality and make them more usable for subsequent analysis using artificial intelligence techniques.

A statistical analysis allowed discovering the data and confirming those factors involved in the ageing process already known due to the studies present in the literature but also to an intrinsic knowledge coming from the direct experience on the field. The analysis also identified some new factors such as the impact of the blowing agent and the type of refrigerating group. The most important factors identified as a result of this analysis were then classified in order of importance, i. e., the blowing agent, the type of refrigerating unit, the kind of transported foodstuff, the manufacturer of trucks, the type of insulation of the enclosure and the type of vehicle.

A first classification model was built using standard classification methods. The metrics of this model are: a Precision of 0.818 and a Recall of 0.783. At this stage the notions of functional dependencies and counterexamples were used, which were useful to improve the available dataset and overcome some of the limits of the classifier. Hence, with this first model available, it was possible to understand what could be done to improve the results and what where the blocking points in the dataset itself.

After this first classification analysis, the available data were analyzed from the point of view of regression using a random forest algorithm. The chosen algorithm was applied to two different databases: the first one containing 2120 extracted vehicles without information on the blowing agent, the second one containing only the 1092 having the information of the blowing agent. The model results show higher prediction efficiency when applied to the 1092 vehicle dataset containing the blowing agent information. MAPE and RMSE are, in this case, respectively equal to 5.76% and 0.117 whereas for the 2120 vehicles dataset, their value reaches 6.73% and 0.132. The most important features used for the construction of each node of the trees were analyzed. This analysis showed that the numerical model relies on mechanisms that make sense with respect with the domain knowledge and a match was found with the results shown through statistical analysis. The interaction between experts in refrigeration, refrigerated transport and thermal processes (Cemafroid and CETHIL laboratory sides) and experts in data science (LIRIS laboratory) has been fruitful and has shown that it is not possible to ignore the field reality, and to only see the problem as a matrix of data: the physical phenomena are as important as the data itself, and bridges have to be built between physical and numerical models. Therefore, the modelling of ageing is presented in the next chapter from a purely physical point of view.

4.6 References

Breiman, L., 2017: Classification and regression trees. Routledge.

Boldrin, B., Minotto G., Panozzo, G., Toniolo, B., Varotto, G., 1990. Ageing of insulated vehicles: statistical elaboration of test result. Proceedings of Commissions B2, C2, D1, D2/3, Dresden, Germany, IIF/IIR, (839-845).

Boldrin, B., Minotto., G., Panozzo, G., Toniolo, B., Lanza, W., Florio, G., Jacobini, A., Sallusti, L., 1993. New data about ageing of insulated vehicles in service: a statistical analysis. Proceedings of Commissions B1, B2, D1, D2/3, Palmerston North, New Zealand, IIF/IIR, (555-564).

Capo, C., Latchan, F., Michineau, T., Petit, J.M., Revellin, R., Bonjour, J., Cavalier, G., 2018. Factors affecting the ageing of refrigerated transport equipment. Proceedings of the 5th IIR Conference on Sustainability and the Cold Chain, Beijing, China.

Fernández-Delgado, M., Cernadas, E., Barro, S., Amorim, D., 2014. Do we need hundreds of classifiers to solve real world classification problems?. Journal of Machine Learning Research 15, (3133-31).

Garavaglia, S., Sharma, A., 1998. A smart guide to dummy variables: four applications and a macro. Proceedings of the Northeast SAS Users Group Conference.

Han, J., Kamber, M. (2006) Data Mining: Concepts and Techniques. 2nd Edition, Morgan Kaufmann Publishers, San Francisco.

Le Guilly, M., Capo, C., Petit, J.M., Scuturici, V-M., Revellin, R., Bonjour, J., Cavalier, G., 2020. Attempt to better trust classification models: Application to the Ageing of Refrigerated Transport Vehicles. Proceedings of the 25th International Symposium on Methodologies for Intelligent Systems.

Le Guilly, M., 2020. Guided Data Selection for Predictive Models. INSA, Lyon.

Panozzo, G., Alberti, O., Toniolo, B., Barizza, A., Boldrin, B., 1999. Parameters affecting the ageing of insulated vehicles. Proceedings of the 20th International Congress of Refrigeration, IIR/IIF, Sydney, Vol. IV (Paper 472).

Panozzo, G., Boldrin B., Minotto, G., Toniolo, B., Biancardi, N., 1995. Ageing of insulated vehicles: theoretical model and experimental analysis. Proceedings of the 19th International Congress of Refrigeration., Den Hague, Netherlands, Vol. II, (583-589).

Pedregosa, F., Varoquaux, G., Gramfort, A., Michel, V., Thirion, B.,Grisel, O., Blondel, M., Prettenhofer, P.,Weiss, R., Dubourg, V., Vanderplas, J., Passos, A., Cournapeau, D., 2011. Scikit-learn: Machine Learning in Python. Journal of Machine Learning Research 12, (2825–2830).

Schapire, R., 1990. The strength of weak learnability. Machine learning 5(2), (197-227).

Chapter 5

Physical model

Nomenclature of Chapter 5

Abbreviations

ATP	Agreement on the International Carriage of Perishable Foodstuffs and on the Special Equipment to be Used for such Carriage
PIR	Polyisocyanurate foam (
PU	Polyurethane foam
PVC	Polyvinyl chloride

Greek

Δ	Variation	
δ	Thickness	[m]
λ.	Thermal conductivity,	[$W.m^{-1}.K^{-1}$]

Roman

h	Height	[m]
h	Covective heat transfer coefficient	[$W.m^{-2}\ K^{-1}$]
K	Overall heat transfer coefficient	[$W.m^{-2}\ K^{-1}$]
L	Lenght	[m]
l	Width	[m]
$\dot{Q}$	Heating power	[W]
R	Thermal Resistance	[$K.W^{-1}$]
S	Mean surface area	[m^2]
T	Temperature	[K]
$u(x)$	Composed uncertainity of x	[same of x]

Subrscripts

0	Initial/immediately after manufaturing(refferd to real vehicle)
12	
*calculate*d	Calculated
coat	Coating
conv	Convective
ext	External
foam	Foam
floor	Floor
i	i-th
int	Internal
n	n-th year of life
p	Prototype
tot	Total

5. Physical model

After dealing with the ageing from a statistical point of view with a data centric approach and numerically modelling with the use of artificial intelligence techniques, this Chapter presents the development of a 1D model to study the phenomenon from a heat transfer point of view .

As already seen, after the vehicle has been manufactured, the ATP does not currently prescribe the K coefficient test for the entire series of vehicles but only for the prototype vehicle. It has been seen, however, that the K_p coefficient of the prototype vehicle is not the best reference indicator for studying the ageing of refrigerated vehicles. In this section, therefore, the objective is to produce a simple model which allows calculating the initial performance of the vehicle (K_p and K_0 values) and simulating the vehicle's ageing after twelve years of life.

Thess goals arise from the fact that there are currently very few models of this type in the literature (Glouannec et al., 2014)

The model presented in this chapter is developed thanks to the experimental activity carried out in the official Cemafroid ATP test station, where several vehicles have been tested every day, since 1953. The study also benefited from the support of the engineers and technicians working in Cemafroid. The creation of the model was made possible thanks to collaboration with the Aubineau company, which provided detailed plans of its vehicles.

5.1 Case study

A refrigerated truck with an internal air volume of 52 $m^3$and a mean surface area, S, equal to 98 m^2 has been considered to develop the model of the present study. The considered truck body was produced by the manufacturer Aubineau. The main dimensions of its insulated body are reported in Table 5.1. Inside the truck, there are four PVC plastic lighting recessed in the ceiling, five meat rails on the ceilind and four steel anchoring rails, two on each lateral wall.

This truck was tested at the beginning of its life to compare its initial K_0 coefficient to the K coefficient of the respective prototype, K_p. On the basis of this prototype another truck that had been built in the series was tested in the Cemafroid test chamber after twelve years of life. Since this vehicle has the same main dimensions and characteristics as the new vehicle under study, it may be taken into consideration to evaluate the ageing of the new vehicle after twelve years of life.

The measured K coefficient values of these three trucks with the respective measurement uncertainties (calculated using Eq. 3.47) are reported in Table 5.2.

Table 5.1 Main dimensions of the studied insulated truck.

Internal dimensions			**External dimensions**		
L_{int} (m)	l_{int} (m)	h_{int} (m)	L_{ext} (m)	l_{ext} (m)	h_{ext} (m)
9.00	2.47	2.35	9.17	2.59	2.60

Table 5.2 Measured K values with associated measurement uncertainties of the 3 trucks.

	Prototype vehicle K_p	**New truck on the series** K_0	**Truck on the series after twelve years of life** K_{12}
K [W.m^{-2}.K^{-1}]	0.34	0.36	0.42
u(K)	±2.4 %	±2.7 %	±3.7 %

Based on the widespread sandwich panel technology, the walls of this truck are made up of three layers consisting of polyurethane foam enclosed between two thin polyester layers. The floor includes two additional layers of plywood plate, necessary to meet the requested mechanical resistance, being generally the most stressed wall. The complete stratigraphy of the walls was provided by the manufacturer and is presented in Table 5.3.

Table 5.3 Specifications and complete stratigraphy of the insulated enclosure.

	Ceiling	**Floor**	**Lateral walls**	**Front wall**	**Rear door**
Nature of the interior coating	Polyester	Polyester and Plywood	Polyester	Polyester	Polyester
Thickness of the interior coating (mm)	1.5	1.5 (polyester) 18 (plywood)	2	1.5	2
Nature of the insulated foam	Polyurethane foamed with cyclopentane	Polyurethane foamed with cyclopentane	Polyurethane foamed with cyclopentane	Polyurethane foamed with cyclopentane	Polyurethane foamed with cyclopentane
Thickness of the insulated foam (mm)	102	108	56	62	82
Nature of the exterior coating	Polyester	Plywood Poyester	Polyester	Polyester	Polyester
Thickness of the exterior coating (mm)	1.5	18 (plywood) 2 (polyester)	2	1.5	2
Total thickness of the wall (mm)	105	149	60	65	84

5.2 Development of the model

This section presents the development of the model for the calculation of the initial K coefficient of a refrigerated truck and the subsequent prediction of the K coefficient at twelve years of life, taking simply into account the possible ageing of the panels of which the truck is composed. The model was developed in Excel environment.

5.2.1 Calculation of the initial K_0 coefficient of the truck

First, the simplest case of a truck consisting simply of sandwich panels is presented. The accessories inside the enclosure are then taken into account and the model is thus modified.

5.2.1.1 Simple case of a truck consisting only of sandwich panels

For the development of the model, the new truck described in the previous paragraph is taken into account. This truck is modeled considering the conditions prescribed by the ATP K coefficient test (see Figure 3.4): it is placed in a climatic chamber at T_{ext} equal to + 7°C. Thus, the problem initially consists in determining the heating power, $\dot{Q}$ to be extracted from the insulated enclosure of the truck, in order to maintain, under stationary conditions, an internal temperature, T_{int}, equal to +33°C.

For this study a mono-dimensional approach can be considered by choosing, for each wall, an appropriate reference area, which may be assumed to be constant with respect to thickness. In the first instance, this reference area could be considered to be equal to the average area, S, of the heat passage section, i.e. the area of the passage section at the half of the wall thickness.

Neglecting the side effects, from the point of view of thermal transmission, each wall diffuses heat in parallel with the others. The thermal circuit related to the problem under study, without initially considering the presence of accessories inside the vehicle, is presented in Figure 5.1.

In the picture each i-th branch corresponds to a wall (i=1, 2, …6). In particular:

- branch labeled 1 corresponds to the ceiling;
- branch labelled 2 concerns the floor;
- branches 3 and 4 refer to the lateral walls;
- branches 5 and 6 are respectively the front and the rear walls.

The model accounts for the convective heat exchanges, insisting on the average internal and external surfaces. These exchanges are represented by the internal and external convective resistances, $R_{int,conv,i}$ and $R_{ext,conv,i}$. The convective heat transfer coefficients on the internal and external and outer surfaces of the walls, $h_{int,conv}$ and $h_{ext,conv}$, are respectively equal to 10 W.m^{-2}. K^{-1} and 15 W. m^{-2}. K^{-1}.(Moran et al., 2010)

The other resistances correspond to the different layers that make up the walls:

- $R_{coat,i}$, the resistance of the polystyrene coating;
- $R_{foam,i}$, the resistance of the polyurethane foam;
- $R_{plywood,i}$, the resistance of the plywood plate, introduced in this case in the floor to meet the requested mechanical resistance.

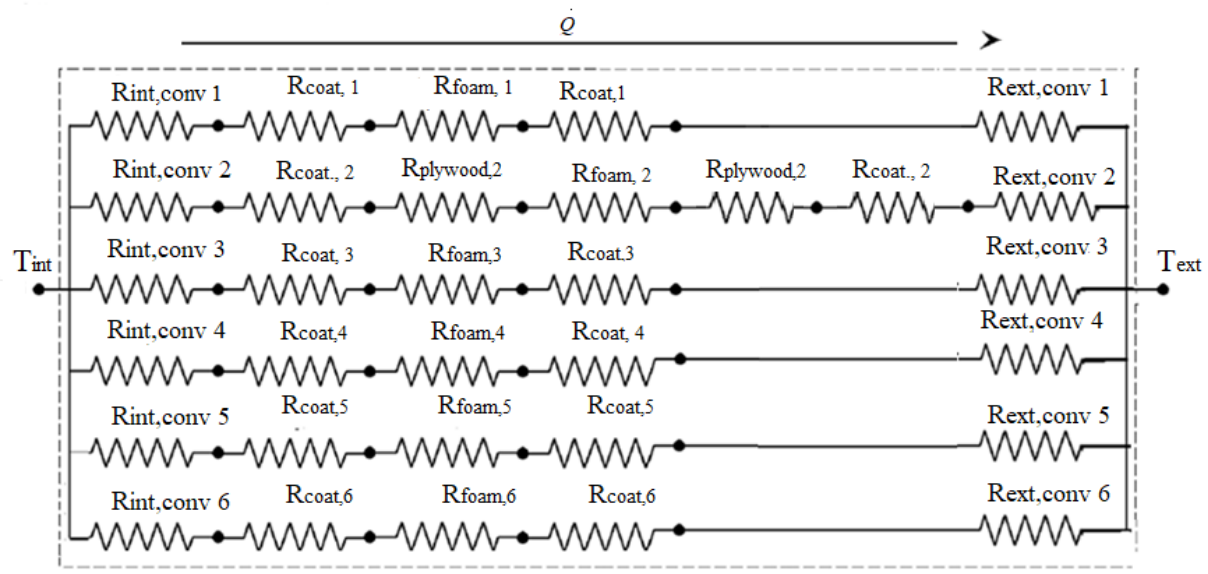

Figure 5.1Thermal circuit describing the studied truck without considering the presence of accessories.

Considering the equivalent (total) resistances ($R_i \; where \; i = 1, 2, \dots, 6$) of each of the six parallel branches, the previous scheme can be simplified as presented in Figure 5.2. The total resistance of a generic branch, R_i can be calculated as the sum of the internal and external convective resistances and those of each layer of material composing the i-th wall.

For example, considering the branch number 2, related to the floor, its total resistance, R_2 is calculated as follows:

$$R_2 = \frac{1}{S_{floor}}\left(\frac{1}{h_{int,conv}} + \frac{\delta_{coat}}{\lambda_{coat}} + \frac{\delta_{plywood}}{\lambda_{plywood}} + \frac{\delta_{foam}}{\lambda_{foam}} + \frac{\delta_{plywood}}{\lambda_{plywood}} + \frac{\delta_{\mathrm{coat}}}{\lambda_{coat}} + \frac{1}{h_{ext,conv}}\right) \qquad \text{Eq. (5.1)}$$

Where S_{floor} is the average surface of the floor, δ indicates the thickness of the generic material composing the sandwich panel and λ the associated thermal conductivity. The used values of thermal conductivities are shown in Table 5.4.

The thermal power that must be continuously supplied inside the insulated enclosure in order to maintain a temperature permanently equal to the desired value of +33 °C, may be calculated as:

$$\dot{Q} = \frac{T_{int} - T_{ext}}{R_{tot}} \qquad \text{Eq. (5.2)}$$

The total resistance, R_{tot}, to be used in the calculation of $\dot{Q}$ is given by:

$$R_{tot} = \frac{1}{\frac{1}{R_1}+\frac{1}{R_2}+\frac{1}{R_3}+\frac{1}{R_4}+\frac{1}{R_5}+\frac{1}{R_6}} \quad \text{Eq. (5.3)}$$

To obtain the K coefficient, the power held through Eq. (5.2) has to be divided by the temperature difference ($T_{int} - T_{ext}$) and the mean surface area, S of the insulated enclosure. This first circuit of resistors excluding the presence of accessories, allows to obtain the calculated K coefficient of the new truck, $K_{0,calculated}$, whose value was found to be equal to 0.34 W.m^{-2}.K^{-1}. This value results in a decrease by 7.1 % compared to the K_0 value measured in the climate chamber (equal to 0.36 W.m^{-2}.K^{-1}).

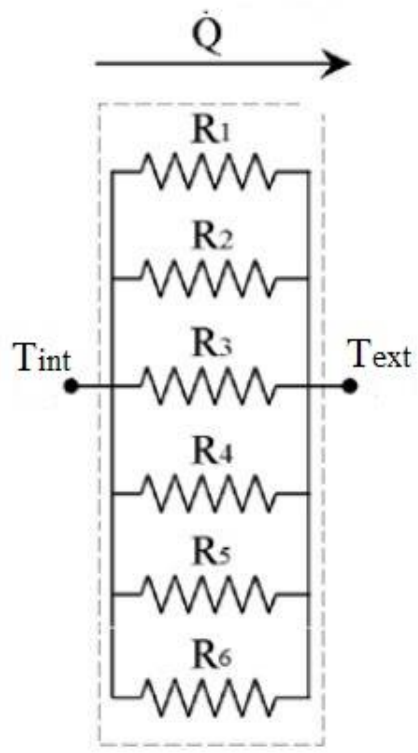

Figure 5.2 Equivalent thermal circuit.

Table 5.4 Thermal conductivities used for the calculation of resistances.

	λ [W.m^{-1}. K^{-1}]
Polyester coating	0.250
Plywood	0.150
Polyurethane foam	0.023
Steel	50
PVC plastic	0.200
Aluminum	200

5.2.1.2 Case of vehicle whose specifications and accessories are known

Since the details of the accessories inside the truck (type and quantity, materials, thermal conductivity, dimensions and position) were provided by the manufacturer (see Table 5.5), their presence was taken into account in the calculation of the K coefficient. Such accessories represent thermal bridges affecting the value of K_0. In addition, the manufacturer provided more details on the floor composition indicating the presence of eleven wooden beams with the purpose of further reinforcing this wall which is generally the most stressed. These wooden beams also had to be considered. These features (accessories in the side walls and in the ceiling, as well as the wooden beams in the floor) were added as parallel elements to the materials that make up the corresponding wall.

The thermal resistances of each of these features were calculated using the values of thermal conductivity shown in Table 5.4. The inverse values of these resistances, which represent the heat flow due to the presence of these accessories, are shown in Table 5.6. As final resut the calculated initial K value, $K_{0,calculted}$ of the truck was equal to 0.35 W. m^{-2}. K^{-1}. It is worth pointing out that the model does not take into account the presence of the refrigeration unit mounted on the enclosure of the truck house. In this regard, the K coefficient obtained considering the presence of accessories has to be increased by the correction factor due to the presence of the refrigerating unit, presented in Chapter 3, section 3.3, and also used in the experimental assessment of the difference between series vehicles and prototypes ones (paragraph 3.5.2). The addition of this factor leads to an increase in the calculated $K_{0,calculated}$ coefficient to a value equal to 0.37. This new value, which takes into account the presence of the accessories, the wooden beams and the refrigerating unit, deviates from the measured value by only 1 %.

Table 5.5 Details of the accessories inside the truck.

Type of accessory and quantity	**Position**	**Material**	**Diameter, D [m]**	**Length, L [m]**	**Height, h [m]**	**Thickness, t [m]**
4 Recessed lighting	Ceiling	PVC plastic	0.10	/	/	0.055
5 Meat rails	Ceiling	steel	/	9.021	0.07	0.025
4 Recessed lashing rails	2 on each lateral wall	steel	/	9.021	0.009	0.012
2 plinths	1 on each lateral wall	alluminium	/	9	0.26	0.003
11 Wooden beams	in the floor	wood	/	2.465	0.106	0.060

Table 5.6 Heat flow through each feature in the truck.

$\frac{1}{R_{feature}}$ [W.K^{-1}]				
Recessed lighting	**Meat rail**	**Recessed lashing rail**	**Plinth**	**Wooden beam**
0.18	**9 000**	**6750.00**	**15 6000**	**7.19**

5.2.2 Prediction of the ageing of the truck after twelve years of use

The presented model allows calculating quite faithfully the K coefficient of the vehicle at the beginning of its life. This is possible thanks to the detailed specifications and characteristics of the truck provided by the manufacturer.

The ageing of a vehicle, as learned from the statistical study carried out in this thesis, depends on several factors (i.e., the blowing agent and the type of insulation, the type of refrigerating unit, the type of realized transport, etc…). Since the developed model is based on the heat transmission through the walls of the truck, to predict the K coefficient value after twelve years of life it was decided to include the ageing of the wall component that most affects the heat exchange: the polyurethane foam. To this end, the knowledge from the studies already present in the literature has been exploited. The Forschungsinstitut für Wärmeschutz e.V. München (1998) conducted long-term tests on rigid polyurethane foam (PU/PIR) insulation panels blown with pentane. The thermal conductivity and cell gas composition of the panels were determined periodically over a storage period of fifteen years at room temperature. Figure 5.3 shows the obtained results highlighting the change in thermal conductivity of rigid polyurethane panels of different thicknesses (i.e. 40 mm and 80 mm) and it highlights that after twelve years of life, the thermal conductivity of a polyurethane panel with a thickness of 80 mm is about 0.026 W.m^{-1}.K^{-1} . This is 13% higher than its value at the beginning of its life (equal to 0.023 W.m^{-1}.K^{-1}). Replacing in the model the initial thermal conductivity value of the polyurethane foam with this aged value, gives an estimation of the K coefficient at twelve years, $K_{12,calculated}$ equal to 0.41 W.m^{-2}.K.$^{-1}$. This value also takes into account the refrigerating unit factor correction equal to 0.02 W.m^{-2}.K.$^{-1}$ and is 2% less than the value of K measured at twelve years of life on a vehicle of the same series having the same dimensions, characteristics and accessories. This difference could be attributed to the use of the truck. This factor contributes to the ageing of a refrigerated vehicle but it is difficult to quantify because it is to be ascribed to the human factor.

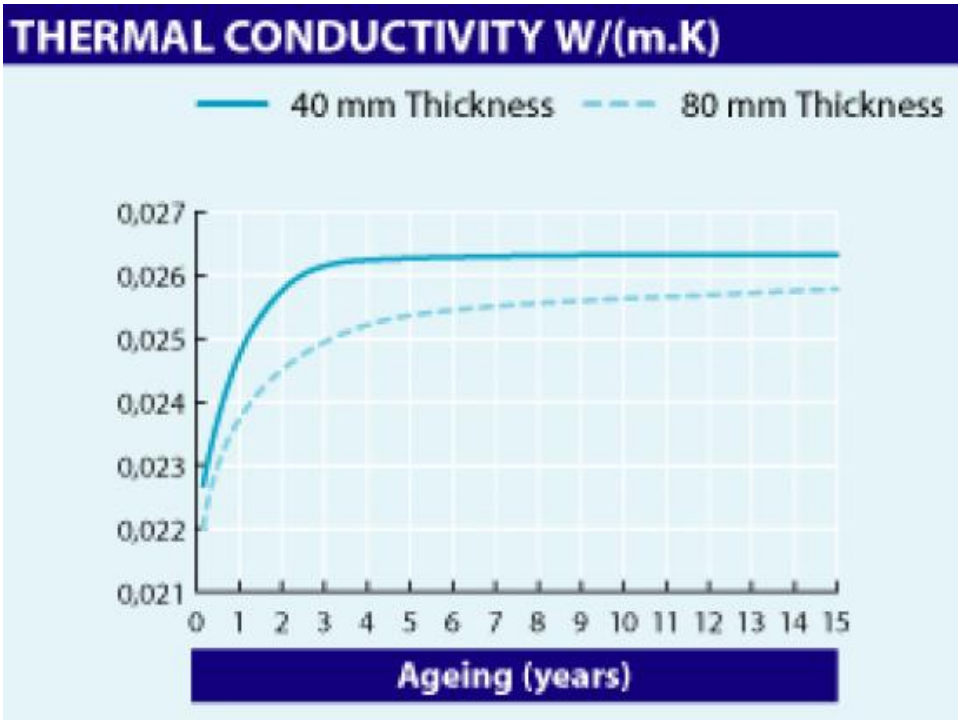

Figure 5.3 Increase in thermal conductivity of rigid polyurethane foam (PU/PIR) insulation panels in the first fifteen years after manufacture (FIW München, 1998).

5.3 Conclusions

This chapter presented a 1D model under steady-state conditions for the calculation of the initial K coefficient of a refrigerated vehicle.

The detailed knowledge of the characteristics of the vehicle and the accessories inside it and the addition of the correction factor due to the presence of the refrigeration unit make it possible to calculate the initial K coefficient quite faithfully.

For the case study considered a difference of only 1% with the measured value was found (i.e., $K_{0,calulated} = 0.37$ W.m^{-2}.K^{-1} whereas $K_{0,measured} = 0.36$ W.m^{-2}.K^{-1}). By adding to this model the information of the aged thermal conductivity acquired from the literature it was possible to predict the value of the K coefficient after twelve years of life. This predicted value is 2% less than the value of the K coefficient measured at twelve years of life on a vehicle of the same series having the same dimensions, characteristics and accessories. This difference could be attributed to the type of use made of the vehicle during its lifetime. Further modeling tests should be performed to confirm the goodness of the model. To this end, it would be useful to have detailed information about the construction and composition of other vehicles including the accessories and features inside the insulated enclosure. In addition, a protocol has been recently developed for carrying out thermal conductivity tests on panels obtained from real vehicles. This protocol is not part of the work of this thesis but of its follow-up. The main objective of these future tests is to experimentally obtain equivalent thermal conductivity values both at the beginning and after twelve years of life to be inserted in the model. The development of this experimental assessment is in partnership with Petit Forestier company, which will supply panels from its vehicles for

testing. The expected results from this future study could allow obtaining more accurate values of the calculated K coefficients.

5.4 References

Glouannec, P., Michel, B., Delamarre, G., Grohens., Y., 2014. Experimental and numerical study of heat transfer across insulation wall of a refrigerated integral panel van. Applied Thermal Engineering, Elsevier, 73, (196 – 204).

Moran, M. J., Shapiro, H. N., Boettner, D. D., Bailey, M. B., 2010. Fundamentals of engineering thermodynamics. John Wiley & Sons.

Prüfbericht Nr. F.2-421, 462, 630, 731, 840/98,1998. Forschungsinstitut für Wärmeschutz e.V. München, FIW München).

Chapter 6

Conclusions and perspectives

Nomenclature of Chapter 6

Abbreviations

ATP	Agreement on the International Carriage of Perishable Foodstuffs and on the Special Equipment to be Used for such Carriage
ANRT	Association Nationale Recherche Technologie
CETHIL	Centre d'Energétique et de THermIque de Lyon
CIFRE	Conventions Industrielles de Formation par la REcherche
MAPE	
RMSE	
VIP	Vacuum insulation panel

Greek

λ.	Thermal conductivity,	[$W.m^{-1}.K^{-1}$]

Roman

K	Overall heat transfer coefficient	[$W.m^{-2}\ K^{-1}$]

Subrscripts

0	Initial/immediately after manufaturing(refferd to real vehicle)
12	
calculated	Calculated
ext	External
i	i-th
int	Internal
measured	Measured
n	n-th year of life
p	Prototype

6. Conclusions and perspectives

The ageing of vehicles used in refrigerated transport is a complex phenomenon involving both physio-chemical and mechanical factors. It may affect the refrigeration and environmental performances of the vehicles and therefore have a significant cost on their exploitation as well as on their lifetime. The study of the ageing of refrigerated vehicles and the investigation of all the factors associated with this phenomenon is of fundamental importance for the design of better performing vehicles, but also for their smart use. The work of the present PhD thesis has been realized in the context of the ANRT's CIFRE device. This device results as a meeting point between academic and industrial Research and has therefore allowed the establishment of a partnership between three different entities: the Cemafroid, recognized by the United Nations as ATP authority competent in France, and two academic laboratories of INSA Engineering School, based in Lyon, i.e. the CETHIL (Centre d'Energétique et de THermIque de Lyon.) and the LIRIS (Laboratoire d'Informatique en Image et Systèmes d'Information). The strength of this partnership has been the diversity and wealth of competences. This has made it possible to study the phenomenon of ageing by means of several approaches:

- experimental, thanks to the expertise of Cemafroid and its laboratories,
- physical modelling based on heat transfer analysis, thanks to the experience in this field of the CETHIL laboratory;
- data science, thanks to the presence of LIRIS which, through the use of artificial intelligence techniques, made it possible to use the large amount of data stored in the Cemafroid Datafrig® databases.

The main outcomes of this study as well as the resulting future works and perspectives are summarized in this Chapter.

6.1 Summary of experimental activities

A comprehensive literature review on the evolution of construction technologies as well as on the phenomena of ageing affecting vehicles, suitable for refrigerated transport, was carried out. It shows that:

- the insulation performance of the new enclosures has been deteriorated due to the ban of halogenated blowing agents (used in the foams of sandwich panels) since the early 1990s. While between 1950 and 1970 the value of the K coefficient was reduced by half, in the last thirty years this has increased by 25%. This development is the opposite of what was desired at a time in history when energy savings were being sought. Producers must therefore reverse the trend. The use of new insulation and new technologies such as aerogels and VIPs are essential to meet this challenge.
- Several studies on ageing are reported in the literature providing important information about the factors involved in this process such as: the influence due to de manufacturer, the type of realized refrigerated transport or the presence of some accessories inside the insulated enclosure (i.e. meat rails and refrigerating unit). However, the studies previously carried out are lacking in important information: the exact knowledge of the K coefficient at the beginning of the life of the vehicle as well as values of the K coefficient at times of life other than those prescribed by the ATP (i. e. after manufacturing and 12 years). The

lack of the real K values at the beginning of the life of the vehicles is due to the process implemented by the ATP regulation which requires, immediately after the manufacturing, only the K coefficient of prototype vehicles to be determined. These vehicles may differ from those of the series both in surfaces and accessories inside them.

Considering what has emerged from the literature review, the experimental activities carried out for the present thesis aimed at filling this lack of information. Experimental activities were thus performed in order to:

- measure K values of different vehicles at key moments in their life (in the first months and in the last years of use of the vehicles);
- confirm already known ageing factors;
- quantify the impact of some accessories in the insulating performance of vehicles as well as on the ageing process;
- assess the existing difference between real vehicles and prototype ones by measuring the initial K values, (K_0) of the vehicles in the series and making a comparison with the K values of the corresponding prototypes (K_p);
- evaluate the energy savings that can be achieved through the use of new materials such as VIP insertions.

The main results obtained from these experimental activities are the following ones:

- several K coefficient tests realized on a semi-trailer at the beginning of its life, allowed finding out that over a period of one hundred and eleven days the ageing of the insulated enclosure of this semi-trailer was equal to 1.33%. This estimation may correspond to about 4.4% over a period of one year and is consistent with previous studies in the literature quantifying the annual ageing at 5%.
- On the same semi-trailer the impact of the refrigerating unit and door inserts was assessed. Removing both these features from the same semi-trailer a relative decrease of the K coefficient by 5.3% was found.
- The impact of the refrigeration unit was deepened: four semi-trailers were tested under two different conditions, i.e. in presence or absence of the refrigerating unit, and the mean value of the difference between K measured in these two conditions was found to be equal to 0.020 $W.m^{-2}.K^{-1}$. Improving the mounting technique and the insulation of the refrigerating unit thus appear to be two useful tracks to enhance the insulation performance of the vehicles realized on the series.
- Ten trucks for which the K coefficients were measured even after twelve years of life were analyzed and it was possible to highlight that in the period between 12 -18 years the relative increase of the K coefficient is equal to 5% whereas in the period 0-12 this increase reaches up to 66 %. However, as pointed out, the ageing between 0 and 12 years could be higher or lower due to the fact that it refers to the K coefficient of the prototype vehicle (K_p) and not to that of the real vehicle.
- Forty-one new vehicles of different categories underwent the K coefficient test and were compared with their respective prototypes. This experimental assessment allowed, for the

first time, to determine the K_0 coefficient of newly produced vehicles. This assessment also made it possible to point out that K_p is not the best reference point for the ageing assessment. As a matter of fact, at the moment of their construction, real vehicles, depending on their type (vans, trucks, semi-trailers) exhibit real K coefficients (K_0) deviating up to 31% from the K values of the corresponding prototypes (K_p). Considering the K value of the prototype (K_p) as the reference measurement, some of the vehicle realized in the series, would have received a wrong insulation class according to the ATP Agreement;

- The experimentation carried out on these forty-one new vehicles also made it possible to calculate an apparent thermal conductivity (λ_{app}). Thus, the results of K_0 of the three series of vehicles were combined as a unique series of vehicles and λ_{app} was found to be equal to 0.030 $W.m^{-1}.K^{-1}$. This parameter takes into account the presence of the solid matrix that improves the mechanical robustness to the structure of the vehicle. This value of λ_{app} is greater, by 20 to 30%, than the conductivity of polyurethane foam declared by the manufacturers.
- Considering the series of trucks of the forty-one vehicles it was possible to apprehend the importance of the doors in the insulation efficiency. Removing doors or changing their type (which is common practice when building real vans after their prototype) significantly affects the value of the K coefficient. Thus, improving the choice of the doors as well as their tightness appears to be a useful challenge to enhance the insulation performance of the vehicles realized on the series;
- Two semi-trailers with VIP insertions in some of the walls were subjected to the K coefficient test and an improvement in insulation performance was found in both vehicles. This new technology of VIP insertions in hybrid form in the classic sandwich panels is one of the solutions for the short-term future to obtain energy savings in refrigerated transport. In fact, the vehicle with the largest VIP insertion has K_p value (measured immediately after its manufacture) equal to 0.27 $W.m^{-2}.K^{-1}$, which is comparable to the average value obtained in the past when R11 was used as blowing agent. In addition, there was also a reduction in energy consumption on this vehicle compared to a vehicle with standard sandwich panels with cyclopentane as blowing agent. These energy savings are equal to 34 % in start and stop mode and 23% in the continuous mode.

6.2 Conclusions arising from the the analysis carried out with a data-centric approach

After carrying out the various experimental activities, the next step in this thesis work was to implement a data-centric analysis using both simple concepts of statistics and Machine Learning methods. Cemafroid has in fact been carrying out K coefficient experiments since 1950 and therefore has a large available database containing the results of these experiments as well as all the characteristics and features of the tested vehicles. The creation of a numerical model was the final objective of such a data centric approach. The results of the statistical analysis and numerical modelling of available data are summarised in the following sub-paragraphs.

6.2.1 Summary of the statistical analysis

In order to gain insights from the available data the first step of such data learning problem was a statistical analysis using simple concepts such as probability density. This analysis was performed on a first dataset containing the information of 1158 vehicles extracted from Datafrig database and allowed confirming the influence of factors already studied: the type of vehicle, the influence of manufacturer and the type of transport realized. However, other important factors not yet considered before were analyzed and the obtained results are as follows:

- The performance in the long-term resulted to be higher for those refrigerated vehicles which insulated enclosures are assembled on their platforms than for vehicles with an integrated insulation.
- The influence of the architecture of the refrigerating unit was studied highlighting that monobloc units are installed through a more homogeneous technology than splits ones but cause a greater reduction of the insulating performance. This may be due to the perforation that must be realized on the wall for their installation.
- Another important aspect, relevant for understanding the ageing phenomena, highlighted by the statistical analysis, concerns the influence of the blowing agent. Three samples of refrigerated semi-trailers foamed with different blowing agents were compared. This comparison showed that semi-trailers foamed with cyclopentane have better performance in the long period.

After the statistical analysis, the phenomenon of ageing was modelled using artificial intelligence techniques, in particular through classification and regression algorithms. The main results obtained from this second stem are summarized in the next paragraph.

6.2.2 Conclusions arising from the numerical modelling

A first classification model was built on the same dataset as that used used for the the statistical analysis and through the use of classification methods. Hence, the ageing of refrigerated vehicles from this dataset has been classified as low and high ageing. This model presented as results a precision of 0.810, a recall of 0.783 and the F1 score is estimated at 0.800. At this stage the notions of functional dependencies and counter-examples were used. These concepts were useful to improve the available dataset and overcome some of the limits of the classifier. Hence, with this first model available, it was possible to understand what could be done to improve the results and what where the blocking points in the dataset itself.

After this first classification analysis the available data were analyzed from the point of view of regression using a random forest algorithm. The chosen algorithm was applied to two different databases: the first one containing 2120 extracted vehicles without information on the blowing agent, the second one containing only the 1092 having the information of the blowing agent. The results of this second model have shown higher prediction efficiency when applied to the 1092 vehicle dataset containing the blowing agent information. MAPE and RMSE were, in this case, respectively equal to 5.76 % and 0.117 whereas for the 2120 vehicles dataset, their value reached values of 6.73 % and 0.132. The most important features used for the construction of each node of the trees were analyzed. This analysis showed that the numerical model relies on mechanisms that make sense with respect with the domain knowledge and a match was found with the results

shown through statistical analysis. As a matter of fact the same factors identified by the statistical analysis are also highlighted by the model, although with different notations (i.e. features as the payload, the empty weight and the average surface area identified by the numerical model rely to the feature type of vehicle highlighted by the statistical analysis).

6.3 Conclusions arising from the physical model

After studying ageing through a learning problem with artificial intelligence techniques that led to the development of classification and regression models, a physical model was also developed. This 1D model under steady-state conditions allows calculating the initial K coefficient of a refrigerated vehicle. The detailed knowledge of the characteristics of the vehicle and the accessories inside it and the addition of the correction factor due to the presence of the refrigeration unit make it possible to calculate the initial K coefficient quite faithfully. For the presented case study a difference of only 1% with the measured value was found (i.e., $K_{0,calculated}$ 0.368 W.m^{-2}.K^{-1} whereas $K_{0,measured}$= 0.365 W.m^{-2}.K^{-1}).

By adding to this model the information of the aged thermal conductivity acquired from the literature ($\lambda_{12} = 0.026$ W.m^{-1}. K^{-1}) it was possible to calculate a hypothetical value of the K coefficient after twelve years of life. This hypothetical value, equal to 0.410 W.m^{-2}. K^{-1}, is 2.4% less than the value of the K coefficient measured at twelve years of life on a vehicle of the same series (0.42 W.m^{-2}.K^{-1}) having the same dimensions, characteristics and accessories. This difference could be attributed to the type of use made of the vehicle during its lifetime. Further modelling tests should be performed to confirm the goodness of the model. To this end, it would be useful to have detailed information about the construction and composition of other vehicles including the accessories and features inside the insulated enclosure. In addition, a protocol has been developed for carrying out thermal conductivity tests on panels obtained from real vehicles. The main objective of these future tests is to experimentally obtain apparent thermal conductivity values both at the beginning and after twelve years of life to be inserted in the model. This could allow obtaining more accurate values of the calculated K coefficients at the beginning of the life of a vehicle and after twelve years of use.

6.4 Future works and perspectives

The short, medium and long-term perspectives aim to pursue the analysis related to the issue of aging of vehicles used in the cold chain with all its related aspects, in order to continue meeting the demand of the industry. This demand is, in fact, in continuous evolution to satisfy the technological innovation to which the refrigerated transport market is subjected.

The identified perspectives as a result of this 3-years study are summarized in the next paragraphs.

6.4.1 Short-to medium term perspectives

The first short-term perspective is to disseminate the scientific results of this study:

- in the scientific community to provide new insights for further studies,
- in the industry in order to train people to a better use and maintainance of refrigerated vehicles.

The dissemination of these results will therefore take place in the form of scientific communications and articles but also through good practices guides and “ad hoc” training for companies involved both in the manufacturing and/or use of refrigerated vehicles. Good practices related to the use of refrigerated vehicles represent an important process to be implemented to reduce the aging process as well as to reduce the energy consumption. This perspective fits in well with the Ecler programme developed by Cemafroid, which aims to achieve large-scale energy savings by training more than 10 000 refrigerated vehicle drivers and labelling the vehicles to raise awareness among players in the cold chain and refrigerated transport.

The second short-term perspective is to continue the insulation performance monitoring programme of new series-produced vehicles, started in 2017 and whose results were presented in section 3.4 of this manuscript. This control program allowed to study for the first time the difference between new prototype vehicles and real new vehicles of the series built on the basis of the corresponding prototype. This experimental assessment shall be continued systematically since the estimation of the existing difference between prototypes and real vehicles is necessary for the study of ageing. However, this assessment is also an important issue for new refrigerated trucks certification.

During these three years the study has been carried out for fourty-one vehicles of different types (i.e, vans, trucks and semi-trailers), all of which had insulated enclosures reported on their frames. In the short-term, the experimentation should also be extended to the equipment with insulation integrated into the structure of the vehicle.

A third step in the short-to-medium-term concerns the modelling work, which should be continued according to the following two perspectives:

- the numerical models developed according to the data-centric approach, presented in Chapter 4 (section 4.4) of this manuscript, could be integrated into the Datafrig® database In this way the manufacturer, by logging into his Datafrig® account may independently run the models and get a statistical result of the ageing of his fleet of vehicles.
- the physical model, presented in Chapter 5, shall be improved and adapted to the construction needs of the various manufacturers in order to predict the insulating performance in the various phases of the vehicle's life. The prediction of these perfromances could help manufacturers in the design and production phases of their vehicles. In addition, the model accounts for the convective and conductive heat exchanges insisting on the average internal and external surfaces. Radiative heat exchanges are also to be taken into account.

6.4.2 Medium-long term perspectives

In the medium-long term, the perspectives arising from this thesis work are as follows.

A first medium-long term perspective still concerns the insulation performance monitoring programme of new series-produced vehicles the control programme presented in Chapter 3, section 3.4. After perfecting this programme and making it systematic on French territory, the goal would be to implement it at the European level. This requires the development and the creation of synergies with the competent authorities and institutions of the other European countries.

A second medium-long term perspective concerns the development of a new kind of test. As anticipated in the conclusions arising from the physical model (see Chapter 5, section 5.3) a test protocol was developed for carrying out thermal conductivity tests on panels obtained from real vehicles. The main objective of these future tests is to experimentally obtain equivalent thermal conductivity values both at the beginning and after twelve years of life of sandwich panels, exported from real vehicles. The development of the methodology and the implementation of this protocol represent an important medium-long term perspective since the results of these experiments would provide new elements for the evaluation of ageing. These results should also be included in the developed physical model to obtain more accurate values of the calculated K coefficients.

The third medium-long term perspective concerns the exploitation of data resulting from the ATP certificate issuing process implemented in France In the issuing scheme of ATP certificates presented in Chapter 2 (section 2.1, subparagraph 2.1.3.7) it has been seen how insulation performance is initially measured on the prototype vehicle and after 12 years of life on all the vehicles produced in the series. The ageing has been studied from the comparison of the K coefficients measured in these two moments (i.e. K_p and K_{12}) It has been seen, however, that at 6 and 9 years of use the vehicles are subjected to a pull-down test, presented in Chapter 2 (section 2.1, subparagraph 2.1.3.6). The results of these tests are available today on Datafrig® in a binary form (i.e. successful test, failed test) and represent a source of information that has not been well explored and exploited.

The results of these data could be analysed from:

- a thermal point of view in synergy with the test centres by recovering the complete results in temperature drop graph form and,
- through the use of Machine Learning techniques.

The combination of these two approaches could lead to the definition of new performance indicators for refrigerated vehicles after 6 and 9 years of life.

Finally, the interaction between Big Data and refrigeration field, already started in this PhD thesis, has to be continued with the development of new studies and analyses closely related to the ageing of vehicles. An example of a study concerns the temperatures traceability during refrigerated transport. The amount of temperatures that can be acquired in the different logistic schemes of products delivery could be studied more efficiently using artificial intelligence techniques.

Appendix

Annex A: calibration certificate of four-wire platinum resistance thermometers type Pt100

CERTIFICAT D'ETALONNAGE
N° 1909MET003

Délivré par :	CEMAFROID SAS 5, avenue des Prés 94266 FRESNES Cedex France
Délivré à :	CEMAFROID SAS 5, avenue des Prés 94266 FRESNES Cedex France

INSTRUMENT ETALONNE

Désignation : Centrale de mesures de température (37 voies avec capteurs de type PT100)

Marque :	AGILENT
Type :	34980A
N° de série :	MY53150776
Configuration :	MY53151071 (34921A SLOT1) MY53151042 (34921A SLOT2)
N° d'identification:	T– FRE– 137

Date d'émission : 23/09/2019

Responsable Fonction Métrologie:

Thomas GIRAUD

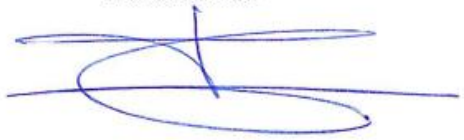

OBJECTIF DE L'ETALONNAGE

L'étalonnage d'une chaîne de mesure de température consiste à déterminer les corrections à appliquer aux valeurs affichées.

MODE OPERATOIRE ET MOYENS UTILISES

L'étalonnage de la chaîne a été réalisé au point de fusion de la glace, ou par comparaison à un thermomètre étalon dans des milieux de comparaison, selon la procédure interne P07523. Les moyens mis en oeuvre sont les suivants:

Thermomètre étalon :

Marque :	AOIP	ou	AOIP	ou	AOIP
Type :	PN 5207 + AN 5847		PHP 601 + AN 5847		PHP 601 + FLUKE 5609
Référence :	MET 97-180		MET 11-031-VRtB/C1		MET 11-031-VRtA/C2

Milieu de comparaison :

• -196°C:	Bain d'azote liquide	Référence : EQT-FRE-174
• de -80°C à 0°C:	Bain d'éthanol	Marque : Fluke Référence : T-FRE-238 Type : 7381
• 0°C	Bain de glace fondante	Référence : EQT-FRE-082 / EQT-FRE-174 / T-FRE-245
• de -30°C à +70°C:	Bain d'eau glycolée	Marque : Fluke Référence : MET 09-002 / MET 11-032 Type : 7340

CONDITIONS D'ETALONNAGE

Date d'étalonnage :	du 20/09/2019 au 23/09/2019	Identification du milieu de comparaison :	MET 11– 032
Température ambiante :	23°C ± 3°C	Identification du thermomètre étalon :	T– MET– 11– 031– VRtB/C1
Immersion du capteur (mm) :	160	Opérateur :	Thomas GIRAUD

CONDITIONS PARTICULIERES

Les incertitudes élargies mentionnées sont celles correspondant à deux fois l'incertitude-type composée.
Les incertitudes élargies ont été calculées en tenant compte des différentes composantes d'incertitudes, étalons de référence, moyens d'étalonnage, conditions d'environnement, répétabilité, dérive...
Ce certificat d'étalonnage garantit le raccordement des résultats d'étalonnage au Système International d'unités (SI).
*Remarque: les moyennes de mesures sont arrondies en tenant compte de la résolution de l'indicateur de la chaîne étalonnée mais les calculs des écarts sont effectués sur les valeurs réelles, ce qui peut engendrer une différence sur la correction égale au maximum à un pas de quantification.

RESULTATS D'ETALONNAGE

Moyenne des températures étalons (°C)	Moyenne des lectures de la chaîne (°C)	Corrections à ajouter aux lectures de la chaîne de mesure (°C)*	Incertitude d'étalonnage (°C) (k=2)	Fonction de correction	Max des résidus de modélisation (°C)	Dérive par rapport au précedent étalonnage (°C)
Capteur T-FRE-137S1-V1001/C221						
-29,96	-30,12	0,16	0,09	0,207 + 1,001*x - 1,173E-5*x^2	0,019672	-0,107178
0,05	-0,17	0,23	0,09			
33,07	32,85	0,21	0,09			
70,14	69,91	0,23	0,09			
Capteur T-FRE-137S1-V1002/C222						
-29,96	-29,93	-0,03	0,09	0,089 + 1,003*x - 2,938E-5*x^2	0,035265	-0,187578
0,05	-0,07	0,12	0,09			
33,07	32,96	0,11	0,09			
70,14	70,00	0,13	0,09			
Capteur T-FRE-137S1-V1003/C223						
-29,96	-30,23	0,27	0,09	0,191 + 0,998*x + 1,156E-5*x^2	0,001172	0,061597
0,05	-0,14	0,19	0,09			
33,07	32,94	0,13	0,09			
70,14	70,04	0,09	0,09			
Capteur T-FRE-137S1-V1004/C224						
-29,96	-29,90	-0,06	0,09	0,037 + 1,002*x - 1,525E-5*x^2	0,024099	-0,122878
0,05	-0,01	0,06	0,09			
33,07	32,99	0,08	0,09			
70,14	69,99	0,14	0,09			

Capteur T-FRE-137S1-V1005/C1245						
-29,96	-30,11	0,15	0,09	0,12 + 0,999*x + 5,42E-6*x^2	0,00005	0,178100
0,05	-0,07	0,12	0,09			
33,07	32,97	0,09	0,09			
70,14	70,05	0,09	0,09			
Capteur T-FRE-137S1-V1008/C1246						
-29,96	-30,14	0,17	0,09	0,135 + 0,999*x + 1,403E-5*x^2	0,0046	0,11838
0,05	-0,08	0,14	0,09			
33,07	32,95	0,12	0,09			
70,14	70,01	0,13	0,09			
Capteur T-FRE-137S1-V1009/C229						
-29,96	-30,26	0,30	0,09	0,2 + 0,997*x + 1,259E-5*x^2	0,002764	0,140522
0,05	-0,15	0,20	0,09			
33,07	32,94	0,12	0,09			
70,14	70,07	0,06	0,09			
Capteur T-FRE-137S1-V1010/C230						
-29,96	-30,15	0,19	0,09	0,048 + 0,996*x + 1,303E-5*x^2	0,001765	0,069722
0,05	0,01	0,05	0,09			
33,07	33,15	-0,08	0,09			
70,14	70,33	-0,19	0,09			
Capteur T-FRE-137S1-V1011/C231						
-29,96	-30,31	0,35	0,09	0,204 + 0,996*x + 1,415E-5*x^2	0,002710	0,058697
0,05	-0,15	0,20	0,09			
33,07	32,98	0,08	0,09			
70,14	70,16	-0,03	0,09			

Capteur T-FRE-137S1-V1012/C232						
-29,96	-30,25	0,29	0,09	0,166 + 0,996*x + 1,415E-5*x^2	0,002156	0,073022
0,05	-0,11	0,16	0,09			
33,07	33,01	0,06	0,09			
70,14	70,16	-0,03	0,09			
Capteur T-FRE-137S1-V1013/C233						
-29,96	-30,20	0,24	0,09	0,163 + 0,998*x + 6,991E-6*x^2	0,002405	0,099022
0,05	-0,11	0,16	0,09			
33,07	32,97	0,10	0,09			
70,14	70,10	0,04	0,09			
Capteur T-FRE-137S1-V1014/C1147						
-29,96	-30,17	0,21	0,09	0,208 + 1*x + 3,378E-6*x^2	0,004186	0,072397
0,05	-0,16	0,21	0,09			
33,07	32,86	0,21	0,09			
70,14	69,91	0,23	0,09			
Capteur T-FRE-137S1-V1015/C235						
-29,96	-30,35	0,39	0,09	0,27 + 0,996*x + 7,445E-6*x^2	0,003323	0,128622
0,05	-0,22	0,27	0,09			
33,07	32,90	0,16	0,09			
70,14	70,08	0,06	0,09			
Capteur T-FRE-137S1-V1016/C1247						
-29,96	-29,98	0,01	0,09	-0,039 + 0,999*x + 5,891E-6*x^2	0,0005	0,15588
0,05	0,09	-0,04	0,09			
33,07	33,14	-0,07	0,09			
70,14	70,23	-0,10	0,09			
Capteur T-FRE-137S1-V1017/C237						
-29,96	-30,15	0,18	0,09	0,064 + 0,996*x + 1,37E-5*x^2	0,002673	0,077822
0,05	-0,01	0,06	0,09			
33,07	33,10	-0,04	0,09			
70,14	70,25	-0,12	0,09			
Capteur T-FRE-137S1-V1018/C238						
-29,96	-30,09	0,13	0,09	0,095 + 0,999*x + 9,775E-6*x^2	0,001023	0,095322
0,05	-0,04	0,09	0,09			
33,07	32,98	0,08	0,09			
70,14	70,04	0,09	0,09			

Capteur T-FRE-137S1-V1019/C239						
-29,96	-30,26	0,30	0,09	0,233 + 0,998*x + 1,117E-5*x^2	0,002627	0,131122
0,05	-0,18	0,23	0,09			
33,07	32,88	0,19	0,09			
70,14	69,98	0,16	0,09			
Capteur T-FRE-137S1-V1020/C240						
-29,96	-30,14	0,18	0,09	0,14 + 0,999*x + 7,039E-6*x^2	0,000505	0,137322
0,05	-0,09	0,14	0,09			
33,07	32,96	0,11	0,09			
70,14	70,04	0,09	0,09			
Capteur T-FRE-137S2-V2020/C260						
-29,96	-29,97	0,01	0,09	-0,005 + 0,999*x - 2,108E-6*x^2	0,000152	0,061227
0,05	0,06	-0,00	0,09			
33,07	33,09	-0,02	0,09			
70,14	70,19	-0,05	0,09			

Capteur T-FRE-137S2-V2001/C1248						
-29,96	-30,02	0,05	0,09	0,041 + 0,999*x + 1,46E-6*x^2	0,0094	0,1589
0,04	-0,01	0,05	0,09			
33,05	33,04	0,01	0,09			
70,05	70,05	0,00	0,09			
Capteur T-FRE-137S2-V2002/C1249						
-29,96	-30,11	0,14	0,09	0,114 + 0,999*x + 2,3E-5*x^2	0,016	0,2211
0,04	-0,09	0,13	0,09			
33,05	32,95	0,10	0,09			
70,05	69,87	0,18	0,09			
Capteur T-FRE-137S2-V2003/C1250						
-29,96	-30,13	0,17	0,09	0,118 + 0,999*x + 1,069E-5*x^2	0,0021	0,0862
0,04	-0,08	0,12	0,09			
33,05	32,97	0,08	0,09			
70,05	69,98	0,07	0,09			
Capteur T-FRE-137S2-V2005/C245						
-29,96	-30,17	0,20	0,09	0,078 + 0,996*x + 1,38E-5*x^2	0,006867	0,057582
0,04	-0,03	0,07	0,09			
33,05	33,07	-0,02	0,09			
70,05	70,16	-0,11	0,09			
Capteur T-FRE-137S2-V2006/C246						
-29,96	-30,24	0,28	0,09	0,21 + 0,998*x + 1,343E-5*x^2	0,006819	0,109382
0,04	-0,16	0,20	0,09			
33,05	32,88	0,17	0,09			
70,05	69,90	0,15	0,09			
Capteur T-FRE-137S2-V2007/C247						
-29,96	-30,18	0,22	0,09	0,124 + 0,997*x + 1,472E-5*x^2	0,006068	0,063182
0,04	-0,08	0,12	0,09			
33,05	32,99	0,06	0,09			
70,05	70,04	0,01	0,09			

Capteur T-FRE-137S2-V2008/C248						
-29,96	-30,17	0,21	0,09	0,084 + 0,996*x + 1,417E-5*x^2	0,006593	0,064282
0,04	-0,04	0,08	0,09			
33,05	33,06	-0,02	0,09			
70,05	70,15	-0,10	0,09			
Capteur T-FRE-137S2-V2009/C249						
-29,96	-30,19	0,23	0,09	0,112 + 0,997*x + 1,356E-5*x^2	0,006482	0,078082
0,04	-0,07	0,11	0,09			
33,05	33,03	0,02	0,09			
70,05	70,11	-0,06	0,09			
Capteur T-FRE-137S2-V2010/C250						
-29,96	-30,30	0,34	0,09	0,201 + 0,996*x + 1,319E-5*x^2	0,006338	0,164682
0,04	-0,16	0,20	0,09			
33,05	32,96	0,09	0,09			
70,05	70,06	-0,01	0,09			
Capteur T-FRE-137S2-V2011/C251						
-29,96	-30,11	0,14	0,09	0,094 + 0,999*x + 1,648E-5*x^2	0,004301	0,052482
0,04	-0,05	0,09	0,09			
33,05	32,97	0,08	0,09			
70,05	69,96	0,09	0,09			
Capteur T-FRE-137S2-V2012/C252						
-29,96	-30,23	0,26	0,09	0,129 + 0,996*x + 1,556E-5*x^2	0,001831	0,068882
0,04	-0,09	0,13	0,09			
33,05	33,03	0,02	0,09			
70,05	70,12	-0,07	0,09			
Capteur T-FRE-137S2-V2013/C253						
-29,96	-30,13	0,16	0,09	0,014 + 0,996*x + 1,73E-5*x^2	0,004025	0,046346
0,04	0,03	0,01	0,09			
33,05	33,16	-0,11	0,09			
70,05	70,26	-0,21	0,09			

Capteur T-FRE-137S2-V2014/C254						
-29,96	-30,21	0,25	0,09	0,12 + 0,996*x + 1,591E-5*x^2	0,004839	0,059982
0,04	-0,08	0,12	0,09			
33,05	33,03	0,02	0,09			
70,05	70,11	-0,06	0,09			
Capteur T-FRE-137S2-V2015/C255						
-29,96	-30,20	0,24	0,09	0,113 + 0,996*x + 1,402E-5*x^2	0,004525	0,063582
0,04	-0,07	0,11	0,09			
33,05	33,04	0,01	0,09			
70,05	70,13	-0,08	0,09			
Capteur T-FRE-137S2-V2016/C256						
-29,96	-30,22	0,25	0,09	0,151 + 0,997*x + 1,425E-5*x^2	0,005186	0,069582
0,04	-0,11	0,15	0,09			
33,05	32,97	0,07	0,09			
70,05	70,04	0,01	0,09			
Capteur T-FRE-137S2-V2017/C257						
-29,96	-30,24	0,27	0,09	0,143 + 0,996*x + 1,447E-5*x^2	0,004850	0,092582
0,04	-0,10	0,14	0,09			
33,05	33,01	0,04	0,09			
70,05	70,11	-0,06	0,09			
Capteur T-FRE-137S2-V2018/C258						
-29,96	-30,16	0,19	0,09	0,038 + 0,995*x + 1,493E-5*x^2	0,005066	0,055682
0,04	0,01	0,03	0,09			
33,05	33,14	-0,09	0,09			
70,05	70,26	-0,21	0,09			
Capteur T-FRE-137S2-V2019/C259						
-29,96	-30,13	0,16	0,09	0,012 + 0,996*x + 1,46E-5*x^2	0,005140	0,055182
0,04	0,03	0,01	0,09			
33,05	33,16	-0,12	0,09			
70,05	70,28	-0,23	0,09			

Annex B: Wattmeter calibration certificate

CERTIFICAT D'ETALONNAGE

N° C07E161365

DELIVRE A : CEMAFROID SAS
5 avenue des prés
94260 FRESNES

INSTRUMENT ETALONNE

Désignation : WATTMETRE NUMERIQUE MONOPHASE

Constructeur : YOKOGAWA

Type : WT210 N° de série : 91G232492
N° d'identification: LTA 07-002

Ce certificat comprend 4 pages Date d'émission : 16 décembre 2016

LE RESPONSABLE DU LABORATOIRE

P. T. JADIN

C. CROZIER

Portée disponible sur www.cofrac.fr

cofrac ETALONNAGE

APPAREIL

Désignation :	WATTMETRE NUMERIQUE MONOPHASE	Date de l'étalonnage :	15 décembre 2016
Constructeur :	YOKOGAWA	MILIEU AMBIANT	
Type :	WT210	Température :	(23 ± 2)°C
N° de série :	91G232492	Hygrométrie :	< 70% H.R.
N° d'identification :	LTA 07-002	Opérateur :	T. JANIN

FONCTION ETALONNEE	MESURE DE TENSION ALTERNATIVE	MESURE DE COURANT ALTERNATIF	MESURE DE PUISSANCE ACTIVE	MESURE DU FACTEUR DE PUISSANCE	MESURE D'ENERGIE ACTIVE
INCERTITUDE D'ETALONNAGE (1)	(3)	(3)	(2)	(3)	(3)

(1) Dans le cas où les indications de l'appareil fluctuaient au cours des mesures, l'incertitude de mesure correspondant à ces fluctuations à court terme est prise en compte dans l'incertitude d'étalonnage, et les résultats sont des valeurs moyennes estimées, le cas échéant arrondies de façon appropriée.

(2) Valeur indiquée dans le tableau des résultats.
(3) Fonction non étalonnée.
(4) Fonction ne concernant pas l'appareil.

PROCEDURES TECHNIQUE D'ETALONNAGE - ETALONS DE REFERENCE - TRACABILITE

L'étalonnage a été réalisé selon la ou les méthode(s) et procédure(s) suivante(s):

Etalonnage en mesure de puissance active par comparaison directe à un wattmètre numérique étalon selon la procédure technique PT-07E-18/b.

"Les incertitudes élargies mentionnées sont celles correspondant à deux fois l'incertitude-type composée. Les incertitudes types ont été calculées en tenant compte des différentes composantes d'incertitudes, étalons de référence, moyens d'étalonnage, conditions d'environnement, contribution de l'instrument étalonné, répétabilité..."

Dans le cas présent, la composante d'incertitude dûe à l'appareil en étalonnage et provenant de l'incertitude sur la mesure de la température n'est pas prise en compte.

« Ce certificat d'étalonnage garantit le raccordement des résultats d'étalonnage au Système International d'unités (SI) pour les seuls étalonnages couverts par l'accréditation, ceux qui ne le sont pas sont repérés par le symbole* »

"Le dossier de mesure dans lequel figurent les étalons utilisés, le nom de l'opérateur, la date, le numéro de ce certificat d'étalonnage est archivé par le laboratoire accrédité."

"L'accréditation par le Cofrac atteste de la compétence des laboratoires pour les seuls étalonnages couverts par l'accréditation."

Le Cofrac est signataire de l'accord multilatéral de EA (European co-operation for Accreditation) et d'ILAC (International Laboratory Accreditation Cooperation) de reconnaissance de l'équivalence des documents d'étalonnage.

CONDITIONS DES MESURES

L' appareil séjournait à la température ambiante du laboratoire depuis au moins vingt quatre heures et était mis en fonctionnement, sous sa tension d'alimentation nominale (230 V - 50 Hz), quatre heures au moins avant le début des mesures.

Sauf indication contraire, l'appareil a été étalonné dans la configuration présente lors de sa mise sous tension et a été effectué pour des valeurs croissantes de la valeur lue sur l'afficheur de l'appareil.

Les résultats figurent dans les tableaux ci-après sous forme de correction à apporter à la valeur lue pour obtenir la valeur exacte.

1- ETALONNAGE DE L'APPAREIL SUR LA FONCTION "MESURE DE PUISSANCE ACTIVE " A LA FREQUENCE DE 50 Hz

L'étalonnage à été effectué en puissance fictive (1) en courant alternatif sinusoïdal,à la fréquence de 50 Hz

La tension de mesure était appliquée une demi-heure au moins avant le début des mesures et le courant de mesure cinq minutes au moins avant le début des mesures

Les points " bas " des circuits " VOLTAGE " et " CURRENT " étaient mis à la terre

1-1 Etalonnage de la voie 1 en mesure de puissance active

CALIBRE TENSION	CALIBRE COURANT	POLARITE FREQUENCE	TENSION APPLIQUEE	COURANT APPLIQUE	FACTEUR DE PUISSANCE	PUISSANCE ACTIVE NOMINALE	CORRECTION DE L'APPAREIL		± INCERTITUDE GLOBALE D'ETALONNAGE (k=2)
Unité →			(V)	(A)		(W)	(W)	(%) (1)	(W)
300 V	0,2 A	50 Hz	230,0	0,02	1,000	4,600	0,01	0,13	0,036
300 V	0,2 A	50 Hz	230,0	0,10	1,000	23,000	0,02	0,11	0,055
300 V	0,2 A	50 Hz	230,0	0,18	1,000	41,400	0,05	0,11	0,091
300 V	0,2 A	50 Hz	230,0	0,26	1,000	59,800	0,06	0,10	0,068
300 V	0,5 A	50 Hz	230,0	0,05	1,000	11,50	0,0	0,05	0,14
300 V	0,5 A	50 Hz	230,0	0,25	1,000	57,50	0,1	0,20	0,14
300 V	0,5 A	50 Hz	230,0	0,45	1,000	103,50	0,1	0,13	0,19
300 V	0,5 A	50 Hz	230,0	0,65	1,000	149,50	0,2	0,16	0,24
300 V	1 A	50 Hz	230,0	0,10	1,000	23,00	0,0	0,00	0,13
300 V	1 A	50 Hz	230,0	0,50	1,000	115,00	0,2	0,21	0,20
300 V	1 A	50 Hz	230,0	0,90	1,000	207,00	0,2	0,12	0,29
300 V	1 A	50 Hz	230,0	1,30	1,000	299,00	0,4	0,13	0,39
300 V	2 A	50 Hz	230,0	0,20	1,000	46,00	0,0	0,03	0,13
300 V	2 A	50 Hz	230,0	1,00	1,000	230,00	0,2	0,07	0,32
300 V	2 A	50 Hz	230,0	1,80	1,000	414,00	0,5	0,12	0,50
300 V	2 A	50 Hz	230,0	2,60	1,000	598,00	0,9	0,15	0,68
Unité →			(V)	(A)		(kW)	(kW)	(%) (1)	(kW)
300 V	5 A	50 Hz	230,0	0,5	1,000	0,11500	0,000	0,03	0,00094
300 V	5 A	50 Hz	230,0	2,5	1,000	0,5750	0,001	0,20	0,0014
300 V	5 A	50 Hz	230,0	4,5	1,000	1,0350	0,002	0,21	0,0019
300 V	5 A	50 Hz	230,0	6,5	1,000	1,4950	0,002	0,15	0,0024
300 V	10 A	50 Hz	230,0	1,0	1,000	0,2300	0,000	-0,03	0,0011
300 V	10 A	50 Hz	230,0	5,0	1,000	1,1500	0,002	0,18	0,0020
300 V	10 A	50 Hz	230,0	9,0	1,000	2,0700	0,004	0,20	0,0029
300 V	10 A	50 Hz	230,0	13,0	1,000	2,9900	0,005	0,17	0,0039
300 V	20 A	50 Hz	230,0	2,0	1,000	0,4600	0,001	0,25	0,0013
300 V	20 A	50 Hz	230,0	10,0	1,000	2,3000	0,003	0,14	0,0032
300 V	20 A	50 Hz	230,0	18,0	1,000	4,1400	0,006	0,15	0,0050
300 V	20 A	50 Hz	230,0	26,0	1,000	5,9800	0,007	0,12	0,0069

(1) Valeurs données à titre indicatif
Correction relative (%) = ((Valeur étalon - Valeur appareil) / Valeur étalon) x 100

FOLIO ADMINISTRATIF

THESE DE L'UNIVERSITE DE LYON OPEREE AU SEIN DE L'INSA LYON

NOM : CAPO DATE de SOUTENANCE :16/03/21

Prénoms : Claudia

TITRE : When physical experiments meet machine learning experiments for the understanding and prediction of the ageing of refrigerated transport vehicles.

NATURE : Doctorat Numéro d'ordre : 2021LYSEI017

Ecole doctorale : MEGA (Mécanique – Energétique – Génie civil – Acoustique)

Spécialité : Thermique - énergétique

RESUME :

L'isolation thermique de la caisse des véhicules utilisés dans le transport sous température dirigée est un élément critique tant pour la qualité de la chaîne du froid que pour la consommation énergétique de ces véhicules. Son efficacité est caractérisée par le coefficient d'isolation global ("coefficient K"), qui tend à augmenter au cours du temps en raison du vieillissement de la caisse. Cette thèse présente les résultats de travaux réalisés selon trois approches complémentaires pour comprendre le vieillissement. Des résultats de campagnes d'essais expérimentaux ont été confrontés à des résultats produits par des méthodes du monde de la science des données pour conforter des efforts de modélisation physique. Les expériences ont consisté à réaliser des mesures du coefficient K d'engins prototypes après leur fabrication et d'engins en service depuis 12 ans. Ceci a permis d'évaluer l'impact du groupe frigorifique et de quantifier la différence entre les nouveaux engins et leurs prototypes. Par ailleurs, les performances thermiques et énergétiques d'un nouveau type d'engin construit avec des panneaux sandwich ayant des inserts sous vide dans les parois ont été déterminées. La disponibilité d'un grand nombre de données stockées dans les bases de données Datafrig® du Cemafroid permet d'étudier le phénomène de vieillissement par une approche centrée sur les données. Les données ont été analysées statistiquement en utilisant des concepts simples de densité de probabilité et des techniques d'intelligence artificielle. Un modèle numérique de vieillissement a été développé à partir d'un algorithme de forêt aléatoire : il permet de prédire le vieillissement avec une erreur inférieure à 6%. Enfin, un modèle physique 1D a été développé afin de comprendre le phénomène de vieillissement d'un point de vue thermique. Ce modèle reproduit les performances d'isolation initiales (K_p et K_0) d'un véhicule frigorifique et permet de simuler le vieillissement du véhicule après 12 ans de vie.

MOTS-CLÉS : Ageing Phenomenon, K coefficient, Refrigerated Transport, Refrigerated Vehicles, Prototype vehicles, In-service Vehicles, Numerical Model, Random Forest Algorithm, Datafrig® database.

Laboratoire (s) de recherche : CETHIL, LIRIS.

Directeur de thèse: Professeur Jocelyn BONJOUR

Président de jury : Mme Silvia MINETTO

Composition du jury : M. Brice TREMEAC, Mme Silvia MINETTO, Mme Claudia RONCANCIO, M. Arthur MONTI, M. Jocelyn BONJOUR, M. Rémi REVELLIN, M. Jean-Marc PETIT, M. Gérald CAVALIER